

Sensor-based determination of the fruit bearing  
capacity in *Malus x domestica* BORKH. aimed at  
precise crop load management

vorgelegt von  
Dipl. Ing. (FH), M.Sc.  
Martin Penzel  
ORCID: 0000-0001-9617-2082

an der Fakultät V - Verkehrs- und Maschinensysteme  
der Technischen Universität Berlin  
zur Erlangung des akademischen Grades

Doktor der Ingenieurwissenschaften  
- Dr.-Ing. -

genehmigte Dissertation

Promotionsausschuss:

Vorsitzender: Prof. Dr.-Ing. Henning Jürgen Meyer

Gutachter: Prof. Dr. agr. Henryk Flachowsky

Gutachter: Dr. agr. Martin Geyer

Gutachterin: Prof. Dr.-Ing. Cornelia Weltzien

Gutachterin: Dr. rer. hort. habil. Manuela Zude-Sasse

Tag der wissenschaftlichen Aussprache: 06.12.2021

Berlin, 2022

## Abstract

One major goal of commercial fruit production is a homogenous fruit quality throughout the whole orchard. For this purpose, crop load management practices in apples intend to reduce the number of fruit per tree in order to (i) optimise the carbon supply to demand balance and the (ii) fruit quality in the current season, and (iii) ensure flower bud formation for the following season. Currently, crop load management is routinely performed field uniform without taking into consideration the inter-tree variability in flower or fruit set and the photosynthetic capacity of the trees, which frequently occurs in commercial orchards. Because of the variability among the trees, uniform crop load management can lead to sub-optimal numbers of fruit per tree when targeting homogenous fruit qualities. Currently, no tree-adapted crop load management practices have been developed. One reason is the lack of plant physiological and agronomic models to evaluate the actual fruit set of individual trees and to derive management decisions from these data. For tree-adapted crop load management, the fruit set and growth capacity of all trees within an orchard, often exceeding 2,500 trees per hectare, need to be mapped. Frequent studies of georeferencing and sensing individual trees' data are available, but the developed approaches lack further application in decision support models.

The aim of this thesis was (i) to investigate inter-tree variability in flower set, fruit set, and total leaf area per tree in apple, (ii) to develop a modelling approach to estimate the trees' capacity to produce fruit of desired diameters, the fruit bearing capacity, which is based on spatially recorded sensor data of individual trees, and finally (iii) to investigate the application of the model, future possibilities, and advantages of tree-adapted crop load management.

The variance in flowers per tree was investigated in two commercially relevant apple cultivars ('Elstar': 200 trees in 2011, 2014, 2015; 'Gala': 100 trees in 2014, 200 trees in 2015, 2016). Trees of the cultivar 'Elstar' were more susceptible to alternate bearing in comparison to 'Gala' trees and, therefore, included a higher percentage of trees with a low flower set, unable to meet the desired number of fruit per tree at harvest. Field uniform flower thinning led to yield reductions by over-thinning of trees with low and medium flower set on both cultivars ranging from 1.4 - 7.6 t ha<sup>-1</sup>.

The leaf area per tree was recorded in three commercial apple orchards, taking into consideration the cultivars 'Gala' (996 trees), 'Pinova' (50 trees) and 'RoHo 3615' (100 trees), with a terrestrial 2-D light detection and ranging (LiDAR) laser scanner. A method

to estimate individual trees' photosynthetic and fruit bearing capacity (FBC) has been introduced. The method utilises the total leaf area per tree, monthly recorded gas exchange variables of the fruit and the leaves, fruit growth rates, and weather data and considers these data in a carbon balance model. The leaf area and photosynthetic capacity of the investigated trees was highly variable in all three orchards. In 'Gala', the variance in leaf area per tree and the FBC was similar in two consecutive years. However, the spatial location of cold and hot spots in the FBC, highlighting trees with FBC below or above the average of the surrounding trees, varied between the years. Consequently, for precise crop load management that targets homogenous average fruit diameters in orchards with inter-tree variability in total leaf area, the FBC need to be recorded annually. The FBC can be used to derive optimum fruit numbers per tree to achieve desired fruit diameters. The FBC of individual trees ('Gala' 2018: 100 trees, 2019: 70 trees; 'Pinova' 2018: 35 trees; 'RoHo 3615' 2018: 45 trees) was calculated for the actual average harvested fruit diameter. The modelled FBC of the trees, with little deviation, corresponded to the actual number of marketable fruit per tree. The results additionally revealed that, in the two orchards of the cultivars 'Pinova' and 'RoHo 3615', field-uniform thinning of heterogeneous trees can result in avoidable yield losses on 23%, 31 %, respectively, of the investigated trees. Furthermore, 16 % of the trees of 'RoHo 3615' had numbers of fruit per tree that exceeded the FBC and led to an average fruit diameter below 65 mm, the minimum requirement for fresh market access. In 'Gala' in two consecutive years, the mean fruit mass and mean soluble solids content per tree correlated with the amount of photons that the tree, after the foliage was fully developed, had absorbed per fruit, demonstrating the physiological limitations of the trees to produce fruit of a desired quality. Minimum thresholds of seasonally intercepted photons per fruit to achieve a specific fruit quality were generated. In the period after the foliage of the trees was fully developed until harvest, the total incident photosynthetically active radiation (PAR) was 440 MJ m<sup>-2</sup>, 508 MJ<sup>-2</sup> in 2018, 2019, respective, of which the trees absorbed 19-62 %, depending on the available leaf area and the associated light interception. On average, 7.5 MJ PAR in 2018 and 5.9 MJ in 2019 per fruit was required, that 80% of the fruit reached a marketable fruit diameter. To absorb this amount of PAR, at least 550 cm<sup>2</sup> of leaf area per fruit were required.

For the implementation of tree adapted crop load management, both flower and fruit thinning would be feasible. Flower thinning has two advantages: it is independent of the weather conditions, and the same settings of the thinning device leads to consistent thinning results over several years. However, after flower thinning is performed, late frost can reduce the fruit set of the trees, which may lead to low crop loads below the FBC.

Chemical fruit thinning is usually carried out when there is no longer a risk of late frost. However, the thinning efficacy depends on temperature, irradiation, humidity and the physiological condition of the trees. Therefore, thinning results often differ between years. In this work it was confirmed that for successful chemical thinning with the photosynthesis inhibitor metamitron, warm weather conditions (night: 15°C, day: 20°C) in the days before and after application are favourable. At these temperatures, one application of the active ingredient is sufficient to reduce the fruit set of the trees to the desired target values, whereas at lower temperatures further applications may be required.

Tree adapted crop load management practices would be beneficial to avoid over-thinning and yield losses on trees with low and medium flower set, to optimise the crop load of all the trees and, consequently, to tap into the full economic potential of an orchard. For future crop load management strategies, the developed model can be utilised to evaluate the actual fruit and flower set in order to make management decisions for individual trees. For this purpose, it is required to utilise tree individual data in plant physiological and agronomic models. The models can potentially serve as algorithms to control machinery that is able to treat trees individually. Tree adapted crop load management would significantly advance the management of apple orchards taking into consideration the desired production targets and the physiological limitations of individual trees.

## Zusammenfassung

Bei der erwerbsmäßigen Erzeugung von Obst wird eine homogene Fruchtqualität innerhalb der gesamten Produktionsanlage angestrebt. Zu diesem Zweck wird bei Äpfeln die Anzahl an Früchten pro Baum durch Ausdünnung reduziert, um in der laufenden Saison (i) das Verhältnis zwischen dem Kohlenstoffbedarf wachsender Früchte und dem Angebot an assimilierten Kohlenstoff für das Fruchtwachstum, sowie (ii) die Fruchtqualität zu optimieren und (iii) die Blütenbildung für die folgende Saison sicherzustellen. Die Ausdünnung wird derzeit feldeinheitlich durchgeführt, ohne dabei die Variabilität des Blüten- und Fruchtansatzes oder der Wachstumskapazität der Bäume zu berücksichtigen, die häufig in Obstanlagen auftreten. Eine feldeinheitliche Ausdünnung kann jedoch aufgrund von Unterschieden im vegetativen und generativen Wachstum zwischen den einzelnen Bäumen zu einer suboptimalen Anzahl von Früchten pro Baum führen, wodurch Ertragsverluste auftreten. Bisher sind keine baumangepassten Verfahren für die Ausdünnung verfügbar. Ein Grund dafür ist das Fehlen von pflanzenphysiologischen und agronomischen Modellen, um den tatsächlichen Fruchtansatz einzelner Bäume in Relation zur Fruchtqualität zum Erntezeitpunkt zu bewerten und daraus Entscheidungen für die Kulturführung abzuleiten. Für eine an einzelne Bäume angepasste Ausdünnung ist es notwendig, den Fruchtansatz und die Fruchtertragskapazität aller Bäume innerhalb einer Anlage, die oft mehr als 2.500 Bäume pro Hektar umfasst, zu kartieren. Zwar gibt es zahlreiche Möglichkeiten zur Erfassung und Georeferenzierung von Daten einzelner Bäume, jedoch werden diese bisher noch nicht in Modellen zur Entscheidungsunterstützung verwendet.

Ziel dieser Arbeit war es, (i) die Variabilität des Blüten- und Fruchtansatzes und der Wachstumskapazität aller Bäume einer Apfelproduktionsanlage zu erfassen, (ii) einen Modellierungsansatz der Fruchtertragskapazität der Bäume, um Früchte mit gewünschten mittleren Fruchtdurchmessern zur Ernte zu produzieren, zu entwickeln, der auf räumlich erfassten Sensordaten einzelner Bäume basiert, die zur Simulation der Kohlenstoffbilanz der Bäume in verschiedenen Fruchtentwicklungsphasen verwendet werden und (iii) Anwendungsmöglichkeiten des Modells in technischen Verfahren zur baumangepassten Ausdünnung zu untersuchen.

Die Variabilität der Blüten pro Baum wurde an zwei wirtschaftlich bedeutenden Apfelsorten untersucht ('Elstar': jeweils 200 Bäume in 2011, 2014, 2015; 'Gala': 100 Bäume in 2014, 200 Bäume in 2015, 2016). Die Bäume der Sorte 'Elstar' wiesen im Vergleich zu denen der Sorte 'Gala' einen höheren prozentualen Anteil mit geringem Blütenansatz auf, die bei

der Ernte nicht die Ertragskapazität pro Baum erreichen konnten. Die feldeinheitliche Ausdünnung während des Ballonstadiums (BBCH-Stadium 59) führte bei beiden Sorten zu Ertragsminderungen zwischen 1,4 - 7,6 t ha<sup>-1</sup>, verursacht durch Überdünnung von Bäumen mit geringem und mittlerem Blütenansatz.

Die gesamte Blattfläche einzelner Bäume wurde in drei Apfelproduktionsanlagen ('Gala': 996 Bäume, 'Pinova': 50 Bäume, 'RoHo 3615': 100 Bäume) mit einem terrestrischen zweidimensionalen Light Detection and Ranging (LiDAR) Laserscanner erfasst. Es wurde eine Methode entwickelt, um die Photosynthese- und Fruchtertragskapazität (FBC) einzelner Bäume zu modellieren. Dabei werden die gesamte Blattfläche pro Baum, die saisonalen Gaswechselraten der Früchte und der Blätter, Wachstumsraten der Früchte und lokal erhobene Wetterdaten in einem Kohlenstoffbilanzmodell verwendet. Die Blattfläche und die Photosynthesekapazität der untersuchten Bäume wiesen in allen drei Anlagen eine hohe Variabilität auf. Die Variabilität der Blattfläche pro Baum und der FBC bei 'Gala' war in zwei aufeinanderfolgenden Jahren ähnlich. Durch Anwendung der Getis-Ord's Hot- und Cold-Spot-Analyse wurden Bäume mit einer niedrigeren bzw. höheren FBC als der Durchschnitt der umgebenden Bäume lokalisiert. Dadurch wurde festgestellt, dass sich die räumliche Lage von Coldspots und Hotspots der FBC zwischen den zwei Jahren unterschied. Folglich muss für eine präzise Ausdünnung, mit dem Ziel homogene mittlere Fruchtdurchmesser aller Bäume trotz Variabilität der Blattfläche zwischen den Bäumen zu erreichen, die FBC jährlich ermittelt werden.

Die FBC kann zur Ableitung der optimalen Fruchtanzahl pro Baum verwendet werden, um gewünschte Fruchtdurchmesser zu erreichen. In dieser Arbeit wurde die FBC einzelner Bäume ('Gala' 2018: 100 Bäume, 2019: 70 Bäume; 'Pinova' 2018: 35 Bäume; 'RoHo 3615' 2018: 45 Bäume) für deren tatsächlichen mittleren Fruchtdurchmesser zur Ernte simuliert. Die resultierende FBC der Bäume entsprach, mit geringer Abweichung, der tatsächlichen Anzahl an vermarktungsfähigen Früchten pro Baum. Die Ergebnisse zeigten zudem, dass in zwei Anlagen die feldeinheitliche Ausdünnung heterogener Bäume zu vermeidbaren Ertragsverlusten bei bis zu 31 % der untersuchten Bäume führte. Zusätzlich überschritten in einer Anlage die Anzahl von Früchten pro Baum von 16 % der Bäume die FBC, was zu mittleren Fruchtdurchmessern unter 65 mm führte, der Mindestanforderung für Tafelware.

Bei 'Gala' korrelierten in zwei aufeinanderfolgenden Jahren die mittlere Fruchtmasse und der mittlere Gehalt an löslicher Trockensubstanz pro Baum mit der Menge an Photonen, die der Baum, nachdem die Blattfläche voll entwickelt war, pro Frucht absorbiert hatte. Durch die Korrelation wurden die physiologischen Grenzen der Bäume für die Erzeugung

von Früchten einer angestrebten Qualität aufgezeigt. Außerdem wurden daraus Schwellenwerte der saisonal absorbierten Photonen pro Frucht generiert, um eine bestimmte Fruchtqualität zu erreichen. In dem Zeitraum, nachdem die Blattfläche der Bäume voll entwickelt war bis zur Ernte, betrug die Summe der einfallenden photosynthetisch aktiven Strahlung (PAR)  $440 \text{ MJ m}^{-2}$  in 2018 und  $508 \text{ MJ m}^{-2}$  in 2019, von denen die Bäume, in Abhängigkeit der vorhandenen Blattfläche und der damit verbundenen Lichtinterzeption, 19-62 % absorbierten. Im Mittel waren je Frucht  $7.5 \text{ MJ PAR}$  in 2018 und  $5.9 \text{ MJ PAR}$  in 2019 notwendig, damit 80 % der Früchte eine vermarktungsfähige Qualität erreichten. Um diese Menge an PAR zu absorbieren, waren mindestens  $550 \text{ cm}^2$  Blattfläche pro Frucht erforderlich.

Für die Umsetzung der baumangepassten Ausdünnung eignen sich sowohl Blüten- als auch Fruchtausdünnung. Die maschinelle Blütenausdünnung hat zwei Vorteile: Zum einen ist sie witterungsunabhängig, zum anderen sind die Ausdünnungsergebnisse, bei gleicher Einstellung des Ausdünnungsgerätes, in mehreren aufeinanderfolgenden Jahren reproduzierbar. Nachdem die Blütenausdünnung durchgeführt wurde, kann Spätfrost den Fruchtansatz der Bäume reduzieren, was häufig zu Erntemengen unterhalb der FBC führt. Die chemische Fruchtausdünnung wird in der Regel durchgeführt, wenn keine Gefahr von Spätfrost mehr besteht. Jedoch hängt die Wirksamkeit der Ausdünnung von Temperatur, Einstrahlung, Luftfeuchtigkeit und dem physiologischen Zustand der Bäume ab. Daher unterscheiden sich die Ausdünnungsergebnisse häufig zwischen den Jahren. In dieser Arbeit wurde bestätigt, dass für eine erfolgreiche chemische Ausdünnung mit dem Photosynthesehemmer Metamitron, warme Witterungsbedingungen (Nacht:  $15^\circ\text{C}$ , Tag:  $20^\circ\text{C}$ ) in den Tagen vor und nach der Anwendung förderlich sind. Bei diesen Temperaturen ist eine Applikation des Wirkstoffes ausreichend, um den Fruchtansatz der Bäume auf die gewünschten Zielwerte zu reduzieren, während bei niedrigeren Temperaturen dafür häufig weitere Applikationen notwendig sind.

Eine baumangepasste Ausdünnung hat den Vorteil, dass sich dadurch Überdünnung, und damit verbundene Ertragsverluste bei Bäumen mit geringem und mittlerem Blütenansatz, vermeiden lassen. Zudem kann durch eine baumangepasste Ausdünnung die Ertragsleistung aller Bäume optimiert und somit das volle wirtschaftliche Potenzial einer Obstanlage ausgeschöpft werden. Das entwickelte Modell zur Simulation der FBC einzelner Bäume, kann für zukünftige Ausdünnstrategien genutzt werden, um den tatsächlichen Frucht- und Blütenansatz einzelner Bäume zu bewerten und daraus Entscheidungen bei den einzelnen Schritten der Ausdünnung zu treffen. Dazu ist es

erforderlich, baumindividuelle Daten (Blattfläche, Fruchtansatz) in pflanzenphysiologischen und agronomischen Modellen anzuwenden. Die Modelle können potenziell als Algorithmen zur Steuerung von Geräten dienen, die in der Lage sind, Bäume individuell auszdünnen. Eine baumangepasste Ausdünnung würde durch die Berücksichtigung der gewünschten Produktionsziele und der physiologischen Grenzen der einzelnen Bäume die präzise Bewirtschaftung von Apfelplantagen deutlich voranbringen.



*Essentially, all models are wrong, but some are useful.*

George Box

## Acknowledgements

I sincerely thank Dr. rer. hort. habil. Manuela Zude-Sasse for giving me the opportunity to do the research for my PhD thesis in her working group, her support, advice and criticism while conducting this research project and her patience with the drafts of our joint manuscripts.

I also thank Dr. Werner B. Herppich for many fruitful discussions, for introducing me to the field of gas exchange measurements, his inspiration and consistent support with the data analysis and the proof reading of our manuscripts.

Many thanks to Prof. Dr. Alan N. Lakso for inviting me to Cornell University to the workshop on carbon balance modelling, for sharing his experience from over forty years of tree fruit research, his suggestions and critique.

I thank Dr. Nikos Tsoulas for the collaborative work and friendship during the last four years. Our research topics have complemented each other very well and produced exciting results.

I thank Gabriele Wegener, Corinna Rolleczeck, David Sakowsky, Stefan Elwert and Christian Regen for the great teamwork throughout the whole research project. I enjoyed working with you very much.

I would also like to thank Christian Kröling for the cooperation and the countless discussions during the last years.

The dissertation committee - Dr. agr. Martin Geyer, Prof. Dr. agr. Henryk Flachowsky, Prof. Dr.-Ing. Cornelia Weltzien, - I would like to thank for the willingness to evaluate the thesis and for hints and suggestions that improved the quality of this work.

Undine Stark I thank for the proof reading of the dissertation.

Finally, I would like to thank my lovely wife Sofiia Penzel for her patience, her tolerance for spending many weekends with me doing field measurements, her love and permanent support.

## Table of contents

Abstract.....	I
Zusammenfassung.....	IV
Acknowledgements.....	IX
Table of contents .....	X
List of abbreviations .....	XII
List of figures.....	XVII
List of tables.....	XVIII
1. Introduction .....	- 1 -
1.1. Problem statement .....	- 1 -
1.2. State of knowledge.....	- 3 -
1.3. Hypotheses .....	- 14 -
1.4. Structure of the cumulative dissertation.....	- 14 -
1.5. References .....	- 17 -
2. Thinning efficacy of metamitron on young 'RoHo 3615' apple .....	- 31 -
3. Tree adapted mechanical flower thinning on apple prevents yield losses caused by over-thinning of trees with low flower set.....	- 38 -
4. Carbon consumption of developing fruit and individual tree's fruit bearing capacity of RoHo 3615 and Pinova apple .....	- 50 -
5. Modeling of individual fruit-bearing capacity of trees is aimed at optimizing fruit quality of Malus x domestica Borkh. 'Gala'.....	- 69 -
6. Discussion.....	- 89 -
6.1. Summary and hypotheses.....	- 89 -

6.2. A concept for variable rate management of crop load .....	- 92 -
6.3. Perspective for sensor application and the concept of the fruit bearing capacity into applied thinning trials .....	- 97 -
6.4. Conclusion.....	- 98 -
6.5. References .....	- 99 -
Eidesstattliche Erklärung.....	- 106 -
Lebenslauf .....	- 107 -

## List of abbreviations

Abbreviation	Description
$\Delta w$	leaf-to-air partial pressure deficit for water vapour
6-BA	6-Benzylaminopurine
ANOVA	analysis of variance
ATP	adenosine triphosphate
AV	aerial vehicles
BBCH	scale for phenological development stages of plants
BRF	basic rotational frequency
CLM	crop load management
CV	coefficient of variation
DOY	day of the year
EIP	European Innovation Partnership
$F_1$	accuracy of a segmentation
FAO	Food and Agriculture Organization of the United Nations
FDC	fully developed canopy
GV	ground vehicles
HI	harvest Index
IEEE	Institute of Electrical and Electronics Engineers
INRAE	Institut national de la recherche agronomique
LA:F	leaf area to fruit ratio
Lat	latitude
LiDAR	light detection and ranging
M.9/M.26	denominations of apple rootstocks
MY	marketable yield
NDVI	normalized difference vegetation index
PSI/PSII	photosystem I, II
PT	production target
$R/R^2$	correlation coefficient/coefficient of determination
RGB sensor	colour light sensor (Red/Green/Blue )
RH	relative humidity
RMSE/RRMSE	root mean squared error/relative root mean squared error

Abbreviation	Description
RTK- GPS	real time kinematic global positioning system
RTK-GNSS	real time kinematic global navigation satellite system
SWC	soil water content
$T_{\text{soil}}$	mean soil temperature
UAV	unmanned aerial vehicle
VPD	vapour pressure deficit
VR	variable rate
VRA	variable rate application
$V_{\text{wind}}$	wind speed

Symbol	Description	Unit
$AGR_C$	absolute growth rate in C content	$\text{g d}^{-1}$
$AGR_{FM}$	absolute growth rate in fruit diameter	$\text{g d}^{-1}$
$C_{\text{daily}}$	daily C requirements per fruit	$\text{g d}^{-1}$
$C_{\text{fruit}}$	absolute C content per fruit	g
CL	crop load	fruit tree <sup>-1</sup>
$C_{\text{part}}$	fraction of the assimilated carbohydrates partitioned to fruit	[0-1]
$C_{\text{rel}}$	fraction of elemental C	[0-1]
D	fruit diameter	mm
d	diameter of the inner tube a rotating spindle	m
DABB	days after bud break	d
DAFB	days after full bloom	d
DL	day length	s
$DM_{\text{rel}}$	fraction of dry mass on fresh mass	[0-1]
Eff	thinning efficacy	%
$E_{\text{kin}}$	kinetic energy that one string transfers into the canopy	J
f	the light distribution factor between PS I and PS II	[0-1]
FBC	fruit bearing capacity	fruit tree <sup>-1</sup>
FC	flower clusters per tree	flower cluster tree <sup>-1</sup>
$FC_{\text{yr}+1}$	flower clusters per tree in the subsequent year	flower cluster tree <sup>-1</sup>

Symbol	description	unit
FFS	final fruit set	fruit 100 flowers <sup>-1</sup>
FM	fruit fresh mass	g
$F_m'$	maximum fluorescence signal obtained after a saturating light pulse	-
$F_{max}$	maximum fraction of total radiation incident to the canopy	[0-1]
FS	fruit set	fruit cluster <sup>-1</sup>
$F_t$	terminal steady state fluorescence signal at ambient light conditions	-
$G_{allotted}$	area covered by the tree's canopies	m <sup>2</sup>
$GDD_{TB}$	growing degree days with base temperature $T_B$	-
$GDH_{TB}$	growing degree hours with base temperature $T_B$	-
HTF	Hand-thinned fruit per tree	fruit tree <sup>-1</sup>
$J_F$	rates of photosynthetic electron transport through PSII	$\mu\text{mol m}^{-2} \text{s}^{-1}$
$J_{F, RD}$	average reduction in $J_F$	%
k	canopy light extinction coefficient	-
LA	Leaf area	cm <sup>2</sup> ; m <sup>2</sup>
$L_a$	fraction of photons absorbed by leaves	[0-1]
$LA_{demand}$	required leaf area to assimilate $C_{daily}$	cm <sup>2</sup>
$LAI_{orchard}$	leaf area index of the orchard	m <sup>2</sup> m <sup>-2</sup>
$LA_{lab}$	manually measured leaf area per tree	m <sup>2</sup>
$LA_{LIDAR}$	total leaf area per tree estimated with a regression model of PPT	m <sup>2</sup>
$LA_{tree}$	whole leaf area of a tree	m <sup>2</sup>
LI	light Interception	[0-1]
$LI_{max}$	maximum fraction of total radiation incident to the canopy	[0-1]
$m^1$	mass at the middle of a rotating plastic string	kg
$max J_{CO_2}$	light saturated net CO <sub>2</sub> gas exchange rate	$\mu\text{mol m}^{-2} \text{s}^{-1}$ ; g m <sup>-2</sup> s <sup>-1</sup>
$max \alpha$	maximum quantum efficiency of leaf photosynthesis	mol mol <sup>-1</sup> ; $\mu\text{g J}^{-1}$
n	rotational frequency of a rotating spindle	rad s <sup>-1</sup>

Symbol	Description	Unit
PAR	photosynthetic active radiation	$\mu\text{mol m}^{-2} \text{s}^{-1}$ ; $\text{W m}^{-2}$
$P_{\text{daily}}$	the daily assimilated C per unit ground area	$\text{g m}^{-2} \text{d}^{-1}$
PPFR	photosynthetic photon flux rates	$\mu\text{mol m}^{-2} \text{s}^{-1}$
PPT	LiDAR points per tree	-
$P_T$	temperature dependant fractional reduction in $\text{max } J_{\text{CO}_2}$	[0-1]
$P_{\text{tree}}$	daily assimilated C per tree	$\text{g d}^{-1}$
$Q_{10}$	coefficient of the temperature impact on fruit respiration	-
$R_{\text{C}_{\text{daily}}}/R_{\text{daily}}$	daily respired C per fruit	$\text{g d}^{-1}$
$R_{\text{dT}}$	temperature-dependant fruit dark respiration rate	$\text{mg kg}^{-1} \text{h}^{-1}$
$R_{\text{field}}/R_{\text{d,field}}$	estimated fruit respiration rate in the field	$\text{mg kg}^{-1} \text{h}^{-1}$
rpm	revolutions per minute	-
S	daily integral of solar radiation	$\text{MJ m}^{-2} \text{d}^{-1}$
$S_a$	ambient solar radiation	$\text{W m}^{-2}$
SSC	soluble solids content	%
TAPE	total absorbed photosynthetic energy	MJ
$T_B$	base temperature	$^{\circ}\text{C}$
$T_H$	measured hourly temperature	$^{\circ}\text{C}$
$t_{\text{HT}}$	required time to hand thin one hectare of orchard	h
$T_{\text{leaf}}$	leaf temperature	$^{\circ}\text{C}$
$T_{\text{mean,day}}$	mean temperature of the daily hours with $S>0$	$^{\circ}\text{C}$
$T_{\text{min}}/T_{\text{mean}}/T_{\text{Max}}$	daily minimum, mean or maximum air temperature in 2m height	$^{\circ}\text{C}$
$T_U$	optimum temperature for growth	$^{\circ}\text{C}$
u	circumferential speed of a rotating plastic string	$\text{m s}^{-1}$
$u_x$	vector component of $w_x$ in direction x	$\text{m s}^{-1}$
$u_y$	vector component of $w_x$ in direction x	$\text{m s}^{-1}$
v	speed of the tractor	$\text{m s}^{-1}$
$v_x$	vector component of $w_x$ in direction x	$\text{m s}^{-1}$
$v_y$	vector component of $w_y$ in direction y	$\text{m s}^{-1}$
w	speed at the middle of a rotating plastic string	$\text{m s}^{-1}$
$w_x$	translational movement in direction x	$\text{m s}^{-1}$



Symbol	Description	Unit
$w_y$	rotary movement in direction y	$\text{m s}^{-1}$
Y	yield	kg
$\alpha$	angle which is formed by $w_x$ and $w_y$	rad
$\phi_{\text{PSII}}$	actual quantum yield of linear electron transport through PSII	[0-1]

**List of figures**

**Figure 1-1:** Total apple production (grey bar) and average yield per hectare (diamond) of the 15 countries with the world's highest apple production (2017-2019). (FAOSTAT; access 20. January 2021). .....4

**Figure 6-1:** Integration of the fruit bearing capacity into a concept for precise crop load management of apple according to the phenological stages (BBCH codes, Meier et al., 2009) and required input variables for management decisions. ....114

**List of tables**

**Table 1-1:** Carbon balance models for fruit trees and vines and the utilised approach for scaling up individual leaf’s photosynthetic capacity to the whole canopy. ....10

**Table 1-2:** Application of optical sensors for georeferenced mapping of tree parameters in orchards. ....13

# **1. Introduction**

## **1.1. Problem statement**

It is forecasted that the world population will increase from currently 7.7 billion (2019) to 9.7 billion people within the next thirty years (United Nations, 2019). To meet the food demand of the growing population, an increase in the overall productivity of current food production systems on arable land by approximately 25% - 70% from recent levels is required (Hunter et al., 2017). Fruit crops, including apple, contribute to the world's food supply as an important source of fibre, phytochemicals, minerals, and vitamins (Feliciano et al., 2010; Vincente et al., 2014; Yahia et al., 2019). Therefore, the desired increase in overall production also includes fruit crops. Currently, 30 % - 50% (1.2 - 2 billion tons annually) of all food produced worldwide is lost along the value chain (field, grading, storage, packing, retail, consumer) and therefore, not consumed (Porat et al., 2018). In apples, both field and grading losses were reported to range between 5 % - 25 % of all the fruit produced (Porat et al., 2018). Avoiding field and grading losses, e.g. through optimised pre-harvest management and associated increase in overall fruit quality, can also reduce losses in subsequent steps of the value chain. Consequently, optimised pre-harvest management of fruit crops leads to higher yields, contributing to the food security of the growing world population.

Furthermore, there is a need for a transition in the current agricultural management practices towards more sustainable food production systems, in order to maintain arable land in a good agricultural condition and to minimise the environmental impact of land use. For these reasons, key objectives of the European Union's Farm to Fork strategy, in order to implement the goals of the European Green Deal, are, to significantly reduce the use of agrochemicals in crop production and the occurrence of food losses along the value chain (Guyomard and Bureau et al., 2020). This coincides with consumers' demand for more sustainable produced food, often referring to environmental sustainability indicators. From a fruit grower's perspective, economic and social sustainability indicators are additionally relevant.

Another challenge that farmers are facing is the structural change in the agricultural sector, including horticulture (Garming et al., 2018), seen in the decreasing numbers of farms and increasing average size of the farms (Neuenfeldt et al., 2018). One important driver of the structural changes in the fruit production sector is the increase in production costs, due to the annual increasing minimum salary (Garming, 2016) and the relatively high demand of

manual labour. However, despite minimum salary, the general availability of human labour in the agricultural sector is predicted to decrease (Schuh et al., 2019).

Means of mechanisation and automation in the production process of fruit crops have the potential to increase the precision of orchard management tasks, reduce the amount of agrochemicals applied and to balance labour scarcity. For this purpose, all regular management practices need to be re-examined to evaluate the potential of mechanisation and further automation. In the past two decades, various approaches for mapping of geometrical and structural canopy parameters of tree fruit crops have been developed (Colaço et al., 2018; Huang et al., 2020), as well as actuators and robotic end-effectors (Verbiest et al., 2020) to perform individual management tasks adapted to the tree's canopy. However, up to date, no fully automated and cost-efficient solutions to replace human labour are available in pome fruit production (Verbiest et al., 2020). One reason is the lack of plant physiological models and agronomic models to simulate the plants response to varying treatments on spatio-temporal scales. The current state of the art in decision making in orchard management is based on the subjective evaluation of single plants extrapolated to whole orchards. Consequently, models would be necessary to optimise the available prototypes of actuators and robotic end effectors to the conditions of commercial orchards and for precise decision making beyond the subjective evaluation of single trees. That is especially true for crop load management of apples, which despite decades of intensive research (Dennis, 2000; Costa et al., 2018), is mostly performed chemically with unpredictable responses. In addition, crop load management lacks precise metrics, which would be necessary to reduce field and storage losses of fruit, allow annual bearing, and optimise the amount of fruit per tree of a desired quality.

To meet current and future challenges, dramatic changes of current fruit production systems are required. Additionally, farm machinery equipped with plant sensors need to be developed, which has the ability to treat trees or groups of trees individually. Such machinery may reduce variability in fruit quality, yield losses in the field, and bearing habits among individual apple trees within an orchard. To provide decision support in crop load management of individual trees, a key objective is the development of reliable plant physiological and agronomic models, serving as algorithms for new machinery, which in turn enables sustainable intensification by achieving high yields of high quality fruit annually with low inter-tree and intra-tree variability in fruit quality.

## 1.2. State of knowledge

Apple (*Malus x domestica* BORKH.) is the world's most produced temperate tree fruit crop and the second most produced fruit crop in Europe, covering more than 0.5 % of the total arable land in Europe (2019; FAO, 2021). China is the world's leading apple producing country in terms of quantity, contributing 49 % to the world's apple production (2019), whereas Germany is ranked 14th based on its production volume when compared to all other (2017-2019; Fig. 1-1) apple producing countries. The comparison between countries in terms of annual production volume and productivity (Fig. 1-1) reveals a large difference in the average production per hectare. The reasons for these differences are the diverse climate conditions (Lakso et al., 2001), growing systems (Robinson et al., 1991), and intensities of production. It is acknowledged that the average yield per hectare is calculated by dividing the total production volume of a country by the total orchard surface, taking into consideration bearing and non-bearing orchards and orchards with varying degree of production intensity. Thus, the average yield per hectare may differ considerably from the yield potential of several orchard types in use. The world's most productive orchards are located in New Zealand due to the beneficial climate there (Lakso et al., 2001, Palmer et al., 2002). In New Zealand, annual yields above 100 t ha<sup>-1</sup> (Breen et al., 2021) can be achieved in commercial orchards, significantly exceeding the yields of the most productive German orchards of 80 t ha<sup>-1</sup>.

In the commercial production of apple, the management of the tree's crop load is of outstanding importance. The crop load affects the harvest index (Glenn, 2016), growth potential of vegetative tree organs (Reyes et al., 2016; Liang et al., 2020), cortical cell number (Lakso et al., 1995) and cell size (Link, 2000) of fruit, formation of most fruit's quality properties (Serra et al., 2016; Lakso and Goffinet, 2017), and the resulting crop value (Robinson et al., 2017). The development of the fruit coincides with the development of the flowers for the following year. Therefore, the crop load also affects flower induction (Kofler et al., 2019) and flower morphology (Buszard and Schwabe, 1995). Moreover, the crop load affects the requirements for carbohydrates (Lakso, 2011), water (Suo et al., 2016) and nutrients of the whole tree which, when the supply is limited, determines the physiological conditions of the tree, e.g. the gas exchange of the leaves (Wünsche et al., 2000), stem water potential (Naschitz and Naor, 2005; Sadras and Trentacoste, 2011; Neilsen et al., 2016) and content of mineral nutrients in the leaves (Neilsen et al., 2015). Naturally, the trees set more fruit than is commercially desirable, which can lead to low fruit quality and poor flower initiation. Therefore, crop load management practices, which reduce the number of fruit per tree to desired levels, are often considered the most

important management practices in apple production to ensure that trees annually bear high quality fruit (Link, 2000; Yuan and Greene, 2000; Kon and Schupp, 2019).

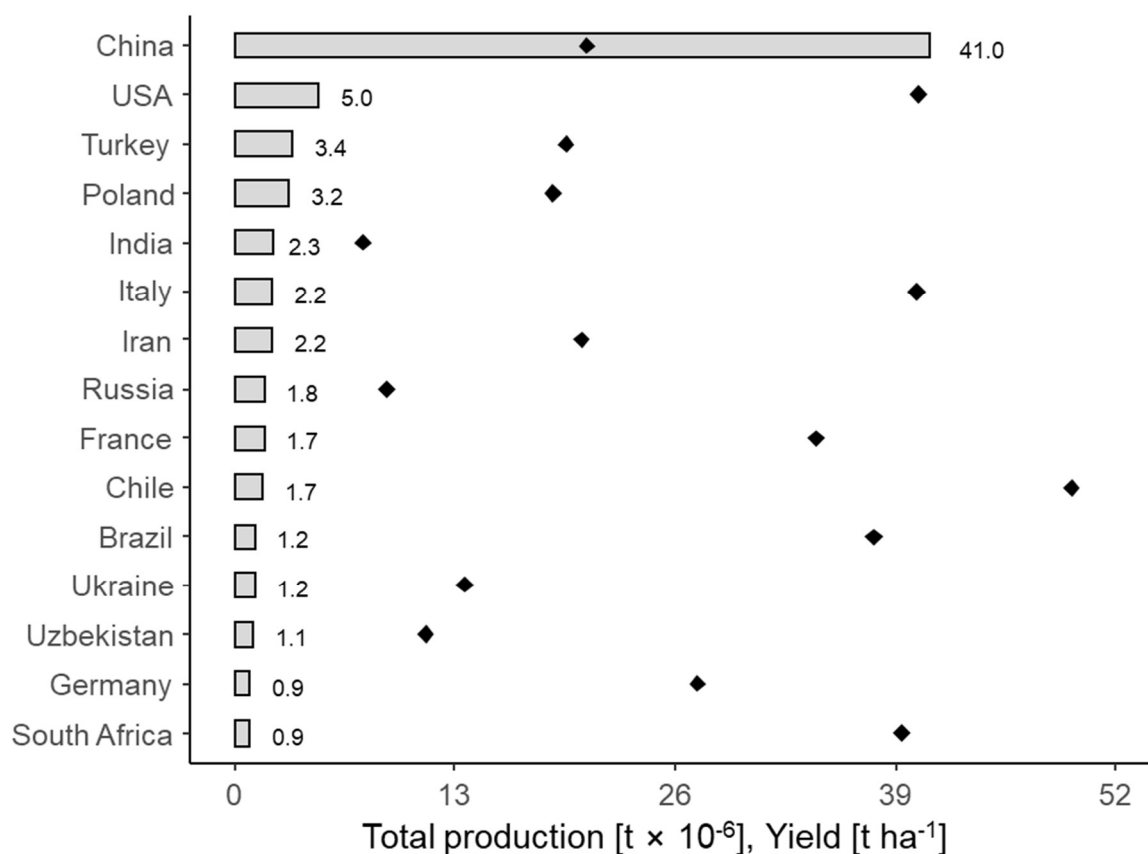


**Figure 1-1**

Total apple production (grey bar) and average yield per hectare (diamond) of the 15 countries with the world's highest apple production (2017-2019). (FAOSTAT; access 20. January 2021).

Variability in flower set (Liakos et al., 2017; Penzel et al., 2020c) and fruit set (Manfrini et al., 2020) among trees or even regions within the same tree canopy frequently occurs. Furthermore, canopy parameters such as leaf area index, canopy light extinction coefficient (Poblete-Echeverría et al., 2015; Sanz et al., 2018), and tree height (Hobart et al., 2020) appear to vary among trees within the same orchards. This indicates variability between the trees in their photosynthetic capacity, which is determined by the total leaf area and associated light interception of a tree (Palmer et al., 2002). Consequently, the trees have variable amounts of fruit and different capacities to produce fruit of a targeted quality, which both need to be considered when managing the tree's crop load.

Traditionally, crop load management practices have consisted of manual removal of surplus fruit and regular pruning of the trees, which removes surplus flower buds and

allows sunlight to penetrate various layers of the canopy and illuminate the leaves and fruit. Both practices were already known in ancient times (Theophrastus, 371 BC - 287 BC; Palladius, 4<sup>th</sup>-5<sup>th</sup> century A.D). In one of his six books on crops, *De Causis Plantarum*, Theophrastus discussed the question:

*[...] why do wild trees, though stronger than the cultivated, fail to ripen their fruit?*

In his answer, he mentioned the effect of crop load on fruit maturity, which is delayed at high levels of crop load (Volz et al., 1993), and the practice of reducing heavy crop loads:

*One cause is the abundance of their fruit. For the superior strength of wild trees is more than offset by their superabundance of fruit; and along with a heavy yield goes a failure to concoct it all, which is why growers remove some fruiting parts when there are too many of them.*

Later, Palladius explained in one of his fourteen books on agriculture, basic cultivation practices of several crops, including apple, and the practice of thinning of surplus fruit:

*If a thick crop loads the tree, all the faulty fruit is to be gathered, that there may be a sufficient supply of juice for the rest, and that the tree may administer abundance of it to the generous fruit, which too large crop rendered of little use.*

Until the 20<sup>th</sup> century, hand thinning and pruning were the main management practices to reduce the crop load of apple trees (Dennis, 2000). During the 20<sup>th</sup> century, when human labour became more expensive or unavailable, chemical and automated mechanical crop load management practices for flower and fruit thinning were developed and integrated into the production process of apples (Dennis, 2000). The mode of action of thinning agents for flower thinning relies on damaging floral tissues and the inhibition of pollen tube growth (Kon and Schupp, 2019). In addition, chemical fruit thinning agents can activate the fruit's abscission zone by means of disturbance of the internal balance of plant hormone streams or by restricting the growing fruitlets' carbon supply below the carbon demand (Bangerth, 2000). Mechanical thinning is mainly performed on flowers by using rotating spindles with attached plastic strings to remove surplus flowers (Kon and Schupp, 2019). Recently, two novel devices have been developed that may enable mechanical fruitlet thinning of apple (Assirelli et al., 2018; Roche, 2020). The principles of chemical and mechanical thinning are further described in Chpts. 2 and 3. Although already implemented into the production process for many years, fruit set response to thinning treatments is highly variable up to date (Jones et al., 2000; Robinson and Lakso, 2004; Lordan et al., 2020), limiting the possibility to reach precise production targets. For a better understanding of the thinning process, physiological and decision support models were



developed in order to integrate several interacting orchard and environmental factors. The models aimed at predicting the timing (Yoder et al., 2013; Peck and Olmstead; 2018), the required frequency of thinning treatments and the fruit set response to thinning treatments (Greene et al., 2013; Robinson et al., 2017; Lordan et al., 2018, 2020). The main interacting factors determining fruit set response to chemical thinning treatments on apple are temperature and solar radiation in the periods before and after the thinning treatment (Greene, 2002; Stover and Greene, 2005) as well as during the early development of the tree's canopy (Lordan et al., 2019). However, thirty factors of the current and the previous year's tree condition and seasonal climate have been described to date that may influence fruit set response to thinning treatments (Costa et al., 2018).

Precise crop load management requires a production target in order to optimise the fruit diameter at harvest and the associated crop value (Robinson et al., 2017) as well as return bloom in the subsequent year (Handsack and Schmidt, 1990; Pellerin et al., 2011). For this purpose, the relationships between harvest fruit diameter, yield, crop load, and flower set in the subsequent year have been intensively studied since the early 20<sup>th</sup> century (Magness et al., 1931; Forshey and Elfving, 1977; Handsack and Schmidt, 1990; Lescourret and Génard, 2003). The negative correlations between fruit per tree and fruit diameter (Iwanami et al., 2018) and fruit per tree and flower set in the subsequent year (Serra et al., 2016) were frequently reported. Consequently, crop load management decisions directly affect the productivity and economic sustainability of an orchard in the year applied and the subsequent year. Decision support in crop load management practices rely on these relationships (Thiele and Zhang, 1992; Hester and Cacho, 2003). However, few metrics are available to estimate production targets for individual trees, either expressed relative to the leaf area per tree (Magness et al., 1931; Preston, 1954), the canopy surface area (Winter, 1976), the trunk cross sectional area (Iwanami et al., 2018) or the branch cross sectional areas of the main branches (Breen et al., 2016). Currently, tree-specific production targets, e.g. to respond to spatial variability in bud numbers per tree, flower and fruit set, can only be addressed with manual crop load management practices such as artificial bud or spur extinction or hand thinning (Breen et al., 2016; Bound, 2019). For chemical and mechanical thinning of blossoms and fruitlets or fruit, tractor speed is the sole option to respond to trees or groups of trees individually. Lack of methods for tree-adapted crop load management can lead to non-optimal numbers of fruit per tree and can, therefore, be seen as a source for heterogeneity in fruit quality, field losses, as well as irregular bearing. In order to adapt mechanical or chemical thinning treatments to the conditions of individual trees or groups of trees, a control system is

required, which integrates sensors to map the trees condition, a control algorithm calculating the required thinning intensity based on the sensor input, and an actuator/robotic end-effector system to adapt the thinning intensity accordingly. Possible systems for tree-adapted mechanical flower thinning of fruit trees were proposed (Wouters, 2014; Lyons et al., 2015; Pflanz et al., 2016). All systems consist of a vision system to map individual trees, or regions within the tree and an algorithm to process the mapped data into the required thinning intensity. This intensity is then translated into an electrical signal controlling the actuator/end-effector, which then convert the electrical signal into mechanical movements (Lyons et al., 2015: Rotating brushes; Pflanz et al., 2016: a rotating spindle) or in case of Wouters (2014), the compressed air supply to nozzles targeting flower buds. Prototypes of all systems were developed, but these have not been commercialised to date (Verbiest et al., 2020). This is, beside economic considerations, due to the lack of suitable models to evaluate a tree's capacity to bear fruit of a targeted harvest fruit quality, often referred to as the fruit bearing capacity, on which an approach of site-specific management can potentially be based.

The mentioned metrics to estimate a target fruit number per tree do not consider the regional seasonal climate and the photosynthetic capacity of a tree. This, however, would be required not only for estimating each tree's fruit bearing capacity, but also to compare it to the actual number of fruit per tree for precise decision making. The resulting management in variable rates would be performed several times after re-evaluation of the actual fruit set until the production target is achieved, analogue to a closed loop control system. A tree's photosynthetic capacity is generally related to light interception (Montheith, 1977; Lakso, 1994; Wünsche et al., 1996; Palmer et al., 2002) of the exposed foliage, which has previously been proven in frequent spacing trials (Verheij and Verwer, 1973; Palmer, 1988; Palmer et al., 1992; Wagenmakers and Callesen, 1995). Most growing systems for apple rely on dwarfing rootstocks such as M.9 or M.26, enabling high-density plantings, early filling of the allotted orchard space per tree, and thus early fruit bearing (Robinson, 2011). In Europe, apple orchards are often planted at 3.5 m × 1.0 m distance, achieving light interception up to 60 % of the incident light. Higher light interception at the same planting system can lead to self-shading of the trees, reduced yield (Wünsche and Lakso, 2000) and fruit quality. Light interception up to 80 % is, however, possible in new two-dimensional growing systems (Breen et al., 2021) with optimised tall, narrow tree architecture, and uniform light distribution giving reduced amount of unproductive leaf area.

A modelling approach for estimating the light interception of orchards was developed (Palmer, 1977; Jackson and Palmer, 1980; Jackson, 1981) and is still frequently used, i.e. in carbon balance models (Tab. 1-1) for scaling up individual leaves' photosynthetic variables to the whole canopy scale (Lakso and Johnson, 1990). With carbon balance models the performance of the orchard system can be simulated to further optimise the planting distance and tree architecture or to estimate the tree's response to climate conditions, crop load, and management practices (Wagenmakers, 1996; Lakso et al., 2001; Pallas et al., 2016). For fruit trees and vines, several carbon balance models were developed (Tab. 1-1) with varying degree of complexity.

The models often consider trees or vines as a collection of semiautonomous organs (DeJong, 2019), where each organ has a genetically determined, organ-specific development pattern and growth potential (Reyes et al., 2016) which is achieved according to the individual carbon supply conditions. The proposed models often consist of several sub-models for the individual tree organs, e.g. fruit, leaves, shoots, roots, or wood (Fishman and Génard, 1998; Lakso and Johnson, 1990; Lakso et al., 2001; Reyes et al., 2020). The carbon supply conditions of each organ are determined by the whole canopy carbon assimilation and partitioning patterns according to the individual organ's relative sink strength for carbohydrates (Cannell, 1985; Buwalda, 1991), hierarchy in carbon partitioning among the tree organs (e.g. shoots>>fruit>roots=wood; Lakso et al., 2001) and, in some models (e.g. Allen et al., 2005; Lescourret et al., 2011; Pallas et al., 2016; Reyes et al., 2020), the proximity of each organ to the carbon source organs. The hierarchy in carbon partitioning among the different organs is especially relevant to simulate carbon source limited conditions (Bepete and Lakso, 1998).

The models often start at bud break (Tab. 1-1). Later starting dates, e.g. full bloom in apples or veraison in grapes, are possible when the initial conditions (e.g. number and size; Tab. 1-1) of the tree organs are set. The photosynthesis of single leaves was scaled up to the whole canopy scale through different approaches (Tab.1-1). The simplest approach is to consider the foliage of the trees as one big leaf, which receives the average irradiance of the canopy (De Pury and Farquhar, 1997). This approach may lead to overestimation of the photosynthetic capacity of a tree, because the light environments within a tree's canopy can be highly variable (Zhang et al., 2016). The photosynthesis of exposed leaves and leaves in sun flecks is mostly light saturated, whereas the photosynthetic response of shaded leaves to irradiance is linear (De Pury and Farquhar, 1997). However, Charles-Edwards (1982) demonstrated the validity of the big-leaf approach for hedgerow apple orchards. Nevertheless, the accuracy of big leaf models may

be increased by considering the sunlit and shaded fraction of the canopy leaf area individually. Models which consider canopy layers, branches, or leaves individually (De Pury and Farquhar, 1997) are most precise. The high level of complexity, however, requires a high computing capacity because the computing time increases with the amount of calculations (Reyes et al., 2020). The application of the models to a high quantity of trees is, therefore, a trade-off between computing capacity, computing time, and accuracy. Depending on the goals of the modelling, the optimal trade-off between simplicity and accuracy/complexity may vary.

Of the mentioned models (Tab. 1-1), the MaluSim model is already being used as an online real-time tool for decision support to forecast the optimum application dates and rates for fruit thinning agents based on overall source-sink balances as affected by weather conditions (Robinson et al., 2017). Furthermore, the model was used to partially explain variations in fruit set responses to thinning treatments (Lordan et al., 2019) and organ growth response to seasonal climate (Lakso and Johnson, 1990; Lakso et al., 2001). The model was developed by Alan N. Lakso at Cornell University (Lakso and Johnson, 1990) in 1990 and continuously advanced since then. The sub-models (leaf area development, canopy net photosynthesis, fruit growth and abscission, carbon partitioning) simulate the growth and respiration of shoots, the associated leaf area development, and the seasonal growth and respiration of other organs (i.e. wood, roots, wood, fruit) as responses to the daily climate conditions.

In comparison to other carbon balance models of fruit crops (Tab. 1-1) the MaluSim model has the highest degree of simplicity, because the big-leaf approach is also applied to the other tree organs (fruit, shoots, spurs, wood, roots) and the time interval is "days" to avoid the complexities of modelling the dynamics of diurnal light availability and distribution in the canopy. Consequently, the model can't simulate distributions in organ size (e.g. fruit size distribution at harvest), which other models (e.g. Pallas et al., 2016; Rahmati et al., 2018; Reyes et al., 2020) are capable of. The more complex models developed by scientists of INRAE in France, i.e. Evelyne Costes, Michel Génard, Françoise Lescourret and co-workers, further consider architectural traits of the trees, which enables the extension of the models to include different growing systems. Furthermore, the models can simulate the seasonal development and distribution in quality parameters among individual fruit (Lescourret et al., 2011; fruit dry mass, fresh mass, sugar contents).

**Table 1-1**

Carbon balance models for fruit trees and vines and the utilised approach for scaling up individual leaf's photosynthetic capacity to the whole canopy.

Author	Crop	Scaling up leaf photosynthesis to the whole canopy	Input parameters <sup>1</sup>		Time steps
			Tree description	Climate	
Lakso and Johnson, 1990; Lakso et al., 2006; Lordan et al., 2019	apple	big leaf	spacing, wood surface area, $F_{\max}$ , k, no. of shoots/spurs, flowers	date of bud break, Lat, PAR, $T_{\min}$ , $T_{\max}$ , DL	days
Pallas et al, 2016	apple	individual shoot	tree organ (e.g. shoots, trunk, branches) dimensions, coordinates at full bloom	$T_{\text{mean}}$ , PAR	days
Reyes et al., 2020	apple	individual leaf	$LA_{\text{tree}}$ , initial cumulative fruit fresh mass, tree organ (e.g. shoots, trunk, branches) dimensions	DOY, hour, PAR, $T_{\text{soil}}$ , $T_{\text{mean}}$ , $V_{\text{wind}}$	hours, days
Lakso, 2006; Poni et al., 2006; Mirás-Avalos et al., 2018	grape	big leaf	spacing, no. of shoots/clusters per shoot/berries per cluster, light interception, k, $J_{\text{CO}_2}^{\max}$	date of bud break, Lat, PAR, $T_{\text{mean}}$	days
Zhu et al., 2019	grape	individual leaf	spacing, organ (root, wood, cordon, fruit) fresh mass, no. of cordons per vine, shoots per cordon, leaves per plant (at veraison)	Lat, PAR, $T_{\text{mean}}$ , RH, SWC	hours
Buwalda, 1991	kiwi	multi canopy layers	C content of vine organs (stem, structural roots, fine roots), no. of buds, fruit	date of budbreak, PAR, $T_{\text{mean}}$	days
Cieslak et al., 2011	kiwi	individual leaf	initial condition of vine organs (e.g. trunk, leaders), no. of canes	PAR	0.1 days
Grossmann and DeJong, 1994	peach	multi canopy layers	initial fresh mass of tree organs (trunk, branches, roots, leaf, fruit), no. of fruit at bloom	PAR, $T_{\min}$ , $T_{\max}$	days
Allen et al., 2005	peach	individual leaf	initial conditions of tree organs (leaves, stem segments, fruit, buds, roots)	date of bud break, SWC, $T_{\text{mean}}$ , PAR	days
Lescourret et al., 2011; Mirás-Avalos et al., 2011; Rahmati et al., 2018	peach	individual shoot	initial conditions of the tree (branch system, no. of leafy shoots, fruit)	RH, PAR, $T_{\text{mean}}$	days

<sup>1)</sup> The table provides a selection of the most important model input parameters, further parameters and constants can be found in the respective reference.

For precise crop load management, a simulation of fruit size distribution at harvest as a response to thinning treatment would be valuable information when targeting the optimization of yield in different fruit quality classes.

All proposed models require complex input data (Tab. 1-1). Extending the model application to the whole orchard scale, which often consists of 2,000-3,000 trees per hectare, would require (1) mapping input parameters for each tree automatically, e.g. by high-throughput phenotyping techniques (Colaço et al., 2018; Coupel-Ledru et al., 2019; Huang et al., 2020) or (2) assuming all trees are the same, an obviously weak assumption if individual tree treatments are desired. Several canopy and architectural traits of the trees can already be mapped and georeferenced with optical sensors with high precision (Tab. 1-2). The sensors can be used on various platforms (Zude-Sasse et al., 2016; Wu et al., 2020), including ground vehicles (GV), aerial vehicles (AV), or satellites.

From a practical point of view, precise crop load management consists of dormant pruning, flower and fruit thinning. For full automation of flower thinning, sensing the number of flower buds or flower clusters per tree is desirable (Pflanz et al., 2016). Knowledge of the number of flower buds or clusters can directly lead to a decision for each tree, e.g. if crop load management is required or not, even when the target number of fruit per tree would assumed to be the same for each tree. It was demonstrated that trees with a low number of flower clusters per tree barely meet the yield potential of the orchards in the respective growing systems (Stopar, 2010; Beber et al., 2016; Penzel et al., 2020c), even without thinning treatment. Consequently, thinning treatments on trees with low flower set can lead to yield losses, which have not yet been quantified. These losses can potentially be avoided by means of variable rate application of thinning treatments, which can distinguish between trees with low flower set and medium or high flower set. Flowers from individual fruit trees were mapped with RGB-sensors mounted on ground vehicles or UAVs (Tab. 1-2). Spatial maps of the number of flower clusters per tree (Vanbrabant et al., 2020) allow management decisions to be made for each tree in a short period of time. To further positively affect fruit size and flower initiation, the subsequent fruit thinning must be performed within three to four weeks post bloom, preferably as early as possible (Lakso and Goffinet, 2017; Belhassine et al., 2019). Management decisions in fruit thinning during this period can be based on the actual flower set or fruit set of the trees relative to the tree's fruit bearing capacity. However, models to precisely evaluate the individual tree's fruit bearing capacity are not yet available. One reason for this is the lack of linkage between existing physiological models and high-throughput sensor data collected from individual trees within an orchard. In order to develop crop load management techniques

which can address trees individual, it is inevitable to develop physiological models to evaluate the fruit bearing capacity of individual trees and agronomic models to evaluate the fruit set of the trees relative to the fruit bearing capacity and derive a management decision out of it. Without such models, the associated application technology capable of treating trees individually would not be operational.

**Table 1-2**

Application of optical sensors for georeferenced mapping of tree parameters in orchards.

Parameter	Crop	Sensor type	Sensor platform	Accuracy (Predicted vs. observed)	Error <sup>1</sup>	Author
flower clusters tree <sup>-1</sup>	pear	RGB-Sensor	UAV	R <sup>2</sup> >0.7	RRMSE<15 %.	Vanbrabant et al., 2020
image pixels belonging to flower clusters	apple	RGB-Sensor	GV	F <sub>1</sub> =85.6%	-	Wang et al., 2020
fruit tree <sup>-1</sup>	apple	RGB-Sensor	UAV	R <sup>2</sup> = 0.8	RMSE=130. 6	Apolo-Apolo et al., 2020
fruit tree <sup>-1</sup>	apple	LiDAR	GV	F <sub>1</sub> =85.8%	-	Gené-Mola et al., 2019
fruit length, width [mm] on tree	mango	RGB-Sensor	GV	R <sup>2</sup> =0.95-0.96	RMSE=4.3-4.9 [mm]	Wang et al., 2017
flowers tree <sup>-1</sup>	almond	RGB-Sensor	UGV	R <sup>2</sup> =0.61	CV=17.9 %	Underwood et al., 2016
canopy volume		LiDAR	UGV	R <sup>2</sup> =0.94-0.99		
canopy volume	apple, grape	LiDAR	GV	R <sup>2</sup> =0.81-0.84	-	Chakraborty et al., 2019
canopy height	apple, grape			R <sup>2</sup> =0.59-0.75	-	
tree row volume, height, leaf area	apple, grape, pear	LiDAR	GV	R <sup>2</sup> =0.84-0.9	-	Sanz et al., 2018
canopy volume, light interception	mango	LiDAR	GV	r=0.8; r=0.89	-	Westling et al., 2020
tree height	apple	LiDAR, RGB-Sensor	GV, AV	R <sup>2</sup> =0.81-0.91	-	Hobart et al., 2020
stem diameter, volume	walnut	LiDAR	AV	R <sup>2</sup> =0.83-0.87	RRMSE=9.4-21.6 [%]	Estornell et al., 2021
canopy height				R <sup>2</sup> =0.69	RRMSE=12.4 %	
light interception	sweet cherry	light sensor bar	GV	-	RE=1.5 -10.3 [%]	Zhang et al., 2015
canopy height, canopy volume	apple	LiDAR	GV	R <sup>2</sup> =0.77-0.87	RRMSE=4.64-5.71 [%]	Tsoulas et al., 2019
stem diameter				R <sup>2</sup> =0.88	RRMSE=2.23 %	

CV: coefficient of variation, F<sub>1</sub>: accuracy of the segmentation, r: correlation coefficient, R<sup>2</sup>: coefficient of determination, RE: relative error, RMSE: root mean squared error, RRMSE: relative root mean squared error



### **1.3. Hypotheses**

Small-scale and large-scale spatial variability of canopy parameters and flower and fruit set is abundant in current apple production systems. Nonetheless, the trees are managed uniformly, which, for crop load management, can be seen as a major cause of inconsistent bearing and inter-tree variability in fruit quality. This variability requires technological solutions to manage individual trees or groups of trees, in order to reduce inter-tree variability in fruit quality within the whole orchard and reduce possible field losses of fruit as consequence to the current uniform crop load management. The overall aim of the study is to consider the variability of tree parameters within orchards utilising individual sensed plant data and seasonal weather data of the orchard. The sensor data serve as input variables into a plant physiological model for the fruit bearing capacity of individual trees, dependant on the desired mean fruit diameter and total leaf area of the tree. The developed model can serve as a part of a control system for variable rate crop load management, targeting individual trees.

In order to quantify differences in fruit bearing capacity of orchards and to develop possible strategies to adapt crop load management to the individual tree level, the following hypotheses were tested:

- 1) The total leaf area, flower and fruit set of apple trees appears variable within commercial apple orchards
- 2) With the modelled fruit bearing capacity the number of fruit per tree can be evaluated in terms of a desired mean fruit diameter
- 3) The average magnitude of fruit quality parameters per tree respond to the number of photons intercepted per fruit during the growing period
- 4) Uniform crop load management leads to yield and fruit quality losses considering individual trees
- 5) Uniform crop load management of apple orchards leads to inaccurate numbers of fruit per tree deviant from the optimum number of fruit per tree defined by the fruit bearing capacity in orchards with inter-tree variability in total leaf area

### **1.4. Structure of the cumulative dissertation**

The thesis starts with an introduction (Chpt. 1) and continues with a series of chapters (Chpts. 2 to 5) which individually have been published by peer reviewed scientific journals. In the final chapter 6 the results and theses are discussed, an overview of the results

obtained is given and an outlook on how crop load management can be improved by using sensor data in physiological models and how this could be implemented in practice.

## **Chapter 1: Introduction**

### **Chapter 2: Thinning efficacy of metamitron on young RoHo 3615 apple.**

In this chapter, a two years experiment was carried out to evaluate the thinning efficacy of a new thinning agent for apples. The chapter gives an introduction into chemical fruit thinning, the inter-year variability in thinning efficacy, and factors which may affect the thinning efficacy of the applied compounds. It was shown that precise applications based to the weather conditions can potentially reduce their required frequency, to successfully reduce the fruit set of apple trees. Furthermore, it was demonstrated, that the labour time required for crop load management, was reduced by chemical thinning treatments in comparison to an untreated control.

The chapter is published in *Scientia Horticulturae* (Penzel and Kröling, 2020). The research was presented as poster presentation at the 4<sup>th</sup> Symposium on Horticulture in Europe in 2021 (Stuttgart, Germany). The research was funded by the Saxon State Office for Environment, Agriculture and Geology.

### **Chapter 3: Tree adapted mechanical flower thinning on apple prevents yield losses caused by over-thinning of trees with low flower set**

Mechanical flower thinning is an environmental friendly thinning technique, showing consistent thinning results independent of weather conditions. In a four years experiment, mechanical thinning treatments were carried out in two orchards with trees heterogeneous in flower set. It was shown that trees can be classified according to their flower set. Trees with low and medium flower set were not able to meet the production target. Consequently, thinning treatment causes yield losses on trees with low and medium flower set, which are avoidable. For better comparison of experiments with different setting of mechanical string thinning devices, an approach was proposed to calculate the kinetic energy that one string transfers to the tree's canopy.

This chapter is published in the *European Journal of Horticultural Science* (Penzel et al., 2021c). The data was, in part, presented as an oral and poster presentation at the XXX. International Horticulture Congress in 2018 (Istanbul, Turkey) at the Symposium: Tree fruit behaviour in dynamic environments (Penzel et al., 2020c). The presentation of the concept of tree-adapted mechanical flower thinning was honoured with the Young Minds Award for the best poster presentation. The research was funded by the German Federal Ministry of

Food and Agriculture and the Landwirtschaftliche Rentenbank, grant number 28-RZ-5IP.013.

#### **Chapter 4: Carbon consumption of developing fruit and individual tree's fruit bearing capacity of RoHo 3615 and Pinova apple**

A method was established to estimate individual trees' total leaf area by means of LiDAR point clouds. The variability in total leaf area per tree was demonstrated in two commercial orchards of different age. Based on the LiDAR estimated total leaf area per tree and measured key carbon related variables of the leaves, the seasonal course of the photosynthetic capacity of the individual trees was calculated. The photosynthetic capacity of the trees showed high seasonal fluctuations as response to temperature and solar radiation as well as variability at the same date among the different trees with varying leaf area. The fruit growth and dark respiration rates were monitored on random fruit and the daily fruit carbon requirement of fruit with varying harvest fruit diameter was quantified. The period of the highest fruit C requirements, which was identical to the periods with the highest growth rates, were identified in order to limit the trees' capacity to produce a certain number of fruit of a mean diameter, which is referred to as the fruit bearing capacity. The fruit bearing capacity was calculated for randomly sampled trees, targeting the measured mean fruit diameter. The results indicated that uniform thinning treatment of trees with variable photosynthetic capacity can lead to sub-optimal numbers of fruit per tree, with either number of fruit per tree below or above the fruit bearing capacity.

This chapter is published in International Agrophysics (Penzel et al., 2020a). The data was presented as an oral presentation at the 1<sup>st</sup> Symposium on Precision Management of Orchards and Vineyards (Palermo, Italy) in 2019 (Penzel et al., 2021b). The research was funded by the Ministry of Agriculture, Environment and Climate Protection of the federal state of Brandenburg and the agricultural European Innovation Partnership (EIP-AGRI), grant number 80168342.

#### **Chapter 5: Modeling of individual fruit-bearing capacity of trees is aimed at optimizing fruit quality of *Malus x domestica* Borkh. 'Gala'**

The fruit bearing capacity to produce fruit of targeted diameters ranging from 65 mm - 80 mm of 996 trees of a commercial orchard for the conditions in two consecutive years was modelled. It was shown that the overall variability in fruit bearing capacity was consistent in both years. However, the spatial distribution of the trees' fruit bearing capacity between both years varied. Consequently, when targeting variable rate application in crop load management according to the trees' fruit bearing capacity, the FBC need to be

mapped annually. The validity of the proposed model in the of two years was demonstrated with the number and average mass of harvested fruit from randomly sampled trees within the same orchard. The mean fruit fresh mass and soluble solids content appeared to correlate to the amount of photons that the tree's canopy had absorbed per fruit during the cell expansion stage of the developing fruit. Additionally, the fresh mass and soluble solids content of individual fruit showed intra-tree variability, which may be reduced with increasing amounts of photons that the tree had absorbed per fruit.

This chapter was submitted to *Frontiers in Plant Science* (Penzel et al., 2021a). The data was presented as oral presentation at the IEEE Workshop on Metrology for Agriculture and Forestry (Trento, Italy) in 2020 (Penzel et al., 2020b). The research was funded by the Ministry of Agriculture, Environment and Climate Protection of the federal state of Brandenburg and the agricultural European Innovation Partnership (EIP-AGRI), grant number 80168342.

## **Chapter 6. Discussion**

### **1.5. References**

Allen, M.T., Prusinkiewicz, P., DeJong, T.M., 2005. Using L-systems for modeling source-sink interactions, architecture and physiology of growing trees: the L-PEACH model. *New Phytol.* 166, 869-880. <https://doi.org/10.1111/j.1469-8137.2005.01348.x>

Apolo-Apolo, O.E., Pérez-Ruiz, M., Martínez-Guanter, J., Valente, J., 2020. A cloud-based environment for generating yield estimation maps from apple orchards using UAV imagery and a deep learning technique. *Front Plant Sci.* 11, 1086. <https://doi.org/10.3389/fpls.2020.01086>.

Assirelli, A., Giovannini, D., Cacchi, M., Sirri, S., Baruzzi, G., Caracciolo, G., 2018. Evaluation of a new machine for flower and fruit thinning in stone fruits. *Sustainability-Basel* 10, 4088. <https://doi.org/10.3390/su10114088>

Bangerth, F., 2000. Abscission and thinning of young fruit and their regulation by plant hormones and bioregulators. *Plant Growth Regul.* 31, 43-49. <https://doi.org/10.1023/A:1006398513703>

Beber, M., Donik Purgaj, B., Veberič, R., 2016. The influence of mechanical thinning on fruit quality and constant bearing of 'Jonagold' apples. *Acta Hortic.* 1139, 513–518. <https://doi.org/10.17660/ActaHortic.2016.1139.88>

- Belhassine, F., Martinez, S., Bluy, S., Fumey, D., Kelner, J.J., Costes, E., Pallas, B., 2019. Impact of within-tree organ distances on floral induction and fruit growth in apple tree: Implication of carbohydrate and gibberellin organ contents. *Front. Plant Sci.* 10, 1233. <https://doi.org/10.3389/fpls.2019.01233>
- Bepete, M., Lakso, A.N., 1998. Differential effects of shade on early season fruit and shoot growth rates in 'Empire' apple branches. *HortScience*, 33, 823-825. <https://doi.org/10.21273/HORTSCI.33.5.823>.
- Bound, S.A., 2019. Precision crop load management of apple (*Malus x domestica* Borkh.) without Chemicals. *Horticulturae* 5, 3. <https://doi.org/10.3390/horticulturae5010003>.
- Breen, K.C., Palmer, J.W., Tustin, D.S., Close, D.C., 2016. Artificial spur extinction alters light interception by 'Royal Gala' apple trees. *Acta Hortic*, 1130, 265–271. <https://doi.org/10.17660/ActaHortic.2016.1130.39>
- Breen, K.C., Tustin, D.S., Van Hooijdonk, B.M., Stanley, C.J., Scofield, C., et al., 2021. Use of physiological principles to guide precision orchard management and facilitate increased yields of premium quality fruit. *Acta Hortic.* (in press)
- Buszard, D., Schwabe, W.W., 1995. Effect of previous crop load on stigmatic morphology of apple flowers. *J. Amer. Soc. Hortic. Sci.* 120, 566-570. <https://doi.org/10.21273/JASHS.120.4.566>
- Buwalda, J.G., 1991. A mathematical model of carbon acquisition and utilisation by kiwifruit vines. *Ecol. Model.* 57, 43-64. [https://doi.org/10.1016/0304-3800\(91\)90054-5](https://doi.org/10.1016/0304-3800(91)90054-5).
- Cannell, M.G.R., 1985. Dry matter partitioning in tree crops. In: Cannell, M.G.R., Jackson, J.E. (Eds), *Attributes of Trees as Crop Plants*. Institute of Terrestrial Ecology, Midlothian, UK
- Chakraborty, M., Khot, L.R., Sankaran S., Jacoby, P.W., 2019. Evaluation of mobile 3D light detection and ranging based canopy mapping system for tree fruit crops. *Comp. Electron. Agric.* 158, 284-293. <https://doi.org/10.1016/j.compag.2019.02.012>.
- Charles-Edwards, D.A., 1982. *Physiological determinants of crop growth*. Academic Press, Sydney
- Cieslak, M., Seleznyova, A. N., Hanan, J., 2011. A functional-structural kiwifruit vine model integrating architecture, carbon dynamics and effects of the environment. *Ann. Bot.-London* 107, 747-764. <https://doi.org/10.1093/aob/mcq180>

- Colaço, A.F., Molin, J.P., Rosell-Polo, J.R., Escolà, A., 2018. Application of light detection and ranging and ultrasonic sensors to high-throughput phenotyping and precision horticulture: current status and challenges. *Hortic. Res.* 5, 35. <https://doi.org/10.1038/s41438-018-0043-0>
- Costa, G., Botton, A., Vizzotto, G., 2018. Fruit thinning: Advances and trends. *Hortic. Rev.* 46, 185-226. <https://doi.org/10.1002/9781119521082.ch4>
- Coupel-Ledru, A., Pallas, B., Delalande, M. et al., 2019. Multi-scale high-throughput phenotyping of apple architectural and functional traits in orchard reveals genotypic variability under contrasted watering regimes. *Hortic. Res.* 6, 52. <https://doi.org/10.1038/s41438-019-0137-3>
- DeJong, T., 2019. Opportunities and challenges in fruit tree and orchard modelling. *Eur. J. Hortic. Sci.* 84, 117-123. <https://doi.org/10.17660/ejhs.2019/84.3.1>
- De Pury, D., Farquhar, G., 1997. Simple scaling of photosynthesis from leaves to canopies without the errors of big-leaf models. *Plant Cell Environ.* 20, 537-557 <https://doi.org/10.1111/j.1365-3040.1997.00094.x>
- Dennis, F.G., 2000. The history of fruit thinning. *Plant Growth Regul.* 31, 1-16. <https://doi.org/10.1023/A:1006330009160>
- Estornell, J., Hadas, E., Martí, J., López-Cortés, I., 2021. Tree extraction and estimation of walnut structure parameters using airborne LiDAR data. *Int. J. Appl. Earth Obs.* 96, 102273. <https://doi.org/10.1016/j.jag.2020.102273>
- FAO, 2021. Faostat database. [www.fao.org](http://www.fao.org), access 20.02.2021
- Feliciano, R.P., Antunes, C., Ramos, A., Serra, A.T., Figueira, M.E., et al., 2010. Characterization of traditional and exotic apple varieties from Portugal. Part 1-Nutritional, phytochemical and sensory evaluation. *J. Funct. Food.* 2, 35-45. <https://doi.org/10.1016/j.jff.2009.12.004>
- Fishman, S., Génard, M., 1998. A biophysical model of fruit growth: simulation of seasonal and diurnal dynamics of mass. *Plant Cell Environ.* 21, 739-752. <https://doi.org/10.1046/j.1365-3040.1998.00322.x>
- Forshey, C.G., Elfving, D.C., 1977. Fruit numbers, fruit size and yield relationships in McIntosh apples. *J. Amer. Soc. Hortic. Sci.* 102, 399-402
- Garming, H., 2016. Auswirkungen des Mindestlohns in Landwirtschaft und Gartenbau: Erfahrungen aus dem ersten Jahr und Ausblick. Thünen Working Paper 53, Johann

Heinrich von Thünen Institut, Braunschweig, Germany, <http://nbn-resolving.de/urn:nbn:de:gbv:253-201603-dn056425-0>

Garming, H., Dirksmeyer, W., Bork, L., 2018. Entwicklungen des Obstbaus in Deutschland von 2005 bis 2017: Obstarten, Anbauregionen, Betriebsstrukturen und Handel. Thünen Working Paper 100, Johann Heinrich von Thünen Institut, Braunschweig, Germany

Gené-Mola, J., Gregorio, E., Guevara, J., Auat, F., Sanz-Cortiella, R., et al., 2019. Fruit detection in an apple orchard using a mobile terrestrial laser scanner. *Biosyst. Eng.* 187, 171-184. <https://doi.org/10.1016/j.biosystemseng.2019.08.017>

Glenn, D. M., 2016. Dry matter partitioning and photosynthetic response to biennial bearing and freeze damage in “Empire” apple. *Sci. Hortic.-Amsterdam* 210, 1-5. [doi:10.1016/j.scienta.2016.06.042](https://doi.org/10.1016/j.scienta.2016.06.042)

Gongal, A., Silwal, A., Amatya, S., Karkee, M., Zhang, Q., Lewis, K., 2016. Apple crop-load estimation with over-the-row machine vision system. *Comp. Electron. Agric.* 120, 26-35. <https://doi.org/10.1016/j.compag.2015.10.022>

Greene, D.W., 2002. Chemicals, timing, and environmental factors involved in thinner efficacy on apple. *HortScience* 37, 477-481. <https://doi.org/10.21273/HORTSCI.37.3.477>

Greene, D.W., Lakso, A.N., Robinson, T.L., Schwallier, P., 2013. Development of a fruitlet growth model to predict thinner response on apples. *HortScience* 48, 584–587. <https://doi.org/10.21273/HORTSCI.48.5.584>

Grossman, Y.L., DeJong, T.M., 1994. PEACH: a simulation model of reproductive and vegetative growth in peach trees. *Tree Physiol.* 14, 329-345. <https://doi.org/10.1093/treephys/14.4.329>

Guyomard, H., Bureau J.-C. et al. (2020), Research for AGRI Committee – The Green Deal and the CAP: policy implications to adapt farming practices and to preserve the EU's natural resources. European Parliament, Policy Department for Structural and Cohesion Policies, Brussels.

Handsack, M., Schmidt, S., 1990. Grafisches Modell zur Beschreibung der Ertragsbildung bei Apfel unter Berücksichtigung von Wechselwirkungen zwischen den Ertragskomponenten. *Arch. Gartenbau* 38, 399-405

Hester, S., Cacho, O., 2003. Modelling apple orchard systems. *Agr. Syst.* 77, 137-154. [https://doi.org/10.1016/S0308-521X\(02\)00106-3](https://doi.org/10.1016/S0308-521X(02)00106-3)

- Hobart, M., Pflanz, M., Weltzien C., Schirrmann, M., 2020. Growth height determination of tree walls for precise monitoring in apple fruit production using UAV photogrammetry. *Remote Sens.-Basel* 12, 1656. <https://doi.org/10.3390/rs12101656>.
- Huang, Y., Ren, Z., Li, D., Liu, X., 2020. Phenotypic techniques and applications in fruit trees: a review. *Plant Methods* 16, 107. <https://doi.org/10.1186/s13007-020-00649-7>
- Hunter, M., Smith, R., Schipanski, M., Atwood, L., Mortensen, D., 2017. Agriculture in 2050: recalibrating targets for sustainable intensification. *BioScience* 67, 385–390. <https://doi.org/10.1093/biosci/bix010>
- Iwanami, H., Moriya-Tanaka, Y., Honda, C., Hanada, T. Wada, M., 2018. A model for representing the relationships among crop load, timing of thinning, flower bud formation, and fruit weight in apples. *Sci. Hortic.-Amsterdam* 242, 181-187. <https://doi.org/10.1016/j.scienta.2018.08.001>.
- Jackson, J.E., Palmer, J.W., 1980. A computer model study of light interception by orchards in relation to mechanised harvesting and management. *Sci. Hortic.-Amsterdam* 13, 1-7. [https://doi.org/10.1016/0304-4238\(80\)90015-1](https://doi.org/10.1016/0304-4238(80)90015-1)
- Jackson, J.E., 1981. Theory of light interception by orchards and a modelling approach to optimiz-ing orchard design. *Acta Hortic.* 114, 69-79 <https://doi.org/10.17660/ActaHortic.1981.114.4>
- Jones, K., Bound, S., Oakford, M., Gillard, P., 2000. Modelling thinning of pome fruits. *Plant Growth Regul.* 31, 75–84. <https://doi.org/10.1023/A:1006315000499>
- Kofler, J., Milyaev, A., Capezzone, F., Stojnić, S., Mičić, N., et al., 2019. High crop load and low temperature delay the onset of bud initiation in apple. *Sci. Rep.* 9, 17986. <https://doi.org/10.1038/s41598-019-54381-x>
- Kon, T.M., Schupp, J.R., 2019. Apple crop load management with special focus on early thinning strategies: a US perspective. *Hortic. Rev.* 46, 255-298. <https://doi.org/10.1002/9781119521082.ch6>
- Lakso, A.N. 1994. Apple. in: Schaffer, B., Andersen, P.C. (Eds), *Environmental physiology of fruit crops*, Vol. 1, Temperate crops, CRC Press, Boca Raton, FL, USA. pp. 3-42.
- Lakso, A.N. 2006. “VitiSim” - A simplified carbon balance model of a grapevine. in: Walker, R.R., (ed.), *Proc. Int. Workshop on carbohydrate dynamics in grapes*, CSIRO Merbein, Vic., Australia. pp. 4-11



- Lakso, A.N., 2011. Early fruit growth and drop: The role of carbon balance in the apple tree, *Acta Hort.* 903, 733-742. <https://doi.org/10.17660/ActaHortic.2011.903.102>
- Lakso, A.N., Goffinet, M.C., 2017. Advances in understanding apple fruit development. in Evans, K. (Ed.), *Achieving sustainable cultivation of apples*, Burleigh Dodds Science Publishing, Cambridge, UK, pp. 103-133
- Lakso, A.N., Johnson, R.S., 1990. A simplified dry matter production model for apple using automatic programming simulation software. *Acta Hortic.* 276, 141-148. <https://doi.org/10.17660/ActaHortic.1990.276.15>.
- Lakso, A.N., White, M.D., Tustin, D.S., 2001. Simulation modeling of the effects of short and long-term climatic variations on carbon balance of apple trees. *Acta Hortic.* 557, 473-480. <https://doi.org/10.17660/ActaHortic.2001.557.63>
- Lakso, A.N., Corelli-Grappadelli, L., Barnard, J., Goffinet, M.C., 1995. An expolinear model of the growth pattern of the apple fruit. *J. Hort. Sci.*, 70, 389-394. <https://doi.org/10.1080/14620316.1995.11515308>
- Lakso, A.N., Greene, D.W., Palmer, J.W., 2006. Improvements on an Apple Carbon Balance Model. *Acta Hortic.* 707, 57-61. <https://doi.org/10.17660/ActaHortic.2006.707.6>
- Lescourret, F., Génard, M., 2003. A multi-level theory of competition for resources applied to fruit production. *Écoscience* 10, 334-341, <https://doi.org/10.1080/11956860.2003.11682782>
- Lescourret, F., Moitrier, N., Valsesia, P., Génard, M., 2011. QualiTree, a virtual fruit tree to study the management of fruit quality. I. Model development. *Trees* 25, 519–530 <https://doi.org/10.1007/s00468-010-0531-9>
- Liang, B., Sun, Y., Li, Z., Zhang, X., Yin, B., Zhou, S., Xu, J., 2020. Crop load influences growth and hormone changes in the roots of “Red Fuji” Apple. *Front. Plant Sci.* 11, 665. <https://doi.org/10.3389/fpls.2020.00665>
- Liakos, V., Tagarakis, A., Aggelopoulou, K., Fountas, S., Nanos, G.D., Gemtos, T., 2017. In-season prediction of yield variability in an apple orchard. *Eur. J. Hortic. Sci.* 82, 251-259 <https://doi.org/10.17660/eJHS.2017/82.5.5>
- Link, H., 2000. Significance of flower and fruit thinning on fruit quality. *Plant Growth Regul.* 31, 17-26. <https://doi.org/10.1023/A:1006334110068>.

- Lyons, D.J., Heinemann, P.H., Schupp, J.R., Baugher T.A., Liu, J., 2015. Development of a selective automated blossom thinning system for peaches. *Trans. ASABE*. 58, 1447-1457. <https://doi.org/10.13031/trans.58.11138>.
- Lordan, J., Alins, G., Àvila, G., Torres, E., Carbó, J., Bonany, J., Alegre, S., 2018. Screening of eco-friendly thinning agents and adjusting mechanical thinning on 'Gala', 'Golden Delicious' and 'Fuji' apple trees. *Sci. Hortic.-Amsterdam* 239, 141-155. <https://doi.org/10.1016/j.scienta.2018.05.027>.
- Lordan, J., Reginato, G.H., Lakso, A.N., Francescatto, P., Robinson, T.L., 2019. Natural fruitlet abscission as related to apple tree carbon balance estimated with the MaluSim model. *Sci. Hortic.-Amsterdam* 247, 296–309. <https://doi.org/10.1016/j.scienta.2018.11.049>.
- Lordan, J., Reginato, G.H., Lakso, A.N., Francescatto, P., Robinson, T.L., 2020. Modelling physiological and environmental factors regulating relative fruit set and final fruit numbers in apple trees. *J. Hortic. Sci. Biotech.* 95, 600-616. <https://doi.org/10.1080/14620316.2020.1718555>
- Magness, J.R., Overley, F.L., Luce, W.A., 1931. Relation of foliage to fruit size and quality in apples and pears. *Wash. State Agric. Exp. Sta. Bull.* 249
- Manfrini, L., Corelli-Grappadelli, L., Morandi, B., Losciale, P., Taylor, J.A., 2020. Innovative approaches to orchard management: assessing the variability in yield and maturity in a 'Gala' apple orchard using a simple management unit modelling approach. *Eur. J. Hortic. Sci.* 85, 211-218. <https://doi.org/10.17660/eJHS.2020/85.4.1>
- Mirás-Avalos, J.M., Egea, G., Nicolas, E., Génard, M., Vercambre, G., et al., 2011. QualiTree, a virtual fruit tree to study the management of fruit quality. II. Parameterisation for peach, analysis of growth-related processes and agronomic scenarios. *Trees* 25, 785-799. <https://doi.org/10.1007/s00468-011-0555-9>
- Mirás-Avalos, J.M., Uriarte, D., Lakso, A.N., Intrigliolo, D.S., 2018. Modeling grapevine performance with "VitiSim", a weather-based carbon balance model: Water status and climate change scenarios. *Sci. Hortic.-Amsterdam* 240, 561–571. <https://doi.org/10.1016/j.scienta.2018.06.065>
- Monteith, J.L., 1977. Climate and the efficiency of crop production in Britain. *Philos. Trans. R. Soc. Lond. Ser. B* 281, 277-294. <https://doi.org/10.1098/rstb.1977.0140>

- Naschitz, S., Naor, A., 2005. The effect of crop load on tree water consumption of 'Golden Delicious' apples in relation to fruit size: an operative model. *J. Amer. Soc. Hortic. Sci.* 130, 7-11. <https://doi.org/10.21273/JASHS.130.1.7>
- Neilsen, G.H., Neilsen, D., Guak, S., Forge, T., 2015. The effect of deficit irrigation and crop load on leaf and fruit nutrition of fertigated 'Ambrosia'/'M.9' apple. *HortScience* 50, 1387-1393. <https://doi.org/10.21273/HORTSCI.50.9.1387>.
- Neilsen, D., Neilsen, G.H., Guak, S., Forge, T., 2016. Consequences of deficit irrigation and crop load reduction on plant water relations, yield and quality of 'Ambrosia' apple. *Hortscience* 51, 98-106. <https://doi.org/10.21273/HORTSCI.51.1.98>
- Neuenfeldt, S., Gocht, A., Heckeley, T., Ciaian, P., 2019. Explaining farm structural change in the European agriculture: a novel analytical framework. *Eur. Rev. Agric. Econ.* 46, 713–768. <https://doi.org/10.1093/erae/jby037>
- Palladius, R.T.Æ., 4<sup>th</sup>-5<sup>th</sup> century A.D. The pear, the apple, the silique, &c. In: The fourteen books of Palladius Rutilius Taurus Æmilianus, on agriculture. Trans. 1807 by Owen, T., Printed for J. White, London, UK. <http://catalog.hathitrust.org/Record/009713447/Home>
- Pallas, B., Da-Silva, D., Valsesia, P., Yang, W., Guillaume, O., et al., 2016. Simulation of carbon allocation and organ growth variability in apple tree by connecting architectural and source-sink models. *Ann. Bot.-London* 118, 317-330. <https://doi.org/10.1093/aob/mcw085>.
- Palmer, J.W., 1977. Diurnal light interception and a computer model of light interception by Hedgerow apple orchards. *J. Appl. Ecol.* 14, 601-614. <https://doi.org/10.2307/2402570>
- Palmer, J.W., 1988. Annual dry matter production and partitioning over the first 5 years of a bed system of Crispin/M. 27 apple trees at four spacings. *J. Appl. Ecol.* 25, 569-578. <https://doi.org/10.2307/2403845>
- Palmer, J.W., Avery, D.J., Wertheim, S.J., 1992. Effect of apple tree spacing and summer pruning on leaf area distribution and light interception. *Sci. Hortic.-Amsterdam* 52, 303-312. [https://doi.org/10.1016/0304-4238\(92\)90031-7](https://doi.org/10.1016/0304-4238(92)90031-7)
- Palmer, J.W., Wünsche, J.N., Meland, M., Hann, A., 2002. Annual dry matter production by three apple cultivars at four within-row spacings in New Zealand. *J. Hortic. Sci. Biotech.* 77, 712-717. <https://doi.org/10.1080/14620316.2002.11511561>
- Peck, G., Olmstead, D. 2018. Implementing the Pollen Tube Growth Model on NEWA. *NY Fruit Quarterly* 26(4), 11-15

- Pellerin, B.P., Buszard, D., Iron, D., Embree, C.G., Marini, R.P., et al., 2011. A theory of blossom thinning to consider maximum annual flower bud numbers on biennial apple trees. *HortScience*, 46, 40-42. <https://doi.org/10.21273/HORTSCI.46.1.40>
- Penzel, M., Kröling, C., 2020. Thinning efficacy of metatriton on young 'RoHo 3615' (Evelina®) apple. *Sci. Hortic.-Amsterdam* 272.  
<https://doi.org/10.1016/j.scienta.2020.109586>
- Penzel, M., Lakso, A.N., Tsoulas, N., Zude-Sasse, M., 2020a. Carbon consumption of developing fruit and individual tree's fruit bearing capacity of RoHo 3615 and Pinova apple. *Int. Agrophys.* 34, 409-423. <https://doi.org/10.31545/intagr/127540>
- Penzel, M., Tsoulas, N., Herppich, W.B., Weltzien, C., Zude-Sasse, M., 2020b. Mapping the fruit bearing capacity in a commercial apple (*Malus x domestica* BORKH.) orchard. *IEEE Int. Worksh. Metrol. Agric. Forest.* 283-287.  
<https://doi.org/10.1109/MetroAgriFor50201.2020.9277563>
- Penzel, M., Pflanz, M., Gebbers, R., Zude-Sasse, M., 2020c. Mechanical thinning of apples reduces fruit drop. *Acta Hortic.* 1281, 533-538.  
<https://doi.org/10.17660/ActaHortic.2020.1281.70>
- Penzel, M., Herppich, W.B., Tsoulas, N., Weltzien, C., Zude-Sasse, M., 2021. Modeling of individual fruit-bearing capacity of trees is aimed at optimizing fruit quality of *Malus x domestica* Borkh. 'Gala'. *Front. Plant Sci.* 12, 1-15.  
<https://doi.org/10.3389/fpls.2021.669909>
- Penzel, M., Tsoulas, N., Lakso, A.N., Zude-Sasse, M., 2021b. Spatial variability of the individual tree's fruit bearing capacity in commercial orchards of 'RoHo 3615' and 'Pinova' apple. *Acta Hortic.* 1314, 125-132. <https://doi.org/10.17660/ActaHortic.2021.1314.17>
- Penzel, M., Pflanz, M., Gebbers, R., Zude-Sasse, M., 2021c. Tree adapted mechanical flower thinning prevents yield loss caused by over thinning of trees with low flower set in apple. *Eur. J. Hortic. Sci.* 86, 88-98. <https://doi.org/10.17660/eJHS.2021/86.1.10>
- Pflanz, M., Gebbers, R., Zude, M., 2016. Influence of tree-adapted flower thinning on apple yield and fruit quality considering cultivars with different predisposition in fructification. *Acta Hortic.* 1130, 605–612. <https://doi.org/10.17660/ActaHortic.2016.1130.90>
- Poni, S., Palliotti, A., Bernizzoni, F., 2006. Calibration and evaluation of a STELLA software-based daily CO<sub>2</sub> balance model in *Vitis vinifera* L. *J. Amer. Soc. Hortic. Sci.* 131, 273-283. <https://doi.org/10.21273/JASHS.131.2.273>

- Poblete-Echeverría, C., Fuentes, S., Ortega-Farias, S., Gonzalez-Talice, J., Yuri, J.A., 2015. Digital cover photography for estimating leaf area index (LAI) in apple trees using a variable light extinction coefficient. *Sensors-Basel* 15, 2860 - 2872. <https://doi.org/10.3390/s150202860>
- Porat, R., Lichter, A., Terry, L.A., Harker, R., Buzby, J., 2018. Postharvest losses of fruit and vegetables during retail and in consumers' homes: Quantifications, causes, and means of prevention. *Postharvest. Biol. Tec.* 139, 135-149. <https://doi.org/10.1016/j.postharvbio.2017.11.019>
- Preston, A.P., 1954. Effects of fruit thinning by the leaf count method on yield, size and biennial bearing of the apple Duchess Favorite. *J. Hortic. Sci.* 43, 373–381. <https://doi.org/10.1080/00221589.1954.11513819>.
- Rahmati, M., Mirás-Avalos, J.M., Valsesia, P., Lescourret, F., Génard, M., et al., 2018. Disentangling the effects of water stress on carbon acquisition, vegetative growth, and fruit quality of peach trees by means of the QualiTree model. *Front. Plant Sci.* 9. <https://doi.org/10.3389/fpls.2018.00003>
- Reyes, F., DeJong, T., Franceschi, P., Tagliavini, M. Gianelle, D., 2016. Maximum growth potential and periods of resource limitation in apple tree. *Front. Plant Sci.* 7. <https://doi.org/10.3389/fpls.2016.00233>
- Reyes, F., Pallas, B., Pradal, C., Vaggi, F., Zanotelli, D., Tagliavini, M., Costes, E., 2020. MuSCA: a multi-scale source–sink carbon allocation model to explore carbon allocation in plants. An application to static apple tree structures. *Ann. Bot.-London* 126, 571-585. <https://doi.org/10.1093/aob/mcz122>
- Robinson, T.L., 2011. Advances in apple culture worldwide. *Rev. Bras. Frutic.* 33, 37-47. <https://dx.doi.org/10.1590/S0100-29452011000500006>
- Robinson, T.L., Lakso, A.N., 2004. Between year and within year variation in chemical fruit thinning efficacy of apple during cool springs. *Acta Hortic.* 636, 283–294. <https://doi.org/10.17660/ActaHortic.2004.636.34>
- Robinson, T. L., Lakso, A. N., Ren, Z., 1991. Modifying apple tree canopies for improved production efficiency. *HortScience*, 26, 1005-1012
- Robinson, T.L., Lakso, A.N., Greene, D., 2017. Precision crop load management: The practical implementation of physiological models. *Acta Hortic.* 1177, 381–390. <https://doi.org/10.17660/ActaHortic.2017.1177.55>.

Roche, L., 2020. Mechanical fruitlet thinning - New tool shows promise in trials by French researchers, especially when paired with mechanical bloom thinning. Good Fruit Grower, August 2020. <https://www.goodfruit.com/roche-mechanical-fruitlet-thinning/>, access 18.02.2021

Sadras, V.O., Trentacoste, E.R., 2011. Phenotypic plasticity of stem water potential correlates with crop load in horticultural trees. *Tree Physiol.* 31, 494-499. <https://doi.org/10.1093/treephys/tpr043>

Sanz, R., Llorens, J., Escolà, A., Arnó, J., Planas, S., Roman, C., Rosell-Polo, J.R., 2018. LIDAR and non-LIDAR-based canopy parameters to estimate the leaf area in fruit trees and vineyard. *Agric. Forest Meteorol.* 260, 229-239. <https://doi.org/10.1016/j.agrformet.2018.06.017>

Schuh, B et al. 2019, Research for AGRI Committee – The EU farming employment: current challenges and future prospects, European Parliament, Policy Department for Structural and Cohesion Policies, Brussels

Serra, S., Leisso, R., Giordani, L., Kalcsits, L., Musacchi, S., 2016. Crop load influences fruit quality, nutritional balance, and return bloom in ‘Honeycrisp’ apple. *HortScience* 51, 236-244. <https://doi.org/10.21273/HORTSCI.51.3.236>.

Stopar, M., 2010. Fruit set and return bloom of light, medium and high flowering apple trees after BA applications. *Acta Hortic.* 884, 351-356. <https://doi.org/10.17660/ActaHortic.2010.884.41>

Stover, E.W., Greene, D.W., 2005. Environmental effects on the performance of foliar applied plant growth regulators: a review focusing on tree fruits, *HortTechnology* 15, 214-221. <https://doi.org/10.21273/HORTTECH.15.2.0214>

Suo, G.D., Xie, Y.S., Zhang, Y., Cai, M.Y., Wang, X.S., Chuai, J.F., 2016. Crop load management (CLM) for sustainable apple production in China. *Sci. Hortic.-Amsterdam* 211, 213-219. <https://doi.org/10.1016/j.scienta.2016.08.029>

Theophrastus, 371 BC - 287 BC. The modes of generation In: *De Causis Plantarum* Book I. Trans. 1976 by Einarson, B., Link, G.K.K. Harvard University Press, Cambridge, MA, USA, pp. 1-195

Thiele, G.F., Zhang, J., 1992. The dynamic apple tree system: relationships to AID management strategies. *Acta Hortic.* 313, 249-256. <https://doi.org/10.17660/ActaHortic.1992.313.31>.

- Tsoulias, N., Paraforos, D.S., Fountas, S., Zude-Sasse, M., 2019. Estimating canopy parameters based on the stem position in apple trees using a 2D LiDAR. *Agronomy* 9, 740. <https://doi.org/10.3390/agronomy9110740>
- Underwood, J.P., Hung, C., Whelan, B., Sukkarieh, S., 2016. Mapping almond orchard canopy volume, flowers, fruit and yield using lidar and vision sensors. *Comp. Electron. Agric.* 130, 83-96. <https://doi.org/10.1016/j.compag.2016.09.014>
- Vanbrabant, Y., Delalieux, S., Tits, L., Pauly, K., Vandermaesen, J., Somers B., 2020. Pear flower cluster quantification using RGB drone imagery. *Agronomy* 10, 407. <https://doi.org/10.3390/agronomy10030407>
- Verbiest, R., Ruysen, K., Vanwalleghem, T., Demeester, E., Kellens, K., 2020. Automation and robotics in the cultivation of pome fruit: Where do we stand today?. *J. Field Robot.* 2020, 1-19. <https://doi.org/10.1002/rob.22000>
- Verheij, E.W.M., Verwer, F.L.J.A.W., 1973. Light studies in a spacing trial with apple on a dwarfing and a semi-dwarfing rootstock. *Sci. Hortic.-Amsterdam* 1, 25-42. [https://doi.org/10.1016/0304-4238\(73\)90004-6](https://doi.org/10.1016/0304-4238(73)90004-6)
- Vincente, A.R., Manganaris, G.A., Ortiz, C.M., Sozzi, G.O., Crisosto, C.H., 2014. Nutritional quality of fruits and vegetables. In: Florkowski, W.J., Shewfelt, R.L., Brueckner, B., Prussia, S.E. (Eds.), *Postharvest handling – A systems approach*, Academic Press, Cambridge, MA, USA, pp. 69-122. <https://doi.org/10.1016/B978-0-12-408137-6.00005-3>
- Volz, R.K., Ferguson, I.B., Bowen, J.H., Watkins, C.B., 1993. Crop load effects on fruit mineral nutrition, maturity, fruiting and tree growth of 'Cox's Orange Pippin' apple. *J. Hortic. Sci.* 68, 127-137. <https://doi.org/10.1080/00221589.1993.11516336>
- Wagenmakers, P.S., 1996. Effects of light and temperature on potential apple production. *Acta Hortic.* 416, 191-198. <https://doi.org/10.17660/ActaHortic.1996.416.23>
- Wagenmakers, P.S., Callesen, O., 1995. Light distribution in apple orchard systems in relation to production and fruit quality. *J. Hort. Sci.* 70, 935-948. <https://doi.org/10.1080/14620316.1995.11515369>
- Wang, Z., Walsh, K.B., Verma, B., 2017. On-tree mango fruit size estimation using RGB-D images. *Sensors-Basel* 17, 2738. <https://doi.org/10.3390/s17122738>
- Wang, X., Tang, J., Whitty, M., 2020. Side-view apple flower mapping using edge-based fully convolutional networks for variable rate chemical thinning. *Comp. Electron. Agric.* 178, 106573. <https://doi.org/10.1016/j.compag.2020.106573>

- Westling, F., Mahmud, K., Underwood, J., Bally, I., 2020. Replacing traditional light measurement with LiDAR based methods in orchards. *Comp. Electron. Agric.* 179, 105798. <https://doi.org/10.1016/j.compag.2020.105798>
- Winter, F., 1976. A simulation model for studying the efficiency of apple and pear orchards. *Gartenbauwissenschaft* 41, 26-34
- Wouters, N., 2014. Mechatronics for efficient thinning of pear. Ph.D. thesis. KU Leuven
- Wu, D., Johansen, K., Phinn, S., Robson, A., Tu, Y.-H., 2020. Inter-comparison of remote sensing platforms for height estimation of mango and avocado tree crowns. *Int. J. Appl. Earth Obs.* 89, 102091. <https://doi.org/10.1016/j.jag.2020.102091>
- Wünsche, J.N., Lakso, A.N., Robinson, T.L., Lenz, F., Denning, S.S., 1996. The bases of productivity in apple production systems: The role of light interception by different shoot types. *J. Amer. Soc. Hortic. Sci.* 121, 886-893. <https://doi.org/10.21273/JASHS.121.5.886>
- Wünsche, J.N., Palmer, J.W., Greer, D.H., 2000. Effects of crop load on fruiting and gas-exchange characteristics of 'Braeburn'/M.26 apple trees at full canopy. *J. Amer. Soc. Hortic. Sci.* 125, 93-99. <https://doi.org/10.21273/JASHS.125.1.93>
- Wünsche, J.N., Lakso, A.N., 2000. The relationship between leaf area and light interception by spur and extension shoot leaves and apple orchard productivity. *HortScience* 35, 1202-1206. <https://doi.org/10.21273/HORTSCI.35.7.1202>
- Yahia, E.M., García-Solís, P., Celis, M.E.M., 2019. Contribution of fruits and vegetables to human nutrition and health. in: Yahia, E.M., (Ed.), *Postharvest physiology and biochemistry of fruits and vegetables*, Woodhead Publishing, Cambridge, MA, USA, pp. 19-45. <https://doi.org/10.1016/B978-0-12-813278-4.00002-6>
- Yoder, K.S., Peck, G.M., Combs, L.D., Byers, R.E., 2013. Using a pollen tube growth model to improve apple blossom thinning for organic production. *Acta Hortic.* 1001, 207-214. <https://doi.org/10.17660/ActaHortic.2013.1001.23>
- Yuan, R., Greene, D.W., 2000. Benzyladenine as a chemical thinner for 'McIntosh' apples. I. Fruit thinning effects and associated relationships with photosynthesis, assimilate translocation, and nonstructural carbohydrates. *J. Am. Soc. Hortic. Sci.* 125, 169-176. <https://doi.org/10.21273/JASHS.125.2.169>
- Zhang, J., Zhang, Q., Whiting, M.D., 2015. Mapping interception of photosynthetically active radiation in sweet cherry orchards. *Comput. Electron. Agric.* 111, 29-37. <http://dx.doi.org/10.1016/j.compag.2014.11.024>



Zhang, J., Serra, S., Leisso, R.S., and Musacchi, S., 2016. Effect of light microclimate on the quality of 'd'Anjou' pears in mature open-centre tree architecture. *Biosyst. Eng.* 141, 1-11. <https://10.1016/j.biosystemseng.2015.11.002>

Zhu, J., Génard, M., Poni, S., Gambetta, G.A., Vivin, P., et al., 2019. Modelling grape growth in relation to whole-plant carbon and water fluxes, *J. Exp. Bot.* 70, 2505-2521 <https://doi.org/10.1093/jxb/ery367>.

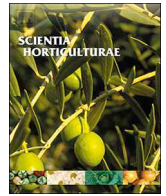
Zude-Sasse, M., Fountas, S., Gemtos, T.A., Abu-Khalaf, N., 2016. Applications of precision agriculture in horticultural crops - review. *Eur. J. Hortic. Sci.* 81, 78-90. <https://doi.org/10.17660/eJHS.2016/81.2.2>.

## **2. Thinning efficacy of met amitron on young 'RoHo 3615' apple**

In: Scientia Horticulturae 272, pp. 1-6, 2020

Cite as:

Penzel, M., Kröling, C., 2020. Thinning efficacy of met amitron on young 'RoHo 3615' (Evelina®) apple. Sci. Hortic.-Amsterdam 272. <https://doi.org/10.1016/j.scienta.2020.109586>



# Thinning efficacy of metamitron on young 'RoHo 3615' (Evelina®) apple

Martin Penzel<sup>a,\*</sup>, Christian Kröling<sup>b,\*</sup>

<sup>a</sup> Leibniz Institute for Agricultural Engineering and Bioeconomy (ATB), Max-Eyth-Allee 100, 14469 Potsdam, Germany

<sup>b</sup> Saxon State Office for Environment, Agriculture and Geology, Lohmener Straße 12, 01326 Dresden, Germany

## ARTICLE INFO

### Keywords:

6-Benzyladenine  
Chemical thinning  
Chlorophyll fluorescence analysis  
Fruit quality  
*Malus x domestica*  
Photoinhibition  
Plant growth regulator

## ABSTRACT

To achieve a high quantity of premium class fruit, chemical thinning is an important component of crop load management in apples. For this purpose, the triazine-type photosynthetic inhibitor metamitron was registered for fruit thinning in Germany. Frequent studies demonstrated consistent thinning effects of metamitron on trees of different apple and pear cultivars. In the present study, the efficacy of metamitron applied at a low concentration ( $165 \text{ g ha}^{-1}$ ) was investigated in 2016 and 2017 on young 'RoHo3615' apple trees, planted in 2014. The highest fruit set reduction was achieved when metamitron was applied twice. Single application, in contrast, led to variable results and pointed out the strong dependence of the thinning efficacy of metamitron on favourable weather conditions. Adding citric acid or the growth regulator prohexadione-Ca in combination with ammonium sulphate did not affect the thinning efficacy of metamitron. The fruit quality was high in any treatment and no effects of thinning treatment on fruit colouration or percentage of skin russetting were observed. Consequently, metamitron is an effective fruit thinning agent for young apple trees, which can be additionally used in combination with the mentioned substances, while maintaining a high fruit quality.

## 1. Introduction

Important quality attributes of apples, determining the market value, are fruit size and colouration. These parameters are positively correlated with the tree-specific leaf area to fruit ratio (Hansen, 1980; Palmer, 1992) and, consequently, with the fruit carbohydrate supply. Low carbon supply reduces fruit growth (Zibordi et al., 2009; Lakso and Goffinet, 2017) and potentially delays fruit development. The reduction of crop load increases the leaf area per fruit ratio within individual trees and thus improves the carbon supply per fruit. This, in turn, enhances fruit size and quality and is, therefore, an essential tool in fruit production. Crop load reduction can be achieved by reducing the number of flower buds per tree via pruning (Breen et al., 2015), mechanical removal of flowers (Kon et al., 2013) or by triggering fruit abscission (Bangerth, 2000), e.g. as reaction of trees to carbohydrate deficit, or by increasing the competition for carbohydrates between fruit and other sink organs (Byers et al., 1990; Zibordi et al., 2009).

The triazine-type herbicide metamitron acts as photosynthesis inhibitor and restricts the photosynthetic electron transport, affecting the photochemical efficiency and consequently the carbon assimilation of the leaves. Metamitron can be active for up to 29 d after application, depending on cultivar, applied concentration and fruit development stage (Köpcke, 2004; McCartney et al., 2012; Gonzalez et al., 2019). This

substance affects the carbon supply to demand-balance within trees, which potentially leads to a carbon supply deficit for the individual fruit. Therefore, metamitron is an effective thinning agent for apples when applied once or twice in the period from petal fall to 20 mm fruit diameter at concentrations of  $150 - 700 \text{ g ha}^{-1}$  (Köpcke, 2004; Stern, 2014; Gonzalez et al., 2019). However, the temperature before, during and after the application is crucial for the thinning efficacy of metamitron (Clever, 2018). When the carbon demand of all fruit exceeds the supply for more than 3 d, abscission of surplus fruit potentially adapts the sink demand for carbon to the actual conditions (Lakso, 2011). High temperatures, especially at night, promote fruit abscission (Kondo and Takahashi, 1987) due to increased growth rates of fruit and terminal shoots. Furthermore, high temperatures generally enhance the mitochondrial respiration of tree organs and, thus, the sink strength for carbohydrates. Additionally, low photon flux rates during the rapid foliage development in the early season (i.e. two to three weeks after full bloom) intensify this effect (Lakso, 2011).

Therefore, the susceptibility of fruit to thinning agents is highest during the initial three weeks after full bloom on warm days with low solar radiation (S) (Lakso et al., 2006). Recent reports specified the required weather conditions for effective thinning with metamitron in the period from 5 d prior to 5 d subsequent to the application as night temperatures  $> 10^\circ \text{C}$  and  $S > 16 \text{ MJ m}^{-2} \text{ d}^{-1}$  for at least 2–3 d

\* Corresponding authors.

E-mail addresses: [mpenzel@atb-potsdam.de](mailto:mpenzel@atb-potsdam.de) (M. Penzel), [Christian.Kroeling@smul.sachsen.de](mailto:Christian.Kroeling@smul.sachsen.de) (C. Kröling).

<https://doi.org/10.1016/j.scienta.2020.109586>

Received 24 March 2020; Received in revised form 19 June 2020; Accepted 30 June 2020

0304-4238/ © 2020 The Author(s). Published by Elsevier B.V. This is an open access article under the CC BY-NC-ND license (<http://creativecommons.org/licenses/by-nc-nd/4.0/>).

(Clever, 2018). To optimally schedule the application of metamitron, warm days with low solar radiation should be forecasted. However, the prediction of the efficacy of fruit abscission as a response to the thinning treatment from measured temperature and solar radiation is currently not possible, because it has not yet been related to accumulated heat units or photothermal units. So far, to quantify fruit abscission, manual measurements of the growth of individual fruit are necessary to predict thinning response, because those fruit going to abscise will terminate their growth (Greene et al., 2013).

In 2016, metamitron was registered as fruit thinning agent for apples and pears in Germany at concentrations between  $165 \text{ g ha}^{-1}$  –  $330 \text{ g ha}^{-1}$ . The application recommendations of the product advise not to apply metamitron for thinning of apples and pears in orchards younger than 4–5 years and 7–8 years, respectively. However, both young and mature trees require crop load management to balance the generative and vegetative growth and to ensure flower bud development for the subsequent year. To avoid disproportionate or unpredictable effects, the lowest concentrations of metamitron recommended by the manufacturer for mature trees should be used on young trees, also, due to economic considerations. The compatibility of metamitron with other compounds in one tank-mix has not been sufficiently investigated or the findings have not been published, and, therefore, results are limited to studies with metamitron in combination with surfactants (Köpcke, 2004). No agent, so far, has been identified to increase or reduce the thinning efficacy of metamitron. In practice, knowledge on compatibility of metamitron with other compounds, applied to apple trees in the same period, would be beneficial in order to reduce the frequency of single applications in orchards, to potentially increase thinning efficacy of metamitron, to reduce the risk of over-thinning and to avoid adverse effects.

The aim of the present study was to evaluate (i) the optimal timing for the application of a low concentration of metamitron on young trees of the apple cultivar 'RoHo3615', and, (ii), whether additives can influence the thinning efficacy of metamitron.

## 2. Materials and methods

Two field trials were carried out in 2016 and 2017 on trees of *Malus x domestica* BORKH. 'RoHo 3615'/M.9 (a red mutant of 'Pinova'; Evelina®) planted in 2014 in a sandy loam soil at the Saxon State Office for Environment, Agriculture and Geology research orchard (51.003919 N, 13.887303 E) in Dresden, Germany. Trees were trained as a slender spindle with a spacing of  $3.2 \text{ m} \times 1.0 \text{ m}$ . The orchard was managed according to the federal regulations of integrated production. The trial was arranged in randomised blocks with four replications of five-tree plots per treatment. To minimise the variance between the trees, those with a similar numbers of flower clusters (FC) were pre-selected (2016:  $165 \pm 29 \text{ FC}$ ; 2017:  $149 \pm 18 \text{ FC}$ ). Flower clusters per tree were counted manually and the variance analysed at confidence level = 5 %. Full bloom was on 03.05.2016 and 27.04.2017. Metamitron at  $165 \text{ g ha}^{-1}$  (Brevis, Adama Deutschland GmbH, Köln, Germany) was applied with a tunnel sprayer (TSG NO1, Lipco, Sasbach, Germany), using a water volume of  $500 \text{ L ha}^{-1}$ , twice, at  $D = 8 \text{ mm}$  and  $12 \text{ mm}$ ; once at  $D = 8 \text{ mm}$ ; once at  $D = 12 \text{ mm}$ ; once in tank-mix with  $106 \text{ g ha}^{-1}$  prohexadione-Ca and  $563 \text{ g ha}^{-1}$  ammonium sulphate (Regalis®Plus, BASF SE, Ludwigshafen, Germany); once at  $D = 8 \text{ mm}$  in tank-mix with  $500 \text{ g ha}^{-1}$  citric acid. Furthermore,  $150 \text{ g ha}^{-1}$  6-benzyladenine (6-BA; Exilis®, Fine Agrochemicals Ltd., Worcester, UK) was applied at  $D = 8 \text{ mm}$  for comparison while the controls remained untreated. The applications were carried out 16 d after full bloom (DAFB), 24 DAFB in 2016 ( $D = 8 \text{ mm}$ : 19.05.;  $D = 12 \text{ mm}$ : 27.05.) and 23 DAFB, 31 DAFB in 2017 ( $D = 8 \text{ mm}$ : 17.05.;  $D = 12 \text{ mm}$ : 25.05.). The temperature at 2 m height and solar radiation,  $S$ , were recorded in 1 h intervals in the periods from 5 d prior to 5 d subsequent to the applications with a PT100 temperature sensor and a pyranometer, in the spectral range from 350 nm to 1100 nm, attached to a weather station

(TOSS GmbH, Potsdam, Germany) located in the same orchard. From the hourly temperature ( $T_H$ ), the accumulated growing degree hours ( $\text{GDH}_{TB}$ ) in the periods 5 d prior, 5 d after and  $\pm 5 \text{ d}$  from each application, were calculated (Eqn. 1);  $T_U$  is the optimum temperature for growth and  $T_B$  the base temperature, which were set to  $25^\circ\text{C}$  and  $10^\circ\text{C}$ , respectively (Anderson et al., 1986). The average temperatures at night ( $T_{\text{night}}$ ) and day ( $T_{\text{day}}$ ) were calculated, considering the hours when  $S$  was  $= 0$  and  $> 0$ , respectively. The average daily integral of  $S$ ,  $S_{\text{daily}}$ , in the same periods was expressed in  $[\text{MJ m}^{-2} \text{ d}^{-1}]$ .

$$\text{GDH}_{TB} = \sum_{i=\text{prior}}^{\text{post}} (T_U - T_B) - 2 \cdot (1 + \cos(\pi + \pi \cdot (T_H - T_B) \cdot (T_U - T_B) - 1)) \quad (1)$$

In 2016 at 20 DAFB, 24 DAFB, 30 DAFB, the actual quantum yield of linear electron transport through PSII ( $\phi_{\text{PSII}}$ ;  $((F_m' - F_t) \cdot F_m'^{-1})$ ) was measured around noon on 5 exposed spur leaves per treatment in 1.2 m height under ambient daylight conditions, using a portable chlorophyll fluorometer (JUNIOR-PAM, H. Walz GmbH, Effeltrich, Germany).  $F_m'$  is the maximum fluorescence signal, obtained after a saturating light pulse, while  $F_t$  denotes the terminal steady state fluorescence signal at the ambient light conditions (Matyssek and Herppich, 2019). Rates of photosynthetic electron transport through PSII,  $J_F$  [ $\mu\text{mol m}^{-2} \text{ s}^{-1}$ ], were estimated (Eqn. 2; c.f. Herppich et al., 1998) as

$$J_F = \phi_{\text{PSII}} \cdot \text{PPFR} \cdot L_a \cdot f \quad (2)$$

The photosynthetic photon flux rates, PPFR [ $\mu\text{mol m}^{-2} \text{ s}^{-1}$ ], were estimated by multiplying ambient  $S$ ,  $S_a$  [ $\text{W m}^{-2}$ ], with the conversion factor 4.57 (McCree, 1972). The fraction of photons absorbed by leaves,  $L_a$ , and the light distribution factor,  $f$ , between PS I and PS II were set to 0.85 (Palmer, 1977) and 0.5, respectively. The average reduction in  $J_F$  in comparison to the control,  $J_{F, \text{RD}}$  [%], was calculated as (Eqn. 3)

$$J_{F, \text{RD}} = 100 - (\text{mean } J_{F, \text{treatment}} \cdot \text{mean } J_{F, \text{control}}^{-1} \cdot 100) \quad (3)$$

After physiological fruit drop, all trees were hand thinned to one or two fruit per cluster and the number of removed fruit per tree, HTF [fruit tree $^{-1}$ ], recorded (20.06.2016; 30.06.2017). The fruit set after physiological fruit drop, FS [fruit cluster $^{-1}$ ], and the thinning efficacy of the different treatments in comparison to the control, Eff [%], were determined for every tree (Eqs. 4, 5).

$$\text{FS} = (F + \text{HTF}) \cdot \text{FC}^{-1} \quad (4)$$

$$\text{Eff} = 100 - (\text{FS}_{\text{treatment}} \cdot \text{mean FS}_{\text{control}}^{-1} \cdot 100) \quad (5)$$

All fruit were harvested when a starch index [1–10] of 5 (Zude-Sasse et al., 2000) was achieved (29.09.2016, 27.09.2017). The harvested fruit of each individual tree,  $F$  [fruit tree $^{-1}$ ], were size and colour graded and the fresh mass, FM [g], of the individual fruit determined with a commercial grading machine (Vision, Aweta, Pijnacker, The Netherlands). In 2016, subsamples of 100 randomly selected fruit per treatment were manually assessed for the percentage of skin russetting on the fruit surface. To assess the effect of the thinning treatments on the flower clusters per tree in the subsequent year,  $\text{FC}_{\text{yr}+1}$ ,  $\text{FC}_{\text{yr}+1}$  was counted before flowering (2017: -13 DAFB; 2018: -10 DAFB).

The variances of  $F$ ,  $\text{FC}$ ,  $\text{FC}_{\text{yr}+1}$ ,  $\text{FM}$ ,  $\text{FS}$ ,  $J_F$ , percentage of yield with  $> 60\%$  red skin, percentage of russetting on fruit surface and yield between the different treatments (confidence level = 5 %) were analysed with the software R (Version 3.4.1; R Core Team, 2018) using the package userfriendlyscience (Peters, 2018).

## 3. Results and discussion

### 3.1. Weather conditions in the period 5 d prior to 5 d subsequent to the application

In 2016, the minimum requirements for successful thinning with metamitron (Clever, 2018) were exceeded in the periods  $\pm 5 \text{ d}$  of both applications (Table 1). Both, the night temperatures and the

**Table 1**

Time of application of thinning treatments and average temperatures at night and day ( $T_{\text{night}}$ ,  $T_{\text{day}}$ ), average daily integral of solar radiation ( $S_{\text{daily}}$ ) and accumulated growing degree hours on base of 10 °C ( $\text{GDH}_{10^\circ\text{C}}$ ) in the period from 5 d prior to 5d after thinning applications.

Year	Time of application	Period	$T_{\text{night}}$ [°C]	$T_{\text{day}}$ [°C]	$S_{\text{daily}}$ [ $\text{MJ m}^{-2} \text{d}^{-1}$ ]	$\text{GDH}_{10^\circ\text{C}}$
2016	8 mm, 16 DAFB	5 d prior application	7.9	11.7	13.4	285
		5 d after application	14.0	19.8	16.3	997
		application $\pm$ 5 d	11.1	15.6	14.6	1282
	12 mm, 24 DAFB	5 d prior application	14.4	18.7	14.4	909
		5 d after application	15.4	20.7	15.1	1132
		application $\pm$ 5 d	14.9	19.7	14.6	2040
2017	8 mm, 23 DAFB	5 d prior application	12.3	20.2	19.7	872
		5 d after application	14.3	18.0	20.4	1011
		application $\pm$ 5 d	13.3	19.5	19.9	1884
	12 mm, 31 DAFB	5 d prior application	10.7	16.6	18.2	703
		5 d after application	15.4	21.3	23	1232
		application $\pm$ 5 d	13.5	19.9	20.6	1935

accumulated  $\text{GDH}_{10^\circ\text{C}}$  were considerably higher before the application at  $D = 12$  mm than before that at  $D = 8$  mm. Therefore, the weather conditions before the treatment at  $D = 12$  mm were more beneficial for fruit thinning, which was also visible in the thinning efficacy. In 2017, the night temperatures during both thinning treatments were permanently above 10 °C, but solar radiation dose did not drop below  $16 \text{ MJ m}^{-2} \text{d}^{-1}$ .

In 2017, in the period 5 d after application at  $D = 12$  mm,  $\text{GDH}_{10^\circ\text{C}}$  were slightly elevated in comparison to 5 d after application at  $D = 8$  mm. However, no difference in thinning efficacy of single application of metatriton occurred between the two application dates. Thinning efficacy of metatriton applied at  $D = 12$  mm in 2017 was lower than thinning efficacy of the same treatment in 2016, despite  $\text{GDH}_{10^\circ\text{C}}$  after the application exceeded that of 2016. However, night temperature prior application at 12 mm  $D$  was elevated, and solar radiation 5 d prior and subsequent to the application was reduced in 2016 in comparison to 2017, possibly explaining the differences in thinning efficacy.

The required temperatures for effective fruit thinning with 6-BA,  $> 20^\circ\text{C}$  after the application (Yuan and Greene, 2000), were not achieved in both years.

### 3.2. Photosynthetic performance of leaves subsequent to the metatriton application

In 2016, photosynthetic electron transport rates,  $J_F$ , were highest in control leaves at any measurement day (Table 2, Fig. 1), but were not significantly different from leaves treated with 6-BA. Four days after the first application,  $J_F$  was reduced in leaves treated with metatriton if compared to the controls and leaves treated with 6-BA. The same was valid 8 d after metatriton application. On these days, chlorophyll fluorescence was measured prior to the 2<sup>nd</sup> application of metatriton. Compared to the measurements at 8 d after the 1<sup>st</sup> application,  $J_F$ ,  $J_F$ ,  $J_F$  of leaves treated once with metatriton at  $D = 8$  mm was lower than 14 d after application. However, 14 d after application, differences in

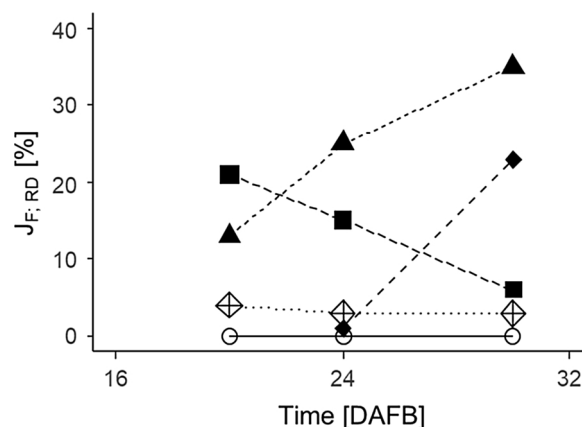


Fig. 1. Relative reduction in the actual photosynthetic electron transport through PS II ( $J_F$ ,  $J_F$ ,  $J_F$ ) of leaves ( $n = 5$ ) of 'RoHo 3615'/M.9 apple trees in response to chemical thinning treatment at different dates in 2016. (Open circle = control; closed triangle = metatriton\* applied at 16 DAFB and 24 DAFB; closed square = metatriton\* applied at 16 DAFB, closed diamond = metatriton\* applied at 24 DAFB, open diamond = 150 g  $\text{ha}^{-1}$  6-benzyladenine applied at 16 DAFB with 500 L  $\text{ha}^{-1}$  water. \*) 165 g  $\text{ha}^{-1}$  with 500 L  $\text{ha}^{-1}$  water).

comparison to untreated leaves still persisted (Table 2). Also, the standard deviation (SD) in  $J_F$  was higher for leaves treated with metatriton in comparison to untreated leaves (Table 2). A minor decrease in SD of  $J_F$  with time was observed. On leaves treated twice with metatriton, SD of  $J_F$  was highest 14 d after the first application, likewise  $J_F$ ,  $J_F$ ,  $J_F$  as a consequence of the additional photosynthetic inhibition, when  $J_F$  was already reduced.

The results indicated that metatriton was presumably metabolised within the third week after the applications. In leaves of 'Cameo' apple trees treated with 300 g  $\text{ha}^{-1}$  metatriton,  $J_F$  recovered to the initial

**Table 2**

Means ( $\pm$  SD;  $n = 5$ ) of the actual photosynthetic electron transport rates through PS II ( $J_F$ ) of leaves of 'RoHo 3615'/M.9 apple trees in response to chemical thinning treatments at 18 d after full bloom (DAFB), 22 DAFB and 28 DAFB in 2016. The respective average ambient photon flux rates (PPFR) were  $1800 \mu\text{mol m}^{-2} \text{s}^{-1}$ ,  $1600 \mu\text{mol m}^{-2} \text{s}^{-1}$  and  $1200 \mu\text{mol m}^{-2} \text{s}^{-1}$ . All treatments were applied with 500 L  $\text{ha}^{-1}$  water. Superscript letters indicate significant differences between means.

Treatment	Time of application	20 DAFB	24 DAFB	30 DAFB
Control	–	$594 \pm 10^b$	$479 \pm 16^b$	$372 \pm 16^d$
Metatriton <sup>1</sup>	16 DAFB, 24 DAFB	$519 \pm 66^a$	$361 \pm 102^a$	$244 \pm 89^a$
Metatriton <sup>1</sup>	16 DAFB	$471 \pm 20^a$	$406 \pm 75^a$	$349 \pm 27^{bc}$
Metatriton <sup>1</sup>	24 DAFB	–	$475 \pm 13^b$	$284 \pm 63^a$
6-BA <sup>2</sup>	16 DAFB	$572 \pm 51^b$	$468 \pm 19^b$	$360 \pm 18^{bcd}$
Metatriton <sup>1</sup> , prohexadione-Ca <sup>3</sup> , $(\text{NH}_4)_2\text{SO}_4$ <sup>4</sup>	16 DAFB	$474 \pm 37^a$	$402 \pm 83^a$	$322 \pm 19^{ab}$
Metatriton <sup>1</sup> , citric acid <sup>5</sup>	16 DAFB	$509 \pm 56^a$	$405 \pm 87^a$	$341 \pm 31^{bc}$

<sup>1</sup>) 165 g  $\text{ha}^{-1}$ ; <sup>2</sup>) 150 g  $\text{ha}^{-1}$ ; <sup>3</sup>) 106 g  $\text{ha}^{-1}$ ; <sup>4</sup>) 563 g  $\text{ha}^{-1}$ ; <sup>5</sup>) 500 g  $\text{ha}^{-1}$ .

value before treatment within 5 d subsequent to the application (McArtney et al., 2012), whereas in 'Fuji' and 'Gala' apples, the period of photosynthetic inhibition, as a consequence of the treatment with metamitron, persisted longer than 20 d after the application (Gonzalez et al., 2019). Fitted curves of the relative photosynthesis inhibition demonstrated differences among cultivars (Gonzalez et al., 2019). Additionally, the phenological stage strongly affected the duration of the inhibition of photosynthesis (Köpcke, 2004). Photosynthesis remained inhibited for up to 29 d when metamitron was applied at petal fall. However, on 'Elstar' and 'Golden Delicious' trees treated with 200 g ha<sup>-1</sup> metamitron, actual photosynthetic efficiency of the leaves fully recovered within 16 d after treatment when the agent was applied at D = 6–8 mm, similar to the findings in the presented trial.

The addition of prohexadione-Ca and ammonium sulphate or citric acid did not affect the photosynthetic electron transport in comparison to the sole application of metamitron at D = 8 mm (Table 1). This confirms earlier findings that the addition of the surfactant Polysorbate 20 did not further reduce the photosynthetic activity of treated leaves in comparison to the exclusive use of metamitron (Köpcke, 2004). The surficial absorption of metamitron by apple leaves generally enables the transport to the PS II, because 2 h after its local application the substance can be located evenly distributed among the vessels of the entire leaf (Köpcke, 2004). At 6 d after the 2<sup>nd</sup> application, J<sub>F</sub> was 34 % lower than that of the controls, whereas that of leaves treated once at D = 12 mm was reduced by 23 % and, thus, similar to the results obtained by one application of metamitron at D = 8 mm (Fig. 1). An additional temperature effect on J<sub>F</sub> could not be observed, since T<sub>H</sub> at each measurement ranged between 22 °C and 23 °C.

### 3.3. Thinning efficacy of metamitron treatments

In both years, the reduction of fruit per tree was highest on trees treated twice with metamitron (Table 3), probably due to the length of J<sub>F</sub> reduction in comparison to that after a single application (Fig. 1). In 2016, however, differences in the thinning efficacy between the different single applications of metamitron occurred. When applied at D = 12 mm, fruit set was reduced by 26 % in comparison to the control, which was not significantly different from the thinning efficacy at the double-application of metamitron. In contrast, fruit set was not reduced in any metamitron treatment at D = 8 mm. The stronger reduction at D = 12 mm can be explained by the higher T<sub>day</sub> and T<sub>night</sub> in the periods before and after application and slightly reduced solar radiation 5 d after application (Table 1). The phenological stage in the range from D

= 8 mm to D = 12 mm had no effect on the thinning efficacy of metamitron because no differences between both treatments occurred in the following year. In general, application of metamitron alone can be used for effective thinning of apple trees until D = 20 mm (McArtney and Obermiller, 2012). In contrast to 2016, thinning efficacy after single application of metamitron at D = 8 mm, was, indeed, higher in 2017. The results further highlighted the pronounced effect of the weather conditions on the thinning efficacy of low concentrations of metamitron. The data tendentially supposed a slight increase in the thinning efficacy when accumulated GDH<sub>10°C</sub> was increased in the days before and after the metamitron treatments (± 5 d).

The presented results confirm earlier finding on young 'Summerred'/M.9 apples that 165 g ha<sup>-1</sup> metamitron given once at D = 15 mm or twice at D = 15 mm and 19 mm significantly reduced fruit set (Maas and Meland, 2016). However, the number of flower clusters in the subsequent year was only enhanced in comparison to the controls at double application. At 330 g ha<sup>-1</sup> metamitron, applied once or twice, over-thinning appeared on the young trees in the above study. Double application of a low concentration (150 g ha<sup>-1</sup>) reduced fruit set of mature 'Gala' trees in a warm climate, where T<sub>night</sub> after application rose above 20 °C (Stern, 2014). In general, on mature apple trees, no or only low reduction in fruit set subsequent to the application of low concentrations (≤ 165 g ha<sup>-1</sup>) of metamitron was expected, especially when applied once (cf. Gonzalez et al., 2019). Despite of the young age of the trees, the canopies nearly filled out the allotted space within the rows from the third year (2016). Hence, a dosage larger than 165 g ha<sup>-1</sup> metamitron may have been helpful to improve thinning during a single application, particular when applied at 8 mm in both years and at 12 mm in 2017. However, since the manufacturer advised not to thin young trees with metamitron, only low concentrations were applied, to avoid unpredictable thinning effects.

The addition of prohexadione-Ca and ammonium sulphate, which is often applied in commercial production to control vegetative growth of the trees, did not affect the thinning efficacy of a single application of metamitron (Table 3). Thus, it can potentially be added when metamitron is applied for fruit thinning without negative consequences. The same is valid for citric acid, which was added to metamitron to potentially facilitate the dissolving of the water-soluble granulate and the absorption of the substance by the leaves. As described before, the absorption of metamitron by the leaves was already sufficient. Therefore, the thinning efficacy could not be enhanced by the addition of citric acid in both years. Furthermore, application of 6-BA did not reduce the number of fruit per tree in treated trees compared to controls,

**Table 3** Please let Tab 3 appear after Tab 2le 3

Effect of chemical thinning treatments on fruit tree<sup>-1</sup>, fruit set (FS, fruit flower clusters<sup>-1</sup>), thinning efficacy (FS of the treatments relative to mean FS of the controls), number of hand-thinned fruit tree<sup>-1</sup> (HTF) and HTF per flower clusters on 'RoHo 3615'/M.9 trees in two consecutive years. Superscript letters indicate significant differences between means.

Treatment	Fruit diameter at application (mm)	Fruit tree <sup>-1</sup> after fruit drop	FS after fruit drop	Thinning efficacy [%]	HTF	HTF clusters <sup>-1</sup>
2016						
Control		173 <sup>c</sup>	1.06 <sup>b</sup>	0 <sup>b</sup>	82 <sup>d</sup>	0.51 <sup>d</sup>
Metamitron <sup>1</sup>	8, 12	104 <sup>a</sup>	0.74 <sup>a</sup>	30 <sup>a</sup>	34 <sup>a</sup>	0.24 <sup>a</sup>
Metamitron <sup>1</sup>	8	158 <sup>bc</sup>	0.98 <sup>b</sup>	6 <sup>b</sup>	71 <sup>cd</sup>	0.44 <sup>cd</sup>
Metamitron <sup>1</sup>	12	139 <sup>b</sup>	0.79 <sup>a</sup>	26 <sup>a</sup>	51 <sup>b</sup>	0.30 <sup>ab</sup>
6-BA <sup>2</sup>	8	164 <sup>bc</sup>	0.99 <sup>b</sup>	7 <sup>b</sup>	72 <sup>cd</sup>	0.43 <sup>cd</sup>
Metamitron <sup>1</sup> , Prohexadione-Ca <sup>3</sup> , (NH <sub>4</sub> ) <sub>2</sub> SO <sub>4</sub> <sup>4</sup>	8	143 <sup>b</sup>	0.92 <sup>b</sup>	14 <sup>b</sup>	60 <sup>bc</sup>	0.39 <sup>bc</sup>
Metamitron <sup>1</sup> , Citric acid <sup>5</sup>	8	164 <sup>bc</sup>	0.95 <sup>b</sup>	11 <sup>b</sup>	70 <sup>cd</sup>	0.41 <sup>cd</sup>
2017						
Control		204 <sup>b</sup>	1.43 <sup>c</sup>	0 <sup>c</sup>	93 <sup>c</sup>	0.64 <sup>c</sup>
Metamitron <sup>1</sup>	8, 12	129 <sup>a</sup>	0.83 <sup>a</sup>	40 <sup>a</sup>	36 <sup>a</sup>	0.24 <sup>a</sup>
Metamitron <sup>1</sup>	8	181 <sup>b</sup>	1.19 <sup>b</sup>	14 <sup>b</sup>	73 <sup>b</sup>	0.48 <sup>b</sup>
Metamitron <sup>1</sup>	12	182 <sup>b</sup>	1.23 <sup>bc</sup>	12 <sup>b</sup>	78 <sup>bc</sup>	0.53 <sup>bc</sup>
6-BA <sup>2</sup>	8	177 <sup>b</sup>	1.15 <sup>b</sup>	14 <sup>bc</sup>	73 <sup>b</sup>	0.49 <sup>b</sup>
Metamitron <sup>1</sup> , Prohexadione-Ca <sup>3</sup> , (NH <sub>4</sub> ) <sub>2</sub> SO <sub>4</sub> <sup>4</sup>	8	176 <sup>b</sup>	1.28 <sup>bc</sup>	8 <sup>bc</sup>	75 <sup>bc</sup>	0.55 <sup>bc</sup>
Metamitron <sup>1</sup> , Citric acid <sup>5</sup>	8	180 <sup>b</sup>	1.24 <sup>bc</sup>	11 <sup>bc</sup>	77 <sup>b</sup>	0.53 <sup>bc</sup>

<sup>1</sup>) 165 g ha<sup>-1</sup>; <sup>2</sup>) 150 g ha<sup>-1</sup>; <sup>3</sup>) 106 g ha<sup>-1</sup>; <sup>4</sup>) 563 g ha<sup>-1</sup>; <sup>5</sup>) 500 g ha<sup>-1</sup>.



which was due to the unfavourable weather conditions. The thinning efficacy of 6-BA-treated trees did not differ from thinning efficacy on trees after a single application of metamitron at  $D = 8$  mm in both years. The capacity of the trees to bear high quality fruit, named fruit bearing capacity (FBC), was estimated from the number of leaves of two randomly selected trees per year divided by 30 (2016: FBC = 90; 2017: FBC = 105). Previously, 30 leaves were reported to be necessary to achieve maximum fruit growth rates (Haller and Magness, 1933). In both years, only the double application of metamitron reduced the number of fruit per tree to nearly the FBC, whereas the natural fruit drop in the controls reduced the fruit per tree to almost double of the FBC. Knowledge of the FBC is important to define a target fruit number per tree for crop load management (CLM) and to evaluate the actual crop load at any time during the season to plan further CLM practices (Robinson et al., 2017). In practice, if the first application of metamitron or any other chemical thinning compound did not sufficiently reduce the crop load, a second application may be necessary. This decision should be well-considered because a second application, especially after a short interval of 5 d, can also cause over-tinning of the trees as a consequence of the prolonged period of photosynthetic inhibition. Köpcke (2004) suggests the application of metamitron for thinning when the target fruit number per tree exceeds actual fruit per tree by minimum 30 %. For the estimation of fruit abscission after chemical thinning treatments, Greene et al. (2013) developed a model where the number of fruit which will abscise can be quantified from measurements of the diameter of random fruit 3–4 d and 7–8 d after each treatment. The model assumes that fruit, with growth rates in  $D \leq 50$  % of growth rates from fruit with the highest growth rates, will abscise. This model can be helpful for decision making.

### 3.4. Effect of thinning treatments on the number of hand thinned fruit, fruit quality and return bloom

After fruit drop has ended, hand thinning of surplus fruit is still an important component of crop load management. In the present trials, the number of hand-thinned fruit per tree to FBC was opposite to the thinning efficacy and, therefore, lowest when metamitron was applied twice. The crop loads in these treatments were hand-thinned below the FBC, because after the thinning treatments at some clusters more than two fruit remained, potentially leading to low fruit size. Therefore, in both years, the yield was reduced when metamitron was applied twice

compared to the controls and the other treatments (Table 4). In 2016, the number of hand-thinned fruit after a single application of metamitron at  $D = 12$  mm was lower compared to a single application at  $D = 8$  mm and that of 6-BA. The results of the latter treatments were not different from the control. In 2017, the number of hand-thinned fruit was reduced compared to controls and similar to the 6-BA treatment, when metamitron was applied once at  $D = 8$  mm. No differences to control was recorded for trees, treated with metamitron at  $D = 12$  mm or with metamitron combined with prohexadione-Ca and ammonium sulphate or citric acid. The time necessary to thin one apple per hand is assumable 1.5 s. Based on this assumption, the required time to hand thin one hectare of orchard,  $t_{HT}$  [h ha<sup>-1</sup>], can be estimated ( $t_{HT} = HTF \cdot 1.5 \text{ s} \cdot \text{tress} \cdot \text{ha}^{-1} \cdot 3600^{-1}$ ). In 2016 and 2017, hand thinning of 1 ha in the present orchard with 3125 trees ha<sup>-1</sup> would have required 108 h and 121 h, respectively, in the controls. The differences between both years were expected, because of differences in flower clusters per tree, magnitude of natural fruit abscission and FBC, which was slightly enhanced in 2017 in comparison to 2016, due to the progressed growth of the young trees. Nevertheless, when metamitron was applied twice, the time to hand-thin 1 ha would have been reduced to 44 h and 48 h, in 2016 and 2017 respectively. In comparison, in 2016, when metamitron was applied once at  $D = 12$  mm,  $t_{HT}$  would have been reduced to 67 h ha<sup>-1</sup>, which is a reduction in comparison to the controls by 62 %.

From an economical perspective, the optimum timing for a single application of metamitron at a low concentration would be generally preferred. It was demonstrated that a single application of a low concentration can reduce fruit per tree almost as effective as a double application, with slightly enhanced  $t_{HT}$ . In 2017, however, thinning efficacy at the single applications of metamitron was considerably lower than for the double application, because the mutual effect of high temperature and low solar radiation were not as beneficial for thinning as in 2016. Therefore, the appearance of beneficial weather conditions and a precise weather forecast are crucial for apple fruit thinning with a single application of metamitron at a low concentration.

The fruit quality was high in all treatments (Table 4) because of the additional hand-thinning after fruit drop. The highest percentage of fruit with diameters below 70 mm was 3.8 % on trees thinned with 6-BA in 2016. The red skin colour, which is one important quality attribute of 'RoHo 3615', was high in the fruit of any treatment. Metamitron did not cause skin russetting, which naturally appears in a low percentage around the pedicle of 'RoHo 3615'. Return bloom, expressed as

**Table 4**

Effect of chemical thinning on yield parameters and flower clusters per tree in the subsequent year,  $FC_{yr+1}$ , of 'RoHo 3615'/M.9 trees in two consecutive years. Superscript letters indicate significant differences between means.

Treatment	Time of application	Fruit tree <sup>-1</sup> at harvest	Yield [kg]	Fresh mass [g]	Yield > 60 % red skin [%]	Fruit with skin russetting > 10 % of fruit surface [%]	$FC_{yr+1}$
2016							
Control		91 <sup>b</sup>	18.3 <sup>b</sup>	203.4 <sup>a</sup>	77 <sup>ab</sup>	44 <sup>a</sup>	147 <sup>a</sup>
Metamitron <sup>1</sup>	8 mm, 12 mm	70 <sup>a</sup>	14.5 <sup>a</sup>	208.4 <sup>a</sup>	84 <sup>ab</sup>	49 <sup>a</sup>	161 <sup>b</sup>
Metamitron <sup>1</sup>	8 mm	87 <sup>b</sup>	17.5 <sup>b</sup>	200.6 <sup>a</sup>	75 <sup>a</sup>	36 <sup>a</sup>	150 <sup>a</sup>
Metamitron <sup>1</sup>	12 mm	86 <sup>b</sup>	17.5 <sup>b</sup>	203.0 <sup>a</sup>	78 <sup>ab</sup>	48 <sup>a</sup>	148 <sup>a</sup>
6-BA <sup>2</sup>	8 mm	92 <sup>b</sup>	18.2 <sup>b</sup>	198.3 <sup>a</sup>	76 <sup>a</sup>	48 <sup>a</sup>	146 <sup>a</sup>
Metamitron <sup>1</sup> , Prohexadione-Ca <sup>3</sup> , (NH <sub>4</sub> ) <sub>2</sub> SO <sub>4</sub> <sup>4</sup>	8 mm	83 <sup>b</sup>	16.3 <sup>ab</sup>	198.6 <sup>a</sup>	88 <sup>b</sup>	43 <sup>a</sup>	142 <sup>a</sup>
Metamitron <sup>1</sup> , Citric acid <sup>5</sup>	8 mm	92 <sup>b</sup>	18.1 <sup>b</sup>	195.5 <sup>a</sup>	76 <sup>ab</sup>	44 <sup>a</sup>	146 <sup>a</sup>
2017							
Control		111 <sup>b</sup>	19.8 <sup>b</sup>	177.7 <sup>a</sup>	96 <sup>a</sup>	–	142 <sup>bc</sup>
Metamitron <sup>1</sup>	8 mm, 12 mm	91 <sup>a</sup>	17.2 <sup>a</sup>	189.6 <sup>b</sup>	96 <sup>a</sup>	–	159 <sup>c</sup>
Metamitron <sup>1</sup>	8 mm	108 <sup>b</sup>	19.2 <sup>ab</sup>	177.7 <sup>a</sup>	94 <sup>a</sup>	–	133 <sup>ab</sup>
Metamitron <sup>1</sup>	12 mm	104 <sup>b</sup>	18.6 <sup>ab</sup>	180.7 <sup>ab</sup>	97 <sup>a</sup>	–	127 <sup>a</sup>
6-BA <sup>2</sup>	8 mm	104 <sup>b</sup>	18.5 <sup>ab</sup>	176.8 <sup>a</sup>	94 <sup>a</sup>	–	155 <sup>c</sup>
Metamitron <sup>1</sup> , Prohexadione-Ca <sup>3</sup> , (NH <sub>4</sub> ) <sub>2</sub> SO <sub>4</sub> <sup>4</sup>	8 mm	101 <sup>ab</sup>	17.9 <sup>ab</sup>	175.5 <sup>a</sup>	95 <sup>a</sup>	–	123 <sup>a</sup>
Metamitron <sup>1</sup> , Citric acid <sup>5</sup>	8 mm	103 <sup>ab</sup>	18.7 <sup>ab</sup>	179.6 <sup>ab</sup>	94 <sup>a</sup>	–	129 <sup>ab</sup>

<sup>1)</sup> 165 g ha<sup>-1</sup>; <sup>2)</sup> 150 g ha<sup>-1</sup>; <sup>3)</sup> 106 g ha<sup>-1</sup>; <sup>4)</sup> 563 g ha<sup>-1</sup>; <sup>5)</sup> 500 g ha<sup>-1</sup>.

flower clusters per tree in the year after thinning treatment ( $FC_{yr+1}$ ), was enhanced in 2017, when in 2016 metamitron was applied twice (Table 4). In 2018, return bloom was reduced, when in 2017 metamitron was applied once at  $D = 12$  mm and at  $D = 8$  mm in tank-mix with prohexadione-Ca and ammonium sulphate. Because, 'RoHo 3615' has a general low susceptibility to alternate bearing,  $FC_{yr+1}$  in the year after the metamitron application was, nevertheless, sufficient to achieve the FBC of the trees, assuming that each flower cluster can generate minimum one fruit at harvest (Breen et al., 2016).

#### 4. Conclusion

Metamitron effectively reduced the actual photosynthetic performance ( $J_F$ ) of the leaves of young apple trees of the cultivar 'RoHo 3615' at a low concentration, when applied once, for at least two weeks. However, fruit set reduction was only achieved when warm weather conditions promoted the fruit abscission in the days prior and subsequent to the application. The results pointed out that metamitron applied once can be used for successful fruit thinning of young 'RoHo 3615' apple trees at a low rate ( $165 \text{ g ha}^{-1}$ ), under conditions of high night temperatures and low solar radiation during the day.

When metamitron was applied twice,  $J_F$  was further reduced and the period of photosynthetic inhibition extended, leading to consistent thinning results. The combination with citric acid or prohexadione-Ca and ammonium sulphate caused similar reductions in  $J_F$  as metamitron alone, without any additional effect on fruit thinning or fruit quality.

#### Funding

The trials were funded by the Saxon State Office for Environment, Agriculture and Geology. The publication costs were covered by the Leibniz Institute for Agricultural Engineering and Bioeconomy.

#### CRediT authorship contribution statement

**Martin Penzel:** Software, Data curation, Validation, Writing - review & editing. **Christian Kröling:** Conceptualization, Project administration, Resources, Supervision, Writing - review & editing.

#### Declaration of Competing Interest

The authors declare that they have no known competing financial interests or personal relationships that could have appeared to influence the work reported in this paper.

#### Acknowledgements

We would like to thank Renate Simora for excellent technical support and Werner B. Herppich for helpful comments on the text.

#### References

Anderson, J.L., Richardson, E.A., Kesner, C.D., 1986. Validation of chill unit and flower bud phenology models for 'Montmorency' sour cherry. *Acta Hortic.* 184, 71–75. <https://doi.org/10.17660/ActaHortic.1986.184.7>.

Bangerth, F., 2000. Abscission and thinning of young fruit and their regulation by plant hormones and bioregulators. *Plant Growth Regul.* 31, 43–49. <https://doi.org/10.1023/A:1006398513703>.

Breen, K.C., Tustin, D.S., Palmer, J.W., Close, D.C., 2015. Method of manipulating floral bud density affects fruit set responses and productivity in apple. *Sci. Hortic.-Amsterdam* 197, 244–253. <https://doi.org/10.1016/j.scienta.2015.09.042>.

Breen, K.C., Tustin, D.S., Palmer, J.W., Hedderley, D.I., Close, D.C., 2016. Effects of environment and floral intensity on fruit set behaviour and annual flowering in apple. *Sci. Hortic.-Amsterdam* 210, 258–267. <https://doi.org/10.1016/j.scienta.2016.07.025>.

Byers, R.E., Barden, J.A., Polomski, R.F., Young, R.W., Carbaugh, D.H., 1990. Apple thinning by photosynthetic inhibition. *J. Am. Soc. Hortic. Sci.* 115, 9–13. <https://doi.org/10.21273/JASHS.115.1.14>.

Clever, M., 2018. Effects of solar irradiation and night-time temperature on the thinning efficacy of metamitron (Brevis®) in apple. *Acta Hortic.* 1221, 23–30. <https://doi.org/10.17660/actahortic.2018.1221.4>.

Gonzalez, L., Torres, E., Carbó, J., Alegre, S., Bonany, J., Àvila, G., Martin, B., Recasens, I., Asin, L., 2019. Effect of different application rates of metamitron as fruitlet chemical thinner on thinning efficacy and fluorescence inhibition in Gala and Fuji apple. *Plant Growth Regul.* 89, 259–271. <https://doi.org/10.1007/s10725-019-00531-0>.

Greene, D.W., Lakso, A.N., Robinson, T.L., Schwallier, P., 2013. Development of a fruitlet growth model to predict thinner response on apples. *HortScience* 48, 584–587. <https://doi.org/10.21273/HORTSCI.48.5.584>.

Haller, M.H., Magness, J.R., 1933. Relation of leaf area and position to quality of fruit and to bud differentiation in apples. U. S. Dept. Agriculture. Technical Bulletin 338.

Hansen, P., 1980. Yield components and fruit development in 'Golden Delicious' apples as affected by the timing of nitrogen supply. *Sci. Hortic.-Amsterdam* 12, 243–257. [https://doi.org/10.1016/0304-4238\(80\)90005-9](https://doi.org/10.1016/0304-4238(80)90005-9).

Herppich, W.B., Herppich, M., Tüffers, A., von Willert, D.J., Midgley, G.F., Veste, M., 1998. Photosynthetic responses to CO<sub>2</sub> concentration and photon fluence rates in the CAM-cycling plant *Delosperma tradescantioides* (Mesembryanthemaceae). *New Phytol.* 138, 433–440. <https://doi.org/10.1046/j.1469-8137.1998.00137.x>.

Kon, T.M., Schupp, J.R., Winzeler, H.E., Marini, R.P., 2013. Influence of mechanical string thinning treatments on vegetative and reproductive tissues, fruit set, yield, and fruit quality of 'Gala' apple. *HortScience* 48, 40–46. <https://doi.org/10.21273/HORTSCI.48.1.40>.

Kondo, S., Takahashi, Y., 1987. Effects of high temperature in the nighttime and shading in the daytime on the early drop of apple fruit 'Starking Delicious'. *J. Jpn. Soc. Hortic. Sci.* 56, 142–150. <https://doi.org/10.2503/jjshs.56.142>.

Köpcke, D., 2004. Untersuchungen Zur Chemischen Fruchtausdünnung Mit Metamitron Bei Apfelbäumen (*Malus X Domestica* Borkh.). Ph.D. Thesis. Universität Hannover.

Lakso, A.N., 2011. Early fruit growth and drop: the role of carbon balance in the apple tree. *Acta Hortic.* 903, 733–742. <https://doi.org/10.17660/ActaHortic.2011.903.102>.

Lakso, A.N., Goffinet, M.C., 2017. Advances in understanding apple fruit development. In: Evans, K. (Ed.), *Achieving Sustainable Cultivation of Apples*. Burleigh Dodds Science Publishing, Cambridge, United Kingdom, pp. 103–133.

Lakso, A.N., Robinson, T.L., Greene, D.W., 2006. Integration of environment, physiology and fruit abscission via carbon balance modelling – implications for understanding growth regulator responses. *Acta Hortic.* 727, 321–326. <https://doi.org/10.17660/ActaHortic.2006.727.38>.

Maas, F.M., Meland, M., 2016. Thinning response of 'Summerred' apple to Brevis® in a northern climate. *Acta Hortic.* 1138, 53–60. <https://doi.org/10.17660/ActaHortic.2016.1138.7>.

Matyssek, R., Herppich, W.B., 2019. Chlorophyllfluoreszenzanalyse. Experimentelle Pflanzenökologie. Springer Reference Naturwissenschaften. Springer Spektrum, Berlin, Heidelberg, pp. 1–56. [https://doi.org/10.1007/978-3-662-53493-9\\_13-1](https://doi.org/10.1007/978-3-662-53493-9_13-1).

McArtney, S.J., Obermiller, J.D., 2012. Use of 1-Aminocyclopropane carboxylic acid and metamitron for delayed thinning of apple fruit. *HortScience* 47, 1612–1616. <https://doi.org/10.21273/HORTSCI.47.11.1612>.

McArtney, S.J., Obermiller, J.D., Arellano, C., 2012. Comparison of the effects of metamitron on chlorophyll fluorescence and fruit set in apple and peach. *HortScience* 47, 509–514. <https://doi.org/10.21273/HORTSCI.47.4.509>.

McCree, K.J., 1972. Test of current definitions of photosynthetically active radiation against leaf photosynthesis data. *Agr. Meteorol.* 10, 443–453. [https://doi.org/10.1016/0002-1571\(72\)90045-3](https://doi.org/10.1016/0002-1571(72)90045-3).

Palmer, J.W., 1977. Light transmittance by apple leaves and canopies. *J. Appl. Ecol.* 14, 505–513. <https://doi.org/10.2307/2402562>.

Palmer, J.W., 1992. Effects of varying crop load on photosynthesis, dry matter production and partitioning of Crispin/M.27 apple trees. *Tree Physiol.* 11, 19–33. <https://doi.org/10.1093/treephys/11.1.19>.

Peters, G., 2018. Userfriendlyscience: Quantitative Analysis Made Accessible. <https://doi.org/10.17605/osc.io/txequ>.

R Core Team, 2018. R: a Language and Environment for Statistical Computing. R Foundation for Statistical Computing, Vienna, Austria. <https://www.R-project.org/>.

Robinson, T.L., Lakso, A.N., Greene, D., 2017. Precision crop load management: the practical implementation of physiological models. *Acta Hortic.* 1177, 381–390. <https://doi.org/10.17660/ActaHortic.2017.1177.55>.

Stern, R., 2014. The photosynthesis inhibitor metamitron is an effective fruitlet thinner for 'Gala' apple in the warm climate of Israel. *Sci. Hortic.-Amsterdam* 178, 163–167. <https://doi.org/10.1016/j.scienta.2014.08.005>.

Yuan, R., Greene, D.W., 2000. Benzyladenine as a Chemical Thinner for 'McIntosh' Apples. I. Fruit Thinning Effects and Associated Relationships with Photosynthesis, Assimilate Translocation, and Nonstructural Carbohydrates. *J. Am. Soc. Hortic. Sci.* 125 (2), 169–176. <https://doi.org/10.21273/JASHS.125.2.169>.

Zibordi, M., Domingos, S., Corelli Grappadelli, L., 2009. Thinning apples via shading: an appraisal under field conditions. *J. Hortic. Sci. Biotechnol.* 138–144. <https://doi.org/10.1080/14620316.2009.11512611>. (ISAFRUIT special issue).

Zude-Sasse, M., Herold, B., Geyer, M., 2000. Comparative study on maturity prediction in 'Elstar' and 'Jonagold' apples. *Gartenbauwissenschaft* 65, 260–265. URL: <https://www.pubhort.org/ejhs/2000/6790.htm>.



### **3. Tree adapted mechanical flower thinning on apple prevents yield losses caused by over-thinning of trees with low flower set**

In: European Journal of Horticultural Science 86, pp. 88-98, 2021

Cite as:

Penzel, M., Pflanz, M., Gebbers, R., Zude-Sasse, M., 2021. Tree adapted mechanical flower thinning prevents yield loss caused by over thinning of trees with low flower set in apple. Eur. J. Hortic. Sci. 86, 88-98. <https://doi.org/10.17660/eJHS.2021/86.1.10>



## Original article

# Tree-adapted mechanical flower thinning prevents yield loss caused by over-thinning of trees with low flower set in apple

M. Penzel<sup>1,2</sup>, M. Pflanz<sup>2</sup>, R. Gebbers<sup>2</sup> and M. Zude-Sasse<sup>2</sup><sup>1</sup> Technische Universität Berlin, Chair of Agromechatronics, Berlin, Germany<sup>2</sup> Leibniz Institute for Agricultural Engineering and Bioeconomy (ATB), Potsdam, Germany

## Summary

Flower thinning compromises the continuous yield and fruit quality in the production of apple fruit. The aim of the present study was to investigate the potential of managing spatial heterogeneity in flower set by adapted tree-individual mechanical flower thinning. In the years 2011, 2014–2016, commercial orchards of 'Elstar'/M26 and 'Gala'/M9 trained as slender spindle, with an abundance of varying flower set were mechanically thinned at balloon stage (BBCH 59) with the Darwin 250 device at constant vehicle speed of 8 km h<sup>-1</sup> with varying rotational frequency ranging from 200 revolutions per minute (rpm) to 380 rpm. Rotational frequency of the thinning device was translated to average kinetic energy ( $E_{kin}$  [J]) that one string transfers into the canopy. Thinning treatments ranged between 0.15 J and 0.66 J. For low and medium flower sets, majority of trees underrun production target of 119 fruit and, therefore, no thinning was necessary. Treatments >0.23 J caused yield loss by over-thinning without any positive effect on fruit mass. At high flower set, thinning treatments of 0.23 J and 0.33 J were adequate settings to reduce crop load in 'Elstar' and 0.33 J in 'Gala' without yield loss. The concept of tree adapted flower thinning in comparison to field uniform thinning would result in the avoidance of yield loss by over-thinning of trees with low and medium flower set by 1.4–4.2 t ha<sup>-1</sup> in 'Elstar' and 2.6–7.6 t ha<sup>-1</sup> in 'Gala'. Results indicate the importance of quantifying flower set for precisely defining the intensity of thinning treatment according to the tree's yield capacity.

## Keywords

crop load, 'Elstar', fruit quality, fruit tree, 'Gala', precision horticulture, yield

## Significance of this study

*What is already known on this subject?*

- In former studies, the principle of mechanical thinning with varying parameters was intensively investigated in apple. The spatial variability of soil was shown for many orchards and heterogeneity in flower set is well known in practise.

*What are the new findings?*

- With the proposed method, the actual impact of mechanical thinning becomes comparable by utilizing kinetic energy as one major variable of the thinning treatment. It is shown that field uniform thinning is a cause for yield loss on trees with low flower set, while tree-adapted thinning can optimize the process considering fruit quality and yield.

*What is the expected impact on horticulture?*

- Cultivars showing high variability of flower set can be managed more precisely resulting in enhanced yield.

## Introduction

Apple trees develop an excessive quantity of flowers exceeding the fruit bearing capacity of the tree (Lakso, 2011). This physiological characteristic is desirable regarding yield reliability even in the case of negative environmental impacts, e.g., late frost, hail and rain, which can cause unfavourable pollination conditions and reduce flower and fruit set (Heinicke, 1917; MacDaniels and Heinicke, 1929). Consequently trees frequently bear more fruit than can be supplied appropriately with carbohydrates (Lakso, 2011), leading to minor fruit size and alternate bearing (Jonkers,

1979; Looney, 1993). Endogenous regulation mechanisms of the tree initiate the reduction of crop load by means of fruit abscission. The fruit drop captures unfertilized and poorly developed fruit, which are dominated by fruit with adequate supply of exogenous and endogenous growth factors, visually measurable by common number of seeds (Luckwill, 1953; Bangerth, 2000). The endogenous regulation of fruit drop is, however, often insufficient to reduce crop load to the optimum level considering fruit quality and prevention of alternate bearing. Therefore, management of surplus fruit is required. The optimum crop load of a tree highly depends on the target of fruit size and the availability of resources, especially carbohydrates and water, per fruit. The supply of carbohydrates is limited by the leaf area to fruit ratio of the tree (Haller and Magness, 1933; Preston, 1954; Silbereisen, 1966; Hansen, 1969, 1977). Crop load management can effectively adjust the leaf area to fruit ratio and, therefore, increase fruit growth rate and advance maturity of apple (Palmer et al., 1997; Wünsche et al., 2000). Until the first half of the 20<sup>th</sup> century, hand thinning was the only production measure of crop load management (Dennis, 2000). Meanwhile, chemical thinning has been widely accepted in practice as efficient method for flower and fruit thinning. However, the efficacy depends highly on weather conditions and the thinning intensity is frequently hardly predictable (Stover and Greene, 2005). As an alternative, devices for mechanical flower thinning were developed during the last 30 years with more reliable effects (Schröder, 1996; Bertschinger et

al., 1998; Damerow et al., 2007). The principle is based on a rotating spindle with elastic strings, which remove flowers and flower clusters by the mechanical impact. The spindle is driven by a mechanical or hydraulic system, which allows the adjustment of rotational frequency in revolutions per minute (rpm). The intensity of flower thinning depends of the length of strings, the rotational frequency and the speed of the vehicle. Enhanced rotational frequencies increases flower removal (Zoth, 2011; Kon et al., 2013; Penzel et al., 2020) by the enhanced kinetic energy ( $E_{kin}$ ), which is transferred by the strings into the canopy. The speed of the tractor influences the frequency of hits per tree. The approach of an integrated thinning coefficient described by Solomakhin and Blanke (2010) regards most of these factors and also includes the factor “Fruit set before June drop” in percentage of the flowers. However, the latter doesn’t allow comparing the effects of different treatments on trees with varying flower set, because the flower set dominates the resulting fruit set compared to the effect of the thinning intensity. The formula developed by Zoth (2011) totalizes the kinetic energy, which every centimeter of one string transfers into the canopy.

Apart from the intended treatment, the strings also hit branches and spur leaves emerging earlier than flowers (Kon et al., 2013). Therefore, it is assumed that mechanical thinning has an effect on ethylene production and export from the tissue (Kong et al., 2009), which might trigger fruit abscission (Bangerth, 2000). In general, flower thinning using a mechanical thinning device potentially improves fruit quality and supports return bloom the same way as chemical or mechanical hand thinning (Weibel et al., 2008; Hehnen, 2012). Moreover the profitability can be enhanced due to reduction of labor input (Schupp et al., 2008). Consequently, machine flower thinning is an effective and environmental friendly way of crop load management (Solomakhin and Blanke, 2010), which can also be applied in organic fruit production (Weibel et al., 2008; Sinatsch, 2014) and at any weather condition. In practice, mechanical thinning is performed with field-uniform rotational frequency in the entire orchard, not considering the tree’s individual flower set. This can potentially lead to yield losses by over-thinning of trees with low flower set or minor fruit quality, considering size and taste, as result of under-thinning trees with heavy flower set. Measures of precision horticulture as mentioned by Zude-Sasse et al. (2016) would analyse the spatial heterogeneity in flower set within orchards, and optimize the thinning intensity according to these information. However, there is still a lack of data on machine thinning and quantified gain in yield when optimizing the thinning measure based on the flower set.

The aim of this study was to analyze the effect of field-uniform thinning intensity on (i) the yield considering trees with low, medium, and high flower set, and (ii) the fruit quality and percentage of marketable yield obtained from trees with low, medium, and high flower set.

## Materials and methods

### Experimental sites

The study was carried out in two commercial orchards of *Malus × domestica* Borkh. in the fruit production region of Werder, Brandenburg, Germany. In 2002, trees of the cultivars ‘Elstar’ and ‘Gala’, trained as slender spindle, were planted with a spacing of 3.2 m × 1.2 m, which accounts for 2,604 trees ha<sup>-1</sup>. The rootstock was M26 for ‘Elstar’ and M9 for ‘Gala’. The soil type was a sandy loam. Trees were irri-

gated by drip irrigation. Management of the trees was performed according to the national regulations of integrated production.

For ‘Elstar’, 200 trees were selected for the years 2011, 2014, 2015, while in ‘Gala’ 100 trees were selected in 2014 and 200 trees in 2015 and 2016. The position of every tree was recorded, using a real time kinematic global positioning systems (RTK-GPS) (HiPer Pro, Topcon Corporation, Japan) to investigate the spatial effect on yield parameters.

Trees were thinned mechanically when 50–80% of the flowers reached balloon stage (2011: 27.04; 2014: 22.04; 2015: 30.04; 2016: 06.05.), BBCH 59 (Meier, 1997). Mechanical thinning was carried out using a rotating string thinner (Darwin 250, FruitTec, Germany) equipped with 270 plastic strings each with a length of 60 cm. Diameter of the internal tube of the spindle was 50 mm. The tractor speed was constant at 8 km h<sup>-1</sup> during the treatment, while varying rotational frequency ranging between 200 rpm and 380 rpm was applied. Thinning at 210 + 10 rpm served as basic rotational frequency (brf) and was considered as control, since no or minimum thinning effect was found. No additional hand thinning was conducted.

### Assessment of flower set, thinning efficacy, yield and average fruit mass

The number of flowers was counted from 12 whole trees of ‘Elstar’ in 2011 and 110 branches per cultivar in 2014 to obtain the conversion factor from flowers to clusters, calculated as arithmetic mean of counts. The factors found in 2014 were applied in 2015 and 2016. Prior to each thinning treatment the number of clusters was counted manually for each tree. All fruits were harvested during commercial harvest of this orchard (2011: 17.08; 2014: 05. and 16.09; 2015: 10.-11.09; 2016: 07.-09.09). Crop load, yield, fruit mass, and percentage of marketable yield considering fruit size >65 mm was measured tree-individual with a commercial sorting line (TrueSort, Ellips B.V., The Netherlands). Total thinning efficacy was determined by the percentage of final fruit set (FFS [%]) as number of fruit at harvest per 100 flowers.

### Fruit quality

In every year, at harvest fruit samples from each treatment (2011: 787; 2014: 63; 2015: 2118; 2016: 165 fruits) were analyzed regarding fruit quality. Soluble solids content (SSC [%Brix]) of squeezed juice was measured using a digital refractometer (DR-301-95, Krüss, Germany). Starch breakdown was analyzed by staining the fruit halves with Lugol’s iodine solution and interpreting the starch hydrolysis on a scale between 1 and 10. Fruit flesh firmness (N cm<sup>-2</sup>) was measured with motor-driven, digital penetrometer (Texture-Analyser, TA.XT, Stable Micro Systems Ltd., UK). A handheld spectrophotometer (Pigment Analyzer PA1101, CP, Germany) was used for non-destructive measurement of chlorophyll-related normalized difference vegetation index (NDVI [-1; 1]; Zude, 2003).

### Thinning coefficient

The thinning coefficient was calculated by the average kinetic energy ( $E_{kin}$  [J]) that one string transfers into the canopy. The  $E_{kin}$  calculated for the middle of the string is affected by the mass,  $m$  [kg], and the speed,  $w$  [m s<sup>-1</sup>] of the string (Eq. 1).

$$E_{kin} = \frac{1}{2} \cdot m \cdot w^2 \quad (\text{Eq. 1})$$

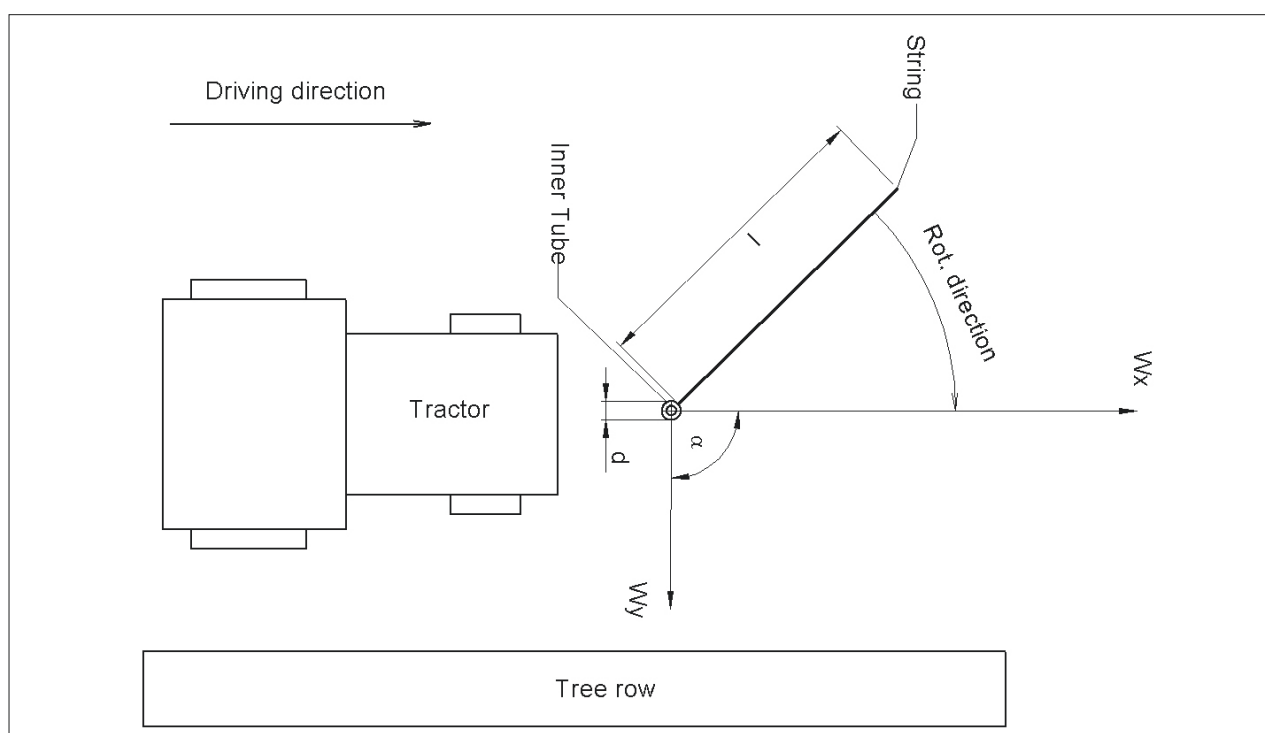


**FIGURE 1.** Scheme of the operating mode of the mechanical thinning device and velocity vectors ( $d$  = diameter of the inner tube of the rotating spindle, where the string is attached;  $l$  = length of the string;  $\alpha$  = the angle between  $w_x$  and  $w_y$ ).

The magnitude of the velocity vector  $w$  of the string consists from the translational movement,  $w_x$ , from the tractor in direction  $x$  and the rotary movement,  $w_y$ , in direction  $y$ , from the spindle (Eq. 2; Figure 1). It is assumed that the rotation is conducted in parallel to the ground and no movement in direction  $z$  occurs.

$$w^2 = w_x^2 + w_y^2 \quad (\text{Eq. 2})$$

The speed  $w_x$  results from the addition of the vector components  $v_x$  and  $u_x$  in the driving direction of the tractor  $x$  (Eq. 3). The vector  $v_x$  equates the speed,  $v$  [ $\text{m s}^{-1}$ ], of the tractor because the motion is rectilinear in one direction.

$$w_x = v_x + u_x \quad (\text{Eq. 3})$$

The speed  $w_y$  results from the addition of the vector components  $v_y$  in direction  $y$ , which equates 0 because the movement of the tractor occurs only in direction  $x$ , and  $u_y$  in direction  $y$  upright to the direction  $x$  (Eq. 4).

$$w_y = v_y + u_y \quad (\text{Eq. 4})$$

The vector components  $u_x$  and  $u_y$  follow from multiplying the circumferential speed  $u$  [ $\text{m s}^{-1}$ ] of the string and the cosine, or sinus respectively of the angle,  $\alpha$  [rad], which is formed by  $w_x$  and  $w_y$ . Because the string hits the tree vertically to the position of the string,  $90^\circ$  are added to  $\alpha$ . (Eq. 5 and 6).

$$u_x = u \cdot \cos(\alpha + 90) \quad (\text{Eq. 5})$$

$$u_y = u \cdot \sin(\alpha + 90) \quad (\text{Eq. 6})$$

The circumferential speed  $u$  [ $\text{m s}^{-1}$ ] results from multiplying the radius,  $r$  [m], at the middle of the string with the rotational frequency  $n$  [ $\text{rad s}^{-1}$ ] of the rotating spindle

(Eq. 7). The radius at the middle of the string,  $r$  [m], captures the half diameter,  $d$  [m], of the inner tube of the rotating spindle, where the string is attached and the half-length,  $l$  [m], of the string (Eq. 8). The rotational frequency  $n$  [ $\text{rad s}^{-1}$ ] results from converting the revolutions per minute (rpm) into the unit  $\text{rad s}^{-1}$  by using Eq. 9.

$$u = r \cdot n \quad (\text{Eq. 7})$$

$$r = \frac{d}{2} + \frac{l}{2} \quad (\text{Eq. 8})$$

$$n = \frac{s}{60} \cdot 2 \cdot \pi \quad (\text{Eq. 9})$$

Eq. 10 displays the resulting overall formula for  $E_{\text{kin}}$  illustrated in Figure 1.

$$E_{\text{kin}} = \frac{1}{2} m \cdot \left( \left( v + \left( \frac{d}{2} + \frac{l}{2} \right) \cdot \frac{s}{60} \cdot 2 \cdot \pi \cdot \cos(\alpha + 90) \right)^2 + \left( \left( \frac{d}{2} + \frac{l}{2} \right) \cdot \frac{s}{60} \cdot 2 \cdot \pi \cdot \sin(\alpha + 90) \right)^2 \right) \quad (\text{Eq. 10})$$

### Statistical analysis

Statistical analyses were carried out in software R v. 3.4.1 (R Core Team, 2018) using the packages 'nlme' (Pinheiro et al., 2018), 'gstat' (Pebesma, 2004), 'sp' (Pebesma and Bivand, 2005), and 'multcomp' (Hothorn et al., 2008). The spatial covariance of latitude and longitude was included in the analysis of variance (ANOVA) when analyzing the effect of thinning treatment on the yield parameters (crop load, final fruit set, average fruit mass, yield and percentage of marketable yield) as described by Crawley (2013). ANOVA results are expressed as  $p$  values in the text. In the case that no significant effect of latitude and longitude on individual traits was found, Dunn's Test (Dinno, 2017) was used for pairwise comparisons of treatments at 5% confidence level.

## Results

### Number of flowers

The average number of flowers per cluster was  $4.3 \pm 0.6$  for 'Elstar' in 2011 and  $4.7 \pm 0.3$  for 'Elstar' and  $5.2 \pm 0.3$  for 'Gala' in 2014. The absolute number and the distribution of the estimated flower set, based on counting clusters of the investigated trees, varied considerably between cultivars and years (Figure 2). 'Elstar' showed a low flower set with arithmetic mean of 249, 246, 646 in 2011, 2014, 2015, respectively, in comparison to 'Gala' with a flower set of 541, 532, 1,434 in 2014, 2015, 2016, respectively. In 'Elstar', trees with no flowers appeared, which were excluded from further analysis (Table 1). The highest flower set of 'Elstar' was 2,162 observed on one single tree in 2015, however the 95<sup>th</sup> quantile of the flower set was 1,206, demonstrating that 'Elstar' possesses a huge variability in flower set. For 'Gala',

the maximum flower set was 3,245 in 2016, representing an extreme value regarding 95<sup>th</sup> quantile of 2,149 in the same year. Trees showing extreme high flower set were excluded as residues to avoid overestimation of the effect of thinning intensity. Trees were grouped in 3 classes according to low, medium, and high flower set per year (Tables 1 and 2).

### Thinning coefficient

The angle of the string to the driving direction has an impact on  $E_{kin}$  (Figure 3). Considering the settings of the Darwin device used in the present trials, the angle of the string generated a difference in  $E_{kin}$  of 0.29 J at 380 rpm, 8 km h<sup>-1</sup> due to the possible angles between 0 and 180 degrees, with 0 degree and 180 degrees resulting in maximum and 90° in minimum  $E_{kin}$  for each rotation.

The speed of the tractor resulted in a reduced effect on  $E_{kin}$  considering the operation speeds described earlier and,

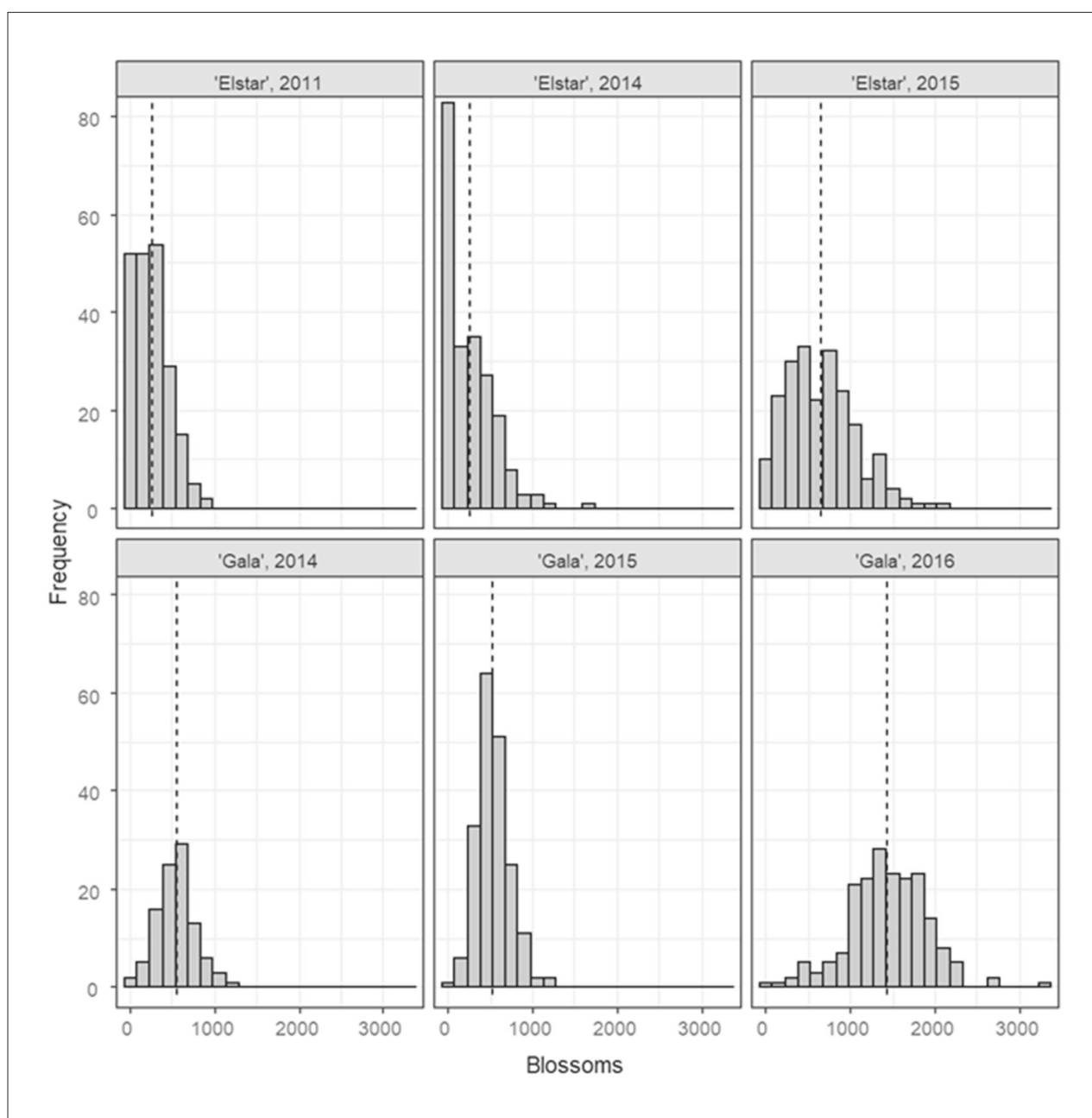


**FIGURE 2.** Distribution of number of flowers per tree estimated by counting the ratio flowers to clusters in one year and clusters in all years in 'Elstar'/M26 and 'Gala'/M9 providing a class width of 150. Dashed line marks the mean value.



**TABLE 1.** Class ranges of flower set defined as low, medium, and high used for further analyses in three years of 'Elstar'/M26.

Flower set	Class	2011		2014		Flower set	Class	2015	
		n	$\bar{x}$	n	$\bar{x}$			n	$\bar{x}$
0	–	–	–	18	0	0	–	2	0
1–200	Low	99	84.5	89	57.5	1–350	Low	57	195.9
201–400	Medium	64	292.8	52	296.5	351–700	Medium	67	519.4
401–800	High	44	529.3	46	556.6	701–1,400	High	82	962.5
Residue	–	2	–	8	–	Residue	–	9	–

**TABLE 2.** Class ranges of flower set defined as low, medium, and high used for further analyses in three years of 'Gala'/M9.

Flower set	Class	2014		2015		Flower set	Class	2016	
		n	$\bar{x}$	n	$\bar{x}$			n	$\bar{x}$
50–350	Low	22	242.5	30	269.2	650–1,150	Low	45	989.6
350–600	Medium	45	510.5	105	479.6	1,151–1,650	Medium	75	1,412.7
600–1,000	High	29	740.9	58	742.7	1,651–2,150	High	56	1,849.5
Residue	–	4	–	7	–	Residue	–	24	–

to our knowledge, applied in practice ranging from 2.5 km h<sup>-1</sup> to 12.0 km h<sup>-1</sup> (Kon et al., 2013). At rotational frequency of 380 rpm, this difference in tractor speed caused a maximum spread of 0.19 J, regarding the angle of the string at 135° to the driving direction. However, the effects of rotational frequency and length of the string represent the major factors with quadratic effect on  $E_{kin}$  per hit calculated for the middle of the rotating string (Eq. 10). For the 60-cm strings and 8 km h<sup>-1</sup> used in the present study, the average  $E_{kin}$  per hit calculated at the middle of the string at an angle of 135 degree, ranged from 0.15 J at 200 rpm to 0.66 J at 380 rpm.

### Thinning efficacy, yield, fruit mass

**1. Spatial autocorrelation.** Variograms (21 figures per trial, not shown) were used for selecting post hoc or adapted post hoc test. For the final fruit set (FFS) and percentage of marketable yield no spatial effect was found in any trial. In 'Elstar', an adapted post hoc test was applied for yield, crop load, and average fruit mass where a spatial effect was found until a distance of 30 m between the trees. For 'Gala' spatial effects were found until a distance of 15 m in 2014 and until 20 m in 2015 and 2016, considering the variables yield, crop load, and average fruit mass.

**2. Influence of thinning treatment on final fruit set.** The FFS, representing the percentage of fruit developed from 100 flowers, differed between cultivars, years and particularly within the same year between the three classes of flower set (Tables 1 and 2). Furthermore, FFS was influenced by thinning treatment in both cultivars in every year. FFS ranged from 2.7% considering trees with high flower set in 2016 to 48.4% considering trees with low flower set in 2015.

For low flower set, in 'Elstar' 2011 (Figure 4) and 2014, thinning treatment of 0.33 J and higher reduced FFS (2011:  $p < 0.01$ ; 2014:  $p = 0.03$ ) in comparison to the basic rotational frequency (brf) of 0.15 J. In 2015, treatment above or equal to 0.28 J had an effect (2015:  $p < 0.001$ ) on FFS in comparison to brf of 0.19 J (Table 3). In 'Gala' 2014, no effect of thinning treatment on FFS was observed for trees with low flower set (Figure 5). In 2015, no statistical evaluation was possible since significant differences in flower set occurred within this class. In 'Gala' 2016, treatments of 0.39 J and higher reduced FFS ( $p < 0.01$ ) considering trees with low flower set from 8.2% to 3.8% and lower.

At medium flower set, in 'Elstar' 2011 treatments of 0.33 J and 0.45 J reduced FFS ( $p < 0.01$ ) in comparison to brf (Figure 4), while in 2014 only 0.45 J caused a significant re-

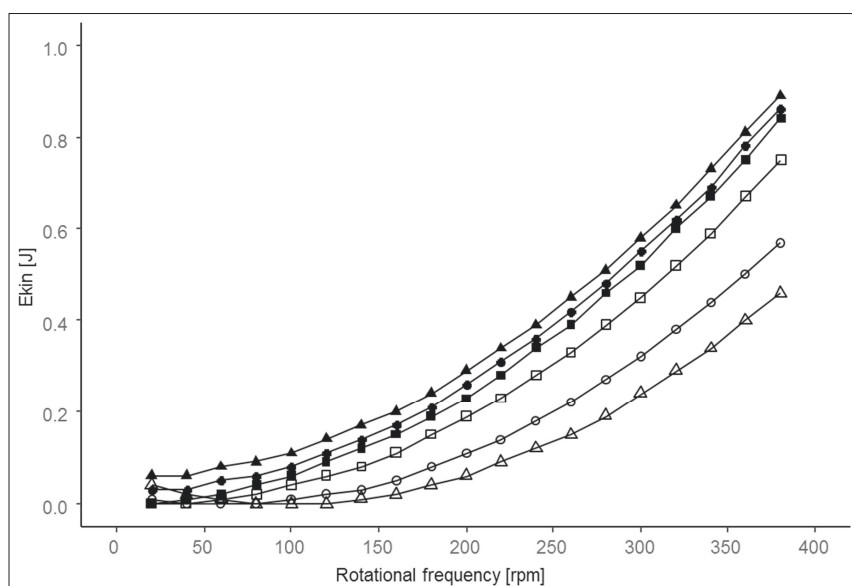


**FIGURE 3.** Calculated  $E_{kin}$  occurring during mechanical thinning, considering one hit of in the middle of the 60 cm string at varying tractor speed (2.5 km h<sup>-1</sup> = square, 8.0 km h<sup>-1</sup> = circle, and 12.0 km h<sup>-1</sup> = triangle) at 90° (open symbol) and 180° (closed symbol) angle of the string to the driving direction.

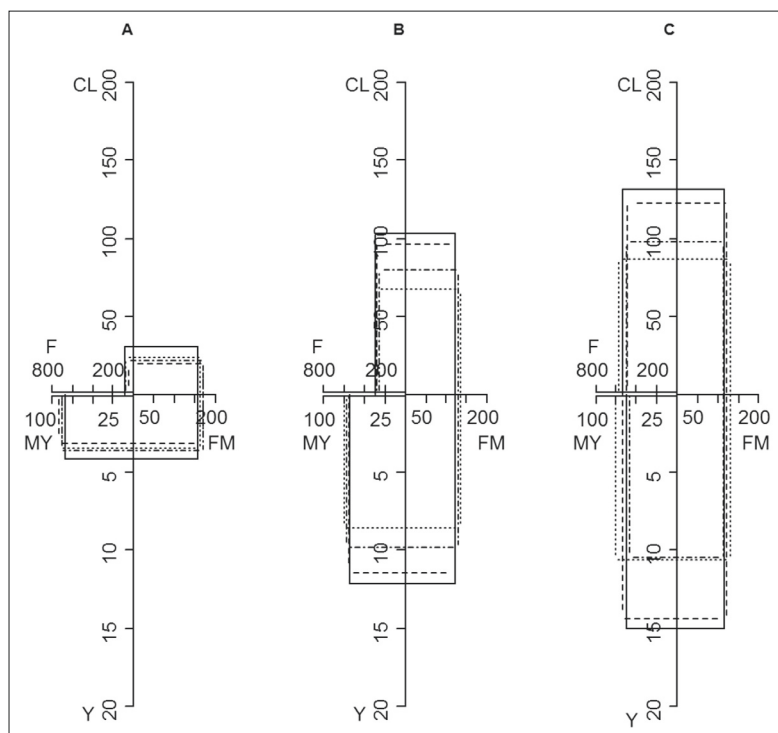


**FIGURE 4.** Effect of mechanical thinning treatment (solid lines = 0.15 J, dashed lines = 0.23 J, dotted lines = 0.33 J, dash-dotted lines = 0.45 J) on crop load (CL as number of fruit per tree), fresh mass (FM in g), absolute yield (Y in kg), and percentage of marketable yield (MY, %) considering classes of flower set: (A) low: 1–200, (B) medium: 201–400, and (C) high: 401–800 flowers (F) of ‘Elstar’/ M26 in 2011.

**TABLE 3.** Effect ( $\alpha=5\%$ ) of mechanical thinning treatment (first letter) and flower set (second letter) on yield parameters of ‘Elstar’ in two years.

Flower set	Thinning treatment $E_{kin}$ (J)	Crop load (fruit/tree)	Final fruit set (fruit $10^{-2}$ flowers)	Yield (kg)	Fruit mass (g)	Marketable yield (%)
2014						
Low	0.15	21.8 <sup>BC, a</sup>	38.9 <sup>B, b</sup>	4.0 <sup>BC, a</sup>	196.9 <sup>A, b</sup>	97.7 <sup>A, b</sup>
	0.23	33.3 <sup>C, a</sup>	39.6 <sup>B, b</sup>	5.3 <sup>C, a</sup>	182.8 <sup>A, b</sup>	95.5 <sup>A, b</sup>
	0.33	14.6 <sup>AB, a</sup>	26.4 <sup>A, a</sup>	2.7 <sup>AB, a</sup>	182.1 <sup>A, b</sup>	96.5 <sup>A, b</sup>
	0.45	16.2 <sup>A, a</sup>	27.8 <sup>A, a</sup>	2.7 <sup>A, a</sup>	171.1 <sup>A, b</sup>	93.8 <sup>A, b</sup>
Medium	0.15	100.5 <sup>A, b</sup>	35.4 <sup>B, b</sup>	13.1 <sup>A, b</sup>	130.8 <sup>A, a</sup>	77.7 <sup>A, a</sup>
	0.23	110.3 <sup>A, b</sup>	39.4 <sup>B, ab</sup>	16.0 <sup>A, b</sup>	145.8 <sup>A, a</sup>	86.2 <sup>A, a</sup>
	0.33	101.4 <sup>A, b</sup>	35.7 <sup>B, b</sup>	15.5 <sup>A, b</sup>	153.4 <sup>A, b</sup>	90.3 <sup>A, b</sup>
	0.45	87.4 <sup>A, b</sup>	26.8 <sup>A, a</sup>	12.4 <sup>A, b</sup>	136.0 <sup>A, a</sup>	84.6 <sup>A, ab</sup>
High	0.15	131.9 <sup>A, c</sup>	25.3 <sup>B, a</sup>	16.0 <sup>A, b</sup>	119.9 <sup>A, a</sup>	67.9 <sup>A, a</sup>
	0.23	126.5 <sup>A, b</sup>	24.5 <sup>AB, a</sup>	14.7 <sup>A, b</sup>	116.6 <sup>A, a</sup>	63.3 <sup>A, a</sup>
	0.33	125.2 <sup>A, b</sup>	22.8 <sup>AB, a</sup>	14.7 <sup>A, b</sup>	117.1 <sup>A, a</sup>	69.7 <sup>A, a</sup>
	0.45	107.3 <sup>A, b</sup>	19.0 <sup>A, a</sup>	12.9 <sup>A, b</sup>	118.6 <sup>A, a</sup>	72.5 <sup>A, a</sup>
2015						
Low	0.19	85.5 <sup>C, a</sup>	48.4 <sup>C, b</sup>	13.4 <sup>C, a</sup>	168.4 <sup>A, b</sup>	91.2 <sup>A, b</sup>
	0.23	58.1 <sup>BC, a</sup>	36.1 <sup>BC, a</sup>	10.0 <sup>BC, a</sup>	176.1 <sup>A, c</sup>	95.7 <sup>A, b</sup>
	0.28	40.3 <sup>AB, a</sup>	21.7 <sup>AB, a</sup>	6.9 <sup>AB, a</sup>	159.0 <sup>A, b</sup>	87.4 <sup>A, b</sup>
	0.45	26.7 <sup>A, a</sup>	11.8 <sup>A, a</sup>	4.3 <sup>A, a</sup>	146.8 <sup>A, a</sup>	89.4 <sup>A, a</sup>
Medium	0.19	123.4 <sup>B, ab</sup>	23.2 <sup>B, a</sup>	17.8 <sup>B, a</sup>	144.9 <sup>A, b</sup>	85.4 <sup>A, b</sup>
	0.23	113.2 <sup>B, b</sup>	22.5 <sup>B, a</sup>	16.4 <sup>B, ab</sup>	141.6 <sup>A, b</sup>	80.8 <sup>A, ab</sup>
	0.28	110.8 <sup>B, b</sup>	21.5 <sup>B, a</sup>	13.6 <sup>AB, b</sup>	131.7 <sup>A, ab</sup>	76.0 <sup>A, ab</sup>
	0.45	73.5 <sup>A, b</sup>	14.3 <sup>A, a</sup>	10.7 <sup>A, b</sup>	149.7 <sup>A, a</sup>	87.8 <sup>A, a</sup>
High	0.19	162.8 <sup>B, b</sup>	17.1 <sup>B, a</sup>	16.1 <sup>A, a</sup>	100.7 <sup>A, a</sup>	55.3 <sup>A, a</sup>
	0.23	172.9 <sup>B, c</sup>	19.1 <sup>B, a</sup>	18.4 <sup>A, b</sup>	106.0 <sup>A, a</sup>	60.7 <sup>A, a</sup>
	0.28	142.3 <sup>AB, c</sup>	15.9 <sup>AB, a</sup>	16.0 <sup>A, b</sup>	113.3 <sup>A, ab</sup>	65.9 <sup>A, a</sup>
	0.45	108.5 <sup>A, b</sup>	10.8 <sup>A, a</sup>	15.3 <sup>A, b</sup>	146.9 <sup>B, b</sup>	87.1 <sup>B, b</sup>

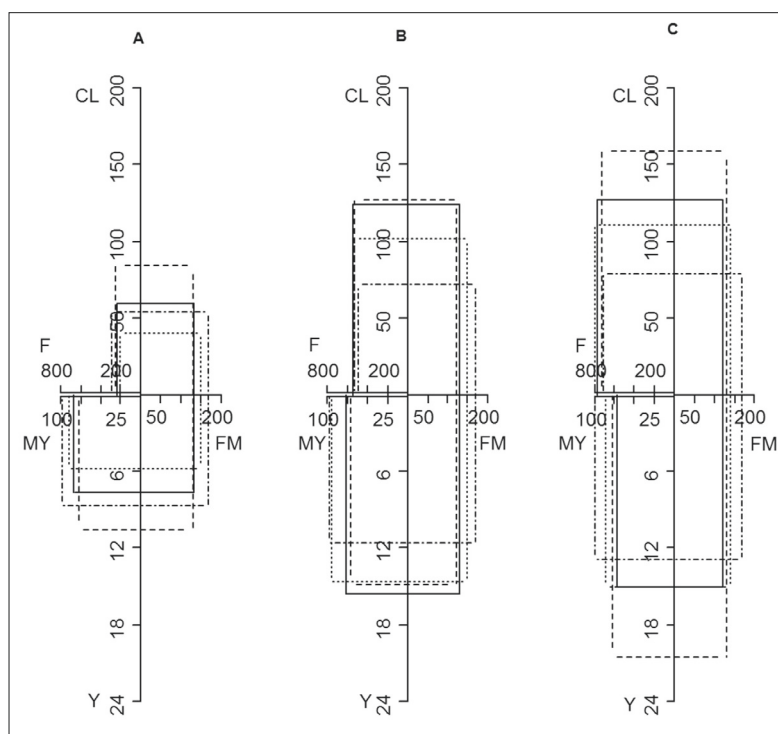


**FIGURE 5.** Effect of thinning intensity (solid lines = 0.15 J, dashed lines = 0.23 J, dotted lines = 0.33 J, dash-dotted lines = 0.45 J) on absolute crop load (CL in number of fruit per tree), fresh mass (FM in g), total yield (Y in kg), and percentage of marketable yield (MY, %) considering classes of flower set: (A) low: 50–350, (B) medium: 351–600, and (C) high: 601–1,000 flowers (F) of ‘Gala’/M9 in 2014.

duction in ‘Elstar’ ( $p=0.05$ ) and in ‘Gala’ ( $p<0.01$ ) (Figure 5). In 2015, treatments of 0.45 J and higher reduced FFS (2015:  $p=0.02$ ) in ‘Elstar’, while 0.28 J and higher resulted in a reduction of FFS in ‘Gala’ 2015 ( $p=0.01$ ) and 0.39 J and higher in 2016 ( $p<0.001$ ).

At high flower set, ‘Elstar’ in 2011 (Figure 4), treatment of 0.33 J and 0.45 J caused again reduction of FFS ( $p=0.04$ ;  $p<0.01$ ), while in 2014 and 2015 (Table 3) only 0.45 J resulted in the same effect (2014:  $p=0.04$ ; 2015:  $p=0.02$ ). In ‘Gala’ 2014 (Figure 5), at high flower set only treatment of 0.45 J had a reducing effect on FFS in comparison to brf ( $p=0.05$ ). In 2015, treatments of 0.28 J and higher  $E_{kin}$  reduced flower set at  $p=0.01$  and  $p<0.01$ , respectively.

**3. Influence of thinning treatment on yield.** The sampling date for laboratory analyses of fruit quality was set at the

commercial harvest date for direct marketing from the same orchards. No correlation was found between crop load and quality parameters except for fruit mass (Figures 4 and 5). In ‘Elstar’, trees with low flower set and thinning treatment equal or higher than 0.33 J in 2011, 2014 and 0.28 J in 2015 had a reduced crop load compared to brf, resulting in yield losses (Figure 4; Table 3). In none of the trials thinning showed a positive effect on fruit mass or percentage of marketable yield (Table 4). In ‘Gala’, trees with low flower set showed no reduction in yield in 2014, however, at 0.45 J average fruit mass was enhanced by 35.8 g ( $p=0.01$ ) to 166.4 g with an effect on percentage of marketable yield ( $p=0.01$ ) which reached 99.0%. In 2016, treatment with 0.39 J caused reduction ( $p=0.02$ ) of marketable yield by 5.4 kg per tree in comparison to brf.

**TABLE 4.** Change of marketable yield (fruit size >65 mm) caused by mechanical thinning treatment in comparison to basic rotational frequency (brf) in ‘Elstar’/M26 considering three classes of flower set.

Year	Marketable yield at brf (kg)	Lowest treatment causing yield reduction* (J)	Reduction* of marketable yield per tree (kg)	Reduction of marketable yield per ha (t)
Low flower set				
2011	4.2	0.33	0.9	1.1
2014	3.9	0.33	1.3	1.4
2015	12.2	0.33	6.2	4.2
Medium flower set				
2011	7.4	No reduction	0	0
2014	10.2	No reduction	0	0
2015	14.5	0.45	5.1	5
High flower set				
2011	12.3	0.33	4	2.2
2014	10.9	0.45	1.5	1.5
2015	8.9	No reduction	0	0

\*: Reduction of marketable yield in comparison to brf calculated as mean value from the total yield and percentage of marketable yield >65 mm per tree.



In 'Elstar' trees with medium flower set, thinning treatment with 0.33 J reduced crop load in 2011 and 0.45 J in 2015, hence yield was reduced. In 2011, thinning at 0.33 increased fruit mass ( $p=0.03$ ) by 14.6 g in comparison to brf, however without effect on percentage of marketable yield (Figure 4). In 2014, 'Gala' showing medium flower set responded to the treatment with 0.45 J ( $p<0.001$ ) (Figure 5). Already at 0.33 J, fruit mass ( $p=0.04$ ) was enhanced. At 0.45 J, average yield per tree was reduced with positive effect on percentage of marketable yield ( $p<0.001$ ), which was enhanced by 20.7% to 97.5% (Figure 5). No effect was found in 2015 and 2016.

At high flower set, in 2011 crop load was reduced in 'Elstar' at 0.33 J ( $p<0.01$ ) and 0.45 J ( $p=0.02$ ) reducing yield per tree with no effect on average fruit mass (Figure 4; Table 4). At high flower set in 'Elstar' 2015 treatment with 0.45 J reduced crop load ( $p=0.02$ ), while gaining fruit mass ( $p=0.02$ ) and increasing the marketable yield ( $p=0.004$ ) (Table 3). In 'Gala' 2014, only treatment with 0.45 J reduced crop load ( $p=0.03$ ) and percentage of marketable yield was enhanced ( $p=0.001$ ) to 99.3% (Figure 5). In 2015 and 2016, at high flower set, 0.28 J reduced crop load and yield per tree in comparison to brf. Average fruit mass was not affected by thinning treatment, as well as percentage of marketable yield, which was already close to 100% at brf. Due to lack of changes in the marketable yield, which was already high in years 2015 and 2016, Tables 3 and 4 weren't reproduced for 'Gala'.

## Discussion

### Flower set

Variability in flower set occurs naturally within orchards and was described earlier (Bukovac et al., 2010; Stopar, 2010; Hočevár et al., 2014; Sinatsch et al., 2014; Beber et al., 2016). In the present study, the variability among flower set was used to classify trees according to the apparent flower set in order to investigate the effect of thinning intensity for each class separately. The size of the classes resulted from the pragmatic approach to meet the requirements for statistical analysis (Table 1). Analysis of variance showed no significant differences in flower set within the classes (Stopar, 2010).

Variability in flower set in the present trials can be explained with the light terrain gradient within the orchard causing spatial distribution of water availability (Moore et al., 1993), nutrients supply (Aandahl, 1948), and occurrence of frost (Weise, 1978). Since these factors have a known effect on crop load (Powell, 1974; Hansen, 1980; Heinicke, 1917), they influence flower bud initiation, leading to spatial variability of flower set. On the hillside, trees showed a tendency of enhanced flower set compared to trees located in region of slightly lower elevation showing stronger vegetative growth assumingly due to late frost events. In cultivar 'Elstar', a higher percentage of trees with low flower set was found compared to 'Gala', which was expected because 'Elstar' is known in practice as biannual bearing cultivar. In order to achieve the growth capacity, trees should bear approximately one apple per 14–42 leaves (Haller and Magness, 1933; Preston, 1954; Silbereisen, 1966; Hansen, 1969) depending on cultivar and growth factors. Unpublished data of 2008 from the same 'Elstar' orchard showed that the leaf number per trees ranged between 2,600 and 4,540. Under the assumption that the necessary leaf number per fruit to produce a marketable size is 30, the trees can hypothetically support 87–151 fruit. This huge variation points to spatial variation

in growth production target (PT) which was in average 117 fruit per tree. The number of flowers to reach the optimum crop load per tree should be slightly enhanced to the PT due to natural fruit drop taking place after flower thinning. In 'Elstar', the fruit drop resulted in crop loads slightly below the PT. In 'Gala', on the other hand, a high percentage of the trees reached PT. The counting of flowers or clusters in practice is time consuming, but necessary to conclude on the target thinning intensity. Automated counting of flowers is required and can be performed with optical sensors and corresponding algorithms (Hočevár et al., 2014; Krikeb et al., 2017). Integrated systems for flower counting and actuator for adaptive mechanical flower thinning are under development (Pflanz et al., 2016), while quantitative data on the thinning requests of individual trees are still rare.

### Thinning coefficient

For comparing the effect of thinning treatments of different experiments, a thinning coefficient is proposed regarding the variables of the devices and treatments. Most important, the coefficient includes the number, length, and mass of the strings, the tractor speed, and the rotational frequency. The formula developed by Zoth (2011) was modified in the present work by adding the angle of the string to the driving direction as a separate factor, which also has an effect on the kinetic energy,  $E_{kin}$  (Figure 3). As simplification, the average  $E_{kin}$  is emphasized, which is achieved in the middle of the string.  $E_{kin}$  at different points of the string varies, consistently according to the distance to the rotating spindle (Figure 3). The  $E_{kin}$  is limited because it ignores the frequency of hits per string in the turbulent application, which is affected by the distance between the device and the tree and the amount of strings of the device. Particularly, the number of stings has a significant effect on thinning efficacy (Kon et al., 2013), but more experiments are needed to test linearity of various numbers of strings and resulting  $E_{kin}$ . For this purpose the distance of the tractor to the tree row needs to be included to calculate the size of the section of tree row which one string possibly hits at one rotation and the depth one string penetrates the canopy. This could be a helpful tool for further optimization of the settings of the device and additionally the shape of the canopy. Clearly visible already with the present simple approach is the effect of the length of one string, which explains the frequently observed phenomenon in practice that used, worn-out strings demand a higher rotational frequency to achieve the same efficacy as new strings.

### Thinning efficacy, yield, fruit mass

Mechanical thinning is an effective measure for crop load management in practice (Schröder, 1996; Bertschinger et al., 1998; Damerow et al., 2007; Weibel et al., 2008; Schupp et al., 2008; Kong et al., 2009; Solomakhin and Blanke, 2010; Hehnen et al., 2012; Kon et al., 2013; Sinatsch et al., 2014; McClure and Cline, 2015; Beber, 2016; Lordan et al., 2018). An overview about the settings of the devices and the thinning efficacy from the literature is given by Kon et al. (2013). A model was developed by Lordan et al. (2018) to predict the final fruit number per tree from the number of flower clusters at different settings of the Darwin thinner considering vehicle speed and rotational frequency. All previous studies report a reduction of fruit set by means of mechanical field-uniform thinning in comparison to the control. Few work was published on thinning intensity adapted to the actual flower intensity (Stopar, 2010; Beber

et al., 2016) although spatial variation within orchards was proved earlier (Manfrini et al., 2009; Aggelopoulou et al., 2010, 2011; Bukovac et al., 2010). Stopar (2010) classified trees according to the number of flower clusters to precisely assess the effect of varying thinning treatments. In the present study, the spatial correlation was recognized by means of semi-variograms (Crawley, 2013).

Results indicate an expected close relationship between flower set and final fruit set. In trees with low flower set, fruit drop was apparently reduced as pointed out earlier (Penzel et al., 2020). Consequently, the comparison of final fruit set (FFS) after varying thinning treatment should be carried out considering trees with similar abundance of flower set, which is a factor with a strong effect on FFS. Furthermore, a positive correlation exists between mechanical thinning and reduction of fruit set regardless of flower set as confirmed in the present study. At low flower set, thinning was not necessary, because in none of the trials the production target of 119 was realized. The 0.23 J treatment showed no effect on FFS in comparison to brf. Consistently, the fruit mass and percentage of marketable yield was hardly affected by thinning treatment, similar to the findings in the literature on mechanical thinning (Beber et al., 2016) and chemical thinning (Greene, 1989; Stophar, 2010). Beber et al. (2016) pointed out that thinning is not necessary to achieve good fruit quality when trees had <80 flower clusters, which equals <400 flowers assuming that one cluster consists of an average of five flowers in the cultivar 'Jonagold'. Mechanical thinning treatment further reduced FFS leading to absolute yield losses. The cortex cell number is positively correlated with fruit mass and thinning at full bloom is the optimum timing for stimulating cell division (Goffinet et al., 1995). However, in the present trials effect on fruit mass was limited, since it can be assumed that the remaining fruit had a sufficient supply of carbohydrates, nutrients and water. Also, no effect of thinning treatments on fruit maturity was found for trees with low crop load as previous studies suggested (Volz et al., 1993; Wünsche and Ferguson, 2005) considering maturity parameters as background color, firmness, and starch index.

At medium flower set, thinning was still hardly necessary as PT of 119 in 'Elstar' was obtained in 2015 and 'Gala' in 2014 at brf. In the other trials, final fruit number at low thinning treatment was below the optimum and further reduced by thinning treatment  $\geq 0.33$  J for 'Gala' and  $\geq 0.33$  J or  $\geq 0.45$  J, depending on the year, in 'Elstar'. However, the percentage of marketable yield showed no increase in 'Elstar' considering any year, pointing out that obviously a crop load equal or lower than the PT will have no effect on percentage of marketable yield. Though, average fruit mass of 'Elstar' 2011 was further enhanced by thinning treatments, which may indeed have a positive effect on market value. In 'Gala', fruit mass was significantly enhanced in two years, whereas the percentage of marketable yield was enhanced only in 2014. In the subsequent years the low fruit set resulted in high percentage of marketable yield of >90% in all treatments. Consequently, thinning at medium flower set results in yield losses as the effect on quality was marginal. Maximum thinning treatment in medium classes of flower set therefore should be 0.23 J for the two cultivars.

At high flower set PT was not exceeded when thinned at brf (Sinatsch et al., 2014; McClure and Cline, 2015). For 'Gala' in 2014 treatment of 0.33 J was appropriate to reach PT. Enhanced thinning treatment reduced fruit set heavily, and fruit mass was increased with every fruit having a

marketable size. Lower thinning treatments resulted in crop load exceeding PT with negative effect on fruit mass. Kon (2013) reported for similar  $E_{kin} \geq 0.27$  J, calculated with prior described thinning coefficient, that leaf injury is high. Such finding may be explained by higher frequency of hits per leaf than in the present study because of the lower vehicle speed. Also, McClure and Cline (2015) noticed leaf injuries when vehicle speed was low. As compromise of thinning response and tree damage, Kon (2013) suggested thinning at lower rotational frequencies equaling 0.14 J or 0.20 J for 'Gala'. However, it was emphasized that these intensities may not thin sufficiently in heavy cropping years and recommended the combination with other thinning methods. McClure and Cline (2015) also reported no effect on fruit mass when thinned up to 0.29 J at low vehicle speed, though marketable yield was adequate already in the control.

In 'Elstar' 2011, treatment of 0.23 J reduced crop load close to PT, though no effect on fruit mass was achieved. This may have resulted from damage on spur leaves, which was not further evaluated. In 2014, treatments of 0.23 J and 0.33 J provided the optimum thinning treatment in terms of crop load, while in 2015 treatments >0.28 J and <0.45 J have caused best results regarding crop load level and fruit mass as crop load at applied treatments exceeded or underrun PT. For practical use, considering high levels of flower set on 'Elstar', 0.23 J and 0.33 J are adequate treatments to reduce crop load. Sinatsch et al. (2014) suggested treatments of 0.19 J or 0.23 J for 'Elstar' trees with high flower set positively affecting fruit size and reducing biannual bearing.

In summary all treatments indicate that different levels of flower set require different settings of the thinning device for best thinning results. A model for thinning response depending on flower set and settings for the Darwin with high  $R^2$  as Lordan and co-workers (Lordan et al., 2018) developed for two cultivars was not possible from the present data. However, data indicate that tree adapted mechanical thinning can decrease possible yield losses by over-thinning at low and medium flower set. High flower set in contrast requires enhanced thinning intensity as crop loads possibly exceed PT. Reduced percentage of marketable yield by field-uniform mechanical thinning ranged from  $1.4 \text{ t ha}^{-1}$  –  $4.2 \text{ t ha}^{-1}$  in 'Elstar' in years 2011, 2014, 2015, and  $2.6 \text{ t ha}^{-1}$  –  $7.6 \text{ t ha}^{-1}$  in 'Gala' in 2014. Consequently, tree-adapted thinning is a promising method to increase production volume without increasing land consumption. When commercial systems for tree-adapted thinning become available, the economic aspect is crucial for the farmer.

## Conclusion

The present study showed that heterogeneity in flower set is existing and trees with different abundance of flowers demand adapted treatment in terms of flower thinning intensity. The concept of mechanical thinning considering the flower set was further evaluated and showed the capability to reduce yield losses by over-thinning of trees with low flower set, while increasing yield per hectare by  $1.4$ – $4.2 \text{ t ha}^{-1}$  in 'Elstar' and  $2.6$ – $7.6 \text{ t ha}^{-1}$  in 'Gala'. When commercially available, this approach of precise management can potentially balance spatial heterogeneity within orchards.

## Acknowledgments

The authors acknowledge Dr. K. Gottschalk for his expertise on developing the formula for calculating kinetic energy of rotating strings and Dr. M. Schirrmann for his support on the application of spatial statistic.

## References

- Aandahl, A.R. (1948). The characterization of slope positions and their influence on the total N content of a few virgin soils in Western Iowa. *Soil Sci. Soc. Am. Proc.* 13, 449–454. <https://doi.org/10.2136/sssaj1949.036159950013000C0081x>.
- Aggelopoulou, K.D., Wulfsohn, D., Fountas, S., Gemtos, T.A., Nanos, G.D., and Blackmore, S. (2010). Spatial variation in yield and quality in a small apple orchard. *Precision Agric.* 11, 538–556. <https://doi.org/10.1007/s11119-009-9146-9>.
- Aggelopoulou, K.D., Pateras, D., Fountas, S., Gemtos, T.A., and Nanos, G.D. (2011). Soil spatial variability and site-specific fertilization maps in an apple orchard. *Precision Agric.* 12, 118–129. <https://doi.org/10.1007/s11119-010-9161-x>.
- Bangerth, F. (2000). Abscission and thinning of young fruit and their regulation by plant hormones and bioregulators. *Plant Growth Regul.* 31, 43–49. <https://doi.org/10.1023/A:1006398513703>.
- Beber, M., Donik Purgaj, B., and Veberič, R. (2016). The influence of mechanical thinning on fruit quality and constant bearing of 'Jonagold' apples. *Acta Hortic.* 1139, 513–518. <https://doi.org/10.17660/ActaHortic.2016.1139.88>.
- Bertschinger, L., Stadler, L., Stadler, W., Weibel, F., and Schumacher, R. (1998). New methods of environmentally safe regulation of flower and fruit set and of alternate bearing of apple crop. *Acta Hortic.* 466, 65–70. <http://dx.doi.org/10.17660/ActaHortic.1998.466.11>.
- Bukovac, M.J., Sabbatini, P., Zucconi, F., and Schwallier, P.G. (2010). A long-term study on native variation of flowering and fruiting in spur-type 'Delicious' apple. *HortScience* 45, 22–29. <https://doi.org/10.21273/HORTSCI.45.1.22>.
- Crawley, M.J. (2013). *The R book*, 2<sup>nd</sup> edn. (Chichester, U.K.: Wiley), p. 860–866.
- Damerow, L., Kunz, A., and Blanke, M. (2007). Mechanische Fruchtbehangsregulierung. *Erwerbs-Obstbau* 49, 1–9. <https://doi.org/10.1007/s10341-007-0029-9>.
- Dennis, F.G. (2000). The history of fruit thinning. *Plant Growth Regul.* 31, 1–16. <https://doi.org/10.1023/A:1006330009160>.
- Dinno, A. (2017). Dunn's test of multiple comparisons using rank sums. R-Package 'dunn.test'. <https://cran.r-project.org/web/packages/dunn.test/dunn.test.pdf>.
- Goffinet, M.C., Robinson, T.L., and Lakso, A.N. (1995). A comparison of 'Empire' apple fruit size and anatomy in unthinned and hand-thinned trees. *J. Hortic. Sci.* 70, 375–387. <https://doi.org/10.1080/14620316.1995.11515307>.
- Greene, D.W. (1989). Regulation of fruit set in tree fruits with plant growth regulators. *Acta Hortic.* 239, 323–334. <https://doi.org/10.17660/ActaHortic.1989.239.51>.
- Haller, M.H., and Magness, J.R. (1933). Relation of leaf area and position to quality of fruit and to bud differentiation in apples. *U.S. Dept. Agric. Techn. Bull.* 338.
- Hansen, P. (1969). <sup>14</sup>C-studies on apple trees. IV. Photosynthate consumption in fruits in relation to the leaf-fruit ratio and to the leaf-fruit position. *Physiologia Plantarum* 22, 186–198. <https://doi.org/10.1111/j.1399-3054.1969.tb07855.x>.
- Hansen, P. (1977). The relative importance of fruits and leaves for the cultivar-specific growth rate of apple fruits. *J. Hortic. Sci.* 52, 501–508. <https://doi.org/10.1080/00221589.1977.11514780>.
- Hansen, P. (1980). Yield components and fruit development in 'Golden Delicious' apples as affected by the timing of nitrogen supply. *Sci. Hortic.* 12, 243–257. [https://doi.org/10.1016/0304-4238\(80\)90005-9](https://doi.org/10.1016/0304-4238(80)90005-9).
- Hehnen, D., Hanrahan, I., Lewis, K., McFerson, J., and Blanke, M. (2012). Mechanical flower thinning improves fruit quality of apples and promotes consistent bearing. *Sci. Hortic.* 134, 241–244. <https://doi.org/10.1016/j.scienta.2011.11.011>.
- Heinicke, A.J. (1917). Factors influencing the abscission of flowers and partially developed fruits of apple (*Pyrus malus* L.). *Cornell Univ. Experim. Station Bull.* 393, 41–114. <https://doi.org/10.5962/bhl.title.36986>.
- Hočevár, M., Širok, B., Godeša, T., and Stopar, M. (2014). Flowering estimation in apple orchards by image analysis. *Precision Agric.* 15, 466–478. <https://doi.org/10.1007/s11119-013-9341-6>.
- Hothorn, T., Bretz, F., and Westfall, P. (2008). Simultaneous inference in general parametric models. *Biometrical J.* 50, 346–363. <https://doi.org/10.1002/bimj.200810425>.
- Jonkers, H. (1979). Biennial bearing in apple and pear: A literature survey. *Sci. Hortic.* 11, 303–317. [https://doi.org/10.1016/0304-4238\(79\)90015-3](https://doi.org/10.1016/0304-4238(79)90015-3).
- Kon, T.M., Schupp, J.R., Winzeler, H.E., and Marini, R.P. (2013). Influence of mechanical string thinning treatments on vegetative and reproductive tissues, fruit set, yield, and fruit quality of 'Gala' apple. *HortScience* 48, 40–46. <https://doi.org/10.21273/HORTSCI.48.1.40>.
- Kong, T., Damerow, L., and Blanke, M. (2009). Einfluss selektiver mechanischer Fruchtbehangsregulierung auf Ethylensynthese als Stressindikator sowie Ertrag und Fruchtqualität bei Kernobst. *Erwerbs-Obstbau* 51, 39–53. <https://doi.org/10.1007/s10341-009-0080-9>.
- Krikeb, O., Alchanatis, V., Crane, O., and Naor, A. (2017). Evaluation of apple flowering intensity using color image processing for tree specific chemical thinning. *Adv. Animal Biosci.* 8, 466–470. <https://doi.org/10.1017/S2040470017001406>.
- Lakso, A.N. (2011). Early fruit growth and drop – The role of carbon balance in the apple tree. *Acta Hortic.* 903, 733–742. <https://doi.org/10.17660/ActaHortic.2011.903.102>.
- Looney, N.E. (1993). Improving fruit size, appearance, and other effects of fruit crop 'quality' with plant bioregulating chemicals. *Acta Hortic.* 329, 120–127. <https://doi.org/10.17660/ActaHortic.1993.329.21>.
- Lordan, J., Alins, G., Àvila, G., Torres, E., Carbó, J., Bonany, J., and Alegre, S. (2018). Screening of eco-friendly thinning agents and adjusting mechanical thinning on 'Gala', 'Golden Delicious' and 'Fuji' apple trees. *Sci. Hortic.* 239, 141–155. <https://doi.org/10.1016/j.scienta.2018.05.027>.
- Luckwill, L.C. (1953). Studies of fruit development in relation to plant hormones. I. Hormone production by the developing apple seed in relation to fruit drop. *J. Hortic. Sci.* 28, 14–24. <https://doi.org/10.1080/00221589.1953.11513767>.
- MacDaniels, L.H., and Heinicke, A.J. (1929). Pollination and other factors affecting the set of fruit, with special reference to the Apple. *Cornell Univ. Experim. Station Bull.* 497.
- Manfrini, L., Taylor, J.A., and Grappadelli, L.C. (2009). Spatial analysis of the effect of fruit thinning on apple crop load. *Eur. J. Hortic. Sci.* 74, 54–60.
- McClure, K.A., and Cline, J.A. (2015). Mechanical blossom thinning of apples and influence on yield, fruit quality and spur leaf area. *Canadian J. Plant Sci.* 95, 887–896. <https://doi.org/10.4141/cjps-2014-421>.
- Meier, U. (1997). *BBCH-Monograph. Growth Stages of Mono- and Dicotyledonous Plants* (Berlin, Wien: Blackwell).
- Moore, I.D., Gessler, P.E., Nielsen, G.A., and Peterson, G.A. (1993). Soil attribute prediction using terrain analysis. *Soil Sci. Soc. Am. J.* 57, 443–452. <https://doi.org/10.2136/sssaj1993.03615995005700020026x>.



- Palmer, J.W., Giuliani, R., and Adams, H.M. (1997). Effect of crop load on fruiting and leaf photosynthesis of 'Braeburn'/M.26 apple trees. *Tree Physiol.* 17, 741–746. <https://doi.org/10.1093/treephys/17.11.741>.
- Pebesma, E.J. (2004). Multivariable geostatistics in S: the gstat package. *Computers & Geosci.* 30, 683–691. <https://doi.org/10.1016/j.cageo.2004.03.012>.
- Pebesma, E.J., and Bivand, R.S. (2005). Classes and methods for spatial data in R. *R News* 5(2). <https://cran.r-project.org/doc/Rnews/>.
- Penzel, M., Pflanz, M., Gebbers, R., and Zude-Sasse, M. (2020). Mechanical thinning of apples reduces fruit drop. *Acta Hort.* 1281, 533–538. <https://doi.org/10.17660/ActaHortic.2020.1281.70>.
- Pflanz, M., Gebbers, R., and Zude, M. (2016). Influence of tree-adapted flower thinning on apple yield and fruit quality considering cultivars with different predisposition in fructification. *Acta Hort.* 1130, 605–612. <https://doi.org/10.17660/ActaHortic.2016.1130.90>.
- Pinheiro, J., Bates, D., DebRoy, S., Sarkar, D., and R Core Team (2018). nlme: Linear and Nonlinear Mixed Effects Models. R Package v. 3.1-137. <https://CRAN.R-project.org/package=nlme>.
- Powell, D.B.B. (1974). Some effects of water stress in late spring on apple trees. *J. Hortic. Sci.* 49, 257–272. <https://doi.org/10.1080/00221589.1974.11514578>.
- Preston, A.P. (1954). Effects of fruit thinning by the leaf count method on yield, size and biennial bearing of the apple Duchess Favorite. *J. Hortic. Sci.* 43, 373–381.
- R Core Team (2018). R: A language and environment for statistical computing (Vienna, Austria: R Foundation for Statistical Computing). URL: <https://www.R-project.org/>.
- Schröder, M. (1996). Maschinell ausdünnen. *Obst und Garten* 3, 116–117.
- Schupp, J.R., Baugher, T.A., Miller, S.S., Harsh, R.M., and Lesser, K.M. (2008). Mechanical thinning of peach and apple trees reduces labor input and increases fruit size. *Hort Technology* 18, 660–670. <https://doi.org/10.21273/HORTTECH.18.4.660>.
- Silbereisen, R. (1966). Beziehungen zwischen Fruchtausbildung, Blatt-Frucht-Verhältnis und Wärmeklima bei 'Golden Delicious': I. Abhängigkeit des Fruchtgewichtes vom Blatt-Frucht-Verhältnis und vom Wärmeklima. *Gartenbauwissenschaft* 3, 267–295.
- Sinatsch, S., Pfeiffer, B., Schult, I., Zimmer, J., and Brockamp, L. (2014). Crop regulation in organic grown apples – Results of different trials on three different sites. *Proc. 16<sup>th</sup> Int. Conf. on Organic Fruit-Growing*, Feb. 17–19, Hohenheim, Germany (Weinsberg: Föko e.V.), p. 142–152.
- Solomakhin, A.A., and Blanke, M.M. (2010). Mechanical flower thinning improves the fruit quality of apples. *J. Sci. Food Agric.* 90, 735–741. <https://doi.org/10.1002/jsfa.3875>.
- Stopar, M. (2010). Fruit set and return bloom of light, medium and high flowering apple trees after BA applications. *Acta Hort.* 884, 351–356. <https://doi.org/10.17660/ActaHortic.2010.884.41>.
- Stover, E.W., and Greene, D.W. (2005). Environmental effects on the performance of foliar applied plant growth regulators. *HortTechnology* 15, 214–221. <https://doi.org/10.21273/HORTTECH.15.2.0214>.
- Volz, R.K., Ferguson, I.B., Bowen, J.H., and Watkins, C.B. (1993). Crop load effects on mineral nutrition, maturity, fruiting and tree growth of 'Cox's Orange Pippin' apple. *J. Hortic. Sci.* 68, 127–137. <https://doi.org/10.1080/00221589.1993.11516336>.
- Weibel, F.P., Chevillat, V.S., Rios, E., Tschabold, J.-L., and Stadler, W. (2008). Fruit thinning in organic apple growing with optimised strategies including natural spray products and rope-device. *Eur. J. Hortic. Sci.* 73, 145–154.
- Weise, A. (1978). Zum Problem der Frostgefährdung im Obstbau unter Berücksichtigung von Gebieten mit geringer Reliefeenergie. *Archiv für Gartenbau* 26, 349–359.
- Wünsche, J.N., and Ferguson, I.B. (2005). Crop load interactions in apple. *Hortic. Rev.* 31, 233–292.
- Wünsche, J.N., Palmer, J.W., and Greer, D.H. (2000). Effects of crop load on fruiting and gas exchange characteristics of 'Braeburn'/M.26 apple trees at full canopy. *J. Am. Soc. Hortic. Sci.* 125, 93–99. <https://doi.org/10.21273/JASHS.125.1.93>.
- Zoth, M. (2011). Untersuchung zur abgestuften Ausdünnungswirkung der 'DARWIN'-Fadenmaschine mittels Staffelung der kinetischen Rotationsenergie. *DGG-Proceedings* 17, 1–5. DOI: 10.5288/dgg-pr-01-17-mz-2011.
- Zude-Sasse, M., Fountas, S., Gemtos, T.A., and Abu-Khalaf, N. (2016). Applications of precision agriculture in horticultural crops. *Eur. J. Hortic. Sci.* 81, 78–90. <https://doi.org/10.17660/ejHS.2016/81.2.2>.

Received: May 23, 2019

Accepted: Apr. 6, 2020

Address of authors:

Martin Penzel<sup>1,2,\*</sup>, Michael Pflanz<sup>2</sup>, Robin Gebbers<sup>2</sup> and Manuela Zude-Sasse<sup>2</sup>

<sup>1</sup> Technische Universität Berlin, Chair of Agromechatronics, Straße des 17. Juni 135, 10623 Berlin, Germany

<sup>2</sup> Leibniz Institute for Agricultural Engineering and Bioeconomy (ATB), Potsdam, Germany

\* Corresponding author;

Tel.: +49-331-5699-915; Fax: +49-331-5699-849

#### **4. Carbon consumption of developing fruit and individual tree's fruit bearing capacity of RoHo 3615 and Pinova apple**

In: International Agrophysics 34, pp. 409-423, 2020

Cite as:

Penzel, M., Lakso, A.N., Tsoulas, N., Zude-Sasse, M., 2020. Carbon consumption of developing fruit and individual tree's fruit bearing capacity of RoHo 3615 and Pinova apple. Int. Agrophys. 34, 409-423. <https://doi.org/10.31545/intagr/127540>

## Carbon consumption of developing fruit and the fruit bearing capacity of individual RoHo 3615 and Pinova apple trees\*\*

Martin Penzel<sup>1,2</sup> , Alan Neil Lakso<sup>3</sup>, Nikos Tsoulas<sup>1,4</sup> , and Manuela Zude-Sasse<sup>1</sup> \*

<sup>1</sup>Department of Horticultural Engineering, Leibniz Institute for Agricultural Engineering and Bioeconomy (ATB), Germany

<sup>2</sup>Agromechatronics – Sensor-based Process Management in Agriculture, Technische Universität Berlin, Germany

<sup>3</sup>Horticulture Section, Cornell AgriTech, Cornell University, Geneva, NY 14456, USA

<sup>4</sup>Department of Natural Resources Management and Agricultural Engineering, Agricultural University of Athens, Greece

Received July 17, 2020; accepted September 3, 2020

**Abstract.** This paper describes an approach to estimate the photosynthetic capacity and derive the optimum fruit number for each individual tree, in order to achieve a defined fruit size, which is named as the fruit bearing capacity of the tree. The estimation of fruit bearing capacity was carried out considering the total leaf area per tree as measured with a 2-D LiDAR laser scanner,  $LA_{LiDAR}$ , and key carbon-related variables of the trees including leaf gas exchange, fruit growth and respiration, in two commercial apple orchards. The range between  $^{min}LA_{LiDAR}$  and  $^{max}LA_{LiDAR}$  was found to be 2.4 m<sup>2</sup> on Pinova and 4.3 m<sup>2</sup> on RoHo 3615 at fully developed canopy. The daily C requirement of the growing fruit and the associated leaf area demand, necessary to meet the average daily fruit C requirements showed seasonal variation, with maximum values in the middle of the growing period. The estimated fruit bearing capacity ranged from 33-95 fruit tree<sup>-1</sup> and 45-121 fruit tree<sup>-1</sup> on the trees of Pinova and RoHo 3615, respectively. This finding demonstrates sub-optimal crop load at harvest time in both orchards, above or below the fruit bearing capacity for individual trees. In conclusion, the LiDAR measurements of the leaf area combined with a carbon balance model allows for the estimation of fruit bearing capacity for individual trees for precise crop load management.

**Keywords:** fruit growth rate, fruit respiration, leaf area, LiDAR, precision horticulture

## INTRODUCTION

As a perennial plant, the production of premium size apples requires a balance of crop level and the ability of the tree to support the crop as well as flower bud development for the following year. Crop load management (CLM) targets the fruit number per tree to enable the growth to optimal fruit sizes by optimizing the carbon supply to demand balance for economically desirable fruit growth. Also, when performed less than 30 days after full bloom, CLM avoids a reduction in flower bud development to prevent alternate bearing on susceptible cultivars (Kofler *et al.*, 2019). CLM may include pruning to reduce flower-bud numbers per branch (Breen *et al.*, 2015), mechanical (Penzel *et al.*, 2021) or chemical thinning of flowers (Janoudi and Flore, 2005) or fruitlets (Penzel and Kröling, 2020), and frequently corrective hand thinning after fruit drop.

In order to optimize CLM for the quantity of profitable fruit size, it is crucial to define the optimum fruit number per tree, which should be considered as the target fruit number for the purposes of making an accurate determination of the intensity of each individual management practice (Treder, 2008; Robinson *et al.*, 2017). The optimum fruit number per tree depends on the economically desirable fruit size at harvest, the daily C demand of growing fruit required to achieve this fruit size and the individual photosynthetic capacity of each tree to support fruit growth versus vegetative growth and flower bud development.

\*Corresponding author e-mail: mzude@atb-potsdam.de

\*\*This work was funded by the Ministry of Agriculture, Environment and Climate Protection of the federal state of Brandenburg and the agricultural European Innovation Partnership (EIP-AGRI), grant number 80168342 (2016-2020).

The photosynthetic capacity of fruit trees is associated with the extent of their generative and vegetative growth, both directly and indirectly determined by interacting factors of intra-plant competition. Furthermore, external factors such as light availability and interception, temperature, mineral nutrition, soil properties and water availability affect the photosynthetic capacity (Monteith, 1977; Xia *et al.*, 2009; Lakso and Goffinet, 2017; Lopez *et al.*, 2018). Physiological crop models can quantify cumulative effects of several factors on the magnitude of vegetative and generative growth of fruit trees (Lakso *et al.*, 2001; Mirás-Avalos *et al.*, 2011; Pallas *et al.*, 2016). Therefore, physiological crop models are helpful in understanding the seasonal growth patterns of fruit trees or they may be used to determine the tree's photosynthetic capacity and they can also be applied as a tool for decision support for precise orchard management (Lakso and Robinson, 2014).

Furthermore, physiological and decision support models may be utilized to predict the optimum timing for the application of thinning agents (Robinson *et al.*, 2017; Yoder *et al.*, 2013), the thinning response (Greene *et al.*, 2013), flower bud formation, fruit mass at harvest (Iwanami *et al.*, 2018) and to estimate the target fruit number per tree (Handsack and Schmidt, 1990). In practice, the target fruit number per tree is, however, often estimated from the average yields of the previous years considering the mean of the entire orchard, divided by the number of trees in the orchard and the targeted fruit fresh mass. This approach leads to one level of treatment for all of the trees. This empirical method is not based on the natural variance in the capacity of each tree to support fruit of an economically desired size, namely the fruit bearing capacity (FBC), which can be highly variable within orchards (Manfrini *et al.*, 2009). Therefore, the individual FBC of a certain number of trees is potentially over or underestimated by the established method. Overestimation of the FBC will lead to excessively high crop levels, poor fruit quality and reduced flower bud induction, while underestimation leads to too few fruits, a loss of crop value, reduced storability and an increased risk of storage disorders (Wójcik *et al.*, 2001; Mussachi and Serra, 2018). As individual trees require a variable intensity of CLM, it is assumed that lack of tree-specific CLM is an important cause of heterogeneity in fruit size, quality, and value.

In order to observe the variability in the growth habits of trees, data from a large quantity of trees is required. Recent approaches used to detect flower clusters and the fruit of individual trees (Tsoulas *et al.*, 2020) or to estimate other canopy parameters such as canopy height, volume or total leaf area, have shown promising results (Bresilla *et al.*, 2019; Tsoulas *et al.*, 2019; Hobart *et al.*, 2020; Vanbrabant *et al.*, 2020). When these techniques are implemented within existing physiological models, the data generated can potentially be applied to estimate the photosynthetic

capacity of individual trees, the optimum and target fruit number per tree, their variability within an orchard, and the required variable intensity for precise CLM practice.

The estimation of leaf area may be of outstanding importance, since the photosynthetic capacity of a tree relies on the total leaf area, especially from the exposed leaves, the quantity of light intercepted by the leaves and the photosynthetic conversion to fixed carbon. The percentage of leaf-assimilated carbohydrates partitioned to fruit,  $C_{\text{part}}$  (%), is dynamic during the whole season, with significant changes in the first weeks after bloom (Hansen, 1967; Corelli-Grappadelli *et al.*, 1994; Pallas *et al.*, 2016). The magnitude of  $C_{\text{part}}$  for a specific date is determined by the C supply to demand balance of the tree, which is influenced by the quantity and actual sink activity of all organs including shoots, fruit, leaves, branches, roots, and stem.  $C_{\text{part}}$  can range from 0% on non-bearing trees to 85% on fruiting trees with a low leaf area to fruit ratio (LA:F) (Hansen, 1969; Palmer, 1992; Lakso, unpublished data).

In periods showing C demand exceeding the supply in a particular apple tree, there is a prioritization in C partitioning among the sink organs, with the highest priority assigned to growing shoots (Bepete and Lakso, 1998). When shoot and leaf growth is complete, the highest priority for C partitioning is the fruit (Wagenmakers, 1996). When integrated over the whole season,  $C_{\text{part}}$  is defined as the harvest index (HI). For fruiting trees of different cultivars, varying HI were reported in previous studies, ranging from 50% - 85% (Koike *et al.*, 1990; Palmer *et al.*, 2002; Glenn, 2016; Lakso, unpublished data). They were typically grown on dwarfing rootstocks including M.9, M.26 and M.27. The HI is negatively correlated to the N supply of the tree, which positively affects the LA:F (Xia *et al.*, 2009).

The C supply to the individual fruit may limit fruit growth at different times during the season (Lakso and Goffinet, 2017) and, therefore, determine the fruit size at harvest time. Hence, assuming the total leaf area per tree is closely related to light interception, the fruit size at harvest is positively correlated to LA:F (Palmer, 1992) and can be further described as a hyperbolic function of the exposed LA:F of healthy LA, not affected by external stress. The effective LA required to produce a specific fruit size from a cultivar varies depending on the exposed versus shaded LA as demonstrated by earlier studies. Hansen (1969) reviewed several early studies concerning the relationship between LA:F and fruit size, pointing out that 300-500 cm<sup>2</sup> LA:F, or 20-30 leaves per fruit, is the minimum requirement to achieve a marketable fruit size. The required LA:F in contemporary orchards may be different, because it may be assumed that at the time when the studies were carried out, the trees were probably not as optimally supplied with nutrients and water as in present day orchards. Other factors which affect the required LA:F are cultivar, rootstock, growing system and seasonal climate, all affecting the light interception of the trees and the HI.

Previous studies have in common that the LA:F was determined at full canopy or at harvest. However, the fruit growth rate and related C consumption of individual fruit underlies seasonal changes (Schechter *et al.*, 1993; Pavel and DeJong, 1995; Lakso and Robinson, 2014). As a consequence, since seasonal leaf area and fruit development occur with different patterns, it may be assumed that the LA:F required for fulfilling the fruit's C requirement varies during fruit development. Additionally, the total LA per tree changes continuously during the season, as does the LA:F, until fruit drop and shoot growth have ended. Schumacher (1962) pointed out the negative effect of temporarily variable LA:F in order to overcome alternate bearing on Glockenapfel/M.13. The LA:F ranged from 35–70 cm<sup>2</sup> at petal fall, 180–265 cm<sup>2</sup> before fruit drop and 530–710 cm<sup>2</sup> after fruit drop. This study indicated increasing leaf area demand per fruit to provide the C required by fruit growth during the growing period, presumably because of the increasing C requirements of the fruit and variable C assimilation by the leaves over the season. This finding was consistent with seasonal simulations applying the MaluSim carbon balance model (Lakso and Robinson, 2014). As a consequence, the FBC of the tree will be determined in phases with the highest leaf area demand per fruit, presumably in the middle of fruit development, when the fruit growth rates achieve their seasonal maximum and temperature is high.

Based on the demand and value of optimizing individual tree crop load, the objectives of the present study were (i) to quantify the fruit's daily C requirement during the growing season, (ii) to estimate the daily C assimilation of individual trees based on 2-D LiDAR measurements of the total LA, and (iii) to calculate the fruit bearing capacity of Pinova and RoHo 3615 apple trees.

#### MATERIAL AND METHODS

Trials were carried out in 2018 in two commercial orchards of *Malus x domestica* Borkh. Pinova/M.26 and RoHo 3615/M.9 (Evelina®; red mutant of Pinova) in the Brandenburg (Germany) fruit growing regions of Werder (52.357 N, 12.867 E) and Altlandsberg (52.607 N, 13.817 E) planted in 2014 and 2006, respectively. The trees were trained as tall thin central leaders with a spacing of 3.5 m × 1.25 m for Pinova and 3.2 m × 0.95 m for RoHo 3615 in Werder and Altlandsberg, respectively. The mean ground area covered by a tree was 1.15 m<sup>2</sup> in

Werder and 1.05 m<sup>2</sup> in Altlandsberg. Both orchards were drip irrigated and managed according to the federal regulations of integrated production. No visible nutrient or water stress symptoms or pathogen symptoms were noted on the considered trees.

In both orchards, 45 trees were labelled and the number of flower clusters counted at green bud stage. At full bloom (Table 1) trees of RoHo 3615 were thinned with two applications of 15 kg ha<sup>-1</sup> ammonium thiosulfate salt (20% N) in 500 L ha<sup>-1</sup> water solution, whereas trees of Pinova were thinned with a rotating string thinner (Darwin 250, FruitTec, Markdorf, Germany) with 270 strings at 8 km h<sup>-1</sup> vehicle speed and a rotational frequency of 280 rpm.

Fruit gas exchange, dry matter, elemental C content, and fruit size from randomly selected fruit, from neighbouring trees to the labelled ones, were analysed in the laboratory in two to five week intervals during the growing season. In the mid-season, when the canopies were fully developed, the total leaf area of 50 trees of Pinova and 100 trees of RoHo 3615, including the 45 labelled trees from each orchard, was estimated by means of a terrestrial mobile light detection and ranging (LiDAR) 2-D laser scanner (Tsoulas *et al.*, 2019). The total yield and fruit number of the labelled trees were measured manually at 143 days after full bloom (DAFB), one day prior to commercial harvest, when randomly sampled fruit in the orchard achieved a starch index (scale ranges from 1–10) of 5.

Fruit fresh mass (FM, g), diameter (D, mm), the fraction of dry matter relative to fresh mass, DM<sub>rel</sub> (0–1), and elemental C content based on fruit dry matter, C<sub>rel</sub> (0–1), were measured during the entire fruit developmental period on 30 fruit per cultivar and 180 fruit per cultivar at harvest time. The samples were taken from exposed spurs in the middle of the canopy at around 2 p.m. in the afternoon. D and FM were recorded directly after sampling. During the next morning, the gas exchange of three samples, each consisting of 10 fruit until 50 DAFB (Pinova: 24 DAFB, 38 DAFB; RoHo 3615: 30 DAFB) and six samples consisting of five fruit after 50 DAFB (Pinova: 52 DAFB, 67 DAFB, 80 DAFB, 108 DAFB; RoHo 3615: 51 DAFB, 74 DAFB, 121 DAFB) were measured in the laboratory in gas-tight acrylic cuvettes, monitoring CO<sub>2</sub> concentration increase with continuously logging IR-CO<sub>2</sub> sensors (FYA600CO<sub>2</sub>, Ahlborn Mess- und Regelungstechnik GmbH, Holzkirchen, Germany). The measurements were carried out in the dark for at least two hours at 10 ± 1°C and 20 ± 1°C after the temperature adjustment of the fruit. Each of the cuvette-

**Table 1.** Reference dates of seasonal tree development and mean air temperature in 2 m height in two apple orchards in 2018

Cultivar	Budbreak	Full bloom	Harvest	Days from full bloom to harvest	Daily mean temperature (°C)	
					0 days after full bloom	46
	Date in 2018				(DAFB) - 45 DAFB	DAFB - harvest
Pinova	26.03.	04.05.	24.09.	143	19.0	19.8
RoHo 3615	22.03.	29.04.	19.09.	143	17.8	19.1



sensor systems was calibrated with technical gases (Linde, Pullach, Germany) using the concentrations 0 ppm CO<sub>2</sub> (N<sub>2</sub>) and 1000 ± 20 ppm CO<sub>2</sub>. The temperature-dependent dark respiration rate,  $R_{dT}$  (mg kg<sup>-1</sup> h<sup>-1</sup>), was calculated ( $R_{dT} = \Delta\text{CO}_2 (\text{FM } \Delta t)^{-1}$ ), considering fruit volume, cuvette volume and actual atmospheric pressure as described earlier for the same measuring system (Brandes and Zude-Sasse, 2019). From the respiration rates obtained at two temperatures, the  $Q_{10-20}$  values were calculated at each measuring date ( $Q_{10-20} = R_{d20} R_{d10}^{-1}$ ). For the purpose of C modelling, CO<sub>2</sub> was converted into C through multiplication by a factor of 0.27, resulting from the fraction of the atomic mass from C (12.01 g mol<sup>-1</sup>) on the molar mass of CO<sub>2</sub> (44.01 g mol<sup>-1</sup>).

Afterwards, 10 fruit (< 50 DAFB), 5 × 0.5 fruit (> 50 DAFB) per measurement were dried at 80°C until a constant mass was reached.  $DM_{rel}$  was calculated by dividing the mass of the dry matter by the initial FM of the sample before drying. The dry matter was homogenized with a mixer mill (MM400, Retsch Technology, Haan, Germany) at a frequency of 30 Hz for 1 min.  $C_{rel}$  of the homogenized dry matter was measured with an elemental analyser (Vario EL III, Elementar Analysensysteme GmbH, Hanau, Germany) at 1150°C. The absolute C content per fruit ( $C_{fruit}$ , g), was then calculated ( $C_{fruit} = \text{FM } DM_{rel} C_{rel}$ ).

After the canopy of the trees was fully developed, usually in mid-July, individual trees (Altlandsberg: 81 DAFB,  $n = 100$ ; Werder: 67 DAFB,  $n = 50$ ) were scanned with a 2-D LiDAR laser scanner (LMS511 pro model, Sick, Düsseldorf, Germany) with an angular resolution of 0.1667° and a scanning frequency of 25 Hz at a vertical scanning angle of 270°. The LiDAR laser scanner was placed together with an inertial measurement unit (MTi-G-710, XSENS, Enschede, The Netherlands) and a RTK-GNSS (AgGPS 542, Trimble, Sunnyvale, CA, USA) on a metal platform at a height of 1.6 m (Tsoulas *et al.*, 2019). The platform was mounted on a tractor and driven along each side of the tree rows with an average speed of 0.13 m s<sup>-1</sup> to acquire the 3-D point cloud of each tree. The LiDAR points were filtered considering only the observations between a height of 0.05 m and 4.00 m, while the points that belonged to the ground were removed utilizing the random sample consensus algorithm. Thus, the LiDAR points per tree (PPT) were extracted from the 3-D point cloud with an own Matlab script (Version 2016b, The Mathworks Inc., Natick, MA, USA) (Tsoulas *et al.*, 2019). In order to calibrate PPT on the total LA per tree,  $LA_{LiDAR}$  (m<sup>2</sup>), six trees per orchard were defoliated and the total LA,  $LA_{lab}$  (m<sup>2</sup>), was measured in the laboratory. All leaves per tree were sorted by size into three fractions (small, medium, large). The number of leaves in each fraction was counted. The average leaf size per fraction was analysed from manual scans of 20% of the leaves, from each fraction, with a desktop scanner (Scanjet 4850, HP, Palo Alto, CA, USA), in groups of 5-15 leaves. The RGB-images were analysed considering the sum of pixels of each leaf, with own Matlab script. An area

of 6241 pixels in the image equalled an area of 1 cm<sup>2</sup>. The number of pixels per leaf was converted into cm<sup>2</sup> leaf area per leaf by division with the factor 6241. The average leaf size per fraction was multiplied by the number of leaves per fraction.  $LA_{lab}$  is the sum of the leaf area from each leaf fraction. Regression analysis between PPT and  $LA_{lab}$  was carried out with software R (Version 3.4.1; R Core Team, 2018). The regression models between PPT and  $LA_{lab}$  were used to convert the individual PPT of individual trees scanned in the orchards into  $LA_{LiDAR}$ . The coefficient of determination,  $R^2$ , and the relative root mean squared error, RRMSE (%) were calculated considering  $LA_{LiDAR}$  and  $LA_{lab}$  (Eqs A1, A2).

The seasonal development of the total leaf area of individual trees,  $LA_{tree}$  (m<sup>2</sup>), was estimated by fitting  $^{mean}LA_{LiDAR}$  of both cultivars into a sigmoid growth model based on the number of days after bud break (DABB) (Eq. A3) with Table Curve 2D (Version 5.01, IBM Corporation, Armonk, NY, USA). It was assumed that  $LA_{tree}$  was 0 at bud break (Table 1), 20% of  $^{mean}LA_{LiDAR}$  at full bloom (cf. Lakso *et al.*, 1984; Wünsche *et al.*, 1996). In an earlier study, it was reported that the canopy of apple trees, grown on a dwarfing rootstock, was fully developed after 1200 accumulated growing degree d on base temperature ( $T_B$ , °C), of 4°C,  $GDD_{4°C}$  (Eq. A4), after bud break (Doerflinger *et al.*, 2015). In the current study 1200  $GDD_{4°C}$  were achieved at 07.07.2018, 13.07.2018 for Pinova and RoHo 3615, respectively. After those dates  $LA_{tree}$  was assumed to remain constant until harvest.  $T_{max}$  and  $T_{min}$  are the daily minima and maxima of T in 2 m height in the orchards.

The maximum quantum yield,  $^{max}\alpha$  (mol mol<sup>-1</sup>), and the light saturated net CO<sub>2</sub> gas exchange rate,  $^{max}J_{CO_2}$  (μmol m<sup>-2</sup> s<sup>-1</sup>), were derived from the light response curves of the net CO<sub>2</sub> gas exchange rates,  $J_{CO_2}$  (μmol m<sup>-2</sup> s<sup>-1</sup>), measured on three mature leaves of RoHo 3615 in exposed positions of the canopy of bearing trees on seven dates during fruit development (DAFB: 7, 27, 32, 66, 71, 92, 108). Measurements were carried out using a portable porometer (LI-6400 XT, LI-COR Inc., Lincoln, NE, USA) coupled with a broadleaf cuvette equipped with a red and blue LED light source (6400-40, LI-COR Inc., Lincoln, NE, USA). An area of 1.7 cm<sup>2</sup> per leaf was fixed inside the cuvette for the measurements. The measurements were performed at ambient leaf temperature,  $T_{leaf}$ , and relative humidity at a constant CO<sub>2</sub> mole fraction of 400 μmol mol<sup>-1</sup> in the reference gas flow and a range of photosynthetic photon flux rates, PPFR (μmol m<sup>-2</sup> s<sup>-1</sup>), (2,000; 1,500; 1,000; 750; 500; 250; 110; 50; 20; 0) with waiting times between 80 and 120 s.  $^{max}\alpha$  was calculated as the initial slope of  $J_{CO_2}$  vs. PPFR between 0 and 110 μmol m<sup>-2</sup> s<sup>-1</sup>, whereas  $^{max}J_{CO_2}$  was considered to be equivalent to  $J_{CO_2}$  at 2000 μmol m<sup>-2</sup> s<sup>-1</sup>.

The means of FM and  $C_{fruit}$  were interpolated over the season and expressed as sigmoid functions of DAFB (Eqs A5, A6). The first derivatives of the equations were calculated and referred to as absolute growth rates considering

FM,  $AGR_{FM}$  ( $g\ d^{-1}$ ) and C,  $AGR_C$  ( $g\ d^{-1}$ ), (Eqs A7, A8). The daily elemental C requirements to account for the observed growth and respiration per fruit ( $C_{daily}$ ,  $g\ d^{-1}$ ), is the sum of  $AGR_C$  and the daily respired C per fruit ( $R_{daily}$ ,  $g\ d^{-1}$ ) ( $C_{daily} = AGR_C + R_{daily}$ ).  $R_{daily}$  ( $C$ ,  $g\ d^{-1}$ ) was calculated (Eq. (1)) from the estimated respiration rate of the fruit in the field ( $R_{field}$ ,  $mg\ kg^{-1}\ h^{-1}$ ), multiplied by the daily interpolated values of FM between the sampling dates, with the simplifying assumption that no diurnal changes in  $R_{dT}$  occurred.

$$R_{daily} = \frac{R_{field} \cdot FM \cdot 24}{1000} \cdot 0.27, \quad (1)$$

$R_{field}$  ( $CO_2$ ,  $mg\ kg^{-1}\ h^{-1}$ ) was estimated (Eq. (2)) from  $R_{d10}$  and  $R_{d20}$  measured in the laboratory, and the average daily temperature ( $T_{mean}$ ,  $^{\circ}C$ ), in the same orchard in Altlandsberg and a neighbouring orchard in Werder (52.453684 N, 12.824633 E), recorded in 2 m height with a PT100 temperature sensor (Pessl Instruments GmbH, Weiz, Austria).

$$R_{field} = R_{d10} + \frac{(T_{mean} - 10^{\circ}C) \times (R_{d20} - R_{d10})}{10^{\circ}C}. \quad (2)$$

To estimate  $C_{daily}$  for varying fruit size at harvest time ( $D = 65, 70, 75, 80$  mm) the equations A5 and A6 were normalized for FM and C at harvest time (143 DAFB). The normalized functions (Eqs A9, A10) were used to fit growth curves for the targeted fruit sizes (Fig. A1b) and the associated daily growth rates,  $AGR_{FM}$  and  $AGR_C$ .  $C_{daily}$  was calculated from these growth curves under the assumption that the respiration rate per fresh mass unit ( $R_{field}$ ) was identical for all fruit sizes.

The necessary LA required to assimilate  $C_{daily}$ ,  $LA_{demand}$  ( $cm^2$ ), was calculated (Eq. (3)) from the daily assimilated C per unit ground area ( $P_{daily}$ ,  $g\ m^{-2}\ d^{-1}$ ), and the percentage of assimilated carbohydrates partitioned to fruit ( $C_{part}$ , %).  $LA_{demand}$  was calculated for variable amounts of  $C_{part}$ . A linear increase in  $C_{part}$  from 40% at full bloom to 80%, when the foliage was fully developed was assumed (cf. Wagenmakers, 1996). It was also assumed that fruit photosynthesis contributes 5% of the fruit's carbon demand. To reduce the effect of local maxima of  $LA_{demand}$ , originating from days with low solar radiation (Eq. (4)), the seasonal course of  $LA_{demand}$  was smoothed with a Savitzky-Golay filter, using the R-Package signal (Ligges *et al.*, 2015; `sgolayfilt`, filter order = 1, filter length = 9).

$$LA_{demand} = \frac{0.95 \cdot C_{daily}}{\frac{P_{daily} \cdot C_{part}}{(LA_{orchard} \cdot 10000)}} \quad (3)$$

$P_{daily}$  ( $C$ ,  $g\ m^{-2}\ d^{-1}$ ) was calculated (Eq. (4)) according to the equation of the canopy daily net photosynthesis integral of Charles-Edwards (1982), adapted to apple (Lakso and Johnson, 1990; Lakso *et al.*, 2001, 2006):

$$P_{daily} = \frac{\max_a \cdot S \cdot DL \cdot \max_{J_{CO_2}} \cdot P_T \cdot LI}{\max_a \cdot k \cdot S + h \cdot \max_{J_{CO_2}} \cdot P_T} \cdot 0.27, \quad (4)$$

$$LI[0-1] = F_{max} \cdot (1 - e^{(-k \cdot \frac{LA_{orchard}}{F_{max}})}), \quad (5)$$

$$P_T[0-1] = 0.535 + 0.0384 \cdot T_{day} - 0.0004126 \cdot T_{day}^2 - 0.00001576 \cdot T_{day}^3. \quad (6)$$

For the purpose of the model, the seasonal mean values of  $\max_a$  and  $\max_{J_{CO_2}}$  ( $0.054\ mol\ mol^{-1}$ ;  $17.2\ \mu mol\ m^{-2}\ s^{-1}$ ) were converted into  $5.43\ \mu g\ J^{-1}$  and  $0.000758\ g\ m^{-2}\ s^{-1}$ , respectively, assuming that the fraction of the photosynthetic active radiation, PAR, from the total radiation was 0.5 and the conversion factor from  $\mu mol\ s^{-1}\ m^{-2}$  (PAR) to  $W\ m^{-2}$  (PAR) was 0.2188 (McCree, 1972). The daily integral of solar radiation,  $S$  ( $MJ\ m^{-2}\ d^{-1}$ ), was recorded by a pyranometer (CMP 3, Kipp & Zonen, Delft, The Netherlands) in the spectral range of 300–2800 nm. The day length,  $DL$  (s), resulted from the daily hours, with solar radiation  $> 0\ W\ m^{-2}\ h^{-1}$ , multiplied by  $3600\ s\ h^{-1}$ .  $LI$  (Eq. (5)) is the fraction of light intercepted by the canopy (cf. Jackson and Palmer, 1980). The canopy's light extinction coefficient ( $k$ ), and the fraction of total radiation actually incident to the canopy,  $F_{max}$ , were assumed to be 0.5 and 0.7, respectively (Lakso *et al.*, 2006). An  $F_{max}$  of 0.7 assumes that 30% of the incident radiation is lost to the ground regardless of the tree's leaf area. Daily values of LAI of the whole orchard,  $LA_{orchards}$  were calculated from the ground area allotted per tree ( $G_{allotted}$ ,  $m^2$ ), divided by the daily value of  $LA_{tree}$ .  $G_{allotted}$  is determined by the spacing between the trees and rows, and was 4.375 and 3.040  $m^2$  for Pinova and RoHo 3615, respectively.

The relative effect of temperature on  $P_{daily}$ ,  $P_T[0-1]$ , was included (Eq. (6)), taking into account the average temperature during the daylight period ( $T_{day}$ ,  $^{\circ}C$ ). The normalised equation of  $P_T$  was estimated from several studies at Cornell AgriTech (cf. Lakso *et al.*, 1999). The daily amount of assimilated C per tree,  $P_{tree}$  ( $g\ d^{-1}$ ), and the fruit bearing capacities (FBC, fruit tree $^{-1}$ ) of the trees for several target fruit sizes, FBC, were calculated (Eqs (7), (8)).

$$P_{tree} = P_{daily} \cdot G_{allotted}, \quad (7)$$

$$FBC = \frac{LA_{tree}}{LA_{demand}}. \quad (8)$$

## RESULTS

A sigmoidal growth model was applied to interpolate the measured values of fresh mass and C as a function of time (Fig. 1a, 1e), because the linear interpolation of individual means led to an unrealistic fluctuation in growth rates, which was most likely a consequence of the sampling of random fruit at each date. The model was in good agreement with the measured values (Pinova:  $R^2 = 0.85$ ; RoHo 3615:  $R^2 = 0.87$ ). A high degree of deviation was found in RoHo 3615, at 100 DAFB which would have resulted in very high growth rates  $> 2.5 \text{ g d}^{-1}$  ( $\text{AGR}_{\text{FM}}$ ), more than double that of the neighbouring values. Since the weather data in both periods did not indicate strong changes or extreme weather events and the water supply to the trees was unchanged, this variation wasn't taken into account in the subsequent analysis. Fruit of Pinova developed elevated growth rates ( $\text{AGR}_{\text{C}}$ ,  $\text{AGR}_{\text{FM}}$ ) in comparison to RoHo 3615 from 22 DAFB to 100 DAFB (Figs 1b, 1f), although the average temperatures in the cell division stage was similar in both orchards (Table 1). Both growth rates of Pinova peaked 9 days earlier compared to RoHo 3615. The result was that the average fresh mass (FM) and absolute C content of Pinova fruit exceeded that of RoHo 3615 at harvest time.

The dry matter content ( $\text{DM}_{\text{rel}}$ ) and C content of dry matter ( $\text{C}_{\text{rel}}$ ) of fruit from both cultivars followed similar seasonal courses (Fig. 1c, 1d). While  $\text{DM}_{\text{rel}}$  showed slight seasonal fluctuations,  $\text{C}_{\text{rel}}$  decreased linearly within the range from 0.51 to 0.47 (Eqs A11).

The dark respiration rates per unit of fresh mass of both cultivars decreased during fruit development in a typical course for apple (Jones, 1981), but at  $10^\circ\text{C}$  to a lower extent than at  $20^\circ\text{C}$  (Fig. 2a). At 38 DAFB and 52 DAFB, the  $R_{\text{d20}}$  value of Pinova fruit was elevated in comparison to the fruit of RoHo 3615. The  $Q_{10-20}$  values indicated that an increase in temperature from 10 to  $20^\circ\text{C}$  resulted in a 1.4–4.0 fold increase in  $R_{\text{dT}}$  (Fig. 2b). As a consequence of elevated FM and  $R_{\text{field}}$ , the  $R_{\text{daily}}$  of Pinova was enhanced until 65 DAFB in comparison to RoHo 3615. Accordingly, the total of respired C per fruit from 30 DAFB until harvest (114 d) was higher on Pinova (1.67 g) in comparison to RoHo 3615 (1.33 g), accounting for 10.4 and 10%, respectively, of the accumulated daily C requirement per fruit. The daily fluctuation in the percentage of respiration of  $\text{C}_{\text{daily}}$  ranged from 6–44%. Hence,  $\text{C}_{\text{daily}}$  was mainly determined by C accumulation,  $\text{AGR}_{\text{C}}$ , which is reflected in a similar seasonal course. In total, fruit of RoHo 3615 consumed 13.3 g of C in the period from 30 DAFB till harvest, achieving an average FM of 165 g, whereas Pinova fruit

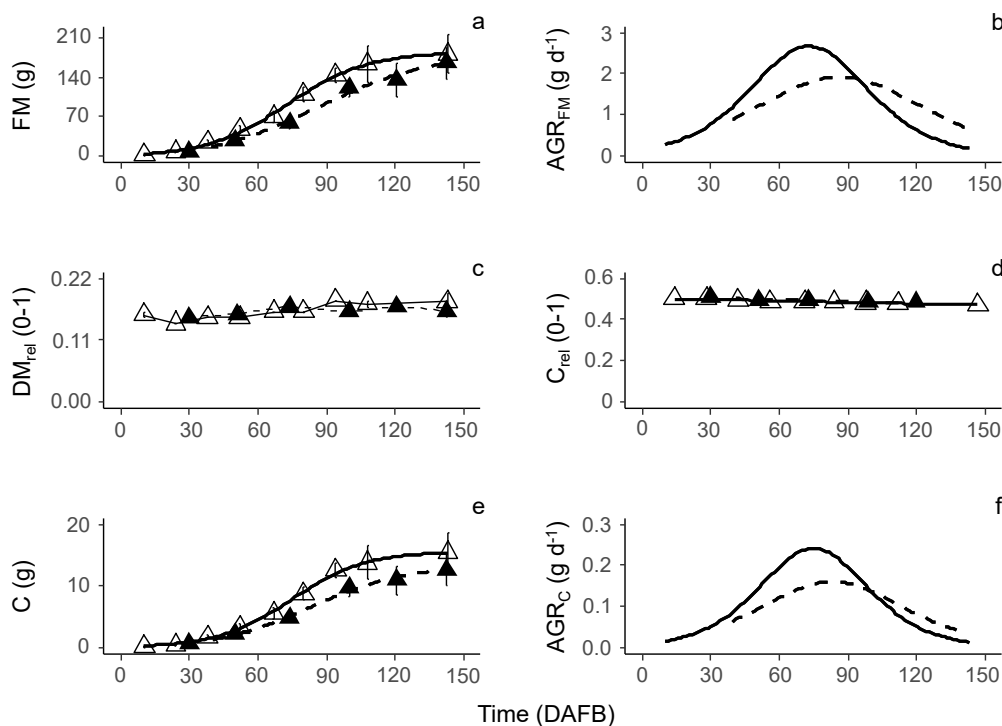


**Fig. 1.** Time course in days after full bloom (DAFB) of (a) fresh mass (FM, g), (b) absolute growth rate of fresh mass ( $\text{AGR}_{\text{FM}}$ ,  $\text{g d}^{-1}$ ), (c) fraction of dry matter ( $\text{DM}_{\text{rel}}$ ) on FM (0–1), (d) fraction of elemental C on  $\text{DM}_{\text{rel}}$  (0–1) ( $\text{C}_{\text{rel}}$ ), (e) absolute C content (g), (f) absolute growth rate in C ( $\text{AGR}_{\text{C}}$ ,  $\text{g d}^{-1}$ ) of developing Pinova/M.26 (open symbol, solid line) and RoHo 3615/M.9 (closed symbol, dashed line) apple fruit during the 2018 growing season. Error bars indicate the standard deviations.

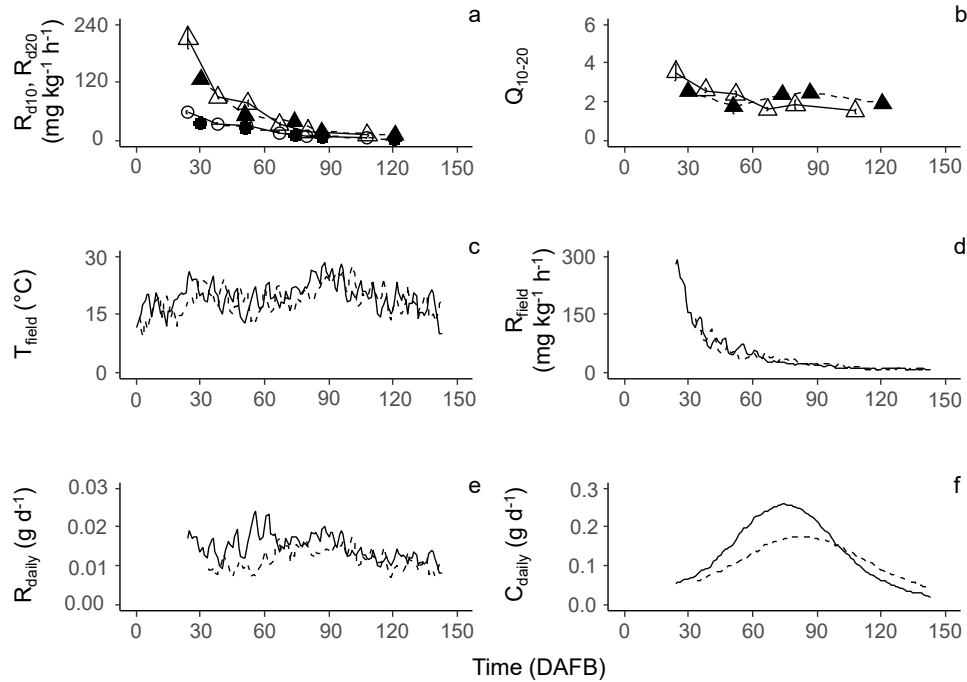


**Fig. 2.** Time course in days after full bloom (DAFB) of: a) fruit CO<sub>2</sub> respiration rate (mg kg<sup>-1</sup> h<sup>-1</sup>) at 10°C (R<sub>d10</sub>, circle) and 20°C (R<sub>d20</sub>, triangle); b) Q<sub>10-20</sub> values for fruit respiration between 10 and 20°C; c) mean daily temperature (T<sub>mean</sub>, °C) at a height of 2 m; d) estimated respiration rates (R<sub>field</sub>, mg kg<sup>-1</sup> h<sup>-1</sup>) calculated for T<sub>mean</sub>; e) daily respired C per fruit (g d<sup>-1</sup>); f) daily C requirement per fruit (g d<sup>-1</sup>) of Pinova/M.26 (open symbol, solid line) and RoHo 3615/M.9 (closed symbol, dashed line) apple fruit during the 2018 growing season. Error bars indicate the standard deviations.

consumed 16.1 g of C in the same period, achieving 182 g FM. When estimated for varying target fruit size, C<sub>daily</sub> rose up to maximum of 0.35 g d<sup>-1</sup> in Pinova fruit (Fig. 3a), while the targeted fruit size was 80 mm, which equates to 244 g FM at harvest (Fig. A1).

The total leaf area per tree measured in the laboratory, LA<sub>lab</sub>, and LiDAR points per tree, PPT, were highly correlated in both orchards (Fig. 4). Although the relationship would be expected to be hyperbolic, within the abundant range of leaf area, linear models between PPT and LA<sub>lab</sub> were adequate to estimate LA<sub>LiDAR</sub> from the PPT of all scanned trees (Eqs A12.1, A12.2). The RRMSE between the measured and estimated leaf area per tree was 3.8 and 3.0% for Pinova and RoHo 3615, respectively.

LA<sub>LiDAR</sub> of Pinova trees was on average 3.8 ± 0.55 m<sup>2</sup> (10.07.2018) showing a wide range of 2.5 m<sup>2</sup> - 4.9 m<sup>2</sup>, whereas LA<sub>LiDAR</sub> of RoHo 3615 was 5.3 ± 0.95 m<sup>2</sup> (19.07.2018) (Fig. 4) with a total range of 3.3 m<sup>2</sup> - 7.6 m<sup>2</sup>. The resulting <sup>mean</sup>LA<sub>orchard</sub> was 0.87, 1.75, on Pinova, RoHo 3615, respectively. The assumed development of the leaf area per tree from bud break till harvest was estimated (Fig. 5) by fitting <sup>mean</sup>LA<sub>LiDAR</sub> into a sigmoidal growth model (Eqs A13.1, A13.2).

The average maximum quantum yield of the leaves, <sup>max</sup>α, (Fig. 6) over the entire season of RoHo 3615 was 0.054 ± 0.003 mol mol<sup>-1</sup>. The light saturated net CO<sub>2</sub> gas exchange at ambient temperature, in comparison, showed

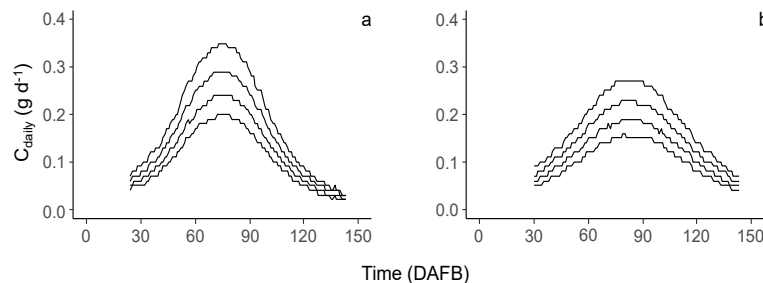


**Fig. 3.** Time course in days after full bloom (DAFB) of daily C requirement per fruit (g d<sup>-1</sup>) considering (a) Pinova/M.26 and (b) RoHo 3615/M.9 apple fruit with varying target fruit sizes (from the bottom up: 65, 70, 75, and 80 mm) estimated for the conditions in the considered orchards in 2018.

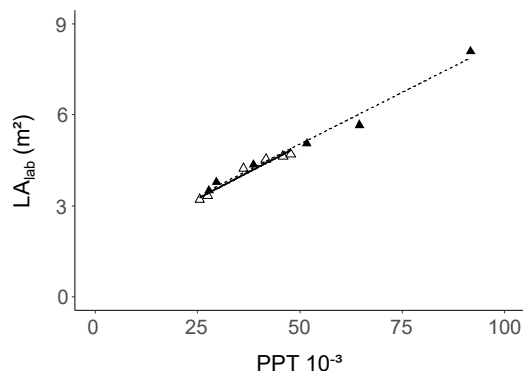


**Fig. 4.** Relationships between laser hits per tree (PPT) and manual measured total leaf area per tree ( $LA_{lab}$ ,  $m^2$ ). (RoHo3615: closed symbol, dotted line;  $LA_{lab} = 1.6 + (6.822 \cdot 10^{-5} \text{ PPT})$ ,  $R^2 = 0.98$ ; Pinova: open symbol, solid line;  $LA_{lab} = 1.49 + (6.987 \cdot 10^{-5} \text{ PPT})$ ,  $R^2 = 0.96$ ).

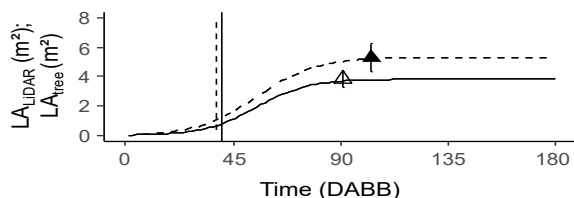


**Fig. 5.** Estimated seasonal course in days after bud break (DABB) of total leaf area per tree ( $LA_{tree}$ ,  $m^2$ ) and LiDAR estimated LA ( $LA_{LiDAR}$ ,  $m^2$ ) of Pinova/M.26 (open symbol, solid line) and RoHo 3615/M.9 (closed symbol, dashed line) in 2018. Vertical lines indicate the date of full bloom, error bars the standard deviation.

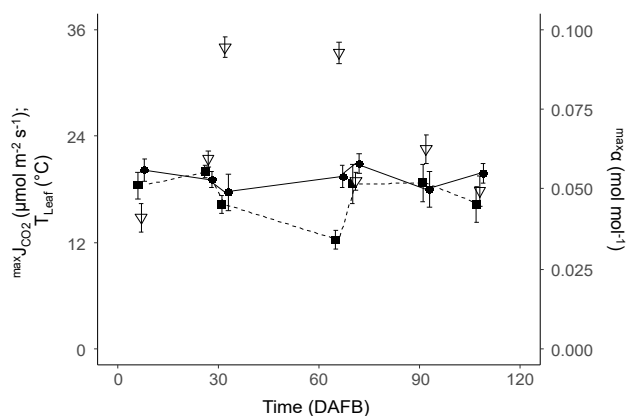


**Fig. 6.** Seasonal course (days after full bloom (DAFB)) of the maximum quantum yield ( $\max \alpha$ ,  $\text{mol mol}^{-1}$ ) (filled circle, solid line), light saturated  $\text{CO}_2$  leaf gas exchange ( $\max J_{\text{CO}_2}$ ,  $\mu\text{mol m}^{-2} \text{s}^{-1}$ ) (filled square, dashed line), and leaf temperature ( $T_{\text{leaf}}$ ,  $^{\circ}\text{C}$ ) (open triangle) during the leaf gas exchange measurements of developing RoHo 3615/M.9 apple leaves during the 2018 growing season. Error bars indicate the standard deviations.

**Table 2.** Leaf area per tree, associated percentage of light intercepted and mean daily carbon assimilation per tree ( $\text{mean } P_{\text{tree}}$ ) of Pinova/M.26 and RoHo 3615/M.9 apple trees in the 2018 growing season after the foliage of the trees was fully developed

Cultivar/ Spacing	$LA_{\text{tree}}$ ( $m^2$ )	Light interception* (%)	$\text{mean } P_{\text{tree}}$ ( $\text{C; g tree}^{-1} \text{d}^{-1}$ )
Pinova/ 3.5 m $\times$ 1.25 m	2.5	23	10.9*
	3.8	32	15*
	4.9	39	17.9*
RoHo 3615/ 3.2 m $\times$ 0.95 m	3.3	38	11.9**
	5.3	50	15.6**
	7.6	58	18.3**

In the period: \*from 66 days after full bloom (DAFB) until harvest, 143 DAFB \*\*76 DAFB until harvest, 143 DAFB.

higher seasonal fluctuations, as a response to varying leaf temperature and vapour pressure deficit (data not shown) at the different measurement dates.

The percentage of light intercepted by the canopy and the average daily assimilated C per tree, when the foliage was fully developed until harvest, was elevated on RoHo 3615 in comparison to Pinova (Table 2, Fig. 7). The difference resulted from the higher leaf area per tree of RoHo 3615 in combination with the reduced distances between trees and rows. Seasonal variation in  $P_{\text{tree}}$  occurred, reflecting the seasonal course in solar radiation (Fig. 7). The daily leaf area demand per fruit,  $LA_{\text{demand}}$ , showed a high degree of fluctuation during the growing season on both cultivars and appeared to be inverse to the seasonal course of S. On 12.07.2018,  $LA_{\text{demand}}$  reached its height, due to the local minima in S (Altlandsberg:  $4.2 \text{ MJ m}^{-2} \text{d}^{-1}$ ; Werder:  $7.1 \text{ MJ m}^{-2} \text{d}^{-1}$ ). Local minima and maxima were smoothed with a Savitzky-Golay filter without affecting the seasonal means in  $LA_{\text{demand}}$ . When dividing the seasonal course of  $LA_{\text{demand}}$  in 30 day intervals, the means of the original and the smoothed values of  $LA_{\text{demand}}$  for each interval differed by a maximum  $3 \text{ cm}^2$  (data not shown). During whole fruit development  $LA_{\text{demand}}$  conformed to  $\text{AGR}_C$  and appeared to reach its highest points when  $\text{AGR}_C$  reached its highest values in the middle of the growing period (Fig. 1f, 3, 7e, 7f).

The mean  $LA_{\text{demand}}$  considering varying fruit size in the period of 30 days after the foliage was fully developed (Pinova: 66 DAFB - 95 DAFB, RoHo 3615: 76 DAFB - 105 DAFB) increased with targeted fruit size (Fig. 8). The estimations, additionally demonstrated that the  $LA_{\text{demand}}$  to produce a target fruit size at harvest increases with total leaf area per tree (Fig. 8), as a consequence of increasing the internal shading of the leaves and the associated decrease in available light per leaf. Models used to estimate  $LA_{\text{demand}}$  for fruit of varying sizes on trees with a range in  $LA_{\text{tree}}$  of the observed trees were developed (Eqs 9.1, 9.2), based on the values plotted in Fig. 8. The average individual leaf

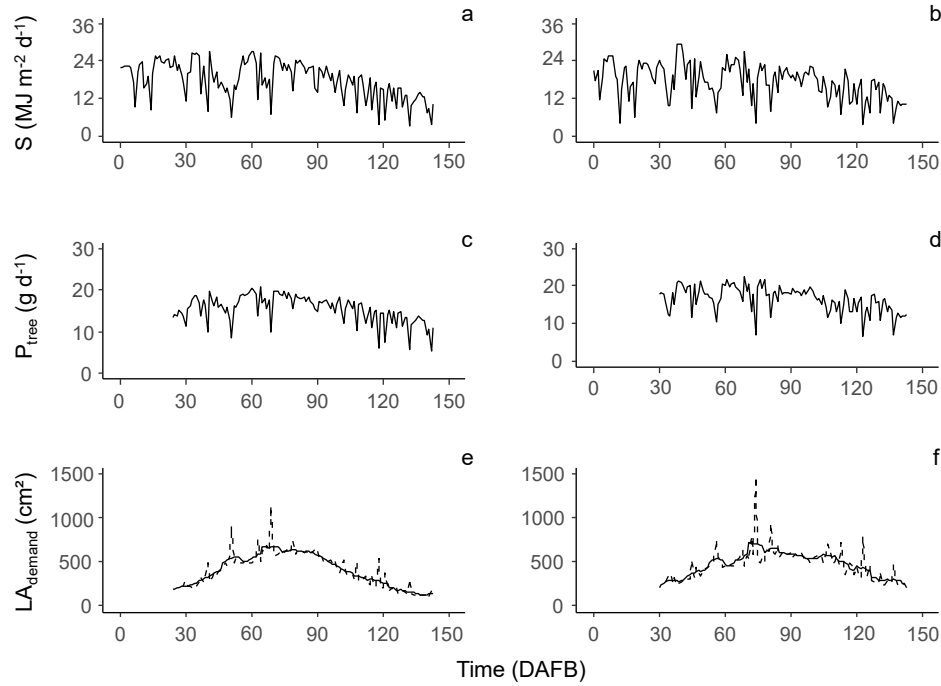


**Fig. 7.** Time course in days after full bloom (DAFB) of (a, b) solar radiation ( $S$ ,  $\text{MJ m}^{-2} \text{d}^{-1}$ ) and (c, d) estimated daily C assimilation per tree ( $P_{\text{tree}}$ ,  $\text{g d}^{-1}$ ) (e, f) daily leaf area demand per fruit ( $LA_{\text{demand}}$ ,  $\text{cm}^2$ ) (percentage of leaf-assimilated C available for fruit: linear increase from 40% (full bloom) to 80% (foliage is fully developed and the period of time after that)) of developing Pinova/M.26 (a, c) and RoHo 3615/M.9 (b, d) apple during the 2018 growing season. The fruit mass and size at harvest time were (e) 182 g / 72 mm, (f) 165 g / 68 mm. (e, f): solid line = smoothed values, dashed line = original values).

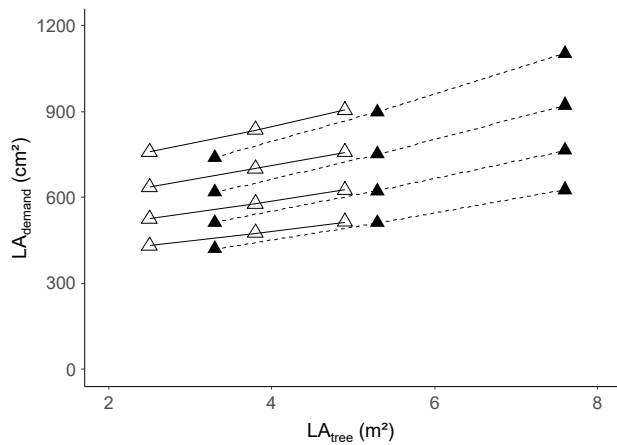


**Fig. 8.** Leaf area demand\* ( $LA_{\text{demand}}$ ,  $\text{cm}^2$ ) per fruit of Pinova/M.26 (open symbol, solid line) and RoHo 3615/M.9 (closed symbol, dashed line) apple with varying harvest fruit size (bottom to top: 65, 70, 75, and 80 mm) for trees with a different total leaf area ( $LA_{\text{tree}}$ ,  $\text{m}^2$ ) (\* mean values in the period of 30 days after foliage was fully developed, Pinova: 66 d after full bloom – 95 DAFB, RoHo 3615: 76 DAFB – 105 DAFB in 2018).

area, considering leaves from spurs and extension shoots in both orchards, was 24  $\text{cm}^2$  (data not shown). The resulting leaf demand per fruit would range from 18 – 38 leaves per fruit for Pinova and 18 – 46 leaves per fruit for RoHo 3615 for the targeted fruit sizes and a given total leaf area per tree

in both orchards. Model equations 9.1 and 9.2 were used to calculate the individual fruit bearing capacity (FBC) of trees with the varying total leaf area (Fig. 9). The difference in FBC between the trees in the range of the measured leaf area per tree is considerable. The FBC for a targeted fruit diameter of 65 mm for trees with a high total leaf area exceeds that of trees with a low leaf area by 50%. Both cultivars are known for their low susceptibility to alternate bearing and, therefore, alternate bearing was not considered in the present study. It may also be assumed that at the crop level equal to the FBC, alternate bearing is not expected.

$$\text{Pinova: } LA_{\text{demand}}(D, LA_{\text{tree}}) = -795.12 + 17.44 D - 79.95 LA_{\text{tree}} + 1.76 D LA_{\text{tree}} \quad (9.1)$$

$$\text{RoHo 3615: } LA_{\text{demand}}(D, LA_{\text{tree}}) = -598 + 13.12 D - 110.9 LA_{\text{tree}} + 2.44 D LA_{\text{tree}} \quad (9.2)$$

$LA_{\text{demand}}$  was estimated using Eqs (9.1), (9.2) taking into account the average fruit size per tree at harvest and the measured  $LA_{\text{tree}}$  of the individual trees. The  $LA_{\text{demand}}$  was applied to calculate the FBC of individual trees to produce fruit of the abundant average fruit size.  $LA_{\text{demand}}$  was compared to the actual LA:F of individual trees, whereas FBC was validated with the number of fruit per tree of the same trees at harvest (Fig. 10). The results demonstrate that the

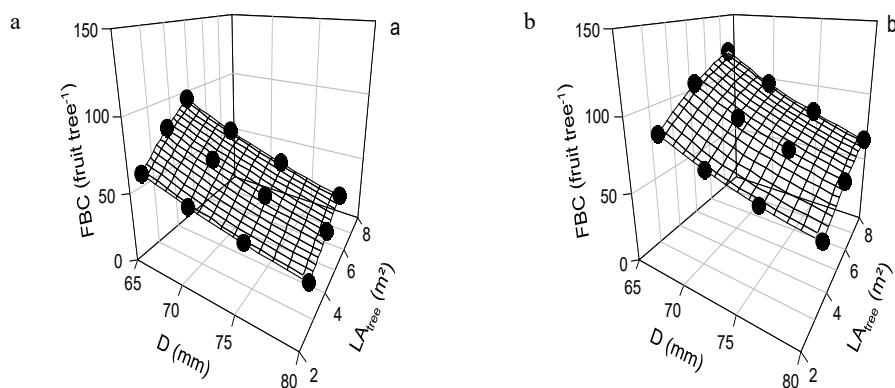


**Fig. 9.** Fruit bearing capacity (FBC, fruit tree<sup>-1</sup>) considering trees with a varying canopy leaf area (m<sup>2</sup>), when the canopy is fully developed, of Pinova (a) and RoHo 3615 (b) in 2018 to produce fruit of a certain target fruit diameter (D, mm). The closed dots represent min, mean and max values of LA<sub>tree</sub> in the considered orchards, cf. Table 2.

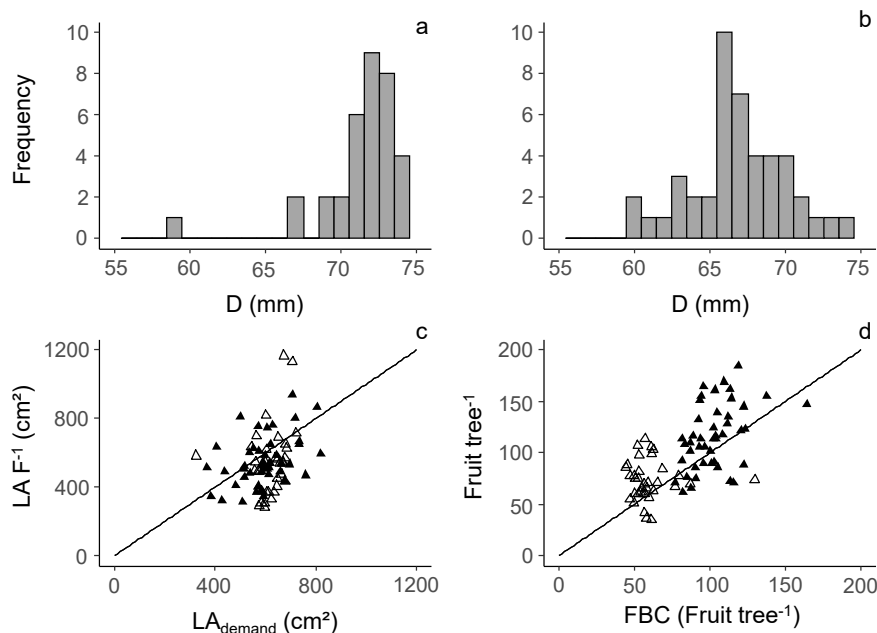


**Fig. 10.** a, b) Distribution of the average fruit diameter\* (mm) of individual apple trees; c) comparison between the modelled LA<sub>demand</sub> (cm<sup>2</sup>) to achieve the average fruit diameter and the measured leaf area to fruit ratio (LA F<sup>-1</sup>, cm<sup>2</sup>); d) estimated fruit bearing capacity (FBC)\*\*, to achieve measured average fruit diameter and harvested fruit per tree of Pinova (a, n = 35; open symbol) and RoHo 361 (b, n = 45; closed symbol) in 2018. Solid lines represent (c) LA:F = LA demand (d) FBC = harvested fruit per tree (\* the average fruit diameter was derived from the average fresh mass as shown in Fig. A1; \*\* in the period 30 days after the tree canopy was fully developed).

mean fruit number per tree in both cultivars was close to the calculated FBC. However, 8 trees out of 35 trees of Pinova and 14 trees out of 45 trees of RoHo 3615 had an LA:F value which was too high, thereby exceeding LA<sub>demand</sub> by an average of 208 cm<sup>2</sup> and 126 cm<sup>2</sup>, respectively (Fig. 10). Consequently, when comparing fruit per tree and FBC, it should be noted that 23% of the Pinova trees and 31% of RoHo 3615 trees had too few fruit per tree below the FBC. The average fruit fresh mass from the latter trees was 165 g, 159 g for Pinova and RoHo 3615, respectively.

When scaled up to the whole orchard level, Pinova could bear 1.9 t ha<sup>-1</sup>, RoHo 3615 3.1 t ha<sup>-1</sup> more fruit, which equates to 6 and 5% of the current yield of the orchards of 29.8 and 59.6 t ha<sup>-1</sup>, respectively. Consequently, the data show that a substantial number of trees are not managed at their optimal FBC. The number of flower clusters per tree in 2018 exceeded the FBC (data not shown) and no late frost reduced the number of fruit per tree in both orchards. The field uniform flower thinning may be seen as the primary source for the reduction in fruit per tree below the FBC.



In contrast, 16% of the trees of RoHo 3615 bore too many fruit per tree, exceeding the FBC by an average of 19 fruits per tree, leading to a low average fruit size below 65 mm (Fig. 10b), which is the minimum requirement for fresh market entry. As a consequence, despite high yields, the crop value from the mentioned trees is reduced.

## DISCUSSION

The purpose of this study was to investigate seasonal fruit growth and the variability in growth and fruit bearing capacity of individual trees within commercial apple orchards. Previous studies demonstrated the variability in yield and fruit per tree within orchards (Manfrini *et al.*, 2009; Aggelopoulou *et al.*, 2010), which is proposed to be considered in orchard management instead of the uniform treatment of all trees. The photosynthetic capacity of the trees and the associated light interception, which is a major determinant of crop growth (Monteith, 1977), was, however, not investigated. To further advance precise crop load management and adapt it to the site specific conditions, knowledge concerning the daily and seasonal carbon fixation of individual trees and the carbon requirements of developing fruit is required, this allows for the optimization of the carbon supply to demand balance of the tree to produce a desired fruit size. Existing carbon balance models (Lakso *et al.*, 2006; Pallas *et al.*, 2016) could adequately express the carbon supply to demand balance of individual apple trees and estimate the resulting number of fruit per tree and their fruit fresh mass at harvest for the conditions of individual seasons as well as the influence of different management practices on them. However, as one major input factor is the quantity of shoots per tree of different shoot populations, to generate leaf areas, it would be time consuming to count them from a high quantity of trees within an orchard for this purpose. The application of LiDAR in horticulture enables the quantification of canopy parameters, such as the total leaf area per tree, georeferenced for all trees of an orchard (Arno *et al.*, 2012; Tsoulis *et al.*, 2019; Hobart *et al.*, 2020). When integrated into the existing carbon balance models or parts of it, these plant data can provide an overview of the variability in carbon fixation per tree and the potential crop growth of whole orchards, for possible application in precision tree-specific crop load management.

A seasonal dynamic in carbon demand per fruit was demonstrated in the presented study, depending on the different development stages and associated sink strength per fruit as determined by the number of cortical cells (Lakso and Goffinet, 2017). The seasonal development of apple fruit from full bloom until harvest may be divided into two main stages, that overlap somewhat: cell division and cell enlargement, both with characteristic growth habits (Schechter *et al.*, 1993). However, there is a smooth transition between the stages as cell division in the cortex ends

around 40–45 DAFB, whereas it continues in the epidermis until 70 DAFB or even longer (Schechter *et al.*, 1993; Skene, 1966). Early fruit growth in fresh mass under the non-limiting conditions of low crop and no environmental stress follows a curvilinear course until about five weeks after full bloom before transitioning into a linear increase (Lakso *et al.*, 1995). A gradual decrease in the growth rate in the last part of the fruit development phase until the final fruit size is achieved is often seen but may reflect a reduced carbon supply or limiting temperatures or radiation (Stanley *et al.*, 2000). Despite the absence of data in the first weeks of fruit growth in the present study, the seasonal growth of fruit from both cultivars followed a course with typical peaks in growth rates in the middle of fruit development (Stanley *et al.*, 2000).

The maximum growth rates of the fruit in the present trials, modelled for different target fruit sizes, were within the range of growth rates in FM of Delicious apple, as reported previously, with a final fruit mass of between 165 g and 260 g (Warrington *et al.*, 1999) and Royal Gala apple with a final fruit mass of 200 g (Stanley *et al.*, 2000). The dry matter content of the fruit was, in comparison to earlier findings (Schechter *et al.*, 1993), relatively stable without noticeable changes occurring between the development stages. Minor fluctuations possibly occurred as a consequence of water flows inside and outside the fruit. The C content of the dry matter appeared to be slightly elevated in comparison with earlier results (Walton *et al.*, 1999). However, a decrease in  $C_{rel}$  from bloom until harvest was also observed, which occurs hypothetically due to changes in the composition of dry matter during fruit development with the accumulation of primarily carbohydrates that consist of approx. 40% C (Pavel and DeJong, 1995).

Dark respiration, generally, provides the chemical energy (*i.e.* ATP) necessary for the maintenance and growth processes in cells. During cell division, relatively more nucleic acids and proteins are formed in comparison to cell enlargement, which involves the vacuoles of the cells being filled with carbohydrates and organic acids for the most part (Walton *et al.*, 1999). Therefore, the respiration rate per unit fresh mass is higher in the cell division period than in the cell enlargement period which is more of a storage process. This leads to the typical seasonal decrease in the fruit respiration rate per unit fresh mass until cortex cell division ends. Afterwards, the respiration rate remains relatively constant (Figs 2a, 2d) until the climacteric rise. The fruit in the present trial, however, was harvested before the climacteric rise in fruit respiration rate occurred.

The seasonal decrease in  $Q_{10-20}$  (Fig. 2b) observed for both cultivars, was also reported previously for the  $Q_{15-25}$  values of the Golden Delicious apple, decreasing from 2.8 in early June to 1.6 in early August (Jones, 1981). The daily integral of respired  $CO_2$  by an apple ( $R_{daily}$ ) is determined by  $R_{dT}$ , fresh mass and temperature, which all change continuously. Consequently,  $R_{daily}$  fluctuated significant during



the whole fruit development process (Fig. 2e). As a result of elevated  $R_{dt}$  and FM,  $R_{daily}$  was higher on Pinova in comparison to RoHo 3615, especially in the period until 67 DAFB (Fig. 2e). Diurnal changes in fruit respiration, independent of fruit temperature, as described earlier (Bepete and Lakso, 1997), were not considered for the current calculations.

Apart from the aforementioned factors, the daily magnitude of fruit growth and respiration, in general, depends on the amount of carbohydrates translocated to the fruit, mainly in the form of sorbitol and sucrose (Hansen, 1967). Because approximately 90% of the annual carbohydrates assimilated by a tree are assimilated in the leaves (Hansen, 1967), the leaf area per fruit ratio, LA:F, and the available light limit fruit growth.

Both the leaf area demand after the canopy was fully developed and the fruit fresh mass were within the normal range of the results described for cultivars with medium size fruit grown on dwarfing rootstocks (cf. Palmer, 1992; Xia *et al.*, 2009). Larger fruit sizes at enhanced leaf area to fruit ratios were reported for the cultivars Braeburn (Palmer *et al.*, 1997) and Fuji (Koike *et al.*, 1990), where the genetic predisposition enables growth to a fresh mass exceeding 320 g at LA:F > 1200 cm<sup>2</sup>.

The daily amount of fixed carbon per tree depends on the amount of intercepted light by the canopy, which also limits its annual yield. The relationship between the fraction of intercepted light by a canopy and the leaf area index of a tree may be described as a hyperbolic function (Eq. (6)). A similar hyperbolic function was expected for the calibration model concerning LiDAR laser hits per tree to total leaf area. However, as a consequence of the given range of leaf area measured in the present study, a linear regression model between both parameters was suitable for describing the leaf area of the abundant trees in both orchards. Since canopy light interception determines canopy photosynthesis, the estimation of the fraction of intercepted light by the canopy directly from the LiDAR point cloud for each tree should be explored in future work. For whole canopies, the relationship between total leaf area and the fraction of intercepted light cannot be linear, as the mutual shading of overlapping leaves is disabling the exposure of a large fraction of the inner leaves to saturating light conditions. An increase in the leaf area per tree in a given space allotted to the tree increases this effect. As a consequence, the leaf area necessary to meet the carbon requirements of a fruit with a defined size varies for trees which are different in total leaf area and associated leaf area index (cf. Fig. 8). This may be one explanation for the achieved higher fruit size on Pinova compared to RoHo 3615, despite similar leaf area to fruit ratios and temperatures in the cell division stage. However, the canopy follows seasonal dynamics, as a consequence of vegetative growth, the loss of leaf area through pathogens and in some orchards, summer pruning. Therefore, the leaf area demand per fruit cannot be a constant. On days with

low solar radiation and a resulting dramatic rise in the leaf area demand per fruit (Fig. 7e, 7f), the woody structures of the tree have the potential to mobilize carbon reserves to maintain fruit growth for a period of approximately 2 days (McQueen *et al.*, 2005). Such a buffering of daily carbon supply has been observed in shading studies as well (Lakso, 2011). Therefore, the smoothing of the seasonal course in  $LA_{demand}$  with the Savitzky-Golay filter, led to a more valid general seasonal pattern.

In future studies, the seasonal development of leaf area and light interception per tree should be measured several times over the season in order to visualize seasonal patterns and identify critical periods. In the present trials, a chronological sigmoid course of the total leaf area per tree was assumed, which is generally valid. However, as temperature is a major driver of shoot and leaf development early in the season (Wagenmakers, 1996), the extent of leaf area development in this critical period for fruit development (Lakso and Goffinet, 2017) should be modelled against degree-days or estimated by LiDAR methods at several measuring dates. Fruit thinning should be realized in less than 30 DAFB, when the leaf area of the tree is still developing. Therefore, it is required to estimate the leaf area at full canopy from the measured values, *e.g.*, after petal fall. Before petal fall, the leaves and petals may not be distinguished by the LiDAR readings. After petal fall, approximately 40% of the total leaf area of a tree is developed (Lakso, 1984; Forshey *et al.*, 1987; Wünsche *et al.*, 1996). In order to estimate the final leaf area per tree immediately after petal fall would enable the consideration of the fruit bearing capacity in chemical fruit thinning, which is, depending on the thinning agent, applicable until fruit diameter of 20 mm is reached. After this, fruit becomes insensitive to the currently available thinning agents (McArtney and Obermiller, 2012).

The comparison between  $LA_{demand}$  and the measured LA:F of trees in both orchards demonstrated that > 20% of the trees had an LA:F value which was too high. This finding demonstrates that Pinova could potentially bear an additional 1.6 t ha<sup>-1</sup> and RoHo 361, 3.1 t ha<sup>-1</sup> more fruit, which is the equivalent of up to 5% of the harvested yields in the orchards, without any negative effect on fruit size. The best fruit size from an economic point of view, however, should be evaluated by each farmer for every orchard and year. The negative relationship between average fruit size and yield per tree is well known. The crop value additionally depends on the specific value-chain and the market situation. Finally, for each variety, the target crop load must not be detrimental to return bloom and sustained cropping. Such economic and tree performance considerations are required to determine the target fruit size, which can lead to the precise calculation of target fruit number per tree. However, a known FBC can support decisions and avoid yield loss.

## CONCLUSIONS

1. It was demonstrated that the estimation of the daily leaf area demand per fruit to satisfy its C requirement,  $LA_{demand}$ , undergoes seasonal changes. When the foliage of the tree is fully developed, the fruit bearing capacity of the tree may be estimated using  $LA_{demand}$  in the period when fruit growth rates achieve their maximum extent.

2. The estimation of the leaf area of individual trees using LiDAR scanning was shown to be feasible to allow for individual tree estimates of target fruit numbers.

3. The fruit bearing capacity of individual trees varied within the orchards investigated. This was due to variation in the total leaf area per tree. Field uniform flower thinning resulted in an avoidable sub-optimal crop load above or below fruit bearing capacity in both orchards. When combined with the modelling of carbon supply and crop carbon demand, the optimal number of fruit may be estimated for each tree.

## ACKNOWLEDGEMENTS

We thank Karin Bergt, Thomas Giese and Lutz Günzel for technical support in their orchards, Michael Pflanz for providing the MATLAB script required to estimate individual leaf area from RGB-images of leaves, and Werner B. Herppich for his general advice concerning gas exchange measurements and the evaluation of raw data.

**Conflict of interest.** The authors declare no conflict of interest

## CREDIT AUTHOR STATEMENT

MP: Conceptualization, Software, Formal analysis, Investigation, Methodology, Writing – Original Draft, Visualisation

AL: Methodology, Validation, Formal analysis, Writing – Review & Editing

NT: Methodology, Software, Investigation, Formal analysis

MZ: Conceptualization, Methodology, Writing – Review & Editing, Supervision, Project administration, Funding acquisition

**Conflict of interest:** The authors declare no conflict of interest.

## REFERENCES

- Aggelopoulou K.D., Wulfsohn D., Fountas S., Gemtos T.A., Nanos G.D., and Blackmore S., 2010. Spatial variation in yield and quality in a small apple orchard. *Precis. Agric.*, 11, 538-556. <https://doi.org/10.1007/s11119-009-9146-9>
- Arno J., Escola A., Valles J.M., Llorens J., Sanz R., et al., 2012. Leaf area index estimation in vineyards using a ground-based LiDAR scanner. *Prec. Agr.*, 14, 290-306. <https://doi.org/10.1007/s11119-012-9295-0>
- Bepete M. and Lakso A.N., 1997. Apple fruit respiration in the field: relationships to fruit growth rate, temperature, and light exposure. *Acta Hortic.*, 451, 319-326. <https://doi.org/10.17660/ActaHortic.1997.451.37>
- Bepete M. and Lakso A.N., 1998. Differential effects of shade on early season fruit and shoot growth rates in 'Empire' apple branches. *HortScience*, 33, 823-825. <https://doi.org/10.21273/HORTSCI.33.5.823>
- Brandes N. and Zude-Sasse M., 2019. Respiratory patterns of European pear (*Pyrus communis* L. 'Conference') throughout pre- and postharvest fruit development. *Heliyon*, 5, e01160. <https://doi.org/10.1016/j.heliyon.2019.e01160>
- Breen K.C., Tustin D.S., Palmer J.W., and Close D.C., 2015. Method of manipulating floral bud density affects fruit set responses and productivity in apple. *Sci. Hortic.-Amsterdam*, 197, 244-253. <https://doi.org/10.1016/j.scienta.2015.09.042>
- Bresilla K., Perulli G.D., Boini A., Morandi B., Corelli Grappadelli L., and Manfrini L., 2019. Single-shot convolution neural networks for real-time fruit detection within the tree. *Front. Plant Sci.*, 611(10), 1-12. <https://doi.org/10.3389/fpls.2019.00611>
- Charles-Edwards DA., 1982. Physiological determinants of crop growth. Academic Press, Sydney.
- Corelli-Grappadelli L., Lakso A.N., Flore J.A., 1994. Early season patterns of carbohydrate partitioning in exposed and shaded apple branches. *J. Am. Soc. Hortic. Sci.*, 119, 596-603. <https://doi.org/10.21273/JASHS.119.3.596>
- Doerflinger F.C., Lakso A.N. and Braun P., 2015. Adapting the MaluSim Apple tree model for the 'Gala' cultivar. *Acta Hortic.*, 1068, 267-272. <https://doi.org/10.17660/ActaHortic.2015.1068.33>
- Forshey C.G., Weires R.W., and van Kirk J.R., 1987. Seasonal development of the leaf canopy of 'Macspur McIntosh' apple trees. *HortScience*, 22, 881-883.
- Glenn D.M., 2016. Dry matter partitioning and photosynthetic response to biennial bearing and freeze damage in 'Empire' apple. *Sci.Hortic.-Amsterdam*, 210, 1-5. <https://doi.org/10.1016/j.scienta.2016.06.042>
- Greene D.W., Lakso A.N., Robinson T.L., and Schwallier P., 2013. Development of a fruitlet growth model to predict thinner response on apples. *HortScience*, 48, 584-587. <https://doi.org/10.21273/HORTSCI.48.5.584>
- Handschack M. and Schmidt S., 1990. Grafisches Modell zur Beschreibung der Ertragsbildung bei Apfel unter Berücksichtigung von Wechselwirkungen zwischen den Ertragskomponenten. *Arch. Gartenbau*, 38, 399-405.
- Hansen P., 1967. 14C-studies on apple trees. I. The effect of the fruit on the translocation and distribution of photosynthates. *Physiol. Plant.*, 20, 382-91. <https://doi.org/10.1111/j.1399-3054.1967.tb07178.x>
- Hansen P., 1969. 14C-Studies on apple trees. IV. Photosynthate consumption in fruits in relation to the leaf-fruit ratio and to the leaf-fruit position. *Physiol. Plant.*, 22, 186-198. <https://doi.org/10.1111/j.1399-3054.1969.tb07855.x>
- Hobart M., Pflanz M., Weltzien C., and Schirrmann M., 2020. Growth Height Determination of Tree Walls for Precise Monitoring in Apple Fruit Production Using UAV Photogrammetry. *Remote Sensing*, 12(10), 1656, 1-17. <https://doi.org/10.3390/rs12101656>

- Iwanami H., Moriya-Tanaka Y., Honda C., Hanada T., and Wada M., 2018.** A model for representing the relationships among crop load, timing of thinning, flower bud formation, and fruit weight in apples. *Sci. Hortic.-Amsterdam*, 242, 181-187. <https://doi.org/10.1016/j.scienta.2018.08.001>
- Jackson J.E. and Palmer J.W., 1980.** A computer model study of light interception by orchards in relation to mechanised harvesting and management. *Sci. Hortic.-Amsterdam*, 13, 1-7. [https://doi.org/10.1016/0304-4238\(80\)90015-1](https://doi.org/10.1016/0304-4238(80)90015-1)
- Janoudi A. and Flore J.A., 2005.** Application of ammonium thiosulfate for blossom thinning in apples. *Sci. Hortic.-Amsterdam*, 104, 161-168. <https://doi.org/10.1016/j.scienta.2004.08.016>
- Jones H.G., 1981.** Carbon dioxide exchange of developing apple (*Malus pumila* Mitt.) fruits. *J. Exp. Bot.*, 32, 1203-1210. <https://doi.org/10.1093/jxb/32.6.1203>
- Kofler J., Milyaev A., Capezzone F., Stojnić S., Mičić N., et al., 2019.** High crop load and low temperature delay the onset of bud initiation in apple. *Sci. Rep.*, 9, 17986 (2019). <https://doi.org/10.1038/s41598-019-54381-x>
- Koike H., Yoshizawa S., and Tsukahara K., 1990.** Optimum crop load and dry weight partitioning in Fuji/M.26 apple trees. *J. Jap. Soc. Hort. Sci.*, 58, 827-834. <https://doi.org/10.2503/jjshs.58.827>
- Lakso A.N., 1984.** Leaf area development patterns in young pruned and unpruned apple trees. *J. Amer. Soc. Hort. Sci.*, 109, 861-865.
- Lakso A.N., 2011.** Early fruit growth and drop - the role of carbon balance in the apple tree. *Acta Hortic.*, 903, 733-742. <https://doi.org/10.17660/ActaHortic.2011.903.102>
- Lakso A.N., Corelli Grappadelli L., Barnard J., and Goffinet M.C., 1995.** An exponential model of the growth pattern of the apple fruit. *J. Hort. Sci.*, 70(4), 389-394. <https://doi.org/10.1080/14620316.1995.11515308>
- Lakso A.N., Piccioni R.M., Denning S.S., Sottile F., and Costa Tura J., 1999.** Validating an apple dry matter production model with whole canopy gas exchange measurements in the field. *Acta Hortic.*, 499, 115-122. <https://doi.org/10.17660/ActaHortic.1999.499.11>
- Lakso A.N., White M.D., and Tustin D.S., 2001.** Simulation modeling of the effects of short and long-term climatic variations on carbon balance of apple trees. *Acta Hortic.*, 557, 473-480. <https://doi.org/10.17660/ActaHortic.2001.557.63>
- Lakso A.N., Greene D.W., and Palmer J.W., 2006.** Improvements on an apple carbon balance model. *Acta Hortic.*, 707, 57-61. <https://doi.org/10.17660/ActaHortic.2006.707.6>
- Lakso A.N. and Johnson R.S., 1990.** A simplified dry matter production model for apple using automatic programming simulation software. *Acta Hortic.*, 276, 141-148. <https://doi.org/10.17660/ActaHortic.1990.276.15>
- Lakso A.N. and Robinson T.L., 2014.** Integrating physiological models in applied fruit crop research. *Acta Hortic.*, 1058, 285-290. <https://doi.org/10.17660/ActaHortic.2014.1058.33>
- Lakso A.N. and Goffinet M.C., 2017.** Advances in understanding apple fruit development. In: *Achieving sustainable cultivation of apples* (Ed. K. Evans), Burleigh Dodds Science Publishing, Cambridge, United Kingdom.
- Ligges U., Short T., Kienzle P., et al., 2015.** Package 'signal'. R Foundation for Statistical Computing.
- Lopez G., Boini A., Manfrini L., Torres-Ruiz J.M., Pierpaoli E., Zibordi M., and Corelli-Grappadelli L., 2018.** Effect of shading and water stress on light interception, physiology and yield of apple trees. *Agr. Water Manag.*, 210, 140-148. <https://doi.org/10.1016/j.agwat.2018.08.015>
- McArtney S.J. and Obermiller J.D., 2012.** Use of 1-Aminocyclopropane carboxylic acid and metamitron for delayed thinning of apple fruit. *Hortscience*, 47, 1612-1616. <https://doi.org/10.21273/HORTSCI.47.11.1612>
- Manfrini L., Taylor J.A., and Corelli-Grappadelli L., 2009.** Spatial analysis of the effect of fruit thinning on apple crop load. *Eur. J. Hort. Sci.*, 74(2), 54-60. [http://www.pubhort.org/ejhs/2009/file\\_968077.pdf](http://www.pubhort.org/ejhs/2009/file_968077.pdf)
- McCree K.J., 1972.** Test of current definitions of photosynthetically active radiation against leaf photosynthesis data. *Agr. Meteorol.*, 10, 443-53. [https://doi.org/10.1016/0002-1571\(72\)90045-3](https://doi.org/10.1016/0002-1571(72)90045-3)
- McQueen J.C., Minchin P.E.H., Thorpe M.R., Silvester W.B., 2005.** Short-term storage of carbohydrate in stem tissue of apple (*Malus domestica*), a woody perennial: evidence for involvement of the apoplast. *Funct. Plant Biol.*, 32, 1027-1031. <https://doi.org/10.1071/FP05082>
- Mirás-Avalos J.M., Egea G., Nicolas E., et al., 2011.** QualiTree, a virtual fruit tree to study the management of fruit quality. II. Parameterisation for peach, analysis of growth-related processes and agronomic scenarios. *Trees*, 25, 785-799. <https://doi.org/10.1007/s00468-011-0555-9>
- Monteith J.L., 1977.** Climate and the efficiency of crop production in Britain. *Philos. Trans. R. Soc. Lond., Ser. B*, 281, 277-294. <https://doi.org/10.1098/rstb.1977.0140>
- Musacchi S. and Serra S., 2018.** Apple fruit quality: overview on pre-harvest factors. *Sci. Hortic.-Amsterdam*, 234, 409-430. <https://doi.org/10.1016/j.scienta.2017.12.057>
- Pallas B., Da Silva D., Valsesia P., Yang W., Guillaume O., et al., 2016.** Simulation of carbon allocation and organ growth variability in apple tree by connecting architectural and source-sink models. *Ann. Bot.*, 118, 317-330. <https://doi.org/10.1093/aob/mcw085>
- Palmer J.W., 1992.** Effects of varying crop load on photosynthesis, dry matter production and partitioning of Crispin/M.27 apple trees. *Tree Physiol.*, 11, 19-33. <https://doi.org/10.1093/treephys/11.1.19>
- Palmer J.W., Giuliani R., and Adams H.M., 1997.** Effect of crop load on fruiting and leaf photosynthesis of 'Braeburn'/M.26 apple trees. *Tree Physiol.*, 17, 741-746. <https://doi.org/10.1093/treephys/17.11.741>
- Palmer J.W., Wünsche J.N., Meland M., and Hann A., 2002.** Annual dry matter production by three apple cultivars at four within-row spacings in New Zealand. *J. Hort. Sci. Biotechnol.*, 77, 712-717. <https://doi.org/10.1080/14620316.2002.11511561>
- Pavel E.W. and DeJong T.M., 1995.** Seasonal patterns of non-structural carbohydrates of apple (*Malus pumila* Mill.) fruits: relationship with relative growth rates and contribution to solute potential. *J. Hort. Sci.*, 70, 127-134. <https://doi.org/10.1080/14620316.1995.11515282>
- Penzel M. and Kröling C., 2020.** Thinning efficacy of metamitron on young 'RoHo 3615' (Evelina®) apple. *Sci. Hortic.-Amsterdam*, 272, 1-6. <https://doi.org/10.1016/j.scienta.2020.109586>

- Penzel M., Pflanz M., Gebbers R., and Zude-Sasse M., 2020.** Tree adapted mechanical flower thinning prevents yield loss caused by over thinning of trees with low flower set in apple. *Eur. J. Hort. Sci.*, 2021 (in press).
- R Core Team, **2018.** R: A language and environment for statistical computing. R Foundation for Statistical Computing, Vienna, Austria. <https://www.R-project.org/>
- Robinson T.L., Lakso A.N., and Greene D., 2017.** Precision crop load management: The practical implementation of physiological models. *Acta Hortic.*, 1177, 381-390. <https://doi.org/10.17660/ActaHortic.2017.1177.55>
- Schechter I., Proctor J.T.A., and Elfving D.C., 1993.** Characterization of seasonal fruit growth of 'Idared' apple. *Sci. Hortic.-Amsterdam*, 54, 203-210. [https://doi.org/10.1016/0304-4238\(93\)90088-8](https://doi.org/10.1016/0304-4238(93)90088-8)
- Schumacher R., 1962.** Fruchtentwicklung und Blütenknospenbildung beim Apfel in Abhängigkeit von der Blattmasse, unter Berücksichtigung der abwechselnden Tragbarkeit. Ph.D. Thesis, ETH Zürich. <https://doi.org/10.3929/ethz-a-000088562>
- Skene D.S., 1966.** The distribution of growth and cell division in the fruit of Cox's Orange Pippin. *Ann. Bot.*, 30(3), 493-512. <https://doi.org/10.1093/oxfordjournals.aob.a084092>
- Stanley C.J., Tustin D.S., Lupton G.B., McArtney S., Cashmore W.M., and De Silva H.N., 2000.** Towards understanding the role of temperature in apple fruit growth response in three geographical regions within New Zealand. *J. Hortic. Sci. Biotech.*, 75(4), 413-422. <https://doi.org/10.1080/14620316.2000.11511261>
- Treder W., 2008.** Relationship between yield, crop density coefficient and average fruit weight of 'Gala' apple. *J. Fruit Orn. Plant Res.*, 16, 53-63
- Tsoulias N., Paraforos D.S., Fountas S., and Zude-Sasse M., 2019.** Estimating canopy parameters based on the stem position in apple trees using a 2D LiDAR. *Agronomy*, 9(11), 740, 1-18. <https://doi.org/10.3390/agronomy9110740>
- Tsoulias N., Paraforos D.S., Xanthopoulos G., Zude-Sasse M., 2020.** Apple shape detection based on geometric and radiometric features using a LiDAR laser scanner. *Remote Sensing*, 12, 2481. <https://doi.org/10.3390/rs12152481>
- Vanbrabant Y., Delalieux S., Tits L., Pauly K., Vandermaesen J., and Somers B., 2020.** Pear Flower Cluster Quantification Using RGB Drone Imagery. *Agronomy*, 10, 407, 1-26. <https://doi.org/10.3390/agronomy10030407>
- Wagenmakers P.S., 1996.** Effects of light and temperature on potential apple production. *Acta Hortic.*, 416, 191-198. <https://doi.org/10.17660/ActaHortic.1996.416.23>
- Walton E.F., Wünsche J.N., and Palmer J.W., 1999.** Estimation of the bioenergetic costs of fruit and other organ synthesis in apple. *Physiol. Plant.*, 106, 129-134. <https://doi.org/10.1034/j.1399-3054.1999.106118.x>
- Warrington I.J., Faulton T.A., Halligan E.A., and de Silva H.N., 1999.** Apple fruit growth and maturity are affected by early season temperatures. *J. Amer. Soc. Hort. Sci.*, 124, 468-477. <https://doi.org/10.21273/JASHS.124.5.468>
- Wójcik P., Rutkowski K., and Treder W., 2001.** Quality and storability of 'Gala' apples as affected by crop load. *Folia Hortic.*, 13(2), 89-96
- Wünsche J.N., Lakso A.N., Robinson T.L., Lenz F., and Denning S.S., 1996.** The bases of productivity in apple production systems: the role of light interception by different shoot types. *J. Amer. Soc. Hort. Sci.*, 121, 886-893. <https://doi.org/10.21273/JASHS.121.5.886>
- Xia G., Cheng L., Lakso A.N., and Goffinet M., 2009.** Effects of nitrogen supply on source-sink balance and fruit size of 'Gala Apple' trees. *Hort. Sci.*, 134, 126-133. <https://doi.org/10.21273/JASHS.134.1.126>
- Yoder K.S., Peck G.M., Combs L.D., and Byers R.E., 2013.** Using a pollen tube growth model to improve apple blossom thinning for organic production. *Acta Hortic.*, 1001, 207-214. <https://doi.org/10.17660/ActaHortic.2013.1001.23>

## APPENDIX

Table A1: Equations used in the materials and method section. Abbreviations are defined in the text

Equation	Description	No.
$R^2 [0-1] = \frac{\sum_{i=1}^n (LA_{LiDAR} - \overline{LA_{lab}})^2}{\sum_{i=1}^n (LA_{lab} - \overline{LA_{lab}})^2}$	Coefficient of determination	(A1)
$RRMSE [\%] = \frac{\sqrt{\frac{1}{n} \times \sum_{i=1}^n (LA_{lab} - LA_{LiDAR})^2}}{\overline{LA_{lab}}} \times 100$	Relative root mean squared error	(A2)
$f(x) = a + \frac{b}{1 + e^{\frac{-(x-c)}{d}}}$	Sigmoid growth model	(A3)
$GDD_{TB} = 0.5 \times (T_{Max} + T_{Min}) - T_B;$		
	Growing degree days	(A4)
if $0.5 \times (T_{Max} + T_{Min}) - T_B > 0$		

Table A2: Functions of fruit and leaf area development and  $LA_{LiDAR}$  fitted with standard regression methods. Abbreviations are defined in the text

Equations	R <sup>2</sup>	Definition	No.
$FM(DAFB) = 185.493 - (12077.2 / ((1.05883)^{DAFB} + 64.6686))$	0.85	Development in FM of Pinova fruit	(A5.1)
$M(DAFB) = 183.972 - (5982.92 / ((1.04047)^{DAFB} + 30.9077))$	0.87	Development in FM of RoHo 3615 fruit	(A5.2)
$C(DAFB) = 15.599 - (1644.78 / ((1.06415)^{DAFB} + 105.827))$	0.85	Development in C content of Pinova fruit	(A6.1)
$C(DAFB) = 13.445 - (674.033 / ((1.04798)^{DAFB} + 49.0924))$	0.84	Development in C content of RoHo 3615 fruit	(A6.2)
$AGR_{FM}(DAFB) = (690.363 \times (1.05883)^{DAFB}) / ((1.05883)^{DAFB} + 64.6686)^2$	-	Daily growth rates in FM of Pinova fruit	(A7.1)
$AGR_{FM}(DAFB) = (237.377 \times (1.04047)^{DAFB}) / ((1.04047)^{DAFB} + 30.9077)^2$	-	Daily growth rates in FM of RoHo 3615 fruit	(A7.2)
$AGR_C(DAFB) = (102.262 \times (1.06415)^{DAFB}) / ((1.06415)^{DAFB} + 105.827)^2$	-	Daily growth rates in C of Pinova fruit	(A8.1)
$AGR_C(DAFB) = (31.5857 \times (1.04798)^{DAFB}) / ((1.04798)^{DAFB} + 49.0924)^2$	-	Daily growth rates in C of RoHo 3615 fruit	(A8.2)
$FM_{norm}(DAFB) = 1.01835 - (66.3031 / ((1.05883)^{DAFB} + 64.6686))$		Development in FM of Pinova fruit, normalized to FM at harvest	A9.1
$FM_{norm}(DAFB) = 1.1124 - (36.176 / ((1.04047)^{DAFB} + 30.9077))$		Development in FM of RoHo 3615 fruit, normalized to FM at harvest	A9.2
$C_{norm}(DAFB) = 1.01451 - (106.971 / ((1.06415)^{DAFB} + 105.827))$		Development in C of Pinova fruit normalized to C at harvest	A10.1
$C_{norm}(DAFB) = 1.06172 - (53.2266 / ((1.04798)^{DAFB} + 49.0924))$		Development in C of RoHo 3615 fruit normalized to C at harvest	A10.2
$C_{rel}(DAFB) = 0.5035 - 0.00023 \times DAFB$	0.94	Fraction of C on the DM of Pinova fruit	(A11.1)
$C_{rel}(DAFB) = 0.5124 - 0.00027 \times DAFB$	0.76	Fraction of C on the DM of RoHo 3615 fruit	(A11.2)
$LA_{LiDAR}(PPT) = 1.62 + (6.822 \times 10^{-5} \times PPT)$	-	Function to estimate $LA_{LiDAR}$ from PPT of Pinova trees.	(A12.1)
$LA_{LiDAR}(PPT) = 1.491 + (6.987 \times 10^{-5} \times PPT)$	-	Function to estimate $LA_{LiDAR}$ from PPT of RoHo 3615 trees.	(A12.2)
$LA_{tree}(DABB) = -0.024 + \frac{3.8301986}{1 + e^{\frac{-(DABB - 54.731847)}{10.847129}}}$	-	Development of the canopy leaf area of Pinova trees	(A13.1)
$LA_{tree}(DABB) = -0.067 + \frac{5.382473}{1 + e^{\frac{-(DABB - 54.766887)}{12.581858}}}$	-	Development of the total leaf area of RoHo 3615 trees	(A13.2)

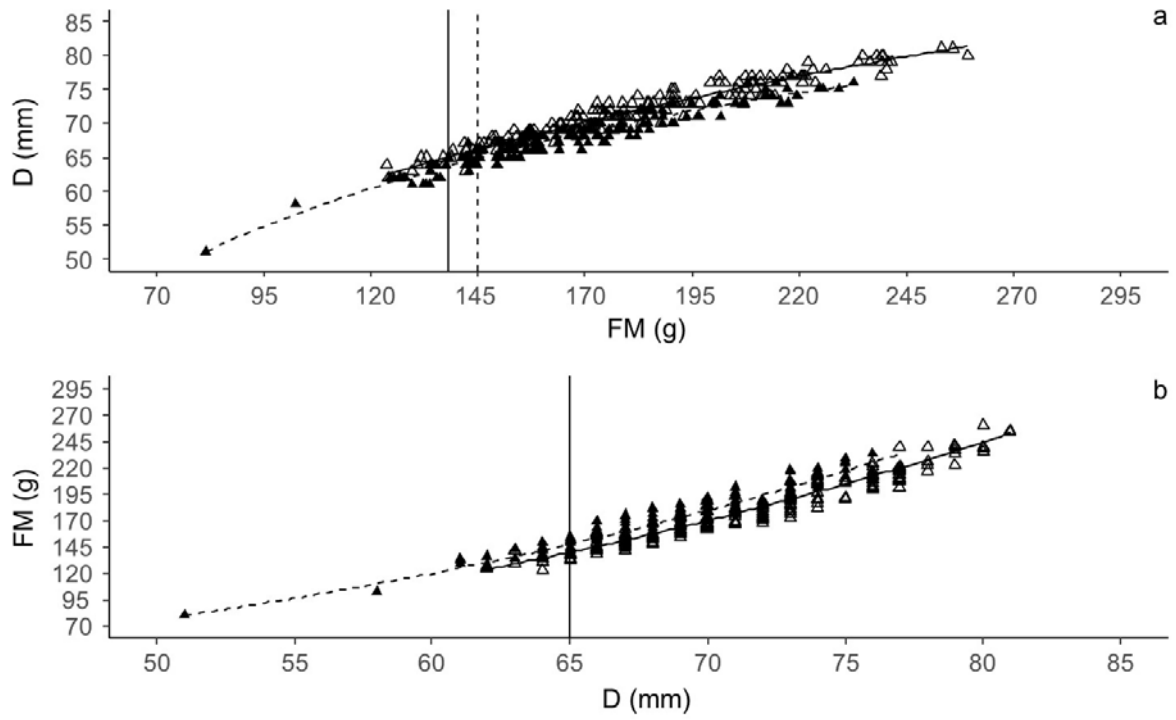


Fig. A1: Relationship between (a) fruit fresh mass (FM) (g) and diameter (D) (mm), (b) D and FM at the harvest time of Pinova/M.26 apple ( $n = 180$ ; open symbol, solid line) and RoHo 3615/M.9 ( $n = 180$ ; closed symbol, dashed line) in 2018. The vertical lines indicate the minimum fruit size for market entry of 65 mm. (Pinova:  $D = 29.275 + 108.34959 \text{ FM} (280.67889 + \text{FM})^{-1}$ ,  $R^2 = 0.94$ ,  $\text{FM} = 18.2 + 0.00044199462 D^3$ ,  $R^2 = 0.94$ ; RoHo 3615:  $D = 10.66 + 96.547187 \text{ FM} (112.84451 + \text{FM})^{-1}$ ,  $R^2 = 0.93$ ,  $\text{FM} = 17.966 + 0.00047130511 D^3$ ,  $R^2 = 0.93$ ).

## **5. Modeling of individual fruit-bearing capacity of trees is aimed at optimizing fruit quality of *Malus x domestica* Borkh. 'Gala'**

In: *Frontiers in Plant Science* 12, pp.1-15, 2021

Cite as:

Penzel, M., Herppich, W.B., Tsoulas, N., Weltzien, C., Zude-Sasse, M., 2021. Modeling of individual fruit-bearing capacity of trees is aimed at optimizing fruit quality of *Malus x domestica* Borkh. 'Gala'. *Front. Plant Sci.* 12, 1-15.  
<https://doi.org/10.3389/fpls.2021.669909>





# Modeling of Individual Fruit-Bearing Capacity of Trees Is Aimed at Optimizing Fruit Quality of *Malus x domestica* Borkh. 'Gala'

Martin Penzel<sup>1,2</sup>, Werner B. Herppich<sup>2</sup>, Cornelia Weltzien<sup>1,2</sup>, Nikos Tsoulas<sup>2</sup> and Manuela Zude-Sasse<sup>2\*</sup>

<sup>1</sup> Chair of Agromechatronics, Technische Universität Berlin, Berlin, Germany, <sup>2</sup> Horticultural Engineering, Leibniz Institute for Agricultural Engineering and Bioeconomy, Potsdam, Germany

## OPEN ACCESS

### Edited by:

Maxwell Ware,  
Colorado State University,  
United States

### Reviewed by:

Riccardo Lo Bianco,  
University of Palermo, Italy  
Youmei Li,  
Yangzhou University, China  
Leo Rufato,  
Santa Catarina State University, Brazil

### \*Correspondence:

Manuela Zude-Sasse  
mzude@atb-potsdam.de

### Specialty section:

This article was submitted to  
Crop and Product Physiology,  
a section of the journal  
Frontiers in Plant Science

**Received:** 19 February 2021

**Accepted:** 07 June 2021

**Published:** 13 July 2021

### Citation:

Penzel M, Herppich WB, Weltzien C,  
Tsoulas N and Zude-Sasse M (2021)  
Modeling of Individual Fruit-Bearing  
Capacity of Trees Is Aimed at  
Optimizing Fruit Quality of  
*Malus x domestica* Borkh. 'Gala'.  
Front. Plant Sci. 12:669909.  
doi: 10.3389/fpls.2021.669909

The capacity of apple trees to produce fruit of a desired diameter, i.e., fruit-bearing capacity (FBC), was investigated by considering the inter-tree variability of leaf area (LA). The LA of 996 trees in a commercial apple orchard was measured by using a terrestrial two-dimensional (2D) light detection and ranging (LiDAR) laser scanner for two consecutive years. The FBC of the trees was simulated in a carbon balance model by utilizing the LiDAR-scanned total LA of the trees, seasonal records of fruit and leaf gas exchanges, fruit growth rates, and weather data. The FBC was compared to the actual fruit size measured in a sorting line on each individual tree. The variance of FBC was similar in both years, whereas each individual tree showed different FBC in both seasons as indicated in the spatially resolved data of FBC. Considering a target mean fruit diameter of 65 mm, FBC ranged from 84 to 168 fruit per tree in 2018 and from 55 to 179 fruit per tree in 2019 depending on the total LA of the trees. The simulated FBC to produce the mean harvest fruit diameter of 65 mm and the actual number of the harvested fruit >65 mm per tree were in good agreement. Fruit quality, indicated by fruit's size and soluble solids content (SSC), showed enhanced percentages of the desired fruit quality according to the seasonally total absorbed photosynthetic energy (TAPE) of the tree per fruit. To achieve a target fruit diameter and reduce the variance in SSC at harvest, the FBC should be considered in crop load management practices. However, achieving this purpose requires annual spatial monitoring of the individual FBC of trees.

**Keywords:** apple, carbon balance, lidar, respiration, precision horticulture, growth, canopy photosynthesis model

## INTRODUCTION

In fruit production, the number of apples per tree is negatively correlated to the mean fruit fresh mass (FM), coloration (Palmer et al., 1997), soluble solids content (SSC) (Link, 2000; Serra et al., 2016), and flower set in the following season (Handsack and Schmidt, 1991). Each individual apple tree may initiate up to 2,000 flowers, which significantly exceeds the commercially desired number of fruit at harvest (Penzel et al., 2021). Although a high percentage of flowers and later fruitlets will be naturally shed in flower or fruit abscission, often too many fruit remain on the tree. High crop load results in low-quality fruit whereas low crop load may reduce yield. Furthermore, the distribution of fruit throughout the canopy may not be uniform,

which is one reason for the variability of fruit quality within the tree. Additionally, the position of the fruit in the cluster (Jakopic et al., 2015), the position and light exposure of the bearing branch as well as the number and proximity of leaves and other fruit affect fruit quality (Belhassine et al., 2019; Reyes et al., 2020). Consequently, crop load management is required to adjust the number of fruit per tree. Various strategies to obtain one to two fruit per flower cluster widely distributed in the canopy exist, targeting a high percentage of high-quality fruit and, thus, high crop value in the current and sufficient flower bud initiation for the subsequent growing season (Costa et al., 2018). However, for developing efficient crop load management, the information on the optimal number of fruit per tree is crucial.

Much work has been done to evaluate the effects of the number of fruit per tree on apple quality parameters. ‘Gala’ apples have a high economic importance worldwide and are well described in crop load experiments. Commercial ‘Gala’ strains show a variability in mean fruit FM per tree up to 90 g affected by crop load (McArtney et al., 1996; Pilar Mata et al., 2006; Xia et al., 2009). The SSC of apples is an additional important internal quality parameter largely influencing the acceptance and buying decision of consumers. Crop load can also slightly affect the mean SSC of ‘Gala’ apples at harvest (Pilar Mata et al., 2006; Yuri et al., 2011). So far, different techniques have been applied to estimate the number of fruit per tree, which would lead to a desired fruit quality. These methods capture continuous yield recording in the orchard (Handsack and Schmidt, 1991) or the assessment of the crop load in relation to the trunk cross-sectional area (Iwanami et al., 2018). Also, the leaf area (LA) per fruit has been identified as an important determinant of fruit quality (Poll et al., 1996; Palmer et al., 1997).

Generally, trees can be considered as a collection of semiautonomous organs (DeJong, 2019), where each organ has a genetically determined, organ-specific development pattern and growth potential (Reyes et al., 2016), which is achieved according to the individual carbon supply conditions. Because only leaves perform net carbon assimilation, the exposed LA of a tree reflects the growth capacity of the tree to intercept solar radiation and serves therefore as a proxy of the fruit-bearing capacity (FBC). Lakso et al. applied LA estimates in carbon balance modeling (Lakso and Johnson, 1990). In their approach, the light interception of each individual shoot was scaled up to the canopy level by considering the tree’s total LA as one big leaf, which receives the average irradiance of the canopy (De Pury and Farquhar, 1997). This approach is valuable as it combines existing knowledge in a modeling approach, providing the potential to simulate the optimum crop load. However, it may lead to an overestimation of the photosynthetic capacity of a tree because the light environments within a tree’s canopy can be highly variable (Zhang et al., 2016). The photosynthesis of the exposed leaves and leaves in sun flecks is mostly light saturated whereas the photosynthetic response of shaded leaves to irradiance is linear (De Pury and Farquhar, 1997). Charles-Edwards (1982) demonstrated the validity of the big-leaf approach for hedgerow apple orchards. Furthermore, this approach was validated by recording the CO<sub>2</sub> exchange of whole trees enclosed in a canopy chamber (Lakso et al., 1996). Nevertheless, the spatial variability

of individual LA of trees was not taken into account in CO<sub>2</sub> balance so far.

Indeed, vegetative and reproductive growths vary spatially in orchards. Variability in the trunk cross-sectional area (Manfrini et al., 2020), number of flower clusters (Vanbrabant et al., 2020; Penzel et al., 2021), yield, mean FM, and the fruit maturity stage of each individual tree (Manfrini et al., 2020) within the same orchard was described. Consequently, both the individual LA (Sanz et al., 2018) and the LA index (Poblete-Echeverría et al., 2015) and the associated FBC of each individual tree may vary spatially. It can also be assumed that such variability in each individual tree affects the optimum number of fruit per tree when targeting a homogenous fruit quality throughout the orchard. However, the actual number of fruit per tree was not yet evaluated in relation to the variable LA and associated FBC.

The mapping of canopy and yield parameters within an orchard can be performed by georeferencing each tree and the application of remote sensing, e.g., based on photogrammetry (Mu et al., 2018), time-of-flight reading (Coupel-Ledru et al., 2019; Tsoulas et al., 2019), or thermal imaging (Huang et al., 2020). Most recently, the number of flower clusters (Vanbrabant et al., 2020) and fruit per tree (Apolo-Apolo et al., 2020; Tsoulas et al., 2020a) were mapped in pome fruit orchards by analyzing the point clouds generated from RGB images or a light detection and ranging (LiDAR) analysis. The sensors may be mounted on various platforms, i.e., ground or aerial vehicles, or satellites, and the measurements carried out throughout the growth season (Zude-Sasse et al., 2016). Indeed, frequent studies of georeferencing and sensing the data of each individual tree are available, but the developed approaches lack further application in decision-support models, which can be utilized for the precise management of crop load.

Recently, the LA of each individual tree was analyzed (Penzel et al., 2020) to quantify the variability of FBC in two apple orchards. LA estimated with LiDAR compared to manual readings was obtained with high coefficient of determination ( $R^2 = 0.96$ ) by considering fully expanded leaves in mid-season. The authors showed that tree-adapted crop load management potentially increases the marketable yield of an orchard by 5%. Carbon balance of each individual tree would enable the adjustment of thinning intensity to each individual tree, introducing the term “variable rate application” (VRA) in crop load management. For this purpose, prototypes of precise thinning systems have been developed (Wouters, 2014; Lyons et al., 2015; Pflanz et al., 2016), but these have not been commercialized to date (Verbiest et al., 2020). This is, besides economic considerations, due to the lack of suitable models to evaluate the actual crop load of a tree in comparison to the tree’s FBC.

For VRA in flower or fruit thinning, it would be advantageous to estimate FBC before full bloom or within subsequent three weeks when fruit are most susceptible to the thinning agents. For this purpose, historical data of FBC in a fully developed canopy could be analyzed, applying the previous years’ data for decision-making in the current year. In viticulture, Taylor et al. (2019) proposed to utilize the crop load information from one year for crop load management decisions in the consecutive year.

However, it has not yet been evaluated whether this approach can be transferred to apple production. In addition, knowledge on the effects of the absorbed light on fruit quality is lacking.

The aim of the present study was to characterize the effect of VRA in crop load management on fruit quality. The objectives were (1) to analyze the inter-year variability in LA and FBC of each individual tree considering their spatial position within a commercial orchard and (2) to generate the minimum thresholds of absorbed photons per fruit for each individual tree to achieve a desired mean fruit size and SSC.

## MATERIALS AND METHODS

### Experimental Site and Trial Design

In 2018 and 2019, trials were carried out on trees of *Malus x domestica* Borkh. 'Gala' strain 'Baigent' (Brookfield®)/M.9 planted in 2006 in a commercial orchard in the fruit-growing region of Brandenburg, Germany (52.607 N, 13.818 E). The 2.3-m slender-spindle trained trees planted at a spacing of  $3.2 \times 1.0$  m, with  $3.2 \text{ m}^2$  allotted orchard surface per tree ( $G_{\text{allotted}}$ ). Trees were drip-irrigated ( $<4 \text{ L tree}^{-1} \text{ d}^{-1}$ ), and managed according to the federal regulations of integrated production preventing any symptoms of nutrient- or water-deficit stress. Soil information were published earlier (Tsoulas et al., 2020b). Trees of five rows (199–200 trees row<sup>-1</sup>) of the orchard were labeled and analyzed. In the green bud stage, trees (2018:  $n = 100$ ; 2019:  $n = 70$ ) were randomly selected and the number of flower clusters per tree was counted. All trees were thinned chemically with ammonium thiosulphate (20% N;  $15 \text{ kg ha}^{-1}$ ) at full bloom (April 29, 2018 to April 24, 2019) and with 6-benzyl adenine ( $500 \text{ g ha}^{-1}$ ) three weeks after full bloom. Subsequently, to generate variable numbers of fruit per tree, 60 trees of the selected samples were hand thinned to low (60 fruit tree<sup>-1</sup>), medium (100 fruit tree<sup>-1</sup>), and high (140 fruit tree<sup>-1</sup>) crop load each year. The average annual yield of the previous years was  $50 \text{ t ha}^{-1}$ , which would equal to 106 fruit per tree on the 3,125 trees per hectare when targeting a fruit of 150 g FM at harvest.

At time intervals of 13–30 d during fruit development, starting 30 d after full bloom (DAFB) in both years until harvest, 30 randomly chosen apples from random trees were picked in the early afternoon and stored at  $10 \pm 2^\circ\text{C}$  until the next morning when respiration rate, dry matter, and C content were measured for estimating the daily carbon requirements during fruit development.

At commercial harvest (September 3, 2018 to September 9, 2019), randomly selected apples (2018:  $n = 180$ ; 2019: all fruit from nine trees,  $n = 1,240$ ) were picked on one day and stored at  $10 \pm 2^\circ\text{C}$  until the next morning for measuring fruit quality. Additionally, each apple of labeled trees (2018:  $n = 100$ ; 2019:  $n = 70$ ) was harvested and measured by using a commercial grading line.

During both seasons, the leaf  $\text{CO}_2$  gas exchange rate was recorded several times on the trees also sampled for fruit analysis. When the canopies were fully developed in July, the total LA per tree from all trees of the five rows ( $n = 996$ ) was estimated from the three-dimensional (3D) point clouds recorded with a tractor-mounted LiDAR laser scanner. The estimations were

based on a regression model of LiDAR points per tree (PPT) and the manually measured total LA of 16 trees with a LA meter (Tsoulas et al., 2021).

### Analyses of Fruit Growth, $\text{CO}_2$ Gas Exchange, and Quality

Fruit diameter (D) and FM were measured by electronic caliper (Type 1108, INSIZE, Suzhou, China) and an electronic balance (CPA22480CE, Sartorius AG, Goettingen, Germany), respectively. The  $\text{CO}_2$  release rate providing the dark respiration rate ( $R_{dT}$ ) of 30 apples was measured by an IR  $\text{CO}_2$  gas analyzer (FYA600CO2, Ahlborn Mess- und Regelungstechnik GmbH, Holzkirchen, Germany) in a self-build closed system (Linke et al., 2010; Huyskens-Keil and Herppich, 2013).  $R_{dT}$  was measured at various temperatures (2018:  $10 \pm 2^\circ\text{C}$ ;  $20 \pm 2^\circ\text{C}$ ; 2019:  $10 \pm 2^\circ\text{C}$ ;  $20 \pm 2^\circ\text{C}$  at 50 DAFB,  $5 \pm 2^\circ\text{C}$ – $25 \pm 2^\circ\text{C}$  in five $^\circ\text{C}$ -steps at 56, 103, and 138 DAFB) after 2 h of temperature acclimation between the measurements.

To quantify the daily amount of C respired per fruit, the dark respiration rates measured in the lab were utilized to generate a model of  $R_{dT}$  of DAFB and  $T_{\text{mean}}$ . The rate of in field fruit respiration ( $R_{d;\text{field}}$ ) was estimated by using the model for the temperature measured in the field ( $T_{\text{mean}}$ ), neglecting diurnal variations  $R_{d;\text{field}}$ , which was used to calculate the daily respiratory C losses per fruit ( $R_{C;\text{daily}}$ ,  $\text{g d}^{-1}$ ) with a factor 0.27 representing relative mass contribution of C in  $\text{CO}_2$  (Equation 1).

$$R_{C;\text{daily}} = R_{d;\text{field}} \times \text{FM} \times 24 \times 0.27 \quad (1)$$

Subsequently, the fruit was dried to constant mass (dry mass, DM) at  $80^\circ\text{C}$ . From DM and FM, the dry matter fraction ( $\text{DM}_{\text{rel}}$ ) was calculated as the ratio of FM to DM.

Dry matter samples were homogenized by using a mixer mill (MM400, Retsch Technology, Haan, Germany), and aliquots (10 mg) of the homogenized DM were analyzed for their relative C contents ( $C_{\text{rel}}$ ) with an element analyzer (Vario EL III, Elementar Analysensysteme GmbH, Hanau, Germany) at an operational temperature of  $1,150^\circ\text{C}$ . The absolute C content per fruit ( $C_{\text{fruit}}$ , g) was calculated as

$$C_{\text{fruit}} = \text{FM} \times \text{DM}_{\text{rel}} \times C_{\text{rel}} \quad (2)$$

In commercial harvest, the SSC of individual fruit was analyzed with a digital refractometer (DR-301-95, Krüss, Hamburg, Germany) and fruit flesh firmness with a texture analyzer (TA.XT, Stable Micro Systems Ltd., Godalming, UK; 11.1 mm Magness-Taylor probe). Flesh firmness was obtained as the maximum force (N) at 10 mm penetration.

In addition, fruit harvested from the labeled trees (2018:  $n = 100$ ; 2019:  $n = 70$ ) were analyzed to capture fruit mass, color, yield per tree, and the number of fruit per tree with a commercial grader (GeoSort, Greefa, Tricht, The Netherlands).

### Leaf $\text{CO}_2$ Gas Exchange

In both seasons (2018: 25, 58, 82, and 99 DAFB; 2019: 40, 47, 97, and 113 DAFB), light responses of steady-state leaf gas exchange were measured on three mature spur leaves from the

bearing shoots of three randomly selected trees from each of the three crop load classes ( $n = 9$  leaves per measurement date) with a portable gas exchange system (LI-6400 XT with the LI-6400-40 red/blue LED light source, LI-COR Inc., Lincoln, USA). At ambient leaf temperature ( $T_{\text{leaf}}$ ), relative humidity, and a constant  $\text{CO}_2$  mole fraction ( $400 \mu\text{mol mol}^{-1}$  in the reference gas), analyses were performed at photosynthetic photon flux rate (PPFR) of 2,000, 250, 100, 50, 20, and  $0 \mu\text{mol m}^{-2} \text{s}^{-1}$  with the minimum waiting time of 100 s before each measurement. Maximum quantum yield ( $\alpha_{\text{max}}$ ,  $\text{mol mol}^{-1}$ ) and the rate of light saturated  $\text{CO}_2$  gas exchange ( $J_{\text{CO}_2}^{\text{max}}$ ,  $\mu\text{mol m}^{-2} \text{s}^{-1}$ ) were analyzed (Matyssek and Herppich, 2017).

## Measurement of LA per Tree

Bud break was recorded on March 22, 2018 and on March 18, 2019. The canopy LA was assumed to be fully developed after 1,200 growing degree days after bud break (base temperature =  $4^\circ\text{C}$ ; Doerflinger et al., 2015) on July 13, 2018, 80 DAFB and July 7, 2019, 84 DAFB. In the stage of fully developed canopy, all trees ( $n = 996$ ) of the five labeled rows were scanned by using a mobile two-dimensional (2D) LiDAR laser scanner (LMS511 pro model, Sick, Düsseldorf, Germany) at a scanning frequency of 25 Hz and a vertical scanning angle of  $270^\circ$ . The LiDAR laser scanner was mounted on a tractor at 1.6 m height, together with an inertial measurement unit (MTi-G-710, XSENS, Enschede, The Netherlands) and an RTK-GNSS positioning system (AgGPS 542, Trimble, Sunnyvale, CA, USA) as described previously (Tsoulas et al., 2019). The sensor system was driven ( $0.13 \text{ m s}^{-1}$ ) along both sides of the trees, acquiring the 3D point cloud of each individual tree for the five rows.

For tree segmentation, the position of each tree trunk was located from the bivariate density histograms of LiDAR points with an in-house developed (Tsoulas et al., 2019) Matlab script (Version 2018b, The Mathworks Inc., Natick, MA, USA). A vertical cylinder with a radius of 50 cm was projected based on the trunk position. The points within the cylinder boundaries were considered to belong to this tree and referred to as LiDAR PPT. Reference trees were defoliated after LiDAR scanning, and the area of each individual leaf was measured by using a LA meter (CI-203, CID Bio-Science, Camas, WA, USA). The regression model to convert PPT into total LA per tree ( $\text{LA}_{\text{LiDAR}}$ ,  $\text{m}^2$ ) from Tsoulas et al. (2021), which was established from the PPT of reference trees ( $n = 6$  in 2018;  $n = 7$  in 2019) and the manually measured total LA (Equations 3 and 4), was utilized to convert PPT of each tree into  $\text{LA}_{\text{LiDAR}}$ .

$${}^{2018}\text{LA}_{\text{LiDAR}}(\text{m}^2) = 9.719 \times 10^{-5} \times \text{PPT} + 1.84 \quad (3)$$

$${}^{2019}\text{LA}_{\text{LiDAR}}(\text{m}^2) = 11.712 \times 10^{-5} \times \text{PPT} + 0.75 \quad (4)$$

## Modeling of Fruit FM and C-Requirement for Target Fruit Diameter

Seasonal changes of FM and  $C_{\text{fruit}}$  were interpolated over time (DAFB) by using a sigmoid-growth model. To derive the growth curves of apples by considering four harvest fruit diameters (65, 70, 75, and 80 mm), the growth equations based on the mean fruit FM and  $C_{\text{fruit}}$  were normalized with the measured mean FM and  $C_{\text{fruit}}$  at harvest. The growth curves of FM and  $C_{\text{fruit}}$  for

target fruit diameters (D) were obtained (Equations 5 and 6) by multiplying the normalized growth functions with the target fruit diameter at harvest and a conversion regression equation from D to FM (Supplementary Figure 1).

$$\text{FM}(\text{g}) = \text{FM}_{\text{norm}}(\text{DAFB}) \times \text{FM}(\text{D}) \times \text{D} \quad (5)$$

$$C_{\text{fruit}}(\text{g}) = C_{\text{norm}}(\text{DAFB}) \times \text{FM}(\text{D}) \times \text{D} \times \text{DM}_{\text{rel}} \times C_{\text{rel}} \quad (6)$$

The first derivation of the resulting growth functions provided the absolute growth rates (AGR,  $\text{g d}^{-1}$ ) considering FM ( $\text{AGR}_{\text{FM}}$ ) and  $C_{\text{fruit}}$  ( $\text{AGR}_C$ ). The integral of  $\text{AGR}_C$  over time in DAFB provided the amount of C representing the fruit growth. The sum of  $\text{AGR}_C$  and  $R_{C_{\text{daily}}}$  denotes the daily C-requirement per fruit. The LA “demanded” ( $\text{LA}_{\text{demand}}$ ,  $\text{cm}^2$ ) to assimilate  $\sum R_{C_{\text{daily}}} + \text{AGR}_C$  was estimated (Equation 7; Penzel et al., 2020) for each tree sampled in the orchard and modeled for varying LA per tree (3.6, 5.5, and  $7.7 \text{ m}^2$  represented the 5th, 50th, and 95th percentile of the measured  $\text{LA}_{\text{LiDAR}}$ , respectively). Daily fluctuations in  $\text{LA}_{\text{demand}}$  were smoothed by a Savitzky–Golay filter, using the R-Package “signal” (Ligges et al., 2015; `sgolayfilt`, filter order = 1, filter length = 9).  $P_{\text{daily}}$  ( $\text{g m}^{-2} \text{d}^{-1}$ ) reflects the C assimilated per unit soil area per day (Equation 8).

$P_{\text{daily}}$  was calculated (Equation 8) as reported earlier (Lakso and Johnson, 1990; Penzel et al., 2020).  $P_{\text{daily}}$  was scaled up for the whole tree ( $P_{\text{tree}}$ ,  $\text{g d}^{-1}$ ) by multiplying it with  $G_{\text{allotted}}$ , which was  $3.2 \text{ m}^2$  in equal planting distance of the orchard.  $C_{\text{part}}$  is a variable carbon-partitioning factor for the fraction of the assimilated carbohydrates partitioned to fruit; it was set to 0.8 when the foliage of trees was fully developed (Xia et al., 2009; Lakso, pers. communication).  $\sum R_{C_{\text{daily}}} + \text{AGR}_C$  was generally reduced by 5% to roughly correct for fruit photosynthesis (Jones, 1981).

$$\text{LA}_{\text{demand}}(\text{cm}^2) = \frac{0.95 \times (\text{AGR}_C + R_{C_{\text{daily}}})}{\left( \frac{P_{\text{daily}} \times C_{\text{part}}}{\text{LA}_{\text{orchard}} \times 10,000} \right)} \quad (7)$$

The daily integral of solar radiation (S,  $\text{MJ m}^{-2} \text{d}^{-1}$ ) was recorded by using a pyranometer (CMP 3, Kipp & Zonen, Delft, The Netherlands) in the spectral range of 300–2,800 nm. The day length (DL, s) was obtained by considering the daily hours with  $S > 0$ . The seasonal means of  $\alpha_{\text{max}}$  and  $J_{\text{CO}_2}^{\text{max}}$  were converted into energy units with the conversion factor of PPFR to S in direct sun light (0.4376; McCree, 1972).  $P_T$  (Equation 9) is a correction for the temperature dependence of  $J_{\text{CO}_2}^{\text{max}}$ , which was provided by Lakso (pers. communication), utilizing the mean temperature of the daily hours when  $S > 0$  ( $T_{\text{mean, day}}$ ). The fraction of light intercepted by the canopy (LI) was calculated (Equation 10) by considering the canopy light extinction coefficient (k) and the fraction of total radiation incidence on the canopy ( $\text{LI}_{\text{max}}$ ), which were set to 0.5 (Poblete-Echeverría et al., 2015) and 0.7 (Doerflinger et al., 2015), respectively. The individual LA index of trees in the orchard ( $\text{LA}_{\text{orchard}}$ ) was calculated by dividing



$LA_{LiDAR}$  with  $G_{allotted}$  (Equation 11).

$$P_{daily}(gd^{-1}) = \frac{\frac{max\alpha \times S \times DL \times \frac{maxJCO2 \times PT \times LI}{max\alpha \times k \times S + DL \times \frac{maxJCO2 \times PT}{0.27}}}{max\alpha \times k \times S + DL \times \frac{maxJCO2 \times PT}{0.27}} \quad (8)$$

$$P_T[0-1] = 0.535 + 0.0384 \times T_{mean,day} - 0.0004126 \times T_{mean,day}^2 - 0.00001576 \times T_{mean,day}^3 \quad (9)$$

$$LI[0-1] = LI_{max} \times (1 - e^{(-k \times \frac{LAI_{orchard}}{LI_{max}})}) \quad (10)$$

$$LAI_{orchard} = \frac{LA_{LiDAR}}{G_{allotted}} \quad (11)$$

## Modeled FBC

The FBC (Equation 12) of 996 trees was calculated by considering the  $LA_{demand}$  for the four target fruit diameters, and the actual LA was analyzed by using LiDAR ( $LA_{LiDAR}$ ). The ratio was built for the relevant time of 15 d before and after the climax of fruit growth.

$$FBC(\text{fruit tree}^{-1}) = \frac{LA_{LiDAR}}{LA_{demand}} \quad (12)$$

## Total Absorbed Photosynthetic Energy

The total absorbed photosynthetic energy (TAPE, MJ; Equation 13) of each tree was considered for the period of fully developed canopy (FDC) LA until harvest. TAPE was divided by the number of fruit per tree for obtaining the TAPE per fruit (MJ fruit<sup>-1</sup>).

$$TAPE(MJ) = LI \times \sum_{FDC}^{Harvest} S \times 0.5 \times G_{allotted} \quad (13)$$

The incident photosynthetic active photon flux rate was estimated by multiplying LI for each individual tree (Equation 10) with the integral of solar radiation,  $S$ , with the assumed fraction of PAR on solar radiation (0.5; Szeicz, 1970), and with  $G_{allotted}$  (3.2 m<sup>2</sup> in the present orchard).

## Statistical Analyses

Descriptive analysis capturing regression analysis and ANOVA were carried out in R (Version 3.4.1, R Core Team, 2018). CI of 95% was used. The value of  $p < 0.05$  was considered as significant. The FBC of each individual tree was visualized by Getis-Ord's analysis at confidence levels  $\geq 90\%$  (c.f. Peeters et al., 2015) calculated in ArcGIS (v.10.2.1, ESRI, Redlands, CA, USA). Hot spot and cold spot analysis (Peeters et al., 2015) indicate trees or clusters of trees having either a very high (hot spot) or a very low (cold spot) Z score, either  $< -1.96$  or  $> 1.96$ , reflecting low and high FBC, respectively.

## RESULTS

### Fruit Development and Its C-Requirement

Fruit development from full bloom to harvest in the beginning of a climacteric peak lasted 11 d longer in 2019 (127 d) than in 2018. Nevertheless, the mean fruit FM at harvest was similar in both years (2018: 145 g; 2019: 150 g). Sigmoid-growth functions were applied to interpolate the measured values of FM and  $C_{fruit}$  and model the increase of FM and  $C_{fruit}$  during

fruit development (Supplementary Equations 1, 2). From the normalized equations, sigmoid-growth curves were calculated by considering the four target fruit diameters. The simulated growth curves showed a horizontal shift explaining the difference of fruit FM and C content multiplicative distributed over the season (Figure 1).

Some data necessary for modeling the FBC, but not relevant to point out the new findings on the effect of measured LA on FBC, were presented in the Supplementary Material: The fraction of DM on fruit FM with a mean of 0.15 in both seasons (Supplementary Figure 2). The carbon content in the fruit DM,  $C_{rel}$ , decreased from 0.51 at 30 DAFB to 0.48 at harvest (Supplementary Equation 3 and Supplementary Figure 2). The maximum values of the absolute fruit growth rate considering C content,  $AGR_C$ , were found at 101 DAFB in 2018 and 92 DAFB in 2019 (Supplementary Figure 3). The fruit dark respiration rate decreased during fruit development and increased with temperature (Supplementary Figure 4). At the last measurement date of harvest,  $R_{dT}$  was slightly enhanced in comparison to the two measurement dates before, indicating the onset of a climacteric rise in fruit respiration. Temperature-corrected  $R_{Cdaily}$  increased during fruit development due to enhanced temperature in the orchard. However, the respiration-related fraction,  $R_{Cdaily}$ , showed a high daily fluctuation (Supplementary Figure 5) ranging from 5 to 15% in 2018 and from 3 to 28% in 2019. Considering fruit of the same target diameter, the modeled total amount of respiratory C loss from 50 DAFB till harvest was in a similar range for 2018 (0.57–1.11 g) and 2019 (0.65–1.26 g). This fruit respiration accounted for 7% (2018) and 10% (2019) of the carbon requirement of fruit in the considered period.

The total carbon requirement of apples (Figure 2) was calculated by the sum of respiratory C loss and fruit growth, which considers four target diameters in the period after cell division till harvest. A horizontal shift of the sum of  $AGR_C + R_{Cdaily}$  appeared for the four target fruit diameters when assuming a similar fruit growth over the season. The total fruit carbon requirement was slightly higher in 2018 than in 2019 (Table 1). The seasonal maximum in the carbon requirements per fruit appeared at 92 and 101 DAFB in 2018 and 2019, respectively (Figure 2). The period  $\pm 15$  d from the seasonal maximum in the carbon requirements per fruit in both years (Figure 2) was considered for estimating the FBC of the trees.

### LA and Canopy Carbon Assimilation

The maximum quantum efficiency of leaf photosynthesis ( $max\alpha$ ) was not affected by either crop load, leaf temperature, season or the actual leaf-to-air partial pressure deficit for water vapor ( $\Delta w$ ) in both years (not shown) and varied marginally during the season as well as between both seasons (Figure 3A). Therefore, the overall mean of  $max\alpha$  0.054 mol mol<sup>-1</sup> was considered in all calculations (Equation 8). The seasonal variation of  $maxJ_{CO2}$  (Figure 3B) was slightly higher than that of  $max\alpha$ , due to the stomatal effects mainly caused by pronounced seasonal changes in  $\Delta w$  (data not shown). In 2019, at 40 and 46 DAFB, the ratio between leaf internal ( $c_i$ ) and ambient CO<sub>2</sub> concentrations ( $c_a$ ), pointing to the degree of stomatal limitation of  $maxJ_{CO2}$ ,

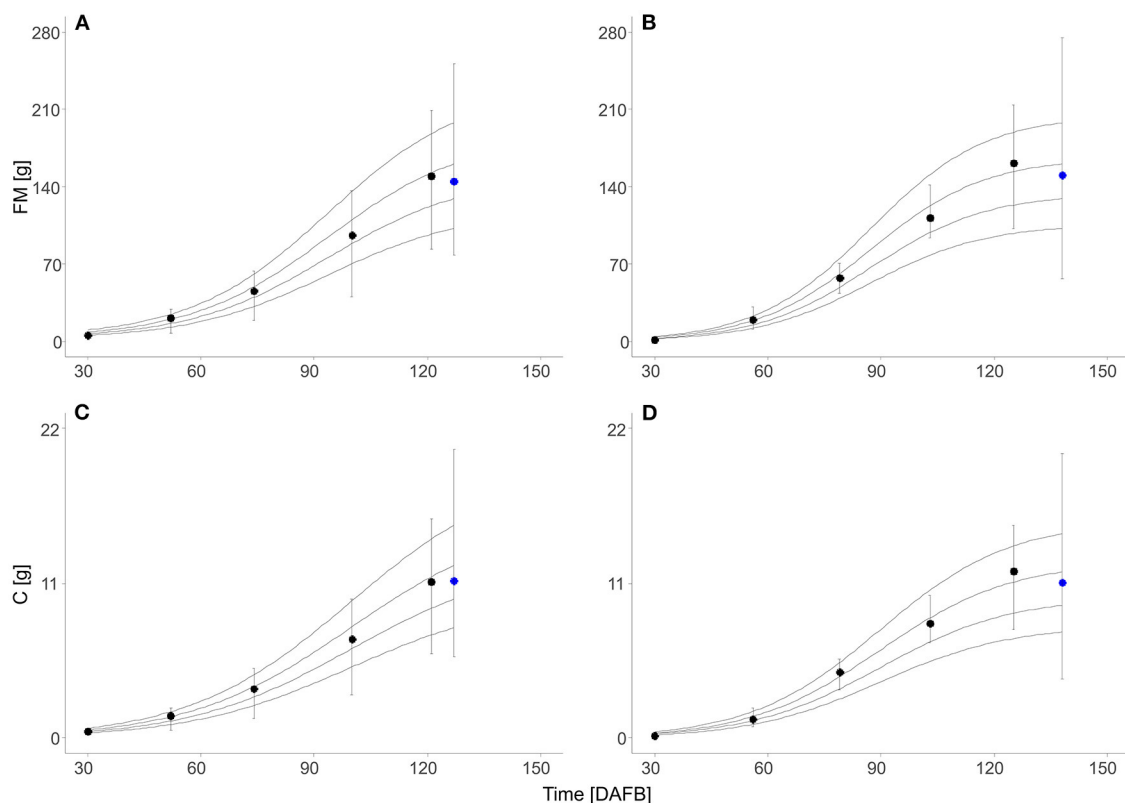


**FIGURE 1 |** Fresh mass (FM) (A,B) and absolute C content ( $C_{\text{fruit}}$ ) (C,D) of 'Gala'/M.9 apples during the season (black circle,  $n = 30$ ) and at harvest (blue circle, 2018:  $n = 180$ ; 2019:  $n = 1,240$ ) in days after full bloom (DAFB) in 2018 (A,C) and 2019 (B,D). Symbols represent the measured means, error bars show the SD, and solid lines show the sigmoid-growth functions simulated for the fruit with 65, 70, 75, and 80 mm diameter at harvest (from the bottom to top).

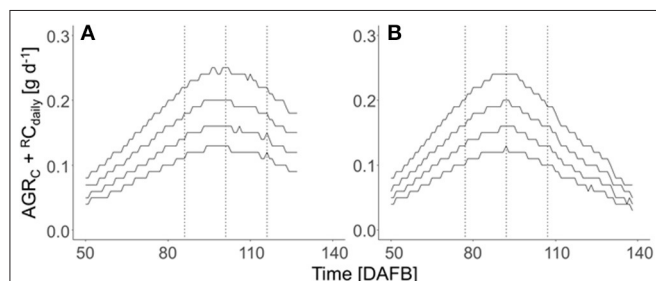


**FIGURE 2 |** Seasonal course of the sum of the C-based daily fruit growth rate ( $AGR_C$ ,  $g\ d^{-1}$ ) and daily respired C per fruit ( $R_{C_{\text{daily}}}$ ,  $g\ d^{-1}$ ) of 'Gala'/M.9 apples with target diameters of 65, 70, 75, and 80 mm (from the bottom to top) during the DAFB in 2018 (A) and 2019 (B) in DAFB. The dotted vertical lines represent the period  $\pm 15$  d of the fruit's highest daily C-requirement (2018: 86–116 DAFB; 2019: 77–107 DAFB).

was lower (0.06–0.22) than the ratio of the measured 77 and 97 DAFB (0.62–0.85). A regression of  $\max J_{CO_2}$  against stomatal conductance showed non-stomatal limited  $\max J_{CO_2}$  at  $19.8\ \mu\text{mol}\ m^{-2}\ s^{-1}$ , which was applied in both years.

The mean LiDAR-estimated total LA per tree ( $LA_{\text{LiDAR}}$ ) was slightly higher in 2018 ( $5.8\ m^2$ ) than that in 2019 ( $5.3\ m^2$ ) (Figure 4A), which corresponds to the slightly enhanced mean

**TABLE 1 |** Total fruit C demand calculated from the sum of absolute C-based growth rates ( $AGR_C$ ) and respiratory C loss ( $R_{C_{\text{daily}}}$ ) of 'Gala'/M.9 apples of the four targeted fruit diameters for the period of 50 d after full bloom (DAFB) till harvest in 2018 and 2019.

Target fruit diameter (mm)	$\sum_{50\ DAFB}^{Harvest} (AGR_C + R_{C_{\text{daily}}})\ (g)$	
	2018	2019
65	7.6	7.5
70	9.5	9.4
75	11.9	11.8
80	14.7	14.5

daily assimilated C in 2018. The estimated fraction of incident light intercepted by the canopy (LI) estimated in Equation (10) ranged between 0.3 and 0.6 in 2018, and 0.2 and 0.6 in 2019, with a mean of 0.5 for both years. The temporal mean of assimilated C (g) was analyzed for each tree to point out the impact of LA on carbon gain without considering the fruit.  $P_{\text{tree}}$  was calculated for each tree in mean conditions (2018: DL = 14 h, S =  $17.5\ MJ\ m^{-2}\ d^{-1}$ ,  $T_{\text{mean;day}} = 25.7^\circ\text{C}$ ; 2019: DL = 15 h, S =  $17\ MJ\ m^{-2}\ d^{-1}$ ,  $T_{\text{mean;day}} = 21^\circ\text{C}$ ) for the period of the maximum fruit carbon

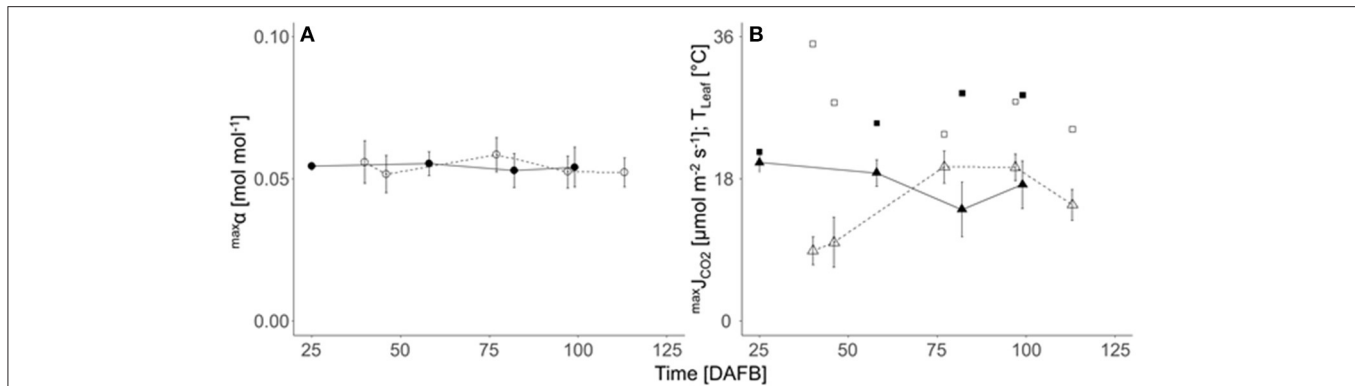


**FIGURE 3 |** Seasonal course (DAFB) of means ( $\pm$  SD;  $n = 9$ ) of (A) the maximum quantum efficiency of photosynthesis ( $^{\max}\alpha$ , circles), (B) light saturated maximum  $\text{CO}_2$  gas exchange rate ( $^{\max}J_{\text{CO}_2}$ , triangles) and leaf temperature ( $T_{\text{leaf}}$ , squares) of fully developed 'Gala'/M.9 apple spur leaves in 2018 (closed symbols, solid lines) and 2019 (open symbols, dashed line).

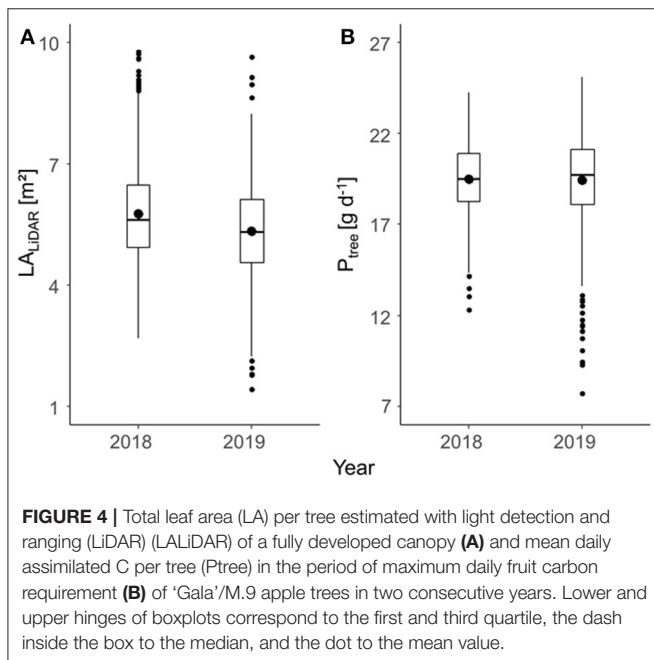


**FIGURE 4 |** Total leaf area (LA) per tree estimated with light detection and ranging (LiDAR) ( $\text{LA}_{\text{LiDAR}}$ ) of a fully developed canopy (A) and mean daily assimilated C per tree ( $P_{\text{tree}}$ ) in the period of maximum daily fruit carbon requirement (B) of 'Gala'/M.9 apple trees in two consecutive years. Lower and upper hinges of boxplots correspond to the first and third quartile, the dash inside the box to the median, and the dot to the mean value.

requirement  $\pm 15$  d (Figure 4B). The data on daily carbon gain per tree reflect the varying  $\text{LA}_{\text{LiDAR}}$  of each individual tree (Figure 4).

The daily integral of solar radiation ( $S$ ) was highly fluctuating in both years (Figure 5A). Consequently, the daily carbon gain of the trees ( $P_{\text{tree}}$ ) fluctuated pronouncedly during the relevant period of maximum carbon requirement by the fruit in both years (Figures 5B,C) with maximum values of 24 (2018) and 25  $\text{g d}^{-1}$  (2019) considering the overall mean LA of 5.5  $\text{m}^2$ . Figure 5 points out the impact of low, mean, and high LA on the daily  $P_{\text{tree}}$ . However, this analysis ignores the shading effects within the canopy.

## LA Demand and FBC Considering Target Fruit Diameters

The LA demand per fruit ( $\text{LA}_{\text{demand}}$ ) varied during fruit development according to  $R_{\text{Cdaily}}$  and  $P_{\text{daily}}$ , which are affected by temperature and solar radiation (Figure 6). Assuming a uniform  $\text{LA}_{\text{demand}}$  for all trees in the orchard and one target fruit diameter, the daily  $\text{LA}_{\text{demand}}$  during the period of maximum fruit C-requirement was slightly higher in 2018 than in 2019.

Regression analyses were carried out to quantify the relationship between the mean  $\text{LA}_{\text{demand}}$  and the actual range of measured LA using LiDAR. The regression models provide the  $\text{LA}_{\text{demand}}$  necessary for the target fruit diameter in 2018 and 2019 (Table 2).  $\text{LA}_{\text{demand}}$  increased with the target fruit diameter (Figures 6, 7). Additionally,  $\text{LA}_{\text{demand}}$  was enhanced with increased actual  $\text{LA}_{\text{LiDAR}}$  (Figure 7). It can be assumed that a hyperbolic response of light interception to  $\text{LA}_{\text{LiDAR}}$  and the associated canopy density (Equation 10) caused this non-linearity.

The mean LA of each individual leaf, capturing the data from both years, was 21  $\text{cm}^2$ . Consequently, the number of leaves necessary per fruit would range from 12 to 57 leaves per fruit.

The FBC, calculated for each tree by the ratio of  $\text{LA}_{\text{LiDAR}}$  and  $\text{LA}_{\text{demand}}$  conferring all four target fruit diameters, ranged from 43 to 168 apples per tree (2018) and 28 to 179 apples per tree (2019) (Figure 8). A maximum difference of 11 apples in FBC between both years for the trees with the same  $\text{LA}_{\text{LiDAR}}$  and fruit diameter was obtained.

In the present orchard, the number of flower clusters per tree was highly variable with 50–220 in 2018 and 73–296 in 2019, sufficient for each tree to meet the FBC when assuming that a tree can generate one to two fruit per cluster at harvest. Trees ( $n = 996$ ) were classified according to their FBC with  $D = 65$  mm to locate the trees having a  $\text{FBC}_{65}$  below (cold spots) or above (hot spots) the majority of trees. The values of  $Z$  between  $-1.96$  and  $1.96$  represented the majority of the trees having a mean  $\text{FBC}_{65}$  of 130 and 135 fruit tree $^{-1}$  in 2018 and 2019, respectively. Cold spots showed a mean  $\text{FBC}_{65}$  of 110 and 106 fruit tree $^{-1}$  whereas the trees representing hot spots had a mean  $\text{FBC}_{65}$  of 156

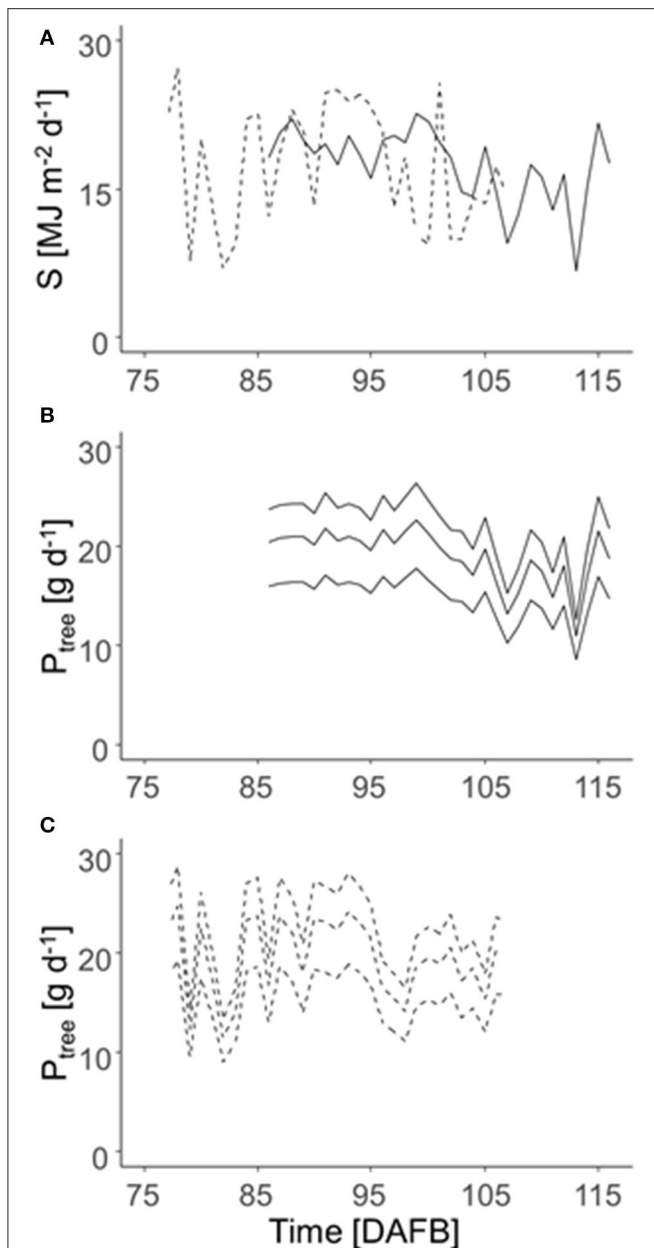


**FIGURE 5 |** Daily integrated solar radiation ( $S$ ) in 2018 (solid lines) and 2019 (dashed lines) (**A**) and daily C gain per tree ( $P_{\text{tree}}$ ) of 'Gala'/M9 during the time of maximum daily fruit C-requirement (2018: 86–116 DAFB; 2019: 77–107 DAFB) (**B**: 2018; **C**: 2019).  $P_{\text{tree}}$  was calculated for the trees of 3.6, 5.5, and 7.7 m<sup>2</sup> total LA (lines from the bottom to top), which represents the 5, 50, and 95th percentile of  $LA_{\text{LiDAR}}$  of all 996 trees measured during both years.

and 155 fruit tree<sup>-1</sup> in 2018 and 2019, respectively (Figure 9). Despite the findings of high variability of LA and FBC in the orchard, the mean values of low, mean, and high crop load were similar. However, cold and hot spots were found in different locations by comparing both years. To conclude, the LA of a certain year cannot be used for predicting hot and cold spots of the following year.

The modeled FBC was validated by using measurements in a commercial grader at harvest, considering each individual tree (2018:  $n = 100$ ; 2019:  $n = 70$ ). The expected fruit diameter from the modeled FBC was compared to the measured values of fruit diameter in the grader: in both years, the actual number of fruit per tree having  $D > 65$  mm and the calculated FBC, considering the actual average fruit diameter and  $LA_{\text{LiDAR}}$  per tree were similar as shown by their ratio (Table 3). The high SD, however, pointed out a high percentage of trees with crop load above or below the FBC.

## Fruit Quality

The effect of TAPE considering  $LA_{\text{LiDAR}}$  of each individual tree per fruit (Equation 13) on fruit quality was analyzed in the laboratory. FM and diameter were enhanced with increasing TAPE per fruit (Figure 10A). The FM of individual fruit showed high SD, which increased with average FM (Figure 10B). A high percentage of apples with  $D > 65$  mm was found in all nine trees analyzed completely in the laboratory (Figure 10C).

Fruit flesh firmness at harvest was  $67 \pm 9$  N in 2018 and  $86 \pm 9$  N in 2019, with a range between maximum and minimum values of 76 N (2018) and 86 N (2019) (Supplementary Table 2). TAPE per fruit had no effect on firmness in both years. In contrast, TAPE per fruit affected SSC but to a different extent comparing both years. The SSC was generally lower in 2019 than in 2018 (Figure 11). The SD of SSC was not related to the mean SSC at harvest (Figure 11B). Enhanced TAPE per fruit caused an increased percentage of fruit having  $SSC \geq 12\%$  from 30 to 80% in 2019 while the effect was less pronounced in 2018 (Figure 11C).

When all fruit per tree (2018:  $n = 100$ ; 2019:  $n = 70$ ) were analyzed on the sorting line, a correlation of total yield per tree and TAPE based on the  $LA_{\text{LiDAR}}$  was found. The  $R^2$  was enhanced in 2018 compared to 2019 (Figure 12A). Additionally, the percentage of fruit with  $D > 65$  mm was correlated with TAPE per fruit (Figure 12B). In enhanced TAPE per fruit, more than 60% of the apples had a marketable fruit  $D > 65$  mm. The slope of the curve indicated over 80% (2018) and 90% (2019) of the marketable fruit at 7.5 and 5.9 MJ fruit<sup>-1</sup>, respectively (Figure 12B).

High quality, considering the blush color, was defined as the fruit showing  $\geq 60\%$  red blush of the entire fruit surface measured with a commercial grader (Supplementary Table 2). In 86% of the trees, high-quality blush color occurred in 80% of the entirely harvested fruit. In 95% of the trees, at least 60% of the fruit showed a high-quality red blush. However, no effect of TAPE per fruit was found on blush color of the red 'Gala' strain in both years.

## DISCUSSION

### Variability of FBC

This study aimed to model the FBC of each individual tree in a commercial orchard for two consecutive years. A considerable range of LA was found in the present study (Figure 4A). The LA differences correspond to the associated mid-season range of photosynthetic performance (Figures 4B, 5B) and, hence, the growth capacity of each individual tree to produce fruit. The FBC



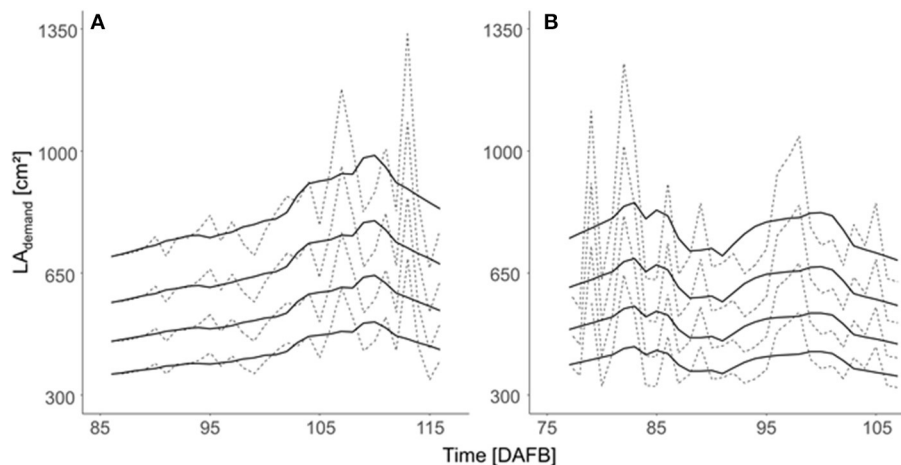


**FIGURE 6** | Daily LA demand [ $LA_{demand}$  ( $cm^2$ )] per fruit estimated for the four target fruit diameters (lines from bottom to top: 65, 70, 75, and 80 mm) of 'Gala'/M.9 trees considering the orchard's mean total LA of 5.5  $m^2$  during the period 15 d before and after maximum daily fruit C-requirement in (A) 2018 and (B) 2019. Dashed lines represent the estimated daily values and solid lines are the values that are smoothed by using a Savitzky-Golay filter.

**TABLE 2** | Regression equations of the relationship between the mean  $LA_{demand}$  and the light detection and ranging (LiDAR)-measured leaf area ( $LA_{LiDAR}$ ) for the estimation of the LA necessary to yield fruit of the target diameter (D) in 2018 and 2019.

Year	Regression equation	Equation
2018	$LA_{demand} = -714.6813 + 14.4682 \times D - 113.006 \times LA_{LiDAR} + 2.2882 \times D \times LA_{LiDAR}$	14
2019	$LA_{demand} = -667.0759 + 13.5078 \times D - 105.5594 \times LA_{LiDAR} + 2.1374 \times D \times LA_{LiDAR}$	15

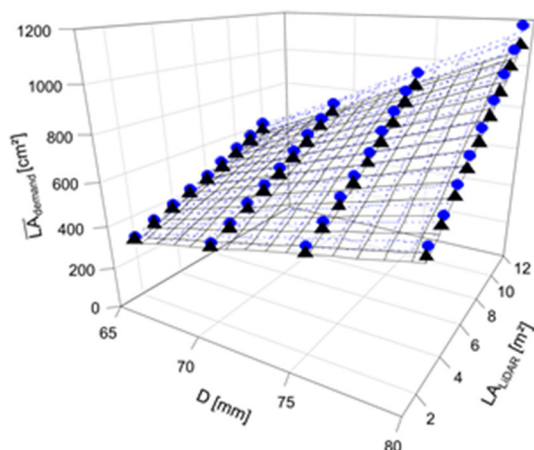


**FIGURE 7** | Mean LA demand per fruit ( $^{2018}LA_{demand}$ ,  $^{2019}LA_{demand}$ ,  $cm^2$ ) considering the four target fruit diameters (D) of 'Gala'/M.9 apple in 2018 (gray circle, dotted line) and 2019 (black triangle, solid line) for the trees with different total LAs ( $LA_{LiDAR}$ ,  $m^2$ ) in the period of 15 d before and after the highest daily C-requirement per fruit (2018: 86–116 DAFB; 2019: 77–107 DAFB).

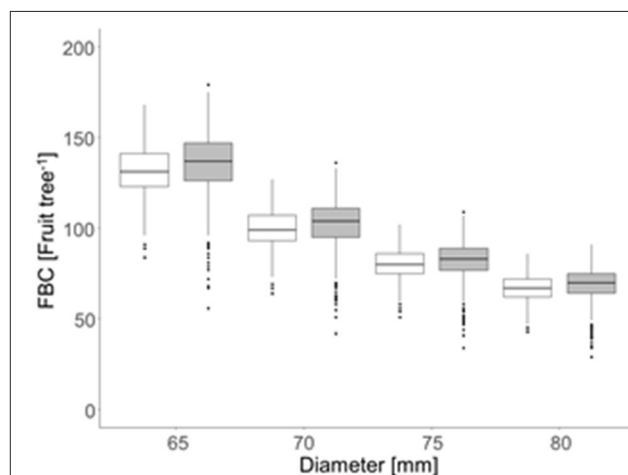


**FIGURE 8** | Mean fruit-bearing capacity [FBC (fruit tree $^{-1}$ )] considering the four target fruit diameters (D) of the 'Gala'/M.9 apple in 2018 (open box plots) and 2019 (gray box plots) for 996 trees per year in the period of 15 d before and after the highest daily fruit C-requirement (2018: 86–116 DAFB; 2019: 77–107 DAFB).

for the desired mean fruit diameter varies between 65 and 80 mm (Figure 8). The FBC was calculated by considering the period of

seasonal maximum in fruit growth and the resulting maximum daily fruit C-requirement. In this period, the LA of the canopy is already fully developed.

The measured input data of the FBC model (fruit growth rate, fruit and leaf  $CO_2$  gas exchange rates) are in close agreement with the ranges reported in the previous studies on apple (Yuri et al., 2011; Baïram et al., 2019; Penzel et al., 2020). Enabling fruit to meet their maximum growth potential, which frequently refers to sink limited fruit growth (Reyes et al., 2016), is commercially always avoided. For maximum fruit growth rates, low crop loads are required, which lead to low yield and possible physiological disorders of fruit (Ferguson et al., 1999). Moreover, low crop load

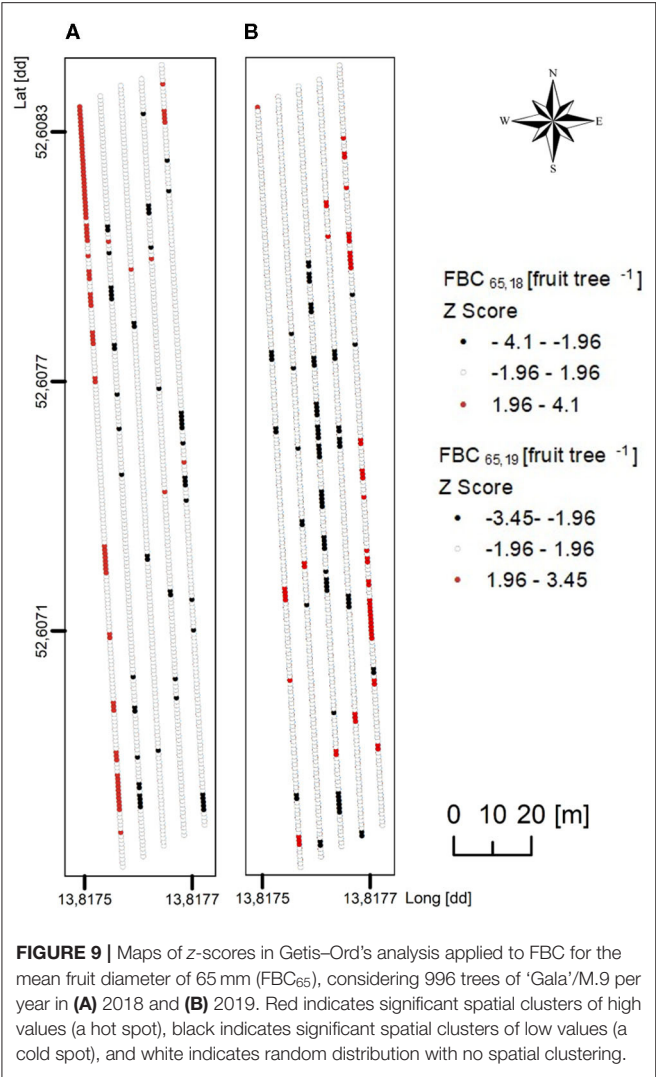
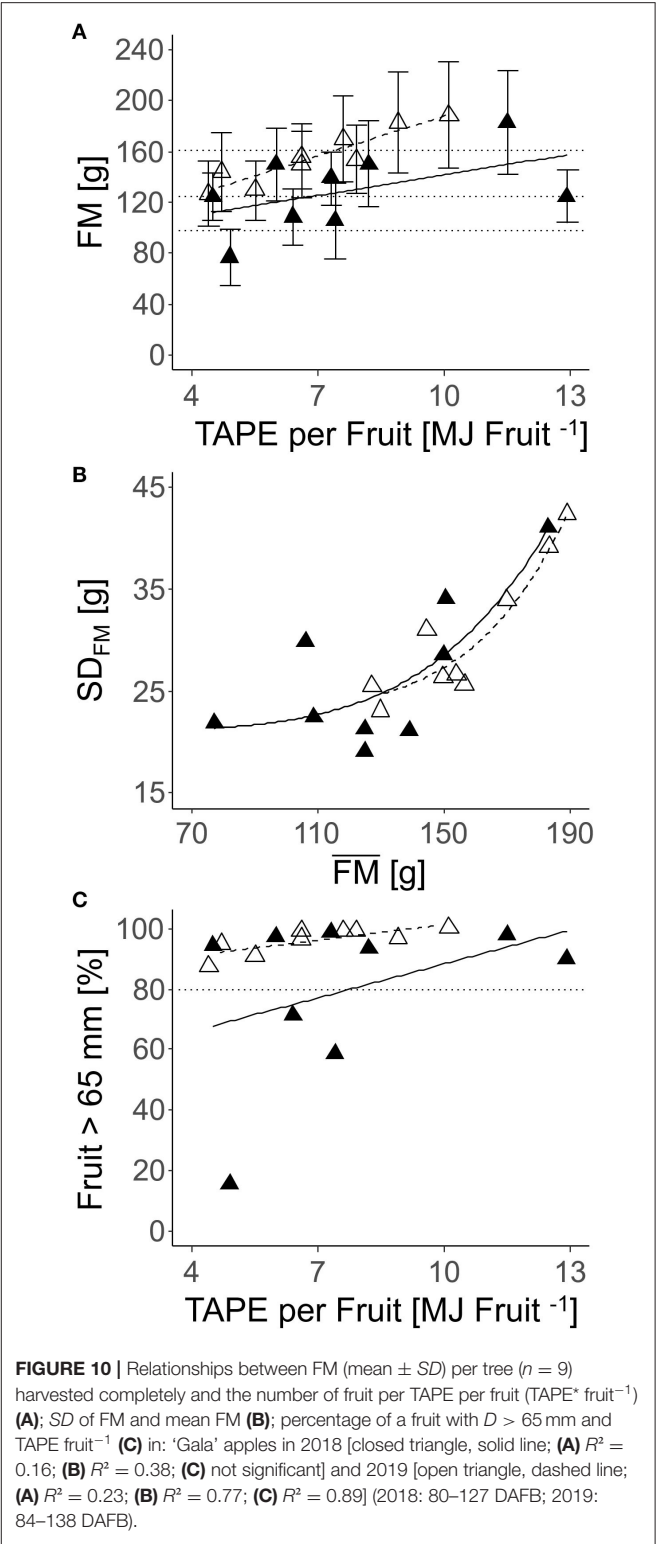


**TABLE 3 |** The ratio between the actual number of fruit per tree with diameter ( $D$ ) > 65 mm considering all fruit measured when harvesting whole trees and modeling fruit-bearing capacity (FBC) for the actual average fruit diameter at harvest of 'Gala' trees in 2 years.

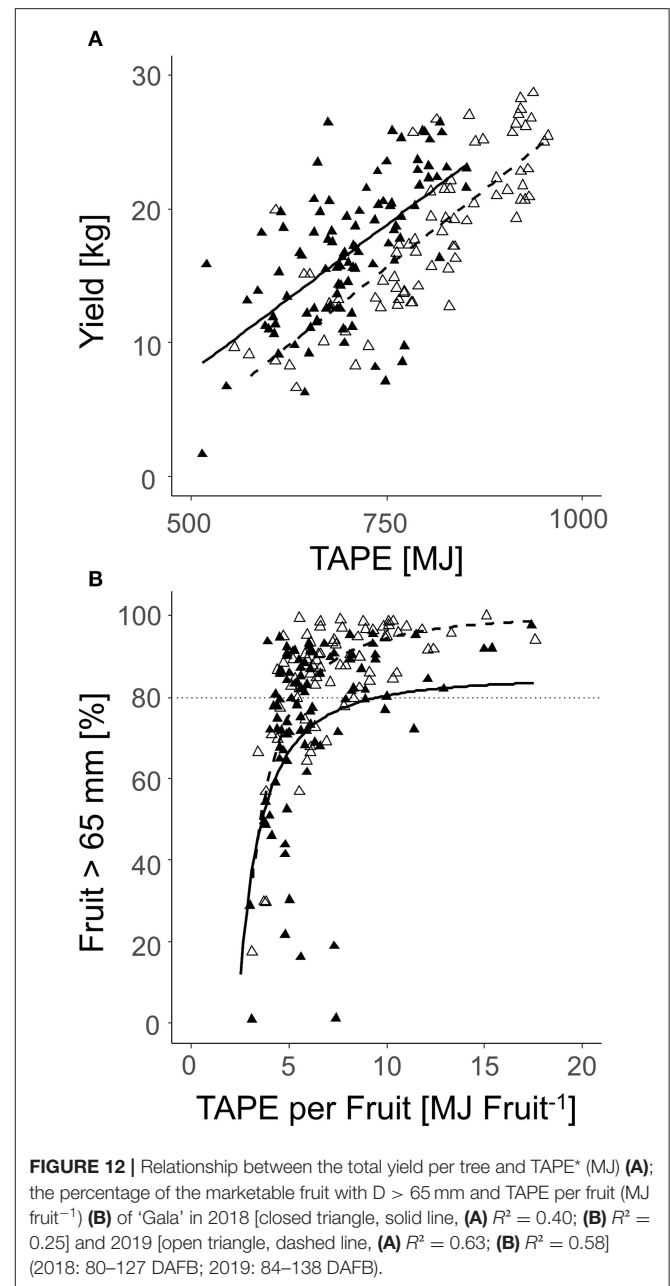
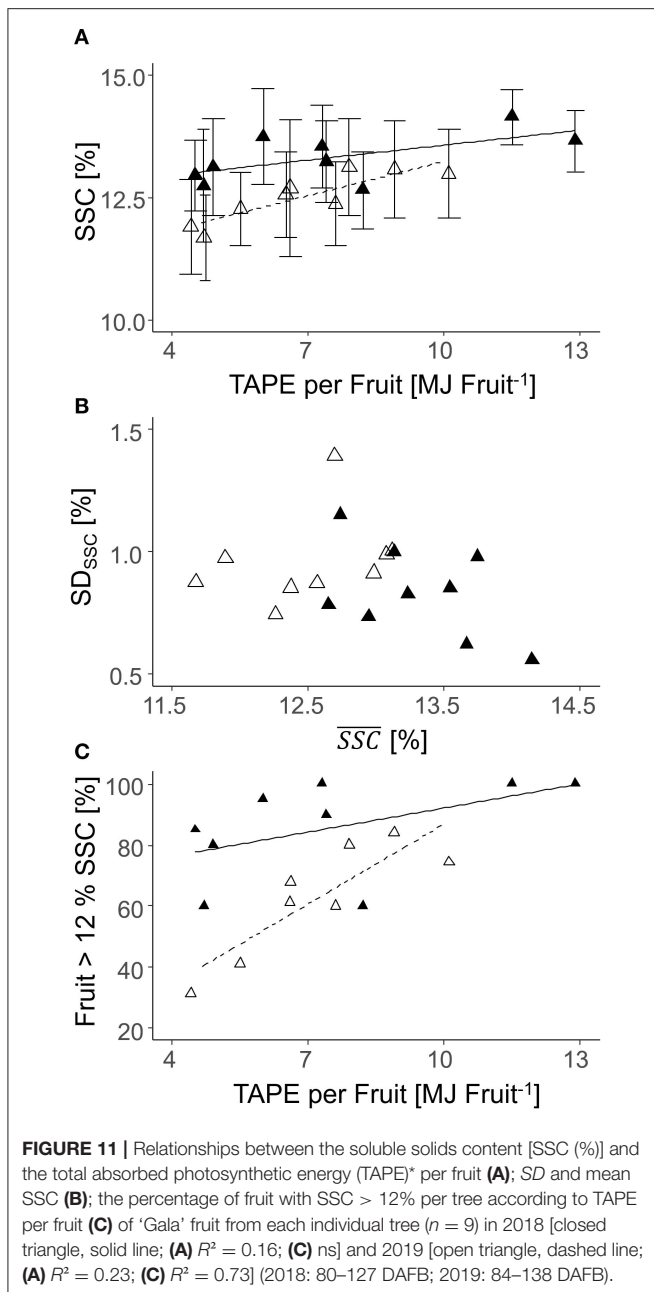
Year	Number of trees	Number of fruit with $D > 65$ mm per tree/FBC (mean $\pm$ SD)
2018	100	0.97 $\pm$ 0.39
2019	75	1.05 $\pm$ 0.29

may negatively affect the net  $CO_2$  exchange rate of apple leaves (Palmer et al., 1997; Pallas et al., 2018). In "Braeburn"/M.26 trees, planted at 5 m  $\times$  2.5 m, mean mid-season leaf net  $CO_2$  exchange rate was reduced when the LA per fruit (LA:F) of the whole tree exceeded 830  $cm^2$  (Palmer et al., 1997). In the present study, however, crop load did not have any effect on  $^{max}J_{CO_2}$  (Figure 3), presumably because the LA:F, ranging from 340  $cm^2$  to 780  $cm^2$  (data not shown), did not exceed this threshold. Consequently,



the reduction of photosynthetic performance can be assumed as a marginal influence on the present findings.

The feasibility of the FBC model was confirmed by comparing the modeled FBC of each individual tree and the measured mean



fruit diameter of the trees as a reference diameter. The ratio obtained was close to 1, proving that the model meets the real-world conditions. Consequently, the FBC provides a concept for simulating the optimum crop load for each tree. The application of FBC for evaluating the actual crop load of each individual tree and addressing the precise management of orchards is potentially based on the decision of each individual tree.

Nevertheless, in the commercial orchard, crop load exceeded the estimated FBC in a considerable number of trees without any negative effects on the mean fruit diameter. It can be assumed that the model fails to account completely for the difference in canopy light extinction coefficient between the trees (Poblete-Echeverría et al., 2015). Actually, a few physiologically

based tree metrics are available for tree design and annual pruning (Breen et al., 2021). Breen et al. (2021) reported that by means of the standardized six limbs per meter of vertical canopy height, light penetration into the inner parts of apple canopies can be increased without any negative consequences on light interception. This improves especially the percentage of a premium class fruit, and reduces variability among the fruit. In the present study, the number of limbs per meter of vertical canopy height varied between 6.6 and 21.3, exceeding the proposed ideal number.

The approach of modeling the LA demand to meet the carbon requirement of developing fruit to specific fruit sizes can provide an additional application. It may contribute to understand the

**TABLE 4 |** FBC considering the four target fruit diameters (D) converted into fresh mass (FM) of 'Gala'/M.9 apple trees in 2018 and 2019 of trees with a mean of 5.5 m<sup>2</sup> total LA; the total absorbed photosynthetic energy (TAPE) (MJ fruit<sup>-1</sup>) per fruit considering the FBC; the measured FM receiving this TAPE per fruit, the ratio between the targeted fruit FM and measured FM.

Year	D (mm), FM (g)	FBC (fruit tree <sup>-1</sup> )	TAPE fruit <sup>-1</sup> (MJ fruit <sup>-1</sup> )	FM (TAPE fruit <sup>-1</sup> ) (g)	Ratio between targeted FM and FM (TAPE fruit <sup>-1</sup> )
2018	65, 102	130	5.4	116.8	0.9
	70, 129	98	7.1	126.0	1.0
	75, 161	79	8.8	135.3	1.2
	80, 198	66	10.5	144.5	1.4
2019	65, 102	139	5.5	141.0	0.7
	70, 129	105	7.3	159.6	0.8
	75, 161	85	9.0	178.1	0.9
	80, 198	71	10.8	196.7	1.0

effect of variable LA:F ratios on fruit mass, which was investigated on either whole trees of a similar size or exposed girdled branches (Palmer et al., 1997; Baïram et al., 2019). Remote sensing provides a new tool to study the LA demand per fruit for specific diameters in different planting systems. However, one limitation is that the LA demand is an average value of the whole tree, not representing the individual types of leaves and distances between leaves and fruit. Consequently, no conclusions about the fruit size distribution in the individual branch level can be made.

## Modeling the LA Demand for Different Fruit Sizes

To meet the consumer's preferences, commercial fruit quality requirements demand a minimum fruit diameter of 65 mm while at least 60% of the fruit surface must be covered with red blush. The firmness of a high-quality 'Gala' fruit should be below 62 N (Harker et al., 2008) and SSC at least 12% (Saei et al., 2011). In the present study, most of the fruit met these consumer preferences when the number of fruit per tree was in the range of the FBC estimated for the target fruit diameters (Figures 8, 10–12 and Supplementary Table 2). With the present approach, an assessment method for the optimum number of fruit per individual tree targeting a certain fruit size becomes available. For applying the FBC in a VRA or field-uniform thinning measure, a few variables are requested: The conversion factor for turning fruit diameter into FM can be obtained on the farm. The LA needs to be known, and here more methods and commercial services are becoming available at present (Tsoulas et al., 2021). For a field-uniform assessment, the mean LA of 5.5 m<sup>2</sup>, found in the present study can be applied as an example (Table 4). With target FM or diameter, known LA, fruit respiration rate from extension service or literature, and weather data from satellite or weather station, the calculation of FBC is enabled (Equation 12). The FBC for the desired fruit diameter can serve as the target crop load in thinning measures (Table 4), e.g., to evaluate whether and to what extent thinning practices are required. In order to account for the production system of the orchard, the TAPE can be considered additionally.

A previous work indicated a lower firmness in apples grown on trees with high crop load compared to low crop load trees (Link, 2000; Serra et al., 2016). Therefore, it was expected that fruit firmness would respond to TAPE per fruit, as did FM and SSC. However, this was not found in the present study.

Both yield and average mass of fruit were directly affected by TAPE and TAPE per fruit confirming the validity of the concept of modeling the FBC of apple trees. With a similar approach, Wünsche et al. (1996) explained differences in productivity of apple growing systems by the amount of intercepted radiation capturing a 2-weeks period. Furthermore, a high TAPE per fruit (2018: 7.4 MJ fruit<sup>-1</sup>; 2019: 5.5 MJ fruit<sup>-1</sup>, Figure 11B) is required for the trees to achieve a high percentage of fruit with D > 65 mm. At this TAPE per fruit, representing a LA:F ratio of approx. 550 cm<sup>2</sup>, 80% of the apples reached D > 65 mm in both years. Thus, this LA:F can be seen as a threshold target for crop load management to achieve a marketable average fruit mass in the present orchard. The threshold is expected to differ in other orchards.

When the number of fruit per tree appeared in the range of FBC, the TAPE per fruit was above the 7.4 MJ fruit<sup>-1</sup> only when targeting D > 70 mm in 2018; and above 5.5 MJ fruit<sup>-1</sup> when targeting D > 65 mm in 2019 (Table 4). The modeled FBC slightly underestimated the actual FBC. However, with the presented empirical model (Figures 7, 8) a target fruit diameter for specific markets can be approached.

The SD of SSC in 2018 was negatively correlated with TAPE per fruit, indicating that differences in SSC can be reduced by the precise management of crop load. The maximum between-tree variability in the mean SSC was 1.4%, which was similar to the data previously reported for 'Gala' apples (Hoehn et al., 2003; Pilar Mata et al., 2006). Within-tree SSC is additionally influenced by the fruit position in the canopy (Nilsson and Gustavsson, 2007) and, thus, fruit exposure to sunlight (Zhang et al., 2016), distance to the leaves, and other sink organs. In 'Gala'/M.26 apples, the mean SSC between fruit from the inner and outer part of canopies differed up to 1.4% (Feng et al., 2014).

The estimation of FBC of each individual tree can be applied to develop VRAs of thinning. Mechanical VRA in thinning based on the flower set of the trees avoided over-thinning of each individual tree with a low flower set, which could increase the fruit yield by 1.4–7.6 t ha<sup>-1</sup> (Penzel et al., 2021). Knowledge on the actual FBC of each individual tree may prevent overestimation and underestimation of thinning intensity and yield as confirmed in two commercial apple orchards earlier. The number of fruit per tree of 23%, 31% of the considered trees were below the FBC, although the per tree flower cluster numbers would have enabled to meet the FBC (Penzel et al., 2020). Yield reduction due to the uniform thinning of trees with variable FBC may be avoided by the knowledge on FBC.

However, for a precise VRA in crop load management of each individual tree, FBC needs to be analyzed each year since the FBC of each individual tree differs between the years (Figure 9). Individual LA of trees of the fully developed canopies may be estimated from the early season LA or the number of

spurs and extensions that shoots in a growth model of growing degree days (Lakso and Johnson, 1990). Furthermore, when the actual crop load data of each individual tree will become available (Apolo-Apolo et al., 2020; Tsoulas et al., 2020a), the difference between FBC and the actual crop load will provide a decision support for each individual tree, enabling VR thinning.

## CONCLUSION

The overall variability of LA per tree and the associated FBC were found in two consecutive years. This finding points to potentially erratic crop load management when field-uniform thinning intensity is applied.

The number of photons per fruit intercepted by the tree during the growing season determined fruit mass and SSC. To produce 80% of the fruit with a  $D > 65$  mm,  $\geq 7.4$  MJ fruit<sup>-1</sup> (2018), and  $\geq 5.5$  MJ fruit<sup>-1</sup> (2019) were needed. Such values represented the LA to fruit ratio above 550 cm<sup>2</sup> in the present orchard. The mean LA of 5.5 m<sup>2</sup> provided the FBC ranging from 66 to 139 fruit when targeting varying harvest fruit diameters (65–80 mm). The corresponding TAPE per fruit ranged from 5.4 to 10.8 MJ fruit<sup>-1</sup>.

Consequently, the FBC to produce a desired mean fruit diameter per tree can be feasibly estimated based on the availability of LA data per tree. The branch autonomy considering source-to-sink and sink-to-sink distances needs to be further investigated, potentially by combining related models and advanced LiDAR readings distinguishing the type of leaf and fruit. With the carbon balance and new sensor data, the variable rate thinning adjusting the thinning intensity for each tree can, therefore, be supported.

## DATA AVAILABILITY STATEMENT

The raw data supporting the conclusions of this article will be made available by the authors, without undue reservation.

## REFERENCES

- Apolo-Apolo, O. E., Perez-Ruiz, M., Martinez-Guanter, J., and Valente, J. (2020). A cloud-based environment for generating yield estimation maps from apple orchards using UAV imagery and a deep learning technique. *Front. Plant Sci.* 11:1086. doi: 10.3389/fpls.2020.01086
- Bairam, E., leMorvan, C., Delaire, M., and Buck-Sorlin, G. (2019). Fruit and leaf response to different source–sink ratios in apple, at the scale of the fruit-bearing branch. *Front. Plant Sci.* 10:1039. doi: 10.3389/fpls.2019.01039
- Belhassine, F., Martinez, S., Bluy, S., Fumey, D., Kelner, J. J., Costes, E., et al. (2019). Impact of within-tree organ distances on floral induction and fruit growth in apple tree: implication of carbohydrate and gibberellin organ contents. *Front. Plant Sci.* 10:1233. doi: 10.3389/fpls.2019.01233
- Breen, K. C., Tustin, D. S., Van Hooijdonk, B. M., Stanley, C. J., Scofield, C., Wilson, J. M., et al. (2021). Use of physiological principles to guide precision orchard management and facilitate increased yields of premium quality fruit. *Acta Hort.*
- Charles-Edwards, D. A. (1982). *Physiological Determinants of Crop Growth*. Sydney: Academic Press.

## AUTHOR CONTRIBUTIONS

MP: conceptualization, methodology, validation, formal analysis, writing—original draft, and writing—review and editing. WH: methodology, resources, and writing—review and editing. CW: writing—review and editing. NT: conceptualization, formal analysis, methodology, and writing. MZ-S: funding acquisition, methodology, writing—review and editing, and supervision. All authors contributed to the article and approved the submitted version.

## FUNDING

This research was funded by the Ministry of Agriculture, Environment and Climate Protection of the federal state of Brandenburg, and the agricultural European Innovation Partnership (EIP-AGRI), grant number 80168342 (2016–2020). We acknowledge the support by the German Research Foundation and the Open Access Publication Fund of TU Berlin.

## ACKNOWLEDGMENTS

We appreciate the excellent cooperation with Karin Bergt and Lutz Günzel, who allowed us to conduct our research in their commercial orchard. We thank Corinna Rolleczeck, David Sakowsky, and Gabriele Wegner for technical support and Michael Schirrmann for helpful comments on the R-Script for analyzing the data.

## SUPPLEMENTARY MATERIAL

The Supplementary Material for this article can be found online at: <https://www.frontiersin.org/articles/10.3389/fpls.2021.669909/full#supplementary-material>

- Costa, G., Botton, A., and Vizzotto, G. (2018). Fruit thinning. *Hortic. Rev.* 46, 185–226. doi: 10.1002/9781119521082.ch4
- Coupe-Ledru, A., Pallas, B., Delalande, M., Boudon, F., Carrié, E., Martinez, S., et al. (2019). Multi-scale high-throughput phenotyping of apple architectural and functional traits in orchard reveals genotypic variability under contrasted watering regimes. *Hortic. Res.* 6:52. doi: 10.1038/s41438-019-0137-3
- De Pury, D., and Farquhar, G. (1997). Simple scaling of photosynthesis from leaves to canopies without the errors of big-leaf models. *Plant Cell Environ.* 20, 537–557. doi: 10.1111/j.1365-3040.1997.00094.x
- DeJong, T. (2019). Opportunities and challenges in fruit tree and orchard modelling. *Eur. J. Hort. Sci.* 84, 117–123. doi: 10.17660/ejhs.2019/84.3.1
- Doerflinger, F. C., Lakso, A. N., and Braun, P. (2015). Adapting the MaluSim apple tree model for the 'Gala' cultivar. *Acta Hort.* 1068, 267–272. doi: 10.17660/ActaHort.2015.1068.33
- Feng, F., Li, M., Ma, F., and Cheng, L. (2014). Effects of location within the tree canopy on carbohydrates, organic acids, amino acids and phenolic compounds in the fruit peel and flesh from three apple (*Malus × domestica*) cultivars. *Hortic. Res.* 1:14019. doi: 10.1038/hortres.2014.19



- Ferguson, I., Volz, R., and Woolf, A. (1999). Preharvest factors affecting physiological disorders of fruit. *Postharvest Biol. Technol.* 15, 255–262. doi: 10.1016/S0925-5214(98)00089-1
- Handsack, M., and Schmidt, S. (1991). Die Bedeutung von Blühstärke, finalem Fruchtansatz und Fruchtmasse für den Ertrag von Apfelbestandseinheiten. *Arch. Gartenbau.* 39, 37–46.
- Harker, F. R., Kupferman, E. M., Marin, A. B., Gunson, F. A., and Triggs, C. M. (2008). Eating quality standards for apples based on consumer preferences. *Postharvest Biol. Technol.* 50, 70–78. doi: 10.1016/j.postharvbio.2008.03.020
- Hoehn, E., Gasser, F., Guggenbühl, B., and Künsch, U. (2003). Efficacy of instrumental measurements for determination of minimum requirements of firmness, soluble solids, and acidity of several apple varieties in comparison to consumer expectations. *Postharvest Biol. Technol.* 27, 27–37. doi: 10.1016/S0925-5214(02)00190-4
- Huang, Y., Ren, Z., Li, D., and Liu, X. (2020). Phenotypic techniques and applications in fruit trees: a review. *Plant Methods* 16:107. doi: 10.1186/s13007-020-00649-7
- Huyskens-Keil, S., and Herppich, W. B. (2013). High CO<sub>2</sub> effects on biochemical and textural properties of white asparagus (*Asparagus officinalis* L.) spears in postharvest. *Postharvest Biol. Technol.* 75, 45–53. doi: 10.1016/j.postharvbio.2012.06.017
- Iwanami, H., Moriya-Tanaka, Y., Honda, C., Hanada, T., and Wada, M. (2018). A model for representing the relationships among crop load, timing of thinning, flower bud formation, and fruit weight in apples. *Sci. Hortic.* 242, 181–187. doi: 10.1016/j.scienta.2018.08.001
- Jakopic, J., Zupan, A., Eler, K., Schmitzer, V., Stampar, F., and Veberic, R. (2015). It's great to be the King: apple fruit development affected by the position in the cluster. *Sci. Hortic.* 194, 18–25. doi: 10.1016/j.scienta.2015.08.003
- Jones, H. G. (1981). Carbon dioxide exchange of developing apple (*Malus pumila* Mitt.) fruits. *J. Exp. Bot.* 32, 1203–1210. doi: 10.1093/jxb/32.6.1203
- Lakso, A. N., and Johnson, R. S. (1990). A simplified dry matter production model for apple using automatic programming simulation software. *Acta Hortic.* 276, 141–148. doi: 10.17660/ActaHortic.1990.276.15
- Lakso, A. N., Mattii, G. B., Nyrop, J. P., and Denning, S. S. (1996). Influence of european red mite on leaf and whole canopy CO<sub>2</sub> exchange, yield, fruit size, quality and return cropping in 'delicious' apple trees. *J. Amer. Soc. Hortic. Sci.* 121, 954–958. doi: 10.21273/JASHS.121.5.954
- Ligges, U., Short, T., Kienzel, P., et al. (2015). *Package 'Signal'*. R Foundation for Statistical Computing.
- Link, H. (2000). Significance of flower and fruit thinning on fruit quality. *Plant Growth Regul.* 31, 17–26. doi: 10.1023/A:1006334110068
- Linke, M., Herppich, W. B., and Geyer, M. (2010). Green peduncles may indicate postharvest freshness of sweet cherries. *Postharvest Biol. Technol.* 58, 135–141. doi: 10.1016/j.postharvbio.2010.05.014
- Lyons, D. J., Heinemann, P. H., Schupp, J. R., Baugher, T. A., and Liu, J. (2015). Development of a selective automated blossom thinning system for peaches. *Trans. ASABE* 58, 1447–1457. doi: 10.13031/trans.58.11138
- Manfrini, L., Corelli-Grappadelli, L., Morandi, B., Losciale, P., and Taylor, J. A. (2020). Innovative approaches to orchard management: assessing the variability in yield and maturity in a 'Gala' apple orchard using a simple management unit modeling approach. *Eur. J. Hortic. Sci.* 85, 211–218. doi: 10.17660/eJHS.2020/85.4.1
- Matyssek, R., and Herppich, W. B. (2017). "Experimentelle pflanzenökologie: physikalische Grundlagen von Transpiration, CO<sub>2</sub>-Aufnahme, Gasleitfähigkeiten und deren Bestimmungen," in *Experimentelle Pflanzenökologie, Springer. Reference Naturwissenschaften*, eds R. Matyssek and W. B. Herppich (Berlin; Heidelberg: Springer Spektrum), 1–30. doi: 10.1007/978-3-662-53493-9\_10-1
- McArtney, S. J., Palmer, J. W., and Adams, H. M. (1996). Crop loading studies with 'Royal Gala' and 'Braeburn' apples: effect of time and level of hand thinning. *New Zeal. J. Crop Hortic. Sci.* 24, 401–407. doi: 10.1080/01140671.1996.9513977
- McCree, K. J. (1972). Test of current definitions of photosynthetically active radiation against leaf photosynthesis data. *Agric. Meteorol.* 10, 443–453. doi: 10.1016/0002-1571(72)90045-3
- Mu, Y., Fujii, Y., Takata, D., Zheng, B., Noshita, K., Honda, K., et al. (2018). Characterization of peach tree crown by using high-resolution images from an unmanned aerial vehicle. *Hortic. Res.* 5:74. doi: 10.1038/s41438-018-0097-z
- Nilsson, T., and Gustavsson, K. E. (2007). Postharvest physiology of 'Aroma' apples in relation to position on the tree. *Postharvest Biol. Technol.* 43, 36–46. doi: 10.1016/j.postharvbio.2006.07.011
- Pallas, B., Bluy, S., Ngao, J., Martinez, S., Clément-Vidal, A., Kelner, J. J., et al. (2018). Growth and carbon balance are differently regulated by tree and shoot fruiting contexts: an integrative study on apple genotypes with contrasted bearing patterns. *Tree Physiol.* 38, 1395–1408. doi: 10.1093/treephys/tpx166
- Palmer, J. W., Giuliani, R., and Adams, H. M. (1997). Effect of crop load on fruiting and leaf photosynthesis of 'Braeburn'/M.26 apple trees. *Tree Physiol.* 17, 741–746. doi: 10.1093/treephys/17.11.741
- Peeters, A., Zude, M., Käthner, J., Ünlü, M., Kanber, R., Hetzroni, A., et al. (2015). Getis-Ord's hot-and cold-spot statistics as a basis for multivariate spatial clustering of orchard tree data. *Comp. Electron. Agric.* 111, 140–150. doi: 10.1016/j.compag.2014.12.011
- Penzel, M., Lakso, A. N., Tsoulas, N., and Zude-Sasse, M. (2020). Carbon consumption of developing fruit and the fruit bearing capacity of individual RoHo 3615 and Pinova apple trees. *Int. Agrophys.* 34, 407–421. doi: 10.31545/intagr/127540
- Penzel, M., Pflanz, M., Gebbers, R., and Zude-Sasse, M. (2021). Tree adapted mechanical flower thinning prevents yield loss caused by over thinning of trees with low flower set in apple. *Eur. J. Hortic. Sci.* 86, 88–98. doi: 10.17660/eJHS.2021/86.1.10
- Pflanz, M., Gebbers, R., and Zude, M. (2016). Influence of tree-adapted flower thinning on apple yield and fruit quality considering cultivars with different predisposition in fructification. *Acta Hortic.* 1130, 605–612. doi: 10.17660/ActaHortic.2016.1130.90
- Pilar Mata, A., Val, J., and Blanco, A. (2006). Prohexadione-calcium effects on the quality of 'Royal Gala' apple fruits. *J. Hortic. Sci. Biotechnol.* 81, 965–970. doi: 10.1080/14620316.2006.11512183
- Poblete-Echeverría, C., Fuentes, S., Ortega-Farías, S., Gonzalez-Talce, J., and Yuri, J. A. (2015). Digital cover photography for estimating leaf area index (LAI) in apple trees using a variable light extinction coefficient. *Sensors* 15, 2860–2872. doi: 10.3390/s150202860
- Poll, L., Rindom, A., Toldam-Andersen, P., and Hansen, P. (1996). Availability of assimilates and formation of aroma compounds in apples as affected by the fruit/leaf ratio. *Physiol. Plant.* 97, 223–227. doi: 10.1034/j.1399-3054.1996.970203.x
- R Core Team (2018). *R: A Language and Environment for Statistical Computing*. R Foundation for Statistical Computing. Vienna. Available online at: <https://www.R-project.org/> (accessed June 7, 2021).
- Reyes, F., DeJong, T., Franceschi, P., Tagliavini, M., and Gianelle, D. (2016). Maximum growth potential and periods of resource limitation in apple tree. *Front. Plant Sci.* 7:233. doi: 10.3389/fpls.2016.00233
- Reyes, F., Pallas, B., Pradal, C., Vaggi, F., Zanotelli, D., Tagliavini, M., et al. (2020). MuSCA: a multi-scale source-sink carbon allocation model to explore carbon allocation in plants. An application to static apple tree structures. *Ann. Bot.* 126, 571–585. doi: 10.1093/aob/mcz122
- Saei, A., Tustin, D. S., Zamani, Z., Talaie, A., and Hall, A. J. (2011). Cropping effects on the loss of apple fruit firmness during storage: the relationship between texture retention and fruit dry matter concentration. *Sci. Hortic.* 130, 256–265. doi: 10.1016/j.scienta.2011.07.008
- Sanz, R., Llorens, J., Escolà, A., Arnó, J., Planas, S., Roman, C., et al. (2018). LIDAR and non-LIDAR-based canopy parameters to estimate the leaf area in fruit trees and vineyard. *Agric. Forest Meteorol.* 260, 229–239. doi: 10.1016/j.agrformet.2018.06.017
- Serra, S., Leisso, R., Giordani, L., Kalcits, L., and Musacchi, S. (2016). Crop load influences fruit quality, nutritional balance, and return bloom in 'Honeycrisp' apple. *HortScience* 51, 236–244. doi: 10.21273/HORTSCI.51.3.236
- Szeicz, G. (1970). *Spectral Composition of Solar Radiation and its Penetration in Crop Canopies*. Ph.D. thesis, University of Reading.
- Taylor, J. A., Dresser, J. L., Hickey, C. C., Nuske, S. T., and Bates, T. R. (2019). Considerations on spatial crop load mapping. *Aust. J. Grape Wine Res.* 25, 144–155. doi: 10.1111/ajgw.12378
- Tsoulas, N., Fountas, S., and Zude-Sasse, M. (2021). Spatio-temporal effects of soil ECA and LiDAR-derived leaf area on fruit quality in the apple production. *Biosyst. Eng.*

- Tsoulias, N., Gebbers, R., and Zude-Sasse, M. (2020b). Using data on soil ECa, soil water properties, and response of tree root system for spatial water balancing in an apple orchard. *Precis. Agric.* 21, 522–548. doi: 10.1007/s11119-019-09680-8
- Tsoulias, N., Paraforos, D. S., Fountas, S., and Zude-Sasse, M. (2019). Estimating canopy parameters based on the stem position in apple trees using a 2D LiDAR. *Agronomy* 9:740. doi: 10.3390/agronomy9110740
- Tsoulias, N., Paraforos, D. S., Xanthopoulos, G., and Zude-Sasse, M. (2020a). Apple shape detection based on geometric and radiometric features using a LiDAR laser scanner. *Remote Sens.* 12:2481. doi: 10.3390/rs12152481
- Vanbrabant, Y., Delalieux, S., Tits, L., Pauly, K., Vandermaesen, J., and Somers, B. (2020). Pear flower cluster quantification using RGB drone imagery. *Agronomy* 10:407. doi: 10.3390/agronomy10030407
- Verbiest, R., Ruysen, K., Vanwalleghem, T., Demeester, E., and Kellens, K. (2020). Automation and robotics in the cultivation of pome fruit: where do we stand today? *J. Field Robot.* 2020, 1–19. doi: 10.1002/rob.22000
- Wouters, N. (2014). *Mechatronics for Efficient Thinning of Pear*. Ph.D. thesis, KU Leuven.
- Wünsche, J. N., Lakso, A. N., Robinson, T. L., Lenz, F. and Denning, S. S. (1996). The bases of productivity in apple production systems: the role of light interception by different shoot types. *J. Amer. Soc. Hortic. Sci.* 121, 886–893. doi: 10.21273/JASHS.121.5.886
- Xia, G., Cheng, L., Lakso, A. N., and Goffinet, M. (2009). Effects of nitrogen supply on source-sink balance and fruit size of ‘Gala’ apple trees. *J. Amer. Soc. Hortic. Sci.* 134, 126–133. doi: 10.21273/JASHS.134.1.126
- Yuri, J. A., Gonzalez-Talice, G., Verdugo, J., and del Pozo, J. (2011). Response of fruit growth, quality, and productivity to crop load in apple cv. Ultra Red Gala/MM.111. *Sci. Hortic.* 127, 305–312. doi: 10.1016/j.scienta.2010.10.021
- Zhang, J., Serra, S., Leisso, R. S., and Musacchi, S. (2016). Effect of light microclimate on the quality of ‘d’Anjou’ pears in mature open-centre tree architecture. *Biosyst. Eng.* 141, 1–11. doi: 10.1016/j.biosystemseng.2015.11.002
- Zude-Sasse, M., Fountas, S., Gemtos, T. A., and Abu-Khalaf, N. (2016). Applications of precision agriculture in horticultural crops – review. *Eur. J. Hortic. Sci.* 81, 78–90. doi: 10.17660/eJHS.2016/81.2.2

**Conflict of Interest:** The authors declare that the research was conducted in the absence of any commercial or financial relationships that could be construed as a potential conflict of interest.

Copyright © 2021 Penzel, Herppich, Weltzien, Tsoulias and Zude-Sasse. This is an open-access article distributed under the terms of the Creative Commons Attribution License (CC BY). The use, distribution or reproduction in other forums is permitted, provided the original author(s) and the copyright owner(s) are credited and that the original publication in this journal is cited, in accordance with accepted academic practice. No use, distribution or reproduction is permitted which does not comply with these terms.

## Supplementary material

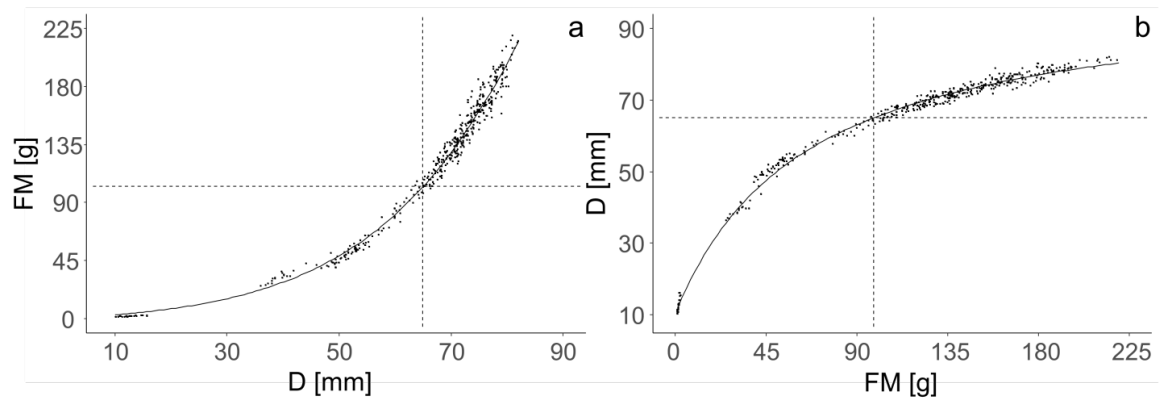


**Figure S1**

Allometric relationships between (a) diameter (D) and fresh mass (FM), (b) FM and D of developing 'Gala'/M.9 apple fruit ( $n = 460$ ) sampled at several dates during the growing seasons in 2018 and 2019 (Fig. 2). The vertical lines indicates the minimum fruit diameter for market entry of 65 mm, the solid lines regression models to convert D into FM and FM into D. ( $FM = 939.73 - 199741/((1.05202)^D + 211.527)$ ,  $R^2 = 0.98$ ;  $D = 10.465 + 90.45152 \times FM \times (64.614448 + FM)^{-1}$ ,  $R^2 = 0.99$ )

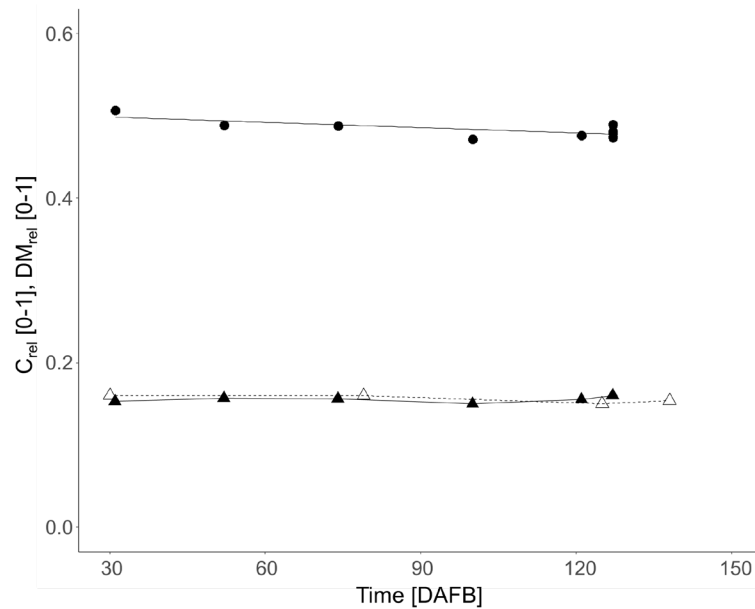


**Figure S2**

Time course in d after full bloom (DAFB) of average fraction of dry matter on fresh mass (triangles,  $DM_{rel}$ ) in 2018 (triangle pointing up), 2019 (triangle pointing down) and fractions of elemental C on  $DM_{rel}$  in 2018 (circle,  $C_{rel}$ ) of developing 'Brookfield Gala'/M.9 apple fruit. ( $C_{rel} = 50.837 - 0.0273 \times DAFB$ ,  $p=0.01$ ,  $R^2 = 0.72$ )

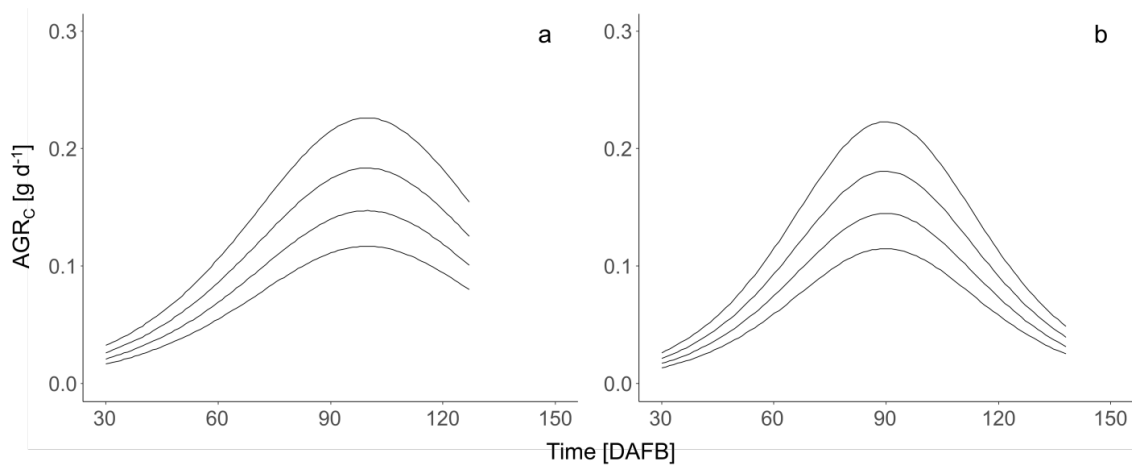


**Table S1**

Normalised equations of seasonal fruit development considering fresh mass ( $FM_{norm}$ ) and elemental C content ( $C_{norm}$ ) of ' Gala' apple fruit expressed over time in days after full bloom (DAFB) in two years.

Year	Equations	No.
2018	$FM_{norm} = 1.16 - \frac{193.1}{(1.056)^{DAFB} + 169.12}$	S1.1
	$C_{norm} = 1.28 - \frac{132.83}{(1.0476)^{DAFB} + 103.39}$	S2.1
2019	$FM_{norm} = 1.04 - \frac{323.99}{(1.068)^{DAFB} + 312.55}$	S1.2
	$C_{norm} = 1.06223 - \frac{189.26}{(1.06)^{DAFB} + 177.63}$	S2.2

$$C_{rel}(DAFB) = 50.837 - 0.0273 \times DAFB, p=0.01, R^2 = 0.72 \quad (\text{Eq. S3})$$

**Figure S3**

Absolute growth rate in C content ( $AGR_C$ ) during 2018 (a) and 2019 (b) in the days after full bloom (DAFB) simulated for ' Gala'/M.9 apples with target fruit diameters of 65 mm, 70 mm, 75 mm and 80 mm (from the bottom to top).

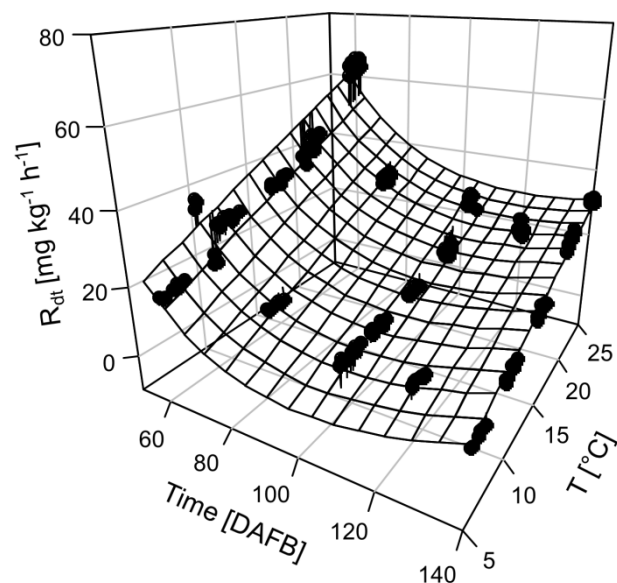


**Figure S4**

Fruit respiration rate,  $R_{dt}$ , of 'Gala' apple during cell expansion and ripening stage of fruit. The  $R_{dt}$  model considers the time, d after full bloom (DAFB), temperature (T):  $R_{dt} = 425.6 - 122.7 \times \ln(\text{DAFB}) - 0.0097 \times \text{DAFB} \times T + 2.31 \times T + 1.31 \times \text{DAFB}$ ,  $p < 0.001$ ;  $R^2 = 0.87$ .

**Table S2**

Fruit firmness, hue angle of 'Gala' apple fruit and percentage of fruit with >60 % red blush of the fruit surface of 'Gala' trees in two years measured at harvest.

Year	$F_{\max}$ [N] <sup>1</sup>			hue angle <sup>1</sup>			Percentage of fruit with > 60 % red blush [%] <sup>2</sup>		
	Min.	Max.	Mean	Min.	Max.	Mean	Min.	Max.	Mean
2018	41	98	67	22	87	38	31	99	82
2019	50	115	86	-	-	-	44	100	64

<sup>1</sup>individual fruit, 2018: n=180, 2019: n=1240; <sup>2</sup>individual trees, 2018: n=100, 2019: n=70

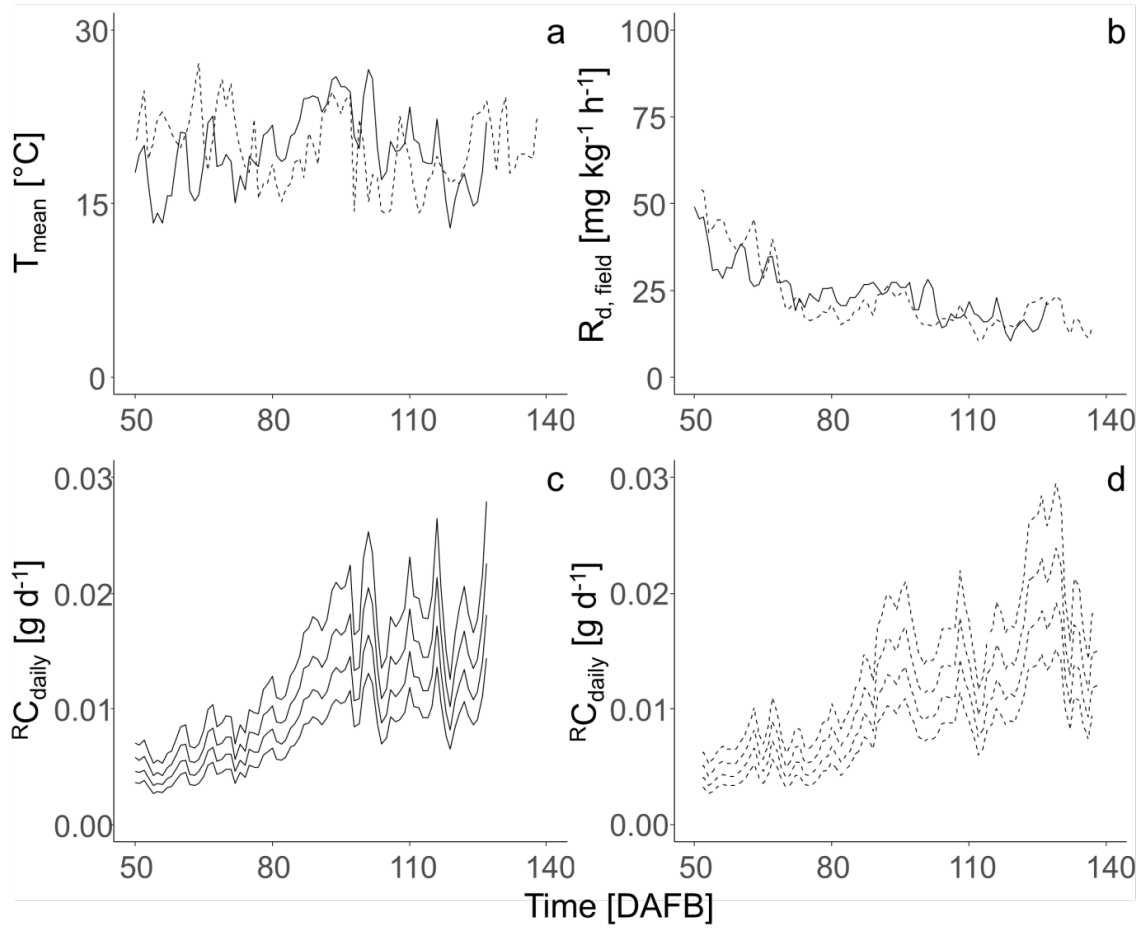


**Figure S5**

(a) Mean daily orchard temperature ( $T_{\text{mean}}$ ) in 2 m height, (b) temperature ( $T_{\text{mean}}$ )-corrected field-measured fruit respiration rate ( $R_{d, \text{field}}$ ; 2018: solid line, 2019: dashed line), (c, d) amount of C respired per fruit and day ( $R_{C, \text{daily}}$ ) of 'Gala'/M.9 apples with the target diameters of 65 mm, 70 mm, 75 mm and 80 mm (from the bottom up) during the days after full bloom (DAFB) in 2018 (c) and 2019 (d).

## 6. Discussion

### 6.1. Summary and hypotheses

Fruit growers will face many challenges in the future, e.g. climate change, labour scarcity, increasing production costs, competition with growers from other countries, and increasing consumer demand for more environmentally sustainable production methods. Means of precision horticulture, including mapping of soil, climate, and plant variables, data management, precise decision making, and site-specific orchard management (Zude-Sasse et al., 2016; Manfrini et al., 2020) may provide solutions to meet some of these challenges. Considering the newly available sensor data, which cannot be used directly in the horticultural process, it is expected that plant physiological and agronomic models will be key elements of future site-specific orchard management. The models will serve a key purpose in the interpretation of mapped data and to derive management decisions out of it. This would allow crop management of individual fruit trees to be adapted to their spatial and temporal conditions (variable rate application), potentially leading to enhanced productivity and overall fruit quality. The main objective of this research was to investigate the potential of adapting crop load management of apples to the conditions of individual trees, in order to manage spatial variability in flower and fruit set and the fruit bearing capacity. A theoretical framework to model the fruit bearing capacity of individual trees and evaluate the actual crop load of trees (Chpts. 4, 5) was developed. The model can be utilised as part of the control system for a mechatronic system for crop load management in variable rates.

In crop load management of apples, no site-specific management solutions to treat individual trees or groups of trees are currently available (Verbiest et al., 2020). However, it was shown that inter-tree and inter-season variability in flower set, fruit set, leaf area per tree, and fruit bearing capacity is abundant in commercial apple orchards (Chpts. 3-5), confirming hypothesis 1:

“The total leaf area, flower and fruit set of apple trees appears variable within commercial apple orchards”

The average capacity of fruit trees to bear fruit of a specific diameter at time of harvest can be estimated by using the stem cross-sectional area (Treder et al., 2010) of sampled trees, historical yield data (Handsack and Schmidt, 1990), or the total leaf area (Preston, 1954). The latter may be most precise, but lacked, until recently, suitable methods to map the leaf area of all the trees within an orchard. However, these methods are not sufficient

to generate target fruit numbers of each individual tree of an orchard, as the trees are heterogeneous in total leaf area. The trunk cross sectional area of a tree is frequently used to calculate the crop density of trees (number of fruit per cm<sup>2</sup> trunk cross sectional area), e.g. in crop load trials (Treder et al., 2010; Anthony et al., 2019). That is, because the total leaf area of a tree canopy appears correlated to the trunk cross sectional area (Lo Bianco, 2019). However, the trunk cross sectional area of each tree increases annually at different rates (Treder et al., 2010), e.g. in response to varying crop load levels (Reyes et al., 2016) or irrigation treatment (Mills et al., 1996). In addition, commercial orchards are routinely pruned, targeting a similar shape of the trees' canopy in each year. Therefore, the relationships between trunk cross sectional area and total leaf area are year sensitive, but differ between individual trees, particularly when crop load and soil properties vary spatially. The latter was frequently observed in commercial fruit orchards (Aggelopoulou et al., 2011; Umali et al., 2012; Tsoulas et al., 2020), especially in orchards located on soils which were formed by glacial and post-glacial deposits (Käthner and Zude, 2015; Käthner et al., 2017). Spatial variability in soil properties is, among others, one important contributor to inter-tree variability in vegetative and reproductive canopy parameters, including the trunk cross sectional area (Peeters et al., 2015; Manfrini et al., 2020). Consequently, the trunk cross sectional area is not suitable for accurately predicting the trees' individual production targets.

In the presented work (Chpts. 4, 5), a novel approach was developed to predict the fruit bearing capacity of individual trees by integrating the total leaf area of each tree, fruit growth rates, and seasonal climate conditions into a carbon balance model. For the mapping of the individual trees' leaf area, a terrestrial two-dimensional light detection and ranging (LiDAR) laser scanner was utilised. The carbon gas exchange of the leaf was measured with a portable photosynthetic system in the field, while the fruit carbon gas exchange was measured with mobile closed respiration chambers in the lab. The climate data were recorded by a weather station in the same orchard. The developed model can be utilised to evaluate the actual crop load of trees and can serve as a potential tool for decision making in crop load management. The modelling approach was orientated on previous work of Alan N. Lakso and co-workers from Cornell University (Francesconi et al., 1996; Lakso et al., 1996). The validity of the model was proven (Chpts. 4, 5) by modelling the fruit bearing capacity of sampled trees in three orchards with different cultivars (2018: 'Gala': 100 trees, 'RoHo 3615': 45 trees, 'Pinova': 35 trees; 2019: 'Gala': 70 trees) and taking into consideration the mean harvest fruit diameter per tree and the measured total leaf area of the individual trees. The estimated optimum number of fruit per

tree to produce fruit of the actual mean harvest fruit diameter and the number of fruit per tree were in good agreement (Chpt. 5), proving hypothesis 2:

“With the modelled fruit bearing capacity the number of fruit per tree can be evaluated in terms of a desired mean fruit diameter”

In the very early studies on the required leaf area to fruit ratio to produce marketable fruit (Magness et al., 1931; Preston, 1954; Hansen, 1969), a linear relationship between leaf area per tree and the number of fruit a tree can produce was expected. However, with increasing leaf area per tree, the mutual shading of neighbouring leaves as well as the fraction of shaded leaves in comparison to sunlit leaves also increases. Therefore, the relationship between total leaf area per tree and light interception was described with a hyperbolic function (Jackson and Palmer, 1980; Chpt. 4: Eq. 5). By utilising the hyperbolic function of total leaf area per tree and determining the light interception, the total absorbed photons per tree during specific periods can be estimated (Chpt. 5: Eq. 13). A linear relationship was found between total yield per tree and total absorbed photons per tree during the cell expansion stage of fruit development (Chpt. 5: Fig. 12). The results confirm earlier studies investigating relationships between orchard yield and light interception (Robinson and Lakso, 1991; Wünsche et al., 1996). Additionally, the magnitude of the mean fruit mass and soluble solids content of the fruit at harvest correlated with the amount of photons that the foliage of the tree has intercepted per fruit during the cell expansion stage of fruit development, confirming hypothesis 3:

“The average magnitude of fruit quality parameters per tree respond to the number of photons intercepted per fruit during the growing period”

This relationship further illustrates the limited ability of trees, variable in leaf area and light interception, to bear fruit with varying requirements in seasonally intercepted photons in order to grow to desired fruit diameters. Additionally, this relationship proves the validity of the modelling approach for the fruit bearing capacity of apple trees here presented. Inter-tree variability in flower clusters (Penzel et al., 2020b; Vanbrabant et al., 2020), fruit (Manfrini et al., 2020; Aggelopoulou et al., 2010) and leaf area per tree (Sanz et al., 2018) were previously reported. However, the effect of uniform crop load management on trees variable in flower set, fruit per tree, or total leaf area were not yet evaluated. Studying mechanical thinning of trees variable in flower set revealed that uniform management led to annual yield reduction in two apple cultivars by up to 7.6 t per hectare (Chpt. 3). Furthermore, it was demonstrated that uniform flower thinning of trees, variable in total leaf area and associated fruit bearing capacity, led to numbers of fruit per tree below the fruit

bearing capacity on 23 % - 31 % of the sampled trees, despite abundant flower clusters (Chpt. 4). If managed according to the fruit bearing capacity, the trees could potentially bear 6 % higher yields. The experimental sets confirmed the hypotheses 4 and 5:

“Uniform crop load management leads to yield and fruit quality losses considering individual trees”

“Uniform crop load management of apple orchards leads to inaccurate numbers of fruit per tree deviant from the optimum number of fruit per tree defined by the fruit bearing capacity in orchards with inter-tree variability in total leaf area”

Since the effect of high crop loads on fruit quality and crop value was not evaluated in the experiments (Chpts. 3-5), no conclusive statement could be made on fruit quality losses as a consequence of field uniform crop load management. However, minimum thresholds of absorbed photons per fruit for individual trees to achieve desired mean fruit fresh mass, soluble solids content (SSC), and percentage of marketable yield (Chpt. 5: Figs. 10-12) were generated. With the thresholds, the effect of high crop load on fruit fresh mass, diameter, and SSC can be evaluated for individual trees in both years. In general, a low crop value is expected on trees with excessive crop load, leading to high yield of low-quality fruit (Robinson et al., 2017; Chpt. 3: Tab. 3; Chpt. 4: Fig. 10), as well as delayed fruit maturity (Anthony et al., 2019).

The observation that high crop loads can lead to low fruit size and delayed maturity also applies to other temperate fruit species e.g. pear (Naor et al., 2000; Bound, 2015), plum (Meland and Birken, 2010), and sweet cherries (Penzel et al., 2020a; Penzel et al., 2021). Therefore, crop load management is also an important management practice in other fruit species in order to achieve a high quantity of high quality fruit annually. Although crop load management practices differ between fruit species, the proposed model of the fruit bearing capacity can potentially be applied for the evaluation of the actual fruit set and decision making in other fruit species.

## **6.2. A concept for variable rate management of crop load**

The application of mechanical and chemical thinning in the apple production has been semi-automated for many years (Dennis, 2000; Costa et al. 2018). However, both practices are performed uniformly within an orchard, which can lead to yield losses (Chpts. 3, 4) and, in case of chemical thinning, to an excess of the used thinning agents. When the thinning is performed in variable rates, taking into consideration the actual flower set or fruit set and the fruit bearing capacity of each tree, yield losses may be avoidable (Chpts.

3, 4). Furthermore, the inter-tree variability in fruit quality may be reduced and a target fruit quality at time of harvest can be approached. A system for fully automated variable-rate thinning of apple trees would consist of a vision system, a control system which integrates tree morphology and physiology, production targets, and an actuator which carries out the thinning (Wouters, 2014; Lyons et al., 2015, Pflanz et al., 2016). The vision system is required to collect and interpret tree-specific data, from which the control system can derive tree-individual management decisions (Fig. 6-1). In this context, the here proposed equations of the fruit bearing capacity (Chpt. 4: Eqs. 8,9; Chpt. 5: Eq. 12, Tab. 2) would serve as plant physiological model to calculate the optimum fruit number per tree based on the mapped total leaf area per tree and the desired production target. The output of the model can further be utilised as an input for an agronomic model comparing the actual number of fruit per tree to the optimum number of fruit per tree to make the decision whether or not and to what extent thinning should be performed in order to achieve the production target. Finally, the thinning decision leads to a command for the thinning device, which takes into consideration the current settings of the thinning device as well as the platform the device is mounted e.g. position, operational speed, vehicle speed, and inclination. Subsequently to each thinning process, further monitoring of the actual crop load is required to evaluate the necessity of further thinning. In the case of sensor-controlled pneumatic flower bud thinning utilising compressed air, Wouters (2014) proposed the installation of a second sensor for the monitoring of the thinning success as a feedback to the control system. However, the fruit set response to thinning treatment is visibly temporally delayed. Following mechanical fruit thinning, the fruit drop, which occurs for several weeks after bloom, frequently appears reduced (Kon et al., 2013; Penzel et al., 2020b). Subsequent to chemical fruit thinning, in contrast, the fruit drop is enhanced (Yuan and Greene, 2000; Chpt. 2) when the thinning process was successful. Therefore, a certain amount of time before re-monitoring of the fruit set as a feedback to the thinning treatment is required. In practice, fruit thinning is frequently performed several times (Chpt. 2), depending on the weather conditions and the fruit set response to the thinning treatment. It would further be possible to evaluate the fruit set and fruit set response to thinning treatments with a fruit abscission model (Greene et al., 2013) before the tree has shed all the fruit whose fate it is to abscise. The crucial period for fruit thinning ends about four weeks after full bloom. Afterwards, the promoting effect of thinning treatment on flower induction (Belhassine et al., 2019) and fruit growth (Lakso et al., 1995) decreases. During this period, repeated measurements of the leaf area may be necessary for accurately modelling of the fruit bearing capacity because of the temporal changes in annual shoots' growth rates (Pallas et al., 2016; Reyes et al., 2016) and the associated total leaf area of



the tree (Chpt. 4). Nevertheless, shoot growth can be accurately predicted based on growing degree-days (Johnson and Lakso, 1985; Reyes et al., 2016).

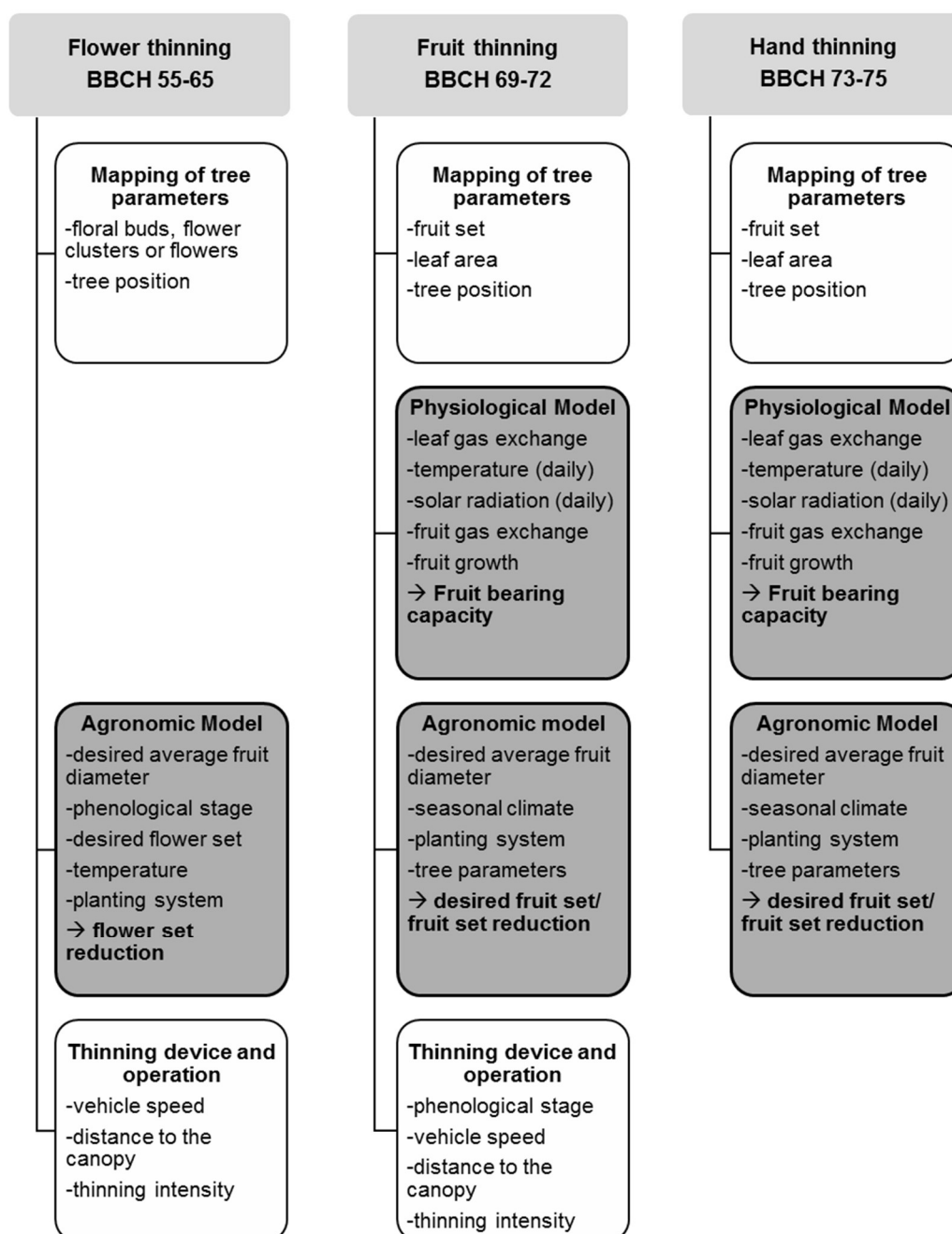


**Figure 6-1**

Integration of the fruit bearing capacity into a concept for precise crop load management of apple according to the phenological stages (BBCH codes, Meier et al., 2009) and required input variables for management decisions

Subsequent to mechanical and chemical thinning, manual hand fruit thinning is frequently performed in commercial orchards. Modelling the fruit bearing capacity and comparing it to the actual fruit set can lead to decision support in manual fruit thinning. With this

approach, individual trees or regions within an orchard can potentially be located, where hand thinning to adjust the number of fruit per tree is required. Besides reducing the number of fruit, hand thinning also intends to remove deformed, shaded, and damaged fruit to prevent their harvest and save the carbon for the harvested fruit. Also this step reduces the sorting out in subsequent steps of the value chain, in which damaged fruit result in food waste.

The required tree-individual input data (Fig. 6-1) to estimate the fruit bearing capacity and evaluate the tree actual flower or fruit set can be recorded with high precision using optical sensors (Chpt. 1: Tab. 1-2). For the fruit detection in apples, frequent studies were carried out (Chpt. 1: Tab. 1-2). In the four week period post-bloom, apple fruit diameters below 20 mm are expected, which have not yet been mapped spatially. However, it was shown that olives, which have similar size and colour ranges as apples in an early developmental stage, can be detected on the tree by utilising RGB-Sensors (Aquino et al., 2020). The application of neuronal networks can further enhance the accuracy of fruit detection (Gongal et al., 2015; Bresilla et al., 2019), which increases with the number of training images (Koirala et al., 2019). Real time availability and processing of the sensor data would be desirable when crop load management is performed in one pass through the orchard. Otherwise, spatial maps of the flower set, fruit set, and fruit bearing capacity can be generated and utilised subsequently in the thinning process. Possible sensor platforms for spatial recording of individual tree data are the existing farm machinery, stationary sensors mounted on the tree, unmanned aerial or ground vehicles, or satellites (Zude-Sasse et al., 2016). In apple orchards, tractors have a great advantage as a platform for sensors because in regular orchard management, they are commonly used for the often over twenty individual applications of plant protection agents and plant growth regulators per year (Roßberg and Harzer, 2015). Other orchard management tasks e.g. fertiliser applications, mechanical pruning, and ground maintenance are additionally performed in each row of an orchard by utilising tractors. Consequently, there is a high potential of mapping individual tree data frequently while performing the regular orchard management. Furthermore, sensors that are mounted on ground vehicles are located relatively close to the canopy, which may increase the accuracy of the mapping in comparison to sensors mounted on air vehicles or satellites as a platform (Zude-Sasse et al., 2016). The thinning in variable rates can be performed either with mechanical thinning devices (Wouters, 2014; Pflanz et al., 2016; Riehle, 2020) or, in the case of chemical thinning, with variable rate orchard sprayers (Wandkar et al., 2018; Zhang et al., 2018; Fessler et al., 2020), capable of targeting individual trees. Knowledge of the individual trees' fruit bearing capacity would

enable a significant improvement in site-specific crop load management in variable rates beyond the current practice of uniform treatment of each tree. The long-term goal is to develop a closed-loop control system to evaluate individual trees' flower and fruit set and to adjust both until the desired levels are achieved (Fig. 6-1).

Verbiest et al., (2020) mentioned that the shape of the trees' canopies are one limitation for the implementation of sensing and automation technology in orchard management. Current canopies often have three-dimensional structures with branches and fruit covering other branches and fruit; one source of errors in their detection (Gongal et al., 2015; Huang et al., 2020). To increase the precision in mapping orchard data, narrow canopy structures with reduced overlapping of neighbouring fruit and leaves and a low fraction of shaded leaves are essential. The accessibility of branches and fruit will be requirements that future tree shapes must meet (He and Schupp, 2018). Various training systems for apple trees with narrow canopies and accessible branches and fruit were developed e.g. planar cordon system, V-trellis system, Y-trellis system, or super spindles (He and Schupp, 2018; Breen et al., 2021). Additionally, on two-dimensional fruit tree canopies, the harvest efficiency is enhanced in comparison to three-dimensional canopies (Ampatzidis and Whiting, 2013). This may also be valid for the labour intensive hand fruit thinning (Chpt. 2) of apple, where accessible branches and visible fruit can potentially simplify the decision making. To create narrow canopies with simple to access branches, annual dormant pruning is one important management practice. While pruning the trees, the number of flower buds and flowers can be adjusted as a first step in crop load management, often referred to as artificial bud or spur extinction (Breen et al., 2015; Breen et al., 2021). Artificial bud or spur extinction further intends to reduce the unproductive leaf area of the trees, leading to an increased exposition of fruit to solar radiation. This relatively novel environmental friendly method of reducing the number of buds per tree is highly effective for treating trees variable in canopy size and for managing the distribution of flower buds within a canopy. Long-term, this may lead to a reduction in inter-tree variability in flower set, fruit set, and leaf area.

The possibilities to optimize the canopies for better access to the branches and fruit and an improved distribution of the fruit set should be realised in order to optimise the sensing of individual trees and to further implement automation approaches in orchards management practices, including crop load management. It is expected that the use of mechanical thinning techniques will increase in future because of the general need to reduce the use of chemicals in food production, the weather-independent mode of action, and the associated high reproducibility of the thinning effects with similar machine settings (Riehle, 2020; Chpt. 3).

### **6.3. Perspective for sensor application and the concept of the fruit bearing capacity into applied thinning trials**

Currently, various thinning trials all around the globe are carried out annually e.g. to evaluate and develop new thinning methods (Costa et al., 2018; Elsysy et al., 2019; Kon and Schupp, 2019) or strategies for individual apple cultivars (Anthony et al., 2019; Chpt. 2). For an accurate evaluation of the thinning efficacy, uniform trees are required. Uniform trees are frequently chosen according to their flower set. For this purpose, the number of flower clusters per tree is manually measured and compared to the roughly estimated canopy size, leaf area (Chpts. 2, 3), or the stem cross sectional area. After choosing nearly uniform trees, the initial and/or final fruit set of the trees (Penzel et al., 2020b) is further measured manually. Additionally, all fruit of the same tree are harvested and sorted (Chpts. 2, 3) when the fruit reaches a desired maturity stage (Zude-Sasse et al., 2000).

The application of sensors to record tree individual data, e.g. number of flower clusters, fruit set, fruit size, leaf area index, stem diameter (Chpt. 1: Tab 1-2; Huang et al., 2020), and fruit quality attributes (Zude et al., 2006; Walsh et al., 2020) would reduce the amount of labour required to perform thinning trials. Sensor application for recording tree individual data can potentially reduce errors in comparison to the time-consuming manual measurements. Furthermore, labour intensive tree individual harvest may be avoidable, if sensors are capable of recording fruit size, colour, and internal quality distribution and their temporal changes on the individual tree scale.

To realise site-specific crop load management, trials to evaluate the potential for several thinning agents and techniques currently in use would be necessary. When the leaf area and the fruit bearing capacity of each tree can be modelled, uniform trees would not necessarily be required anymore in thinning trials because the evaluation of the thinning efficacy can be performed relatively to the optimum number of fruit for each tree for tree-individual production targets. For the development of management decisions in specific situations on several cultivar-rootstock combinations, climates, and growing systems, the thinning efficacy on trees heterogeneous in total leaf area and fruit set would indeed be desired. In case of chemical fruit thinning, new research objectives arise because besides investigating required concentrations of active ingredients within the tank mix, the required amount of spray volume to cover the canopy surface area needs to be studied. For plant protection products, it was proven that the amount of tank mix to cover the surface area varies between trees variable in total leaf area (Berk et al., 2019). Since thinning results in the same location and year are often inconsistent, trials within the same region may be

coordinated and evaluated together, as done by Rosa et al. (2020) or Gonzales et al. (2019), instead of evaluated individually. This would increase the understanding of the performance of several thinning techniques in different situations and make thinning results more reproducible.

## **6.4. Conclusion**

Inter-tree and inter-year variability in flower set, fruit set, and leaf area per tree determining the trees' capacity to produce fruit of desired diameters, the fruit bearing capacity, is abundant in commercial apple orchards. However, inter-tree variability in the fruit bearing capacity, flower and fruit set is frequently not taken into consideration in current crop load management practices.

To enable tree adapted crop load management, the utilisation of sensor data in plant physiological and agronomic models will become inevitable. For this purpose, a modelling approach was developed to estimate the trees' individual fruit bearing capacity out of the LiDAR scanned total leaf area. In the model, the daily assimilated carbon per tree is calculated from seasonally recorded weather data, the leaf area of the trees, the quantum efficiency of leaf photosynthesis, and light saturated leaf assimilation rates, which were recorded with a portable photosynthetic system. Contrary to the assimilated carbon per tree is the daily carbon requirement per fruit, determined by fruit growth and respiration rates. Fruit growth rates as well as the carbon supply conditions to the fruit are continuously changing. During high fruit growth rates, the fruit has the highest seasonal carbon requirements that limits the fruit bearing capacity. After a tree's canopy is fully developed, the period of the highest fruit growth rates is most reasonable to be used as a reference period to calculate the fruit bearing capacity. The model is feasible for individual tree estimations of target fruit numbers. Furthermore, the average fruit fresh mass of a tree appears to correlate with the seasonally intercepted photons per fruit of a tree, demonstrating the physiological limitation of the trees' productivity and the validity of the model. By comparing harvest fruit numbers with the modelled FBC of individual trees, it was proven that uniform flower thinning led to sub-optimal crop load above or below the fruit bearing capacity in two commercial orchards. Tree adapted flower thinning has the potential to reduce yield losses that occur when crop load management is performed uniformly within fields.

In the context of tree adapted crop load management, the model of the fruit bearing capacity would serve as part of the control system for a mechatronic system for mechanical or chemical fruit thinning as well as for decision support in the subsequent corrective hand

thinning. Tree adapted crop load management would be a major step forward in precision orchard management in order to achieve desired production targets in fruit quality.

## 6.5. References

Aggelopoulou, K.D., Wulfsohn, D., Fountas, S., Gemtos, T.A., Nanos, G.D., Blackmore, S., 2010. Spatial variation in yield and quality in a small apple orchard. *Precis. Agric.* 11, 538-556. <https://doi.org/10.1007/s11119-009-9146-9>

Aggelopoulou, K.D., Pateras, D., Fountas, S., Gemtos T.A., Nanos G.D., 2011. Soil spatial variability and site-specific fertilization maps in an apple orchard. *Prec. Agric.* 12, 118-129. <https://doi.org/10.1007/s11119-010-9161-x>

Ampatzidis, Y.G., Whiting, M.D., 2013. Training System Affects Sweet Cherry Harvest Efficiency. *HortScience* 48, 547-555. <https://doi.org/10.21273/HORTSCI.48.5.547>

Anthony, B., Serra, S., Musacchi, S., 2019. Optimizing Crop Load for New Apple Cultivar: “WA38”. *Agronomy* 9, 107. <https://doi.org/10.3390/agronomy9020107>

Aquino, A., Ponce, J.M., Andújar, J.M., 2020. Identification of olive fruit, in intensive olive orchards, by means of its morphological structure using convolutional neural networks. *Comp. Electron. Agric.* 176, 105616. <https://doi.org/10.1016/j.compag.2020.105616>

Belhassine, F., Martinez, S., Bluy, S., Fumey, D., Kelner, J.J., Costes, E., Pallas, B., 2019. Impact of Within-Tree Organ Distances on Floral Induction and Fruit Growth in Apple Tree: Implication of Carbohydrate and Gibberellin Organ Contents. *Front. Plant Sci.* 10, 1233. <https://doi.org/10.3389/fpls.2019.01233>

Berk, P., Stajniko, D., Hočevár, M., Malnersčič, A., Jejčič, V., Belšak, A., 2019. Plant protection product dose rate estimation in apple orchards using a fuzzy logic system. *PLoS ONE* 14, e0214315. <https://doi.org/10.1371/journal.pone.0214315>

Bound, S.A., 2015. Optimising crop load and fruit quality of “Packham”s Triumph’ pear with ammonium thiosulfate, ethephon and 6-benzyladenine. *Sci. Hortic.-Amsterdam* 192, 187–196. <https://doi.org/10.1016/j.scienta.2015.05.030>

Costa, G., Botton, A., Vizzotto, G., 2018. Fruit thinning: Advances and trends. *Hortic. Rev.* 46, 185-226. <https://doi.org/10.1002/9781119521082.ch4>

Breen, K.C., Tustin, D.S., Palmer, J.W., Close, D.C., 2015. Method of manipulating floral bud density affects fruit set responses in apple. *Sci. Hortic.-Amsterdam* 197, 244-253. <https://doi.org/10.1016/j.scienta.2015.09.042>

- Breen, K.C., Tustin, D.S., Van Hooijdonk, B.M., Stanley, C.J., Scofield, C., et al., 2021. Use of physiological principles to guide precision orchard management and facilitate increased yields of premium quality fruit. *Acta Hort.* (In press)
- Bresilla, K., Perulli, G.D., Boini, A., Morandi, B., Corelli-Grappadelli, L., Manfrini, L., 2019. Single-shot convolution neural networks for real-time fruit detection within the tree. *Front. Plant Sci.* 10, 611. <https://doi.org/10.3389/fpls.2019.00611>
- Dennis, F.G., 2000. The history of fruit thinning. *Plant Growth Regul.* 31, 1-16. <https://doi.org/10.1023/A:1006330009160>
- Elsysy, M., Serra, S., Schwallier, P., Musacchi, S., Einhorn, T., 2019. Net enclosure of 'Honeycrisp' and 'Gala' apple trees at different bloom stages affects fruit set and alters seed production. *Agronomy* 9, 478. <https://doi.org/10.3390/agronomy9090478>
- Fessler, L., Fulcher, A., Lockwood, D., Wright, W., Zhu, H., 2020. Advancing sustainability in tree crop pest management: refining spray application rate with a laser-guided variable-rate sprayer in apple orchards. *HortScience* 55, 1522-1530. <https://doi.org/10.21273/HORTSCI15056-20>
- Francesconi, A.H.D., Lakso, A.N., Nyrop, J.P., Barnard, J., Denning, S.S., 1996. Carbon balance as a physiological basis for the interactions of European red mite and crop load on 'Starkrimson Delicious' apple trees. *J. Amer. Soc. Hortic. Sci.* 121, 959-956. <https://doi.org/10.21273/JASHS.121.5.959>
- Gongal, A., Amatya, S., Karkee, M., Zhang, Q., Lewis, K., 2015. Sensors and systems for fruit detection and localization: a review. *Comput. Electron. Agric.* 116, 8-19. <https://doi.org/10.1016/j.compag.2015.05.021>
- Gonzalez, L., Torres, E., Àvila, G., Bonany, J., Alegre, S., Carbó, J., Asin, L., 2019. Evaluation of chemical fruit thinning efficiency using Brevis® (Metamitron) on apple trees ("Gala") under Spanish conditions. *Sci. Hortic.-Amsterdam* 261, 109003. <https://doi.org/10.1016/j.scienta.2019.109003>
- Greene, D.W., Lakso, A.N., Robinson, T.L., Schwallier, P., 2013. Development of a Fruitlet Growth Model to Predict Thinner Response on Apples. *HortScience* 48, 584-587. <https://doi.org/10.21273/HORTSCI.48.5.584>
- Handsack, M., Schmidt, S., 1990. Grafisches Modell zur Beschreibung der Ertragsbildung bei Apfel unter Berücksichtigung von Wechselwirkungen zwischen den Ertragskomponenten. *Arch. Gartenbau* 38, 399-405

- Hansen, P., 1969.  $^{14}\text{C}$ -Studies on apple trees. IV. Photosynthate consumption in fruits in relation to the leaf-fruit ratio and to the leaf-fruit position. *Physiol. Plant.* 22, 186-198. <https://doi.org/10.1111/j.1399-3054.1969.tb07855.x>
- He, L., Schupp, J., 2018. Sensing and automation in pruning of apple trees: A review. *Agronomy* 8, 211. <https://doi.org/10.3390/agronomy8100211>
- Huang, Y., Ren, Z., Li, D., Liu, X., 2020. Phenotypic techniques and applications in fruit trees: a review. *Plant Methods* 16, 107. <https://doi.org/10.1186/s13007-020-00649-7>
- Jackson, J.E., Palmer, J.W., 1980. A computer model study of light interception by orchards in relation to mechanised harvesting and management. *Sci. Hortic.-Amsterdam.* 13, 1-7. [https://doi.org/10.1016/0304-4238\(80\)90015-1](https://doi.org/10.1016/0304-4238(80)90015-1)
- Johnson, R.S., Lakso, A.N., 1985. Relationships between stem length, leaf area, stem weight, and accumulated growing degree days in apple shoots. *J. Amer. Soc. Hortic. Sci.* 110, 586-590
- Käthner, J., Zude-Sasse, M., 2015. Interaction of 3D soil electrical conductivity and generative growth in *Prunus domestica* L. *Eur. J. Hortic. Sci.* 80, 231-239. <http://dx.doi.org/10.17660/eJHS.2015/80.5.5>
- Käthner, J., Ben-Gal, A., Gebbers, R., Peeters, A., Herppich, W.B., Zude-Sasse, M., 2017. Evaluating spatially resolved influence of soil and tree water status on quality of european plum grown in semi-humid climate. *Front. Plant Sci.* 8, 1053. <https://doi.org/10.3389/fpls.2017.01053>
- Kon, T.M., Schupp, J.R., Winzeler, H.E., Marini, R.P., 2013. Influence of mechanical string thinning treatments on vegetative and reproductive tissues, fruit set, yield, and fruit quality of 'Gala' apple. *HortScience* 48, 40-46. <https://doi.org/10.21273/HORTSCI.48.1.40>
- Kon, T.M., Schupp, J.R., 2019. Apple crop load management with special focus on early thinning strategies: a US perspective. *Hortic. Rev.* 46, 255-298. <https://doi.org/10.1002/9781119521082.ch6>
- Koirala, A., Walsh, K.B., Wang, Z., McCarthy, C., 2019. Deep learning - Method overview and review of use for fruit detection and yield estimation. *Comput. Electron. Agric.* 162, 219-234. <https://doi.org/10.1016/j.compag.2019.04.017>
- Lakso, A.N., Corelli-Grappadelli, L., Barnard, J., Goffinet, M.C., 1995. An expolinear model of the growth pattern of the apple fruit. *J. Hort. Sci.*, 70, 389-394. <https://doi.org/10.1080/14620316.1995.11515308>



- Lakso, A.N., Mattii, G.B., Nyrop, J.P., Denning, S.S., 1996. Influence of European red mite on leaf and whole canopy CO<sub>2</sub> exchange, yield, fruit size, quality and return cropping in 'Delicious' apple trees. *J. Amer. Soc. Hortic. Sci.* 121, 954-958. <https://doi.org/10.21273/JASHS.121.5.954>
- Lo Bianco, R. 2019. Water-Related Variables for Predicting Yield of Apple under Deficit Irrigation. *Horticulturae* 5, 8. <https://doi.org/10.3390/horticulturae5010008>
- Lyons, D.J., Heinemann, P.H., Schupp, J.R., Baugher T.A., Liu, J., 2015. Development of a selective automated blossom thinning system for peaches. *Trans. ASABE.* 58, 1447-1457. <https://doi.org/10.13031/trans.58.11138>
- Manfrini, L., Corelli-Grappadelli, L., Morandi, B., Losciale, P., Taylor, J.A., 2020. Innovative approaches to orchard management: assessing the variability in yield and maturity in a 'Gala' apple orchard using a simple management unit modelling approach. *Eur. J. Hortic. Sci.* 85, 211-218. <https://doi.org/10.17660/eJHS.2020/85.4.1>
- Magness, J.R., Overley, F.L., Luce, W.A., 1931. Relation of foliage to fruit size and quality in apples and pears. *Wash. St. Agric. Exp. Sta. Bull.* 249
- Meier, U., Bleiholder, H., Buhr, L., Feller, C., Hacks, H., et al., 2009. The BBCH system to coding the phenological growth stages of plants - history and publications. *J. Kulturpflanz.* 61, 41-52. <https://doi.org/10.5073/JfK.2009.02.01>
- Meland, M., Birken, E., 2010. Ethephon as a blossom and fruitlet thinner affects crop load, fruit weight and fruit quality of the European plum cultivar 'Jubileum'. *Acta Hortic.* 884, 315-321. <https://doi.org/10.17660/ActaHortic.2010.884.36>
- Mills, T.M., Behboudian, M.H., Clothier, B.E., 1996. Water relations, growth, and the composition of 'Braeburn' apple fruit under deficit irrigation. *J. Am. Soc. Hortic. Sci.* 121, 286-291. <https://doi.org/10.21273/JASHS.121.2.286>
- Naor, A., Peres, M., Greenblat, Y., Doron, I., Gal, Y., Stern, R.A., 2000. Irrigation and crop load interactions in relation to pear yield and fruit-size distribution. *J. Hortic. Sci. Biotech.* 75, 555-561. <https://doi.org/10.1080/14620316.2000.11511285>
- Pallas, B., Da-Silva, D., Valsesia, P., Yang, W., Guillaume, O., et al., 2016. Simulation of carbon allocation and organ growth variability in apple tree by connecting architectural and source-sink models. *Ann. Bot.-London* 118, 317-330. <https://doi.org/10.1093/aob/mcw085>

- Peeters, A., Zude, M., Käthner, J., Ünlü, M., Kanber, R., et al., 2015. Getis-Ord's hot-and cold-spot statistics as a basis for multivariate spatial clustering of orchard tree data. *Comp. Electron. Agric.* 111, 140-150. <https://doi.org/10.1016/j.compag.2014.12.011>.
- Penzel, M., Möhler, M., Weltzien, C., Herppich, W.B. and Zude-Sasse, M., 2020a. Estimation of daily carbon demand in sweet cherry (*Prunus avium* L.) production. *J. Appl. Bot. Food Qual.* 93, 149-158 <https://doi.org/10.5073/JABFQ.2020.093.019>
- Penzel, M., Pflanz, M., Gebbers, R., Zude-Sasse, M., 2020b. Mechanical thinning of apples reduces fruit drop. *Acta Hortic.* 1281, 533-538. <https://doi.org/10.17660/ActaHortic.2020.1281.70>
- Penzel, M., Möhler, M., Pflanz, M., Zude-Sasse, M., 2021. Fruit quality response to varying leaf area to fruit ratio on girdled branches and whole trees of 'Bellise' sweet cherry (*Prunus avium* L.). *Acta Hortic.* 1327, 707-714. <https://doi.org/10.17660/ActaHortic.2021.1327.94>
- Pflanz, M., Gebbers, R., Zude, M., 2016. Influence of tree-adapted flower thinning on apple yield and fruit quality considering cultivars with different predisposition in fructification. *Acta Hortic.* 1130, 605–612. <https://doi.org/10.17660/ActaHortic.2016.1130.90>
- Preston, A.P., 1954. Effects of fruit thinning by the leaf count method on yield, size and biennial bearing of the apple Duchess Favorite. *J. Hortic. Sci.* 43, 373–381. <https://doi.org/10.1080/00221589.1954.11513819>
- Reyes, F., DeJong, T., Franceschi, P., Tagliavini, M., Gianelle, D., 2016. Maximum growth potential and periods of resource limitation in apple tree. *Front. Plant Sci.* 7, 233. <https://doi.org/10.3389/fpls.2016.00233>
- Riehle, A., 2020. Maschinelle Blütenausdünnung von Apfelbäumen. Ph.D. thesis, University of Hohenheim
- Robinson, T.L., Lakso, A.N., 1991. Bases of yield and production efficiency in apple orchard systems, *J. Amer. Soc. Hortic. Sci.* 116, 188-194. <https://doi.org/10.21273/JASHS.116.2.188>
- Robinson T.L, Lakso A.N. and Greene D., 2017. Precision crop load management: The practical implementation of physiological models. *Acta Hortic.*, 1177, 381-390. <https://doi.org/10.17660/ActaHortic.2017.1177.55>
- Rosa, N., Àvila, G., Carbó, J., Verjans, W., Pais, I.P., et al., 2020. Metamitron and Shade Effects on Leaf Physiology and Thinning Efficacy of *Malus × domestica* Borkh. *Agronomy* 10, 1924. <https://doi.org/10.3390/agronomy10121924>

Roßberg, D., Harzer, U., 2015. Erhebungen zur Anwendung von Pflanzenschutzmitteln im Apfelanbau (2011–2013). J Kulturpflanz 67, 85-91. <https://doi.org/10.5073/JfK.2015.03.01>.

Sanz, R., Llorens, J., Escolà, A., Arnó, J., Planas, S., Roman, C., Rosell-Polo, J.R., 2018. LIDAR and non-LIDAR-based canopy parameters to estimate the leaf area in fruit trees and vineyard. Agric. Forest Meteorol. 260, 229-239. <https://doi.org/10.1016/j.agrformet.2018.06.017>

Treder, W., Mika, A., Krzewińska, D., 2010. Relations between tree age, fruit load and mean fruit weight. J. Fruit Ornament. Plant Res. 18, 139-149

Tsoulias, N., Gebbers, R., Zude-Sasse, M., 2020. Using data on soil EC<sub>a</sub>, soil water properties, and response of tree root system for spatial water balancing in an apple orchard. Precis. Agric. 21, 522-548. <https://doi.org/10.1007/s11119-019-09680-8>

Umali, B.P., Oliver, D.P., Forrester, S., Chittleborough, D.J., Hutson, J.L., Kookana, R.S., Ostendorf, B., 2012. The effect of terrain and management on the spatial variability of soil properties in an apple orchard. Catena 93, 38-48. <https://doi.org/10.1016/j.catena.2012.01.010>

Vanbrabant, Y., Delalieux, S., Tits, L., Pauly, K., Vandermaesen, J., Somers, B., 2020. Pear flower cluster quantification using RGB drone imagery. Agronomy 10, 407. <https://doi.org/10.3390/agronomy10030407>

Verbiest, R., Ruysen, K., Vanwalleghe, T., Demeester, E., Kellens, K., 2020. Automation and robotics in the cultivation of pome fruit: Where do we stand today?. J. Field Robot. 2020, 1-19. <https://doi.org/10.1002/rob.22000>

Walsh, K.B., Blasco, J., Zude-Sasse, M., Xudong, S., 2020. Review: Visible-NIR 'point' spectroscopy in postharvest fruit and vegetable assessment: the science behind three decades of commercial use. Postharvest Biol. Tech. 168, 111246. <https://doi.org/10.1016/j.postharvbio.2020.111246>

Wandkar, S.V., Bhatt, Y.C., Jain, H.K., Nalawade, S.M., Pawar, S.G., 2018. Real-time variable rate spraying in orchards and Vineyards: A Review. J. Inst. Eng. India Ser. A 99, 385-390. <https://doi.org/10.1007/s40030-018-0289-4>

Wouters, N., 2014. Mechatronics for efficient thinning of pear. Ph.D. thesis. KU Leuven

Wünsche, J.N., Lakso, A.N., Robinson, T.L., Lenz, F., Denning, S.S., 1996. The bases of productivity in apple production systems: The role of light interception by different shoot types. J. Amer. Soc. Hortic. Sci. 121, 886-893. <https://doi.org/10.21273/JASHS.121.5.886>.

Yuan, R., Greene, D.W., 2000. Benzyladenine as a chemical thinner for 'McIntosh' apples. I. Fruit thinning effects and associated relationships with photosynthesis, assimilate translocation, and nonstructural carbohydrates. *J. Amer. Soc. Hortic. Sci.* 12, 169-176. <https://doi.org/10.21273/JASHS.125.2.169>

Zhang, Z., Wang, X., Lai, Q., Zhang, Z., 2018. Review of variable-rate sprayer applications based on real-time sensor technologies. in: Hussmann, S. (Ed.), *Automation in Agriculture- Securing Food Supplies for Future Generations*, IntechOpen, Rijeka, Croatia, pp. 53–79. <https://doi.org/10.5772/intechopen.73622>

Zude-Sasse, M., Herold, B., Geyer, M., 2000. Comparative study on maturity prediction in 'Elstar' and 'Jonagold' apples. *Gartenbauwissenschaft* 65, 260-265. <https://www.pubhort.org/ejhs/2000/6790.htm>

Zude, M., Herold, B., Roger, J.M., Bellon-Maurel, V., Landahl, S., 2006. Non-destructive tests on the prediction of apple fruit flesh firmness and soluble solids content on tree and in shelf life. *J. Food Eng.* 77, 254-260. <https://doi.org/10.1016/j.jfoodeng.2005.06.027>

Zude-Sasse, M., Fountas, S., Gemtos, T.A., Abu-Khalaf, N., 2016. Applications of precision agriculture in horticultural crops. *Eur. J. Hortic. Sci.* 81, 78-90. <https://doi.org/10.17660/eJHS.2016/81.2.2>

## **Eidesstattliche Erklärung**

Hiermit erkläre ich, dass ich die von mir vorgelegte Dissertation mit dem Titel 'Sensor-based determination of the fruit bearing capacity in Malus x domestica BORKH. aimed at precise crop load management' selbstständig und nur unter Verwendung der angegebenen Quellen und Hilfsmittel angefertigt habe. Ich erkläre außerdem, dass diese Dissertation noch keiner anderen Fakultät oder Hochschule zur Prüfung vorgelegt wurde.

Erfurt, den 21.05.2021

Martin Penzel

# Lebenslauf

## Persönliche Daten

Vorname Martin  
Nachname Penzel  
Geburtsdatum 10.02.1988 in Jena

## Studium

2017 - 2021 **Technische Universität Berlin; Fakultät V - Verkehrs- und Maschinensysteme**  
Promotion (Dr. Ing., mit Auszeichnung) an der Professur für Agromechatronik  
2014 - 2016 **Martin-Luther-Universität Halle-Wittenberg**  
M. Sc. Agrarwissenschaften  
2008 - 2012 **Fachhochschule Erfurt**  
Dipl. Ing. (FH) Gartenbau

## Berufspraxis

seit 2021 **Thüringer Landesamt für Landwirtschaft und Ländlichen Raum (TLLLR), Erfurt, Referat Gartenbau und Gartenbauliches Versuchswesen**  
Referent für Obstbau  
2017 - 2021 **Leibniz Institut für Agrartechnik und Bioökonomie e.V. (ATB), Potsdam, Abteilung Technik im Gartenbau**  
Wissenschaftlicher Mitarbeiter  
2016 (Mär-Sep) **Thüringer Landesanstalt für Landwirtschaft (TLL), Erfurt, Referat Pflanzenschutz**  
Sachbearbeiter für Pflanzenschutz im Gemüse- und Zierpflanzenbau  
2012 - 2014 **Landratsamt Breisgau-Hochschwarzwald, Breisach am Rhein**  
Vorbereitungsdienst für den gehobenen Landwirtschaftstechnischen Verwaltungsdienst  
2011 (Mär-Aug) **Washington Tree Fruit Research Commission, Wenatchee, USA**  
Research Assistant  
2009 - 2010 **FitzGerald Nurseries, Stoneyford, Irland**  
Production Assistant